Molekularbiologische Analyse des chemischen Abwehrsystems bei Blattkäferlarven (Coleoptera: Chrysomelina).
In vivo Validierung von Enzymen und Transportproteinen an essentiellen Schnittstellen des Defensiv-Metabolismus mittels RNA interference.

Dissertation
zur Erlangung des akademischen Grades
„doctor rerum naturalium“ (Dr. rer. nat.)

vorgelegt dem Rat der Biologisch-Pharmazeutischen Fakultät
der Friedrich-Schiller-Universität Jena

von René Roberto Gretscher

geboren am 30.11.1983 in Berlin

Die hier vorliegende Arbeit wurde am Max-Planck-Institut für Chemische Ökologie Jena, Abteilung für Bioorganische Chemie in der Arbeitsgruppe „*Chemical defense of leaf beetles*“ von Frau Dr. Antje Burse angefertigt.

Durchgeführt von 05/2010 bis 12/2013

Gutachter: 1. Prof. Dr. Wilhelm Boland, Jena

2. Prof. Dr. Lennart Olsson, Jena

3. Prof. Dr. Gregor Bucher, Göttingen

Tag der öffentlichen Disputation: 27.05.2014

„In einem Zeitalter, wo man Früchte oft vor der Blüte erwartet und vieles darum zu verachten scheint, weil es nicht unmittelbar Wunden heilt, den Acker düngt, oder Mühlräder treibt, […] vergißt man, daß Wissenschaften einen inneren Zweck haben und verliert das eigentlich literarische Interesse, das Streben nach Erkenntnis, als Erkenntnis, aus dem Auge."

Alexander von Humboldt,
Über die Freiheit des Menschen. Auf der Suche nach Wahrheit

Inhaltsverzeichnis

1. Allgemeine Einleitung

Blattkäfer stellen innerhalb der Insekten die artenreichste Gruppe dar (Jolivet 1995). Durch ihre Lebensweise auf buchstäblich allen Pflanzengattungen, haben sie zum Teil Mechanismen entwickelt die oftmals giftige Sekundärchemie der Pflanzen zu detoxifizieren, oder sogar für sich nutzbar zu machen (Wain 1944). Einige Blattkäfer verteidigen sich gegen Prädatoren mit Wehrsektreten, in denen umgewandelte Blattalkohole identifiziert worden sind (Pasteels, Braekman u.a. 1982).

Im Rahmen der vorliegenden Doktorarbeit sollen die molekularen Grundlagen erforscht werden, die in der Biosynthese solcher Wehrsubstanzen bei Blattkäfern eine Rolle spielen. Die Anwendung der RNAi Technologie erlaubt dabei die funktionale Evaluation von Proteinen *in vivo,* um diese in Schlüsselpositionen der realisierten Wehrchemie zu identifizieren. Die durch Hinzunahme von weiteren Analysemethoden erzeugten Modelle können auf andere Insekten übertragen werden und so insgesamt zu einem tieferen Verständnis chemisch-ökologischer Netzwerke in der Natur beitragen.

1.1 Gen-Silencing mittels RNA interference

Das Potential der RNAi-Methode wurde früh für die entomologische Forschung entdeckt (Kennerdell und Carthew 1998). Hierbei wird gezielt die Expression von Genen unterdrückt, was zu einem „loss-of-function"-Phänotyp führt, von dem auf die Funktion des regulierten Genprodukts geschlossen werden kann. RNAi erlaubt die funktionale Charakterisierung ausgewählter Genprodukte, (z.B. Ciudad, Belles u.a. 2007, Araujo, Santos u.a. 2006, Tanaka und Suzuki 2005), kann aber auch in Raster-Analysen (Screens) eingesetzt werden, um aus einer Vielzahl von Kandidaten einzelne zu identifizieren, die für eine gesuchte Funktion verantwortlich sind. In *T. castaneum* wurde zum Beispiel eine Genom-weite Raster-Analyse begonnen, welche Gene identifizieren soll, die für die Entwicklung von Organen und Strukturen der Imagines verantwortlich sind (z.B. N. Posnien, Koniszewski u.a. 2011, http://ibeetle-base.uni-goettingen.de/). Hier zeigte sich, dass RNAi für die Identifizierung von verantwortlichen Genen der Embryogenese und Strukturbildung der Imagines gut geeignet ist, da diese Prozesse oftmals nur *in vivo* untersucht werden können. In *D. melanogaster* hingegen werden derlei Screens häufiger eingesetzt, um in

→ **Abbildung 1: RNAi vermitteltes Gen-Silencing in Insekten.** *A*: Reguläre Transkription-Translation Reaktion. *B*(a): dsRNA oder siRNA wird in die Hämolymphe eingebracht und mittels RNA-Transportern in die Zellen aufgenommen; *B*(b): RNAse III (Dicer) schneidet dsRNA und längere siRNAs auf 21-28bp Länge; *B*(c): einer der beiden siRNA-Stränge wird in den RISC überführt, wo er als Template für die Suche nach passender mRNA dient. *C*(a): Nachdem RISC eine Basenpaarung des siRNA Einzelstranges mit einer mRNA herstellt, wird diese abgebaut; *C*(b): Infolge dessen wird weniger Protein produziert, was den Stoffwechselweg, z.B. der chemischen Abwehr, stört; RNAi-Signale sorgen für ein systemisches Silencen. *D*(a): Wenn die Sequenz der dsRNA einem zweiten Transkript zu ähnlich ist (hier braun), können Off-target-Effekte eintreten, da die nicht-eineindeutigen Sequenzen ebenfalls in RISC eingebaut werden; *D*(b): Die Basenpaarung findet dann nicht mehr nur mit dem Zieltranskript statt, sondern RISC degradiert auch anderen mRNA; *D*(c): Die in der Folge ungewollt verminderte Proteinmenge von off-targets führt zu Veränderungen in anderen Stoffwechselwegen und auch die interzellulären RNAi-Signale sind gemischt. (Verändert nach Siomi und Siomi 2009)

Zelllinien die molekulare Grundlage für einen bestimmten Signalweg oder eines physiologischen Prozesses zu ergründen (z.B. Zhang, Yeromin u.a. 2006). RNAi ist allerdings nicht nur auf genomsequenzierte Modellorganismen beschränkt, sondern wird auf verschiedenste Insektentaxa angewendet (Belles 2010, Mito, Nakamura u.a. 2011).

Für die vorliegende Arbeit wurden Transkriptom-Bibliotheken von mRNA verschiedener Blattkäferarten generiert, die eine *in silico* Identifizierung von Transkripten ermöglichen, die eine Rolle in der Produktion von Wehrsubstanzen spielen könnten. Eine andere Herangehensweise zur Identifizierung wäre die Sequenzierung von Proteomen mittels LC-MS/MS, wobei die resultierenden Peptidsequenzen dann genutzt werden können, um aus der Datenbank die korrespondierenden Transkripte zu erhalten.

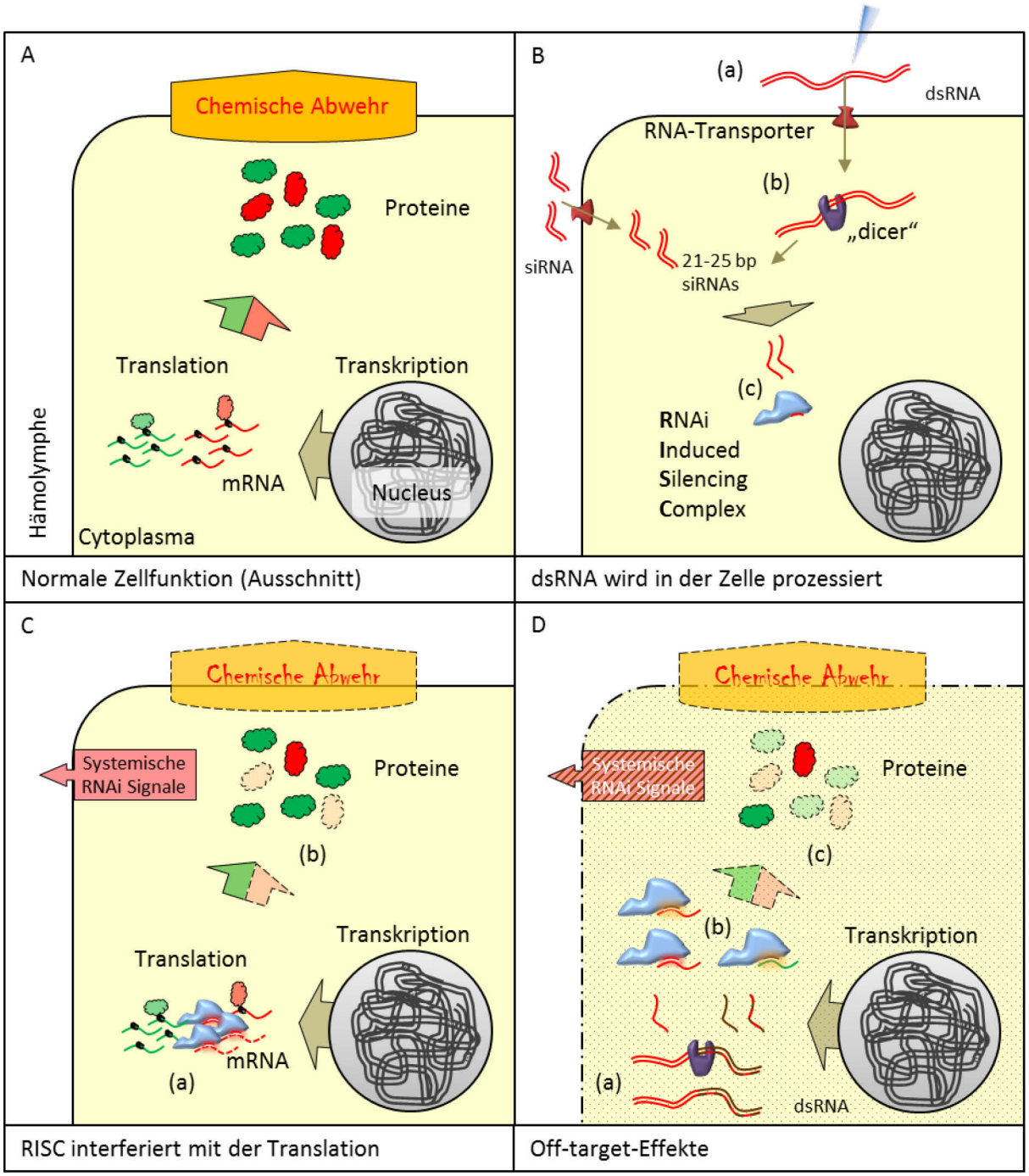

Beide Methoden können Listen mit mehreren Kandidaten erzeugen, die als Verantwortliche für eine bestimmte Funktion im Körper in Frage kommen. Hierbei eignet sich RNAi, um diese Transkripte einer gesuchten Funktion genau zuzuordnen.

Die RNAi-Technik basiert auf einem natürlichen Mechanismus, der in allen eukaryotischen Zellen zu finden ist und der dem Schutz vor Viren und Transposons dient (Burand und Hunter 2013) (s. Abb. 1). Das Genom von Riboviren, sowie ein Abschnitt der aus Transposons stammenden mRNA, kann als doppelsträngige RNA vorliegen (double stranded RNA, dsRNA) und wird gleichermaßen wie künstlich eingeführte dsRNA von RNAse III Enzymen (Dicer) erkannt. Diese zerlegen die dsRNA in 21-28 bp lange Fragmente (short interfering RNA, siRNA), welche dann mittels Argonaut-Protein, in den RNAi induced silencing complex (RISC) geladen werden (Abb. 1*B*). Dieser Proteinkomplex verwendet die nun einzelsträngige siRNA, um zytosolische mRNA auf Basenpaarung zu scannen. Findet eine Basenpaarung zwischen dem siRNA-Strang und der mRNA statt, wird diese mRNA abgebaut und so ihre nachfolgende Translation verhindert. (Meister und Tuschl 2004), (Abb.1*C*). Auf diese Weise wird eine schädigende Produktion von viralen Proteinen ebenso verhindert, wie die der Transposon-Proteine. Vermutlich auch zum Schutz vor Viren kann ein systemisches „RNAi-Signal“ in Form von mobilen RNAs an Nachbarzellen übertragen werden, das dann einen identisch beladenen RISC in einer Zelle erzeugt, die mit dem Auslöser selbst nicht in Kontakt gekommen ist (systemisches RNAi), (Melnyk, Molnar u.a. 2011).

Da der Mechanismus in allen Eukaryoten konserviert ist, hängt es lediglich von der Sensitivität des Organismus' ab, in wieweit RNAi in ihm anwendbar ist. (vgl. z.B. Terenius, Papanicolaou u.a. 2011, Tomoyasu, Miller u.a. 2008). So ist es bspw. nicht möglich durch Mikroinjektion von dsRNA systemisches RNAi in Dipteren und den meisten Lepidopteren zu erzeugen, während es in Coleoptera, Apocrita und allen hemimetabolen Insekten kein Problem darstellt (Terenius, Papanicolaou u.a. 2011). Ein weiteres Beispiel für RNAi-Sensitivität betrifft parentales RNAi, wobei weibliche Puppen oder Imagines nach Behandlung mit dsRNA, ein RNAi-Signal maternal auf die F1-Generation übertragen wird (Bucher, Scholten u.a. 2002).

Im Gegensatz zum vollständigen Ausschalten eines Gens durch Mutageneseverfahren, erzeugt RNAi lediglich die Reduktion eines Genprodukts, so dass Restaktivitäten noch bestehen bleiben können. Außerdem besteht bei genügender Ähnlichkeit der siRNAs zu einer mRNA, die nicht Ziel der RNAi werden sollte, die Gefahr des Sequenz-basierenden Co-Regulation (off-Target-Effekte), (Jackson, Bartz u.a. 2003) (Abb. 1*D*). Um dieser Problematik zu entgehen, werden die dsRNA-Sequenzen auf Ähnlichkeiten mit anderen Transkripten geprüft, um Bereiche mit hoher Ähnlichkeit ggf. aus der dsRNA-Sequenz auszuschließen (beschrieben in Manuskript 3). Für Modellorganismen gibt es bereits freie Software, die eine solche Suche vornimmt (Naito, Yamada u.a. 2005), für Organismen mit Transkriptom-Informationen kann man in manchen Vorhersage Programmen auch

die eigene Datenbank mit einbinden (Iyer, Deutsch u.a. 2007), aber Beispiele ohne jeglichen Sequenzcheck werden auch immer noch publiziert (Ohnishi, Hashimoto u.a. 2009).

Zusammenfassend lässt sich sagen, dass RNAi eine Methode zur genetischen Manipulation von Organismen darstellt, dessen Genom nicht notwendigerweise bekannt ist und/oder welche transgenen Veränderungen nicht zugänglich sind (Belles 2010). Mithilfe von RNAi ist es möglich die *in vivo* Relevanz von Genprodukten in den Tieren selbst zu ermitteln und so Fragen zur molekularen Grundlage der Biosynthese des Wehrsekrets in Blattkäferlarven zu klären. Der Unterstamm, dem die für diese Arbeit relevanten Blattkäferarten zugeordnet werden, wird im folgenden Kapitel näher erläutert.

1.2 Phylogenie und larvale Morphologie der Chrysomelina

Blattkäfer (Chrysomelidae) gehören zu den am weitesten verbreiteten Käferarten und können quasi auf allen grünen Pflanzen der Erde gefunden werden (Jolivet 1995). Ein Teil dieser Arten zeichnet sich durch larvale Verteidigungsstrategien aus, wobei Wehrsekrete aus exokrinen Drüsen eingesetzt werden, deren Wirkstoffe zum Teil auch aus den toxischen Substanzen rekrutiert werden

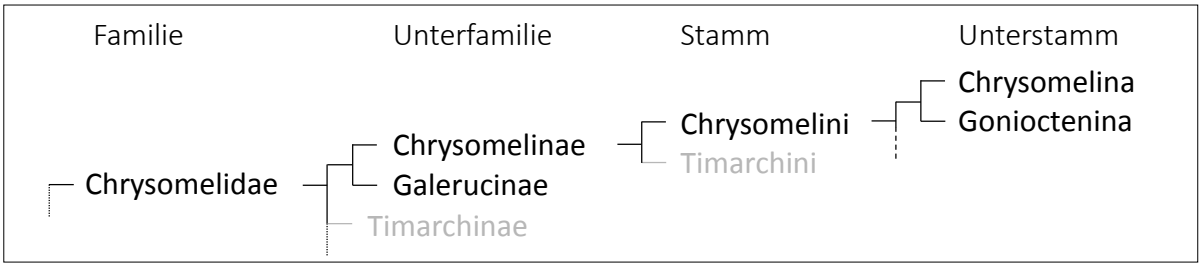

Abbildung 2: Aktuelle Sicht der Phylogenie der Chrysomelina. Gepunktete Linien zeigen weitere Phyla auf diesem Niveau an, die jedoch in der vorliegenden Arbeit keine Referenz darstellen, gestrichelte Linien indizieren weitere Genera auf diesem Niveau, welche keine präzise Zuordnung haben (Leschen und Beutel 2014, S.99).

können, die die Wirtspflanze gegen Fraßfeinde bereit hält (Dettner 1987). Diese Arten ordnen sich taxonomisch in der Unterfamilie der Chrysomelinae ein (Pasteels, Rowell-Rahier u.a. 1984, Leschen und Beutel 2014). Details zur systematischen Einordnung können Abbildung 2 entnommen werden.

Eine Besonderheit der larvalen Morphologie innerhalb der Unterfamilie der Chrysomelinae sind paarige Wehrdrüsenapparate, die ein Sekret produzieren, welches in erster Linie als Verteidigung gegen Prädatoren dient. Zwar ist die relative morphologische Lage der Apparate bei allen drüsentragenden Chrysomelinae gleich (Dettner und Schwinger 1987), doch gibt es Unterschiede im Aufbau und der Anzahl der Apparate, welche zwischen den Gattungen variieren können. Allen Wehrdrüsenapparaten innerhalb des Stammes der Chrysomelini ist gemein, dass sie ein epicuticulär ausgekleidetes Reservoir besitzen (Pasteels und Rowell-Rahier 1989) in welches Klasse III Drüsen-

zellen mittels eines epicuticulären Duktulus Stoffe sezernieren (Quennedey 1998, S. 177-207, Strauss, Peters u.a. 2013) (Abb. 3). Die Lagerung der Sekrete in den Reservoiren stellt unter anderem einen Schutz vor Autointoxikation der teilweise giftigen Sekretkomponenten dar. Die bei einigen *incertae sedis* Arten innerhalb der Chrysomelinae und bei den Gonioctenina zu findenden paarige Abdominaldrüsen (Dettner und Schwinger 1987), handelt es sich entweder um unabhängig von den Chrysomelina entstandene Formen, oder um die ursprüngliche Ausstattung der Larven (ebd.).

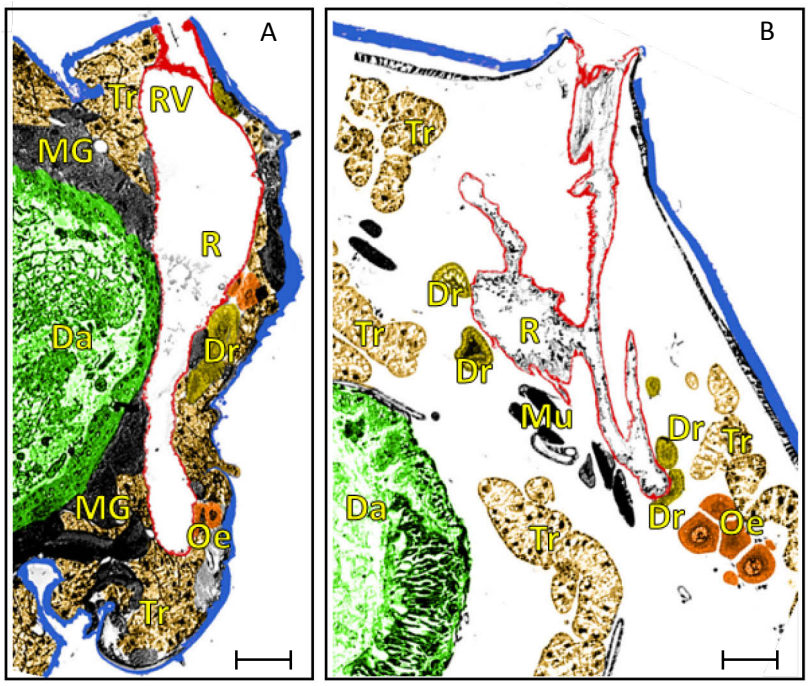

Abbildung 3: Larvale Histologie. *A&B*: Mikrographien aus histologischen Schnittserien (1 µm Schnittdicke), HE gefärbt. Vergößerung 50x *A*: *P. cochleariae*, mittlerer Metathorax, lateraler Ausschnitt rechtsseitig, Blick nach caudal; *B*: *C. populi*, Abdominalsegment VI, dorsolateraler Ausschnitt rechtsseitig, Blick nach caudal. Da: Darm, Mu: Muskulatur, MG: Malpighische Gefäße, Tr: Trophocyten, Oe: Oenocyten, Dr: Wehrdrüsen, R: Reservoir, RV: Reservoir Verschluss. Skala 100µm. Bearbeitung und falschfarben-Einfärbung in Photoshop CS5.

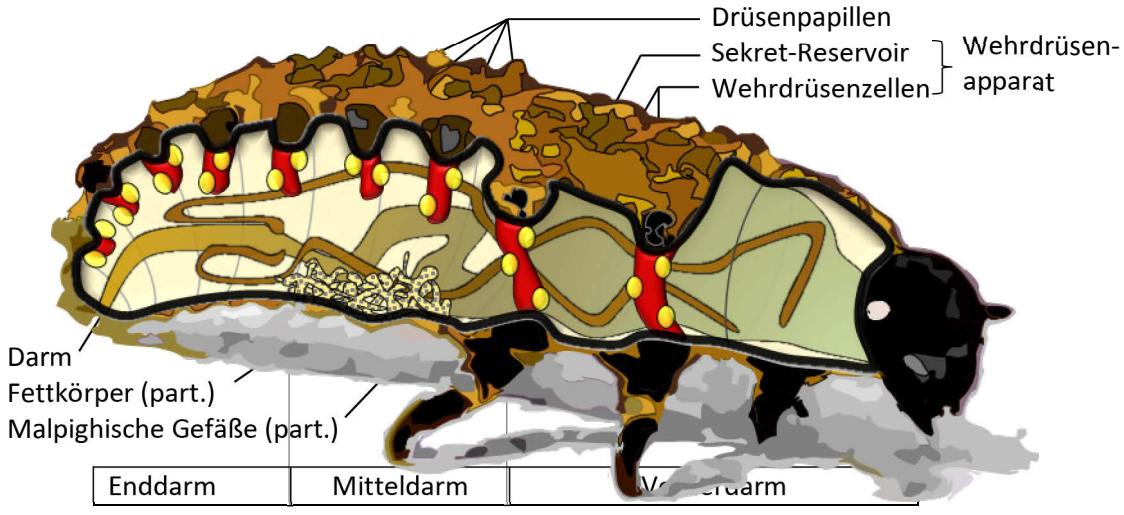

Abbildung 4: Schema der inneren und äußeren Organisation einer L3-Larve von *P. cochleariae*. Die Cuticula der rechten und der dorsalen Prothorax-Seite wurden abgenommen um den Blick auf die darunter liegenden Gewebe zu ermöglichen. Der Fettkörper ist hier nur in einem kleinen Teil eingezeichnet, füllt aber für gewöhnlich die gesamte Körperhöhle im lockeren Zusammenschluss aus. Die Malpighischen Gefäße sind zahlreicher und länger und auch der Darm ist komplexer gewunden.

Von besonderem Interesse für die vorliegende Arbeit, sind jedoch die neun Paare akzessorischer Drüsen, welche sich in den Larven aller Gattungen des Unterstammes der Chrysomelina finden lassen und den am stärksten differenzierten Wehrapparat darstellen. Die Reservoire münden hierbei jeweils in Papillen aus, die dorsolateral auf Meta- und Mesothorax, sowie auf den Abdominalsegmenten I-VII zu finden sind. Die Einzelheiten des inneren Aufbaus der Larven sind am Beispiel des Meerrettichblattkäfers, *Phaedon cochleariae* (Fabr.) in Abbildung 4 schematisiert. In *P. cochleariae* finden sich Sekret-Reservoire, die sich im Thorax beinahe über die komplette Lateralseite spannen und an denen 2-3 Wehrdrüsenzellen sitzen (vgl. Abb. 3*A*, 5*A*). Bei Larven des Pappelblattkäfers, *Chrysomela populi* (L.), finden sich hingegen ballonartige Reservoire an denen 5- 20 Wehrdrüsenzellen zu finden sind (vgl. Abb. 3*B*,5*B*).

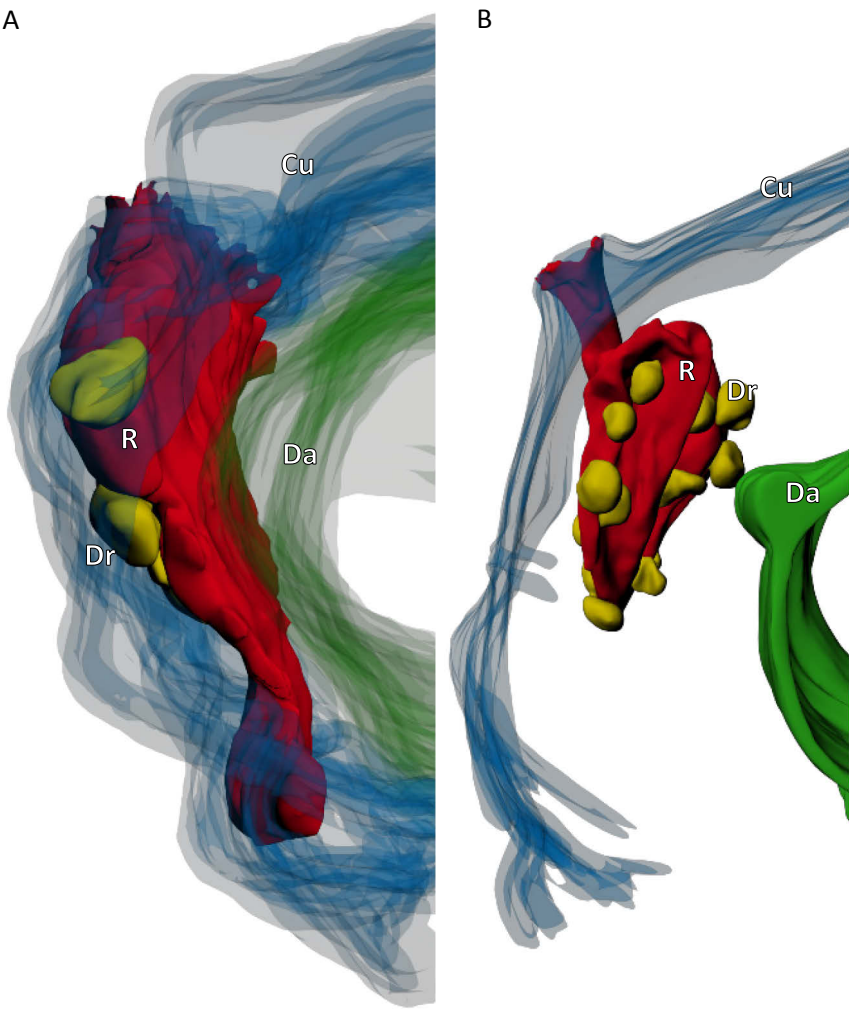

Abbildung 5: 3D-Rekonstruktion von Wehrdrüsenapparaten. Rekonstruktion aus histologischen Schnittserien, aligniert, annotiert, geglättet und fotografiert mit Amira 5.1® (VSG/FEI, Hillsboro, USA). A: *P. cochleariae*, rechter Metathorax, B: C. populi, rechtes Abdominalsegment VI. Blick frontal. Cu: Cuticula, R: Reservoir, Dr: Wehrdrüsenzelle, Da: Darm. (Annotierung und Fotographien von Maximilian Fraulob).

Eine genauere Untersuchung zur Geometrie und Histologie der Wehrapparate von drei verschiedenen Chrysomelina- Arten ist derzeit in Vorbereitung, welche die anfänglichen Arbeiten von (Maraghi 1993) und die subzelluläre Aufklärung in (Strauss, Peters u.a. 2013) ergänzen wird.

Diese Wehrapparate dienen der Produktion und Speicherung von Wehrsekreten, die im Fall des Angriffes durch Fraßfeinde an der Oberfläche der Papillen als Tropfen präsentiert werden (Abb. 6) (Blum, Brand u.a. 1972), (s. Kap. 1.3). Die Wirkstoffe des Sekrets werden als Allomone klassifiziert, da deren Wirkung zumeist keine Vergiftung zur Folge hat, sondern hauptsächlich abwehrend auf Prädatoren wirken soll (Whitman, Blum u.a. 1990). Die Präsentation des Sekretes erfolgt bei Chrysomelina prinzipiell auf zwei Arten, einmal kann das Reservoir aus der Larve heraus umgestülpt werden, sodass das Sekret an der nunmehr zur Außenseite gewordenen Innenseite des Reservoirs, mit den Wehrdrüsenzellen im Inneren, haftet (z.B. bei *P. cochleariae*). Die andere Methode ist ein komprimieren des Reservoirs, wobei das Sekret dann nach außen gepresst wird (z.B. bei *C. populi*). Nach Beendigung der Störung, werden in beiden Fällen die Sekrete wieder in den Körper gesogen und somit für den nächsten Angriff bewahrt. Die adulten Stadien sind ebenfalls in der Lage Wehrsekrete zu produzieren, welches sie, ähnlich wie andere Imagos der Chrysomelidae, durch Klasse III – Drüsenbündel, ohne einen extrazellulären Speicher, im Bedarfsfall durch Poren in der

Abbildung 6: L3-Larven von *C. populi* und *P. cochleariae* mit exponiertem Wehrsekret. links: *C. populi* (Foto: Antje Burse), rechts: *P. cochleariae* (Foto: Sindy Frick).

Cuticula der Elytren, bzw. des Pronotums, entlassen (Pasteels, Rowell-Rahier u.a. 1989). Diese Drüsen sind nach derzeitigem Stand der Erkenntnis nicht homolog zu den larvalen Wehrdrüsenapparaten (vgl. Pasteels, Rowell-Rahier u.a. 1984).

Zusammenfassend lässt sich sagen, dass sich die Larven im Unterstamm der Chrysomelina durch spezielle morphologische Strukturen auszeichnen, die eine Produktion und Speicherung von Wehrsekret ermöglichen, welche im Falle eines Angriffs durch Prädatoren zur Verteidigung eingesetzt werden und welche auch antimikrobielle Eigenschaften besitzen (Gross, Schumacher u.a. 2008). Die Synthese der Sekrete erfolgt auf unterschiedliche Weise, was im folgenden Kapitel unter Betrachtung der Artbildung innerhalb der Chrysomelina näher erläutert wird.

1.2.1 Evolution der Wehrbiochemie

Innerhalb der Chrysomelina bilden sich drei distinkte Arten-Gruppen ab, die die Allomone des Wehrsekretes durch jeweils gleiche Mechanismen synthetisieren (Termonia, Hsiao u.a. 2001) (Abb.

7). Molekulare Ergebnisse von (Termonia, Hsiao u.a.) haben gezeigt, dass die Gruppe der Iridoid-*de-novo*-Produzenten die ursprünglichste Gruppe bildet (Abb. 7, roter Kasten). Larven, die als *de novo*-Produzenten definiert werden, produzieren die Allomone unabhängig vom Sekundärmetabolismus ihrer Wirtspflanze aus dem körpereigenen Stoffwechsel (s. Kap. 1.4.1). Die zweite Gruppe (Abb. 7, grüner Kasten), die der obligatorischen Sequestrierer, nutzen Salicylaldehyd als Allomon welches sie aus Salicin synthetisieren, das sie mit der Nahrung aufnehmen. Die dritte Gruppe schließlich, entwickelte sich unabhängig von den anderen beiden (Mardulyn, Othmezouri u.a. 2011) und nutzt eine Mischung aus sequestrierten Blattalkoholen und einer Veresterung mit autogen produzierten Carbonsäuren, weshalb der Mechanismus hier als „Misch-Modus“ bezeichnet wird (Abb. 7, blauer Kasten). Die Aktivierung der Allomone im Wehrsekret findet über eine schrittweise enzymatische Umwandlung statt, die mechanistisch innerhalb der Chrysomelina in Teilen sehr ähnlich ist. Die enzymatischen Reaktionen, die die jeweiligen Vorstufen zur bioaktiven Substanz katalysieren (Soetens, Pasteels u.a. 1993, Brueckmann, Termonia u.a. 2002), werden in Kapitel 1.4.3 gesondert betrachtet.

Die Entwicklung dieser drei Synthesestrategien hat ihren Ursprung vermutlich in der letzten Eiszeit genommen (Jüngere Tundrenzeit, 10.730-9.700 Jahre v. Chr. mit relativen Durchschnittstemperaturen in Mitteleuropa um -4°C (Ammann 2000)). Die Käferarten überlebten während der Kälteperiode oftmals ausschließlich in den Refugien der Pflanzenarten am Fuß der Gebirge, wobei es wegen der anzunehmenden hohen Individuendichte zu Hybridisierungen zwischen den Arten kam, die zur heutigen Biodiversität beigetragen haben können (Mardulyn, Othmezouri u.a. 2011). Mit der erneuten Erwärmung nach 9700 v.Chr. wurde das Festland dann von krautigen Pflanzen erobert, wonach sich auch der Wald neu bildete. Anhand von Pollenanalysen kann die Wiederbesiedlung abgeleitet werden, wobei sich neben *Pinus spp. und Betula spp.* in der frühen Warmphase auch *Juniperus spp.*, *Salix spp.*, *Populus spp.* und *Rumex spp.* ausbreiteten. Diese robusten Pflanzengattungen verdrängten sich lokal gegenseitig, wanderten aber stets nord- und westwärts. (z. B. Hoek 1997, Theuerkauf und Joosten 2012, Cottrell, Krystufek u.a. 2005).

Die Annahme geht nun dahin, dass die auf Kräutern fressenden Iridoid-Produzenten im Zusammenhang mit der Neuausbreitung der Pflanzen begonnen haben auf einer abundanten Baumart wie *Salix spp.* zu fressen, deren Blätter, durch die Abwesenheit von Proanthocyanidine, für den Metabolismus der Käfer leichter zu verdauen war, als die von anderen Baumarten (z. B. Pasteels, Rowell-Rahier u.a. 1984). Hier entwickelte sich vermutlich auch die Sequestrierung, um mit den anderen Sekundärmetaboliten der Pflanze umgehen zu können. Der dabei mehrfach unabhängige und wiederholte Wechsel von *Salix spp.* als ursprüngliche Wirtspflanze auf *Betula spp.,* wie er bei *Chrysomela lapponica* durch Untersuchungen nachvollzogen werden kann, ist ein Indiz

für eine andauernde funktionale Anpassungen des Wehrsystems (Mardulyn, Othmezouri u.a. 2011, Kirsch, Vogel u.a. 2011a).

Am jüngsten scheint sich der Wirtpflanzenwechsel bei den *Plagiodera spp.* vollzogen zu haben, da sich im Wehrsekret vorwiegend Monoterpene finden lassen aber z.T. auch Salicylaldehyd aus sequestriertem Salicin vorkommt (Pasteels, Rowell-Rahier u.a. 1984). Die obligaten Sequestrierer der *Phratora* und *Chrysomela spp.* wären hiernach die ursprünglichsten Salicaceae-Konsumenten, da bei keiner der Arten Monoterpene im Wehrsekret nachweisbar sind (Pasteels, Rowell-Rahier u.a. 1984).

Die Spezies der Misch-Modus Gruppe, wie z.B. *C. lapponica*, waren dank dieser Synthesestrategie in der Lage, durch die bereits erwähnten zusätzlichen Wirtspflanzenwechsel weit mehr als nur eine Komponente des pflanzlichen Sekundärmetabolismus zu nutzen (Zvereva, Kozlov u.a. 2010). Im Sekret von *C. lapponica* finden sich weit über 60 Komponenten, die durch eine Veresterung der sequestrierten Blattalkohole und Carbonsäuren aus dem eigenen Metabolismus synthetisiert wurden (Schulz, Gross u.a. 1997, Tolzin-Banasch, Dagvadorj u.a. 2011) (Fig. 7*c,d*).

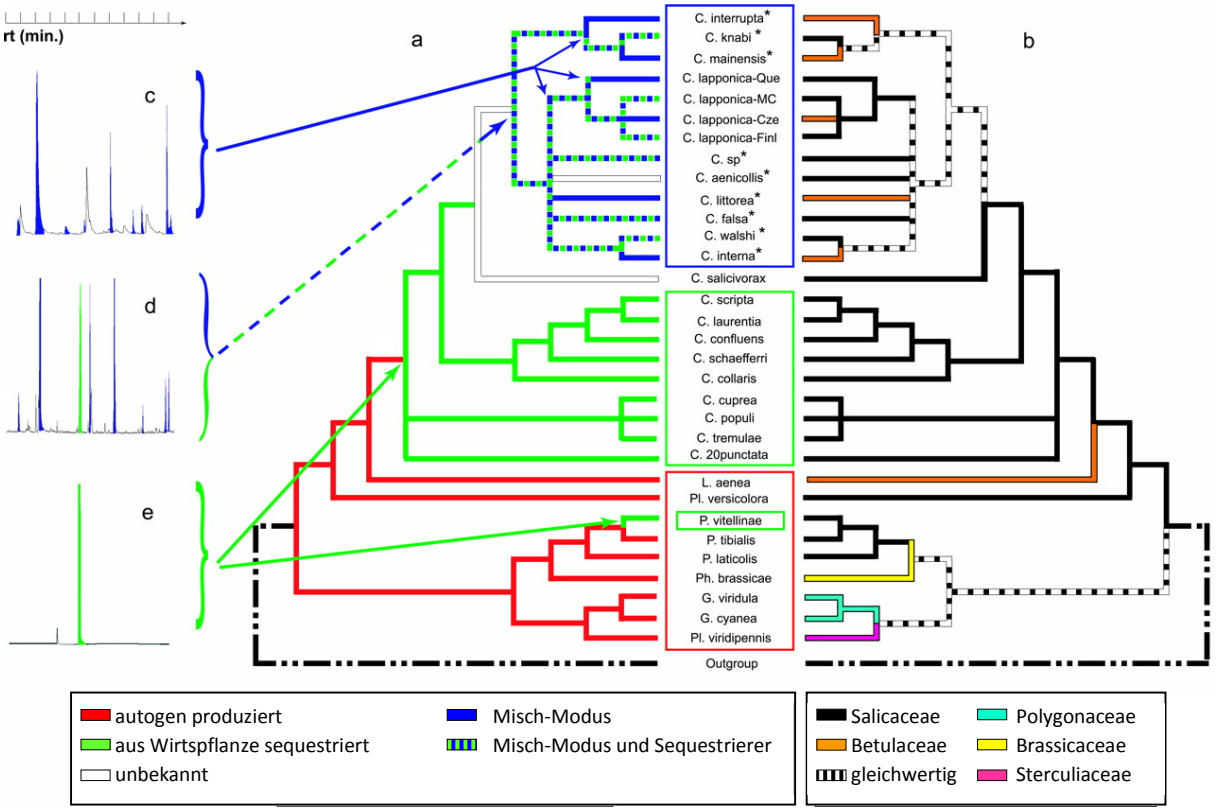

Abbildung 7: Phylogenie innerhalb der Chrysomelina. „Maximum parsimony" Rekonstruktion der chemischen Synthesestrategien *a*: Phylogenie anhand von molekularen Daten in Gegenüberstellung ihrer Wirtspflanzen (*b*). Que, Queyras (Frankreich); MC, Massif Central (Frankreich); Cze, Tschechien; Finl, Finnland. Sterne indizieren Spezies aus Nord Amerika innerhalb der „interrupta Gruppe". *c–e*: Typische Gas-Chromatogramme; Blaue Peaks: Butyl-Säuren und ihre Ester; Grüner Peak: Salicylaldehyd. rt, Retentionszeit. (Entnommen und verändert nach (Termonia, Hsiao u.a. 2001))

1.3 Abwehr von Prädatoren durch Wehrsekret und Lebensweise

Nachdem nun ein Blick auf die Phylogenie der zentralen Arten dieser Dissertation und die vermutliche Entstehung der verschiedenen Synthesestrategien der Wehrsekretkomponenten innerhalb der Chrysomelina geworfen wurde, stellt sich die Frage nach der ökologischen Bedeutung des Wehrsekrets. Das Iridoid Chrysomelidial, die Hauptkomponente des Sekretes von *P. cochleariae,* hat bspw. eine irritierende Wirkung auf andere Arthropoden und der Salicylaldehyd von *C. populi* wirkt auf Fraßfeinde abschreckend (Pasteels, Rowell-Rahier u.a. 1983). Parasitoide Fliegen nutzen hingegen diese Wehrchemie, um die Larven von weidefressenden *C. lapponica* als Wirte für ihre Gelege aufzuspüren (Zvereva, Kozlov u.a. 2010).

Eine Abwehr der Larven gegen andere Prädatoren wie bspw. Vögel oder insektivore Säuger wird weniger dem Sekret zugeschrieben, als vielmehr der Lebensweise der Larven unter den Blättern. Die verwirrende Färbung einiger Larven, die eine genaue Lokalisierung derselben am Blatt erschwert, ist eine weitere Verteidigungsstrategie (Pasteels, Rowell-Rahier u.a. 1984). Die dunkelschwarz gefärbten Larven der meist kleineren Spezies, wie *P. cochleariae*, fressen allerdings eher auf der Blattoberseite, als darunter und hinterlassen ovale Löcher in der Blattspreite. Diese Löcher, die in ungefähr dieselbe Größe wie die Larven selbst haben, erscheinen vor dem dunklen Hintergrund des Schattens oder Bodens wie zusätzliche Larven, sodass die Larven sich inmitten ihrer eigenen Fraßspuren vor einem Angriff aus der Luft schützen können (eigene Beobachtung).

Ein weiterer Schutz ergibt sich aus der Koexistenz von gut bewehrten Imagines zusammen mit den Larven auf der gleichen Wirtspflanze. Diese induzieren aufgrund ihrer deutlichen Färbung einen optischen Aposematismus (Nicolaus, Cassel u.a. 1983), durch Verknüpfung des optischen Reizes mit ihrer giftigen Wehrchemie. Die exponierte Lebensweise der Imagines auf der Oberfläche des Blattes bzw. an dessen Rand schützt daher auch die Larven am gleichen Blatt (Pasteels, Rowell-Rahier u.a. 1984).

Untersuchungen haben gezeigt, dass bei allen Chrysomelina-Arten, deren Imagines ein Wehrsekret mit Isoxazolinon-Derivaten produzieren (Randoux, Braekman u.a. 1991), auch alle anderen Lebensstadien unabhängig von der Fähigkeit zur Sekret-Produktion, durch diese Gifte geschützt sind. Zumindest über die mit Glucose veresterten 3-Nitropropion-Säuren ist bekannt, dass sie als freie Säure den Krebszyklus irreversibel blockieren, was es zu einem potentiellen Gift für sämtliche Eukaryoten macht (Alston, Mela u.a. 1977, Bacsi, Woodberry u.a. 2006). Die auch aus Eiern und Puppen bekannten Isoxazolinone finden sich nach neuesten Untersuchungen auch in nicht unerheblichen Mengen in der Hämolymphe der Larven. Das induziert eine weitere und ob ihrer allgemeinen Gültigkeit für alle Chrysomelina-Arten, grundlegende Verteidigungsstrategie der Larven, nämlich die des olfaktorischen Aposematismus. Hierbei kombiniert sich die Perzeption des volatilen Allomons mit der giftigen Wirkung der Komponenten der Hämolymphe, wobei Fraßfeinde

nach geeigneter Prägung bereits durch den Geruch der Larven vom Verzehr abgehalten werden (Gerhard Pauls, persönliche Mitteilung, (Eisner 1971)).
Im folgenden Kapitel soll der Fokus auf die Biosynthese chemischer Vorstufen für das Wehrsekret im Fettkörper der Larven geworfen werden.

1.4 Biosynthese der Wehrsubstanzen

1.4.1 *De novo* Biosynthese von Iridoiden

Wie bereits eingeleitet können die chemischen Vorstufen der Allomone des Sekrets je nach Spezies entweder sequestrierte Blattalkohole, deren glycosidisch gebunde Transportform, *de novo* produzierten Glucoside oder eine Mischung aus beidem darstellen (vgl. Abb. 7). Am Beispiel von *P. cochleariae* soll hier exemplarisch die Biosynthese des 8-hydroxy-Geraniol-8-*O*-*β*-D-Glucosids gezeigt werden, da dieses Glucosid auch in einer Reihe anderer Chrysomelina-Arten als Iridoid-Vorstufe fungiert (Daloze und Pasteels 1994). Die frühen Stufen des Iridoidkatabolismus finden hierbei im Fettkörper statt, der nicht nur Speicherorgan, sondern auch Ort vieler Stoffwechselvorgänge in Insekten ist (Resh 2009, S. 356).

Ausgehend von Acetyl-CoA aus dem Zitratsäure-Zyklus, wird ein weiteres Acetyl-CoA mittels 3-hydroxy-3-Methylglutaryl CoA (HMG-CoA)-Synthetase angehängt. Das HMG-CoA wird über eine HMG-Reduktase zu Mevalonsäure (Antje Burse, Frick u.a. 2008), welche in mehreren Schritten zu Isopentenyl-Diphosphat umgesetzt wird. Dieses IDP kann nun über eine Isopentenyl-diphosphate Δ-isomerase in Dimethylallyl-Diphosphat (DMADP) umgesetzt werden, welche das Substrat für die Isoprenyl-Diphosphat-Synthase (IDS) darstellt. Aus *P. cochleariae* wurde eine IDS isoliert, welche Metallionenabhängig als Farnesyl-Diphosphat-Synthase oder Geranyl-Diphosphat-Synthase agieren kann. Die C15-Vorstufe (Farnesyl-Diphosphat, FDP) würde für eine Reihe von Produkten des Primärmetabolismus‘ wie Cholesterol, Ubiquinone, und Dolichol sowie Juvenilhormonen benötigt werden (Grünler, Ericsson u.a. 1994). Geranyl-Diphosphat (GDP) hingegen sollte ein Intermediat in der Iridoidproduktion darstellen. In Manuskript 1 konnte mittels RNAi Experimenten gezeigt werden, dass das Enzym vorrangig für die Produktion des Iridoidintermediates zuständig ist. (Manuskript 1). GDP wird anschließend zu Geraniol dephosphoryliert, welches nachfolgend vermutlich über eine Cytochrome P-450 Oxigenase zu 8-Hydroxy-Geraniol umgesetzt wird. Abschließend wird Glucose β-glycosidisch über UDP-Glucose angebunden und die Vorstufe ist fertig für den interzellulären Transport in das Sekret, wo weitere Umwandlungen stattfinden, die in Kapitel 1.4.3 beschrieben werden. (Abbildung in Manuskript 1, Fig. 1).

Die Tatsache, dass die Aufnahme und die Synthese von sämtlichen Komponenten der Wehrbiochemie räumlich voneinander getrennt sind, legt die Existenz eines präzisen Transportnetzwerkes nahe, welches im Folgenden beschrieben wird.

1.4.2 Transportvorgänge von chemischen Vorstufen in Chrysomelina Larven

Von besonderer Bedeutung für die Biosynthese des Wehrsekretes ist der Transport der glycosidisch gebundenen Vorstufe aus der Iridoid-Synthese, sowie der der sequestrierten pflanzlichen Metabolite durch den Körper der Larve.

Funktionale Untersuchungen ergaben, dass der Transport der chemischen Vorstufen durch Ebenen verschiedener Selektivität verläuft (Kuhn, Pettersson u.a. 2007, Maritta Kunert, Soe u.a. 2008). Der unspezifische Transport von Nährstoffen über das Mitteldarm-Epithel in die Hämolymphe führt auch zur unspezifischen Aufnahme von Sekundärmetaboliten aus der Nahrung, welche unter anderen die Vorstufen für die Wehrbiosynthese enthalten können (Abb. 8*B*). Da in der Hämolymphe wenige dieser Pflanzenstoffe nachzuweisen sind (Feld, Pasteels u.a. 2001), wird hier der Transport vermutlich über den Stoffgradienten verwirklicht. Die Vorstufen müssen für den Transport im Tier glycosidisch gebunden sein. Werden über den Gradienten Agluca aufgenommen, also Pflanzenalkohole, die nicht oder nicht mehr glycosidisch gebunden sind, können diese vermutlich im Fettkörper glycosiliert werden (Abb. 8*D*). Diese Glycosilierung hat einerseits die Funktion der Herstellung einer polaren Transportform, zum anderen ist es aber auch eine Methode toxische Stoffe zu inaktivieren.

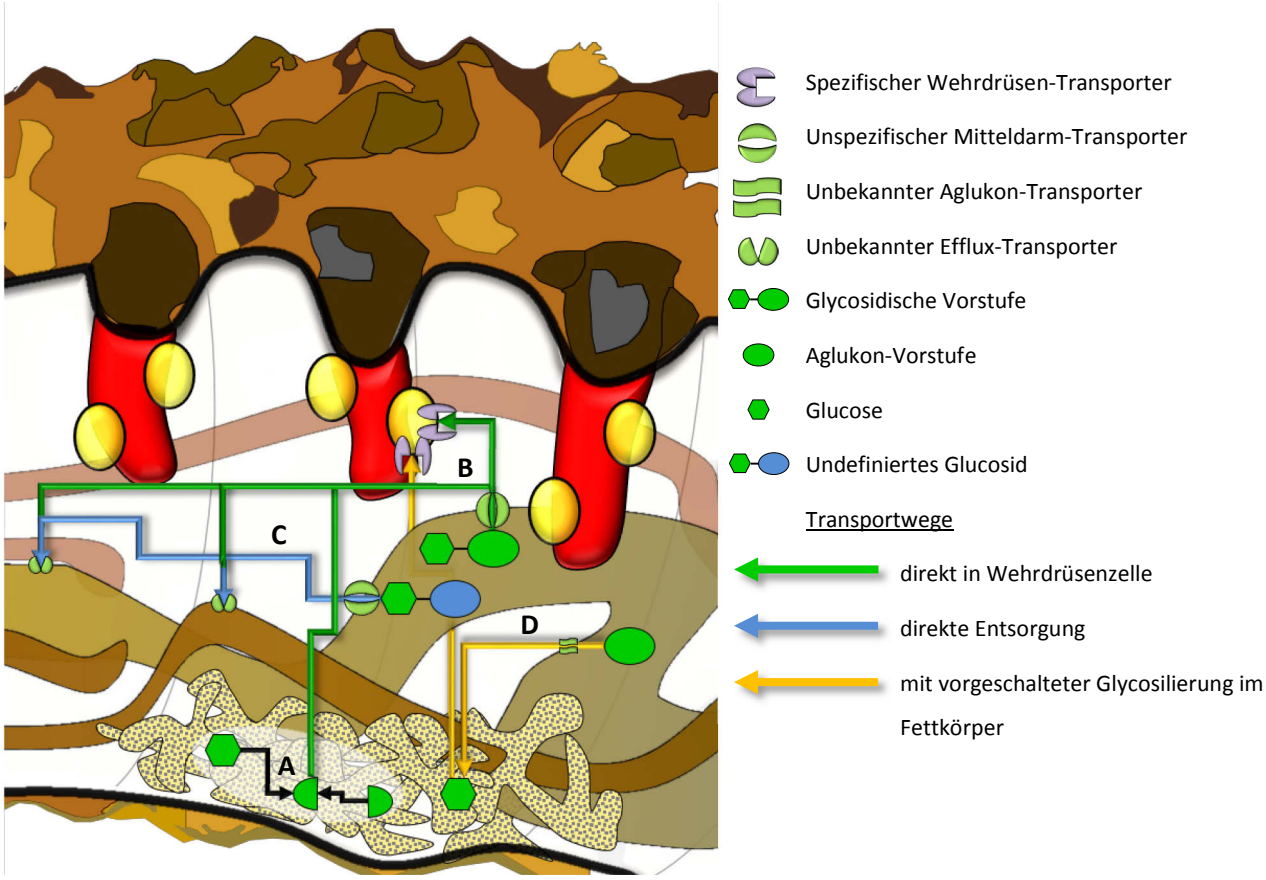

Abbildung 8: Transportmechanismen in der larvalen Leibeshöhle von *P. cochleariae*. *A*: *de novo*-Produktion der chemischen Vorstufen im Fettkörper und anschließender Transport in die Wehrdrüsenzelle (grüner Pfeil); *B*: (grüner Pfeil): Glucosid-Sequestrierungs-Pfad, Überschüsse werden über die Malpighischen Gefäße oder den Enddarm entsorgt; *C*: (blauer Pfeil): unspezifischer Transport von unnutzbaren oder giftigen Nährstoff-Komponenten, die Entsorgung erfolgt wie in *B*; *D*: (gelber Pfeil) Sequestrierung von Agluconen, die im Fettkörper in ihre Transportform glycosiliert werden. (verändert nach Discher, Burse u.a. 2009)

Der spezifische Transport findet aus der Hämolymphe in die Wehrdrüsenzelle statt. Hierbei muss ein aktiver Transport gegen den Stoffgradienten stattfinden, um die Glucoside in der Drüsenzelle im Gegensatz zur Hämolymphe anzureichern. Es konnte gezeigt werden, dass nur jene Vorstufen transportiert werden, die in der jeweiligen Spezies für die Wehrchemie genutzt werden (Kuhn, Pettersson u.a. 2004, Kuhn, Pettersson u.a. 2007). Innerhalb der sekretorischen Zelle vermittelt ein adenine-triphosphate-binding-casette-Transporter (ABC-Transporter) unselektiv den Transfer der chemischen Vorstufen in Vesikel, die dann mittels Exozytose in das extrazelluläre Reservoir gelangen (Strauss, Peters u.a. 2013). Überschüsse von brauchbaren bzw. unbrauchbaren Glucosiden werden aus der Hämolymphe über die Malpighischen Gefäße und den Enddarm ausgeschieden (Abb. 8*C*) (A. Burse, Frick u.a. 2009).

In den Wehrdrüsen von *P. cochleariae* wurden Zucker-Transporter identifiziert, die für die Versorgung der Zelle mit Energie verantwortlich sein können. RNAi in der Anwendung auf Zucker-Transporter zeigte in Manuskript 2 eine Bedeutung für die Drüsenzellen und folglich auch die Synthese des Wehrsekrets, welche im folgenden Kapitel vergleichend für *C. populi* und *P. cochleariae* erläutert wird.

1.4.3 Enzymatische Biosynthese der Wehrsubstanzen im Sekret

Dem Transport der chemischen Vorstufen der Abwehrstoffe folgt eine mehrschrittige enzymatische Umsetzung, die im Wehrsekret selbst stattfindet. Dass die Vorstufen nicht extrazellulär und nicht etwa im Inneren der Zelle umgesetzt werden, beweist die Beobachtung, dass alle Vorstufen in einem *in vitro* Assay zum jeweiligen Endprodukt umgewandelt werden können,

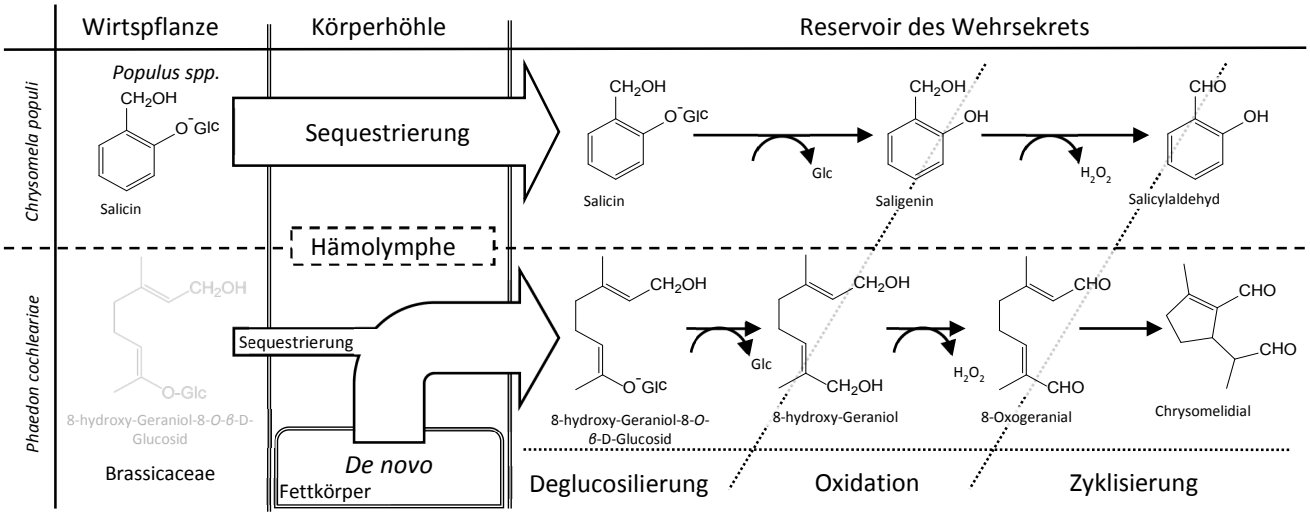

Abbildung 9: Schema der finalen Biosynthese im Sekret von *C. populi* und *P. cochleariae*. *C. populi* sequestriert Salicin durch die Hämolymphe in das Sekret-Reservoir. *P. cochleariae* ist zwar prinzipiell in der Lage 8-hydroxy-Geraniol-8-O-β-D-Glucosid zu sequestrieren, da dieser Stoff in den Brassicaceae aber nicht vorkommt, stammt die benutzte Vorstufe aus der *de novo* Synthese im Fettkörper. Auch dieses Glucosid gelangt via der Hämolymphe ins Reservoir. Hiernach werden in beiden Arten die Glucose-Reste hydrolysiert und die freigewordenen Alkohole oxidiert. In *P. cochleariae* wird das 8-Oxogeranial zyklisiert um Chrysomelidial zu produzieren. In *C. populi* stellt Salicylaldehyd das finale Allomon dar. (nach (Michalski, Mohagheghi u.a. 2008))

sofern dieser mit Sekret versetzt wurde (Brueckmann, Termonia u.a. 2002). Die Enzyme werden also mit den chemischen Vorstufen zusammen in das Sekret sezerniert, wo dann eine schrittweise Aktivierung der Komponenten stattfindet. Diese extrazelluläre Reaktion schützt einerseits den Körper vor den toxischen Endprodukten und erlaubt andererseits eine optimierte Produktion zu bioaktiven Substanzen („Bioreaktor“). Die Wehrsekrete der Chrysomelina, sowie die anderer Arthropoden, die ihr Sekret in abgeschlossenen Reservoiren lagern (Eisner und Meinwald 1966), stellen oftmals biphasische Systeme dar, wobei die organische Phase vom produzierten Endprodukt gebildet wird und die wässrige Phase Proteine enthält (Aldrich, Blum u.a. 1978), die vermutlich an der Phasengrenze ihre Funktion ausüben (Brueckmann, Termonia u.a. 2002).

Die chemischen Vorstufen für die späteren Allomone stammen, wie schon eingeführt wurde (Kap. 1.2.1, 1.4.1), entweder aus dem Sekundärmetabolismus der Wirtspflanze oder aus der Fettkörper-Biosynthese (A. Burse, Schmidt u.a. 2007). Trotz der verschiedenen Ursprünge der Wehrsubstanzen finden sich einige enzymatische Schritte die in allen Arten der Chrysomelina identisch sind. (Pasteels, Duffey u.a. 1990) (vgl. Abb. 9). So werden die jeweiligen glycosidisch gebundenen Vorstufe im Sekret mittels einer β-Glucosidase hydrolysiert (Pasteels, Rowell-Rahier u.a. 1984, Häger 2013). Eine Oxidation des Alkohols führt zu einem Aldehyd (Oldham, Veith u.a. 1996), welcher bei *C. populi* den finalen Wirkstoff Salicylaldehyd darstellt. In *P. cochleariae* wird dem 8-Oxogeranial noch eine Zyklisierungsreaktion nachgeschaltet, die zum Endprodukt Chysomelidial führt (Lorenz, Boland u.a. 1993, M. Kunert, Rahfeld u.a. 2013). Anders verhält es sich bei den Vertretern der „misch-Modus“-Strategie, hier werden den deglucosilierten Blattalkoholen über eine Acyltransferase-Reaktion verschiedene Butylreste angehängt, was zu einem großen Spektrum an Butyrat-Estern im Wehrsekret führt (Tolzin-Banasch, Dagvadorj u.a. 2011).

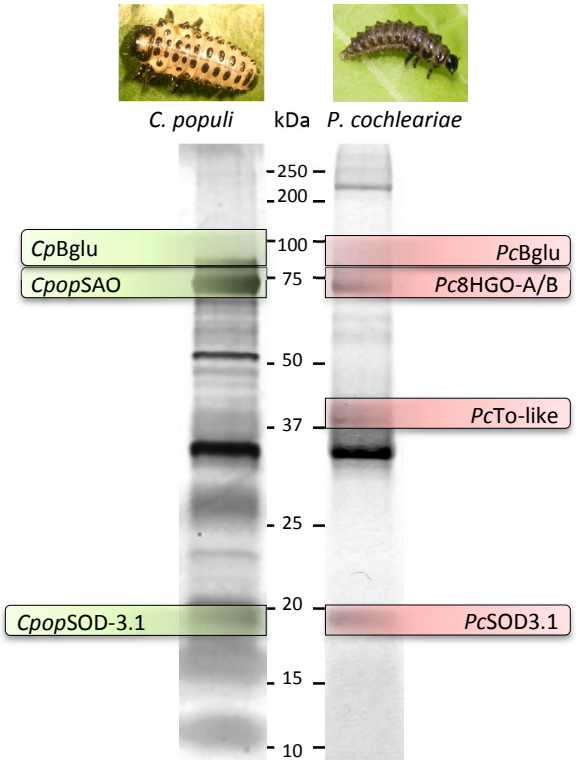

Abbildung 10: Proteinogene Bestandteile des Sekrets von *C. populi* und *P. cochleariae*. 0,5 mg und 0,3 mg des Wehrsekrets von *C. populi* und *P. cochleariae* wurde denaturiert und mittels SDS-PAGE aufgetrennt, Coomassie gefärbt. Die bekannten Enzyme sind mit ihrer Entsprechung in den farbigen Kästen gezeigt. *Cp*Bglu und *Pc*Bglu (Häger 2013), *Pc*8HGO-A/B (Rahfeld, Kirsch u.a. 2014).

Von den hierbei beteiligten Enzymen sind vor dem Beginn dieser Arbeit bereits einige Alkohol-Oxidasen verschiedener Spezies charakterisiert und kloniert worden. Das biochemische Potential

des Enzyms wurde von Brückmann et al. (2002) mittels Voll-Enzym Präzipitaten des Wehrsekrets von *P. vitellinae* und *C. populi* erforscht, wobei Substratspektrum, K_m-Wert und die Produktion von H_2O_2 belegt wurden. In einer Folgearbeit von Michalski et al. (2008) wurden dann die ersten Sequenzen für Salicyl-Alkohol-Oxidasen (SAO) (Abb. 10) veröffentlicht und deren rekombinante Proteine aus *E. coli* mit den Werten von Brückmann verglichen. Durch die erfolgreiche Sequenzierung konnten die SAOs auch den GMC-oxidoreduktasen zugeordnet werden, einer funktional diversen und sehr abundanten Enzymfamilie (Cavener 1992, Rahfeld, Kirsch u.a. 2014).

Interessanterweise gelang anhand desselben Enzyms der Nachweis der Plastizität der Wehrenzymatik. Kirsch et al. (2011a) konnten nachweisen, dass die auf *Betula spp.* fressenden *C. lapponica*, die in mit ihrer Nahrung kein Salicin mehr aufnehmen, keine funktionierende SAO ins Wehrsekret exkretiert, während die *Salix spp.* konsumierenden *C. lapponica* diese noch besitzen.

Bis dato konnte eine *in vivo* Funktionalität der SAO aufgrund der *in vitro* Assays vermutet werden, in Manuskript 3 gelang allerdings der Nachweis, dass dieses Enzym tatsächlich im Sekret für die Oxidation von Saligenin zu Salicyladehyd verantwortlich ist.

Scheinbar unabhängig von der „Makro"-Wirkung der Wehrchemie gegen Fraßfeinde, konnte dem Sekret auch eine Wirkung gegen Mikroorganismen nachgewiesen werden, deren Prinzip nachfolgend erklärt wird.

1.5 Immunologische Abwehr von Pathogenen

Im Wehrsekret von *P. cochleariae*, *C. populi* und beiden bereits beschriebenen Ökotypen von *C. lapponica* wurde mittels LC-MS/MS eine Reihe weiterer, nicht zur Synthese der Allomone gehörender Proteine identifiziert. Darunter war auch eine extrazelluläre Superoxid-Dismutase (SOD, EC 1.15.1.1) (s. Abb. 10), ein Enzym, dessen Funktion es ist, Superoxid- radikale in Sauerstoff und H_2O_2 umzusetzen. SODs spielen in der Wehrbiochemie keine Rolle, da die Oxidasen der Alkohol-Intermediate stets direkt H_2O_2 über einen zwei-Elektronen-Transfer produzieren. Interessanter Weise wurde in *P. cochleariae* das gleiche Protein auch in der Hämolymphe identifiziert, woraufhin ein Zusammenhang mit der Immunreaktion vermutet wurde. Beispiele für einen solchen Zusammenhang gibt es z. B. in decapoden Krebsen, deren extrazelluläre SOD in immunologischen Kontexten eine Rolle spielt (z.B. Johansson, Holmblad u.a. 1999). Da im Manuskript 4 mittels RNAi eine Funktion dieses Enzyms im Kontext der Immunantwort gezeigt wurde, wird im Folgenden die Abwehr gegen mikrobielle Pathogene bei Chrysomelina und Insekten allgemein beschrieben.

Neben der Wirkung der Allomone auf Prädatoren, hat das Wehrsekret auch die Funktion, die larvale Cuticula zu desinfizieren und so die Larve vor der Infektion mit Mikroorganismen zu schützen (Gross, Schumacher u.a. 2008). Hemmhofexperimente und Blastogamie-tests haben für die Wehrsekrete und andere Körperflüssigkeiten verschiedener Chrysomelinae (Gross, Müller u.a.

1998, Gross, Podsiadlowski u.a. 2002, Dossey 2010) und auch für deren Komponenten (Tolzin-Banasch 2009) eine antimikrobielle Wirkung gegen Bakterien und Pilze nachgewiesen. Vergleichbare Wirkungen zeigen bspw. auch die Gifte einiger Hymenopteren (z.B. Moreau 2013) und Spinnen (z.B. Kuhn-Nentwig, Schaller u.a. 2004).

Arthropoden halten eine Vielzahl von Barrieren bereit, die vor einer Infektion des Körpers vom Pathogen überwunden werden müssen. Bakterien und Viren gelangen für gewöhnlich durch Ingestion in den Körper, wo sie sich mit dem pH des Darmes und diversen radikalproduzierenden Enzymen der Darmwand konfrontiert sehen (Siva-Jothy, Moret u.a. 2005, Ha, Oh u.a. 2005). Pilze hingegen lassen ihre Hyphen direkt durch die Cuticula wachsen, wobei sie eine Reihe an Schichten aus hydrophoben Verbindungen, Phenolen und Gerbstoffen überwinden müssen, bevor sie die nährstoffreiche Hämolymphe erreichen (Hajek und Stleger 1994). Zu den häufigsten Verursachern von Krankheiten in Insekten gehören entomopathogene Pilze, die auf die Infektion von Insekten spezialisiert sind und sich auf beinahe allen Pflanzen und im Bodensubstrat finden lassen (ebd.).

Insekten verfügen ferner über ein effektives unspezifisches Immunsystem, dessen Reaktion von bestimmten Signalkaskaden gesteuert wird, die durch die Erkennung von Oberflächenmolekülen des eindringenden Pathogenen aktiviert werden (Siva-Jothy, Moret u.a. 2005). Sämtliche Invertebraten haben kein adaptives Immunsystem, welches mittels Antikörpern eine spezifische Immunantwort gegen ein bestimmtes Pathogen erzielt. Allerdings kann das unspezifische Immunsystem der Invertebraten als Modell für sehr ähnliche Reaktionen in Vertebraten herhalten, da die Abläufe im Prinzip identisch sind (z.B. Wiesner und Vilcinskas 2010).

Das bestehende Modell der Insekten-Immun-Antwort basiert hauptsächlich auf Untersuchungen an *D. melanogaster* (Hoffmann 2003), dessen Komponenten auch in den meisten anderen Untersuchungen wiedergefunden wurden (z.B. Gunaratna und Jiang 2013). Hierbei müssen die konservierten Mechanismen der Pathogen-*Erkennung* von den durch epigenetische Einflüsse überaus flexiblen Immun-*Antworten* unterschieden werden (z. B. Vilcinskas 2013). Mittels in der Hämolymphe zyklisierenden Peptidoglycan recognition proteins (PGRP) und Gram negative binding proteins (GNBP), die an Peptidoglycan bzw. β-Glucan binden, die an der Oberfläche von Bakterien und Pilzen zu finden sind, werden Proteasen aktiviert, welche Kettenreaktionen initiieren, die entweder eine Melanisierungsreaktion durch frei werdende Phenol-Oxidasen einleiten, oder eine Veränderung der zellulären Expression zur Folge haben (Carton, Poirie u.a. 2008). Melanisierung stellt einen Mechanismus dar, bei dem auf der Oberfläche des pathogenen Erregers eine Melanin-Schicht gebildet wird und dieser gleichzeitig durch die radikalischen Intermediate des Phenols oder der bei der Melanisierung produzierten Sauerstoff-Radikale abgetötet wird (Nappi und Christensen 2005).

Die Veränderung der zellulären Expression kann unter anderem zur Folge haben, dass die Erreger mittels Phagozytose aufgenommen werden um sie in zytosolischen Vesikeln zu verdauen, dass eine Apoptose eingeleitet wird, oder, dass antimikrobielle Proteine (AMPs) für das Zytosol oder die Hämolymphe produziert werden (Altincicek, Knorr u.a. 2008). Einige der hier genannten Reaktionen auf eine Infektion werden von Fettkörperzellen oder speziellen Immunzellen (Hämocyten) realisiert, welche in der Hämolymphe zyklisieren (Giulianini, Bertolo u.a. 2003).

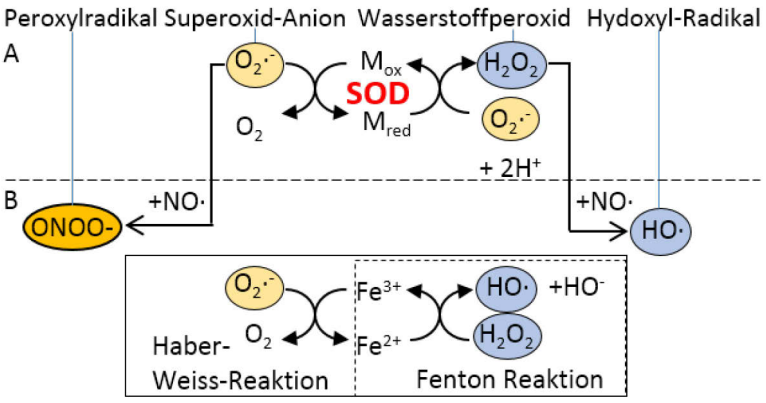

Abbildung 11: Chemische Reaktionen des Superoxid-Radikals und seine Derivate. A: Reaktionen von Superoxid-Dismutasen, B: Reaktionen, die entweder durch Folgereaktionen mit Stickstoffmonooxid oder mit Metallionen eingegangen werden können (nach Nappi und Christensen 2005).

Wie bereits erwähnt, sind in dieser Arbeit (Manuskript 4) die Prozesse der Immunantwort von Interesse, die aufgrund der Produktion von reaktiven Sauerstoffspezies funktionieren und so entweder an den Signalwegen der Zelle, oder an der Anreicherung antimikrobieller Radikale beteiligt sind. In der Insekten-Immunantwort, stellt die Produktion des Superoxid-Radikals durch NADPH-Oxidasen (Nox) einen initialen Schritt für die Aktivierung des Immunsystems dar (Nappi, Vass u.a. 1995). Tatsächlich werden diese *Nox*-Gene, die sowohl in der Membran von Zellorganellen zu finden sind, als auch in der Zellmembran, erst nach der Erkennung einer Infektion mit Pathogenen aktiviert. *Nox*-Gene sind wie viele der Gene der angeborenen Immunantwort stark konserviert. In Insekten finden sich allerdings nur *Nox5*-Gene, welche nicht durch Protein-Protein-Interaktionen, wie die anderen Nox-Varianten, sondern durch Ca^{2+} -Ionen aktiviert werden (Kawahara, Quinn u.a. 2007). Das freie Superoxid kann in der Hämolymphe dann zu einer Reihe weiterer, meist weitaus reaktiverer Radikale reagieren (Abb. 11*B*). Dies kann zur Initiation von Signalkaskaden führen (Rhee 2006), immunologische Reaktionen unterstützen (z.B. Komarov, Slepneva u.a. 2006, Arbi, Pouliliou u.a. 2011), oder immensen Schaden verursachen (Boelsterli 2009). Die herkömmliche Sicht auf die SODs beschreibt sie in diesem Zusammenhang als Schutzenzyme, die für die Beseitigung des überschüssigen Superoxids verantwortlich sind (McCord und Fridovich 1969), (Abb. 11*A*). Die einzige gut charakterisierte extrazelluläre Insekten-SOD wird auch in diesem Kontext beschrieben, wobei allerdings ein *in vivo* Nachweis fehlt (Colinet, Cazes u.a. 2011). Allerdings ist auch ein Umdenken in Gange, welches den Sauerstoff-Radikalen zunehmend positive Mitwirkungen zuschreibt (A. F. Miller 2004). Welche Funktion SODs in *P. cochleariae* haben wurde in Manuskript 4 näher untersucht.

1.6 Zielsetzung der Arbeit

Die Blattkäfer innerhalb der Chrysomelina stellen, wie gezeigt wurde, ein enorm vielseitiges Forschungsfeld dar. Von besonderem Interesse sind dabei stets die Teilbereiche gewesen, die sich auf andere Spezies, auch außerhalb dieses Unterstammes, in phylogenetischen und biochemischen Bezügen übertragen lassen (A. Burse, Frick u.a. 2009, M. Kunert, Rahfeld u.a. 2013, Snyder und Qi 2013). So stellen die Mechanismen der Sequestrierung und die Bereithaltung von Wehrsekreten durchaus häufige Phänomene innerhalb der Insekten dar (Pasteels, Gregoire u.a. 1983).

In der Vergangenheit gelang es, trotz des Fehlens von Sequenzinformationen eines Vertreters der Chrysomelina oder einer phylogenetisch näher verwandten Gruppe als *T. castaneum*, unter Ausschöpfung von (bio-)chemischen Methoden, die grundlegenden Eigenschaften des Transportsystems (Kuhn, Pettersson u.a. 2004, Discher, Burse u.a. 2009) und der Sekret-Biochemie (z.B. Daloze und Pasteels 1994, Veith, Lorenz u.a. 1994) zu ergründen. Basierend auf chemischer Analytik wurden chemotaxonomische Untersuchungen vorgenommen, die die Mechanismen der larvalen Biochemie mit der Sekundärchemie der Wirtspflanze ins Verhältnis setzten (Zusammenfassung in: Dettner 1987). Untersuchungen, die später mit molekularen Methoden bestätigt und vertieft wurden (Termonia, Hsiao u.a. 2001).

2008 wurden in der Arbeitsgruppe von Dietrich Ober die ersten Sequenzen von Sekret-Proteinen (SAO) veröffentlicht (Michalski, Mohagheghi u.a. 2008), wohingegen molekulare Grundlagen eines Wehrsekret-Transportersystems in einem Insekt sind erst seit diesem Jahr von *T. castaneum* (Li, Lehmann u.a. 2013) und durch die Charakterisierung des ABC-Transporters an den Vesikeln von *C. populi* (Strauss, Peters u.a. 2013) publiziert worden.

Mit der Assemblierung des Transkriptoms von *P. cochlearia*e und dann auch von *C. populi* (weitere in Vorbereitung, M. Stock, D. Wang), sind nun Daten zugänglich, die durch *in silico*-Vergleiche mit bekannten Transkripten anderer Spezies via BLAST (Altschul, Madden u.a. 1997) und durch Sequenz-basierende Domänen Vergleiche mit charakterisierten Proteinen anderer Organismen via pfam (Punta, Coggill u.a. 2012), Kandidaten zurückliefern, die für bestimmte biochemische Prozesse verantwortlich sein könnten. In der Regel finden sich aber mehrere Varianten eines Proteins, welches die gleiche vorhergesagte Funktion haben und welche sich durch den Sequenz-Vergleich nicht ausreichend diskriminieren lassen, um für eine distinkte Funktion im Organismus verantwortlich gemacht zu werden.

In diesem Zusammenhang stellt sich die Frage nach der *in vivo* Relevanz eines Kandidaten, welcher durch einen *in vitro* Assay oftmals nicht ausreichend nachgebildet werden kann (Forward Genetics).

Eine Möglichkeit zur Antwort auf die Frage nach der biologischen Rolle eines Proteins ist der Ansatz der „Reverse Genetics“, wobei auf die Funktion eines Genprodukts, über das Fehlen

desselben geschlossen wird („loss-of-function“ Phänotyp) (Ruddle 1984). Die wahrscheinlich am besten funktionierende Methode für einen „Reverse Genetics“ in Nicht-Modellorganismen stellt derzeit die RNA interference dar (Fire, Xu u.a. 1998). Diese Technik ergänzt in unserem Forschungsfeld die bereits etablierten Methoden (vgl. A. Burse, Frick u.a. 2009) mit der Möglichkeit die generierten Daten adäquat auf funktionale Transkripte hin zu untersuchen, indem schnell und präzise eine Analyse von Kandidaten-Genen durch Generierung dieser loss-of-function Phänotypen erfolgen kann. Da RNAi hierbei lediglich die Enzyme aus dem Metabolismus heraus nimmt, muss eine Bewertung des biochemischen Potentials des Kandidaten nach erfolgreicher Identifizierung der funktionalen Variante seines Transkriptes, weiterhin in *in vitro* Assays geklärt werden.

Das Ziel dieser Arbeit ist es daher, durch die Anwendung von RNAi auf allen Ebenen der vorbereitenden und realisierten Wehrbiochemie, ihr Potential zur Aufklärung der molekularen Basis derselben zu nutzen und Beiträge zur Identifizierung von Schlüsselproteinen in diesen metabolischen Netzwerken zu liefern.

Die für diese Arbeit maßgeblichen Manuskripte, werden hier thematisch gereiht, wobei eine Anwendung der Methode auf ein Enzym im Fettkörper, über die Zucker-Transportmechanismen der der Wehrdrüsenzelle, hin zur Enzymatik des Wehrsekretes und zum systemischen Herabregulation von Proteinen im Kontext des oxidativen Stresses und der Immunantwort in Insekten nachvollzogen werden kann.

1) **Identifizierung der *in vivo* Funktionalität der Isoprenyl-diphosphat synthase im larvalen Fettkörper.** (Manuskript 1)

Für *Pc*IDS1, wurde in *in vitro* Assays bereits eine enzymatische Aktivität in der Umsetzung von DMADP zu GDP gezeigt, wobei durch Veränderung des metallsichen Cofactors von Co^{2+} zu Mg^{2+} anstelle von GDP FDP synthetisiert wurde. Mittels RNAi sollte geklärt werden, ob *Pc*IDS1 tatsächlich für die Produktion von GDP, der Vorstufe für 8-hydroxy-Geraniol-8-*O*-*β*-D-Glucosids in der Wehrbiochemie verantwortlich ist und ob das Enzym die Bifunktionalität auch *in vivo* zeigt.

2) **Identifizierung von Zucker-Transportern an der Wehrdüsenzelle**. (Manuskript 2)

Um putative Zucker-Transporter, die eine Rolle in metabolischen Netzwerken der Larven spielen könnten zu identifizieren, wurde ein Data-Mining im Transkriptom von *P. cochleariae* durchgeführt. Putative Zucker-Transporter wurden identifiziert, die sich aufgrund von Homologien nicht präziser im Stoffwechsel der Larve verorten ließen. Via qPCR Analysen wurden 17 Transporter identifiziert, die aufgrund der hohen Expression im Wehrdrüsengewebe für die Versorgung der Drüsenzelle mit Energieträgern in Frage kamen. Mittels RNAi sollten diese Kandidaten auf ihre Funktion im Körper hin untersucht werden, um zu ermitteln ob ein spezifischer Transporter die Wehrdrüsenzelle mit Kohlenhydraten versorgt. In diesem Zusammenhang sollte auch ein Blick auf das Co-regulatorische

Netzwerk innerhalb dieser Transporter geworfen werden, indem durch RNA-seq-Daten Hinweise auf ein solches gesammelt wurden.

3) Anwendung von RNAi auf finale enzymatische Schritte der Wehrbiochemie. (Manuskript 3)

Anhand der *Cpop*SAO aus *C. populi*, einem Enzym, das bereits zuvor *in vitro* charakterisiert wurde (Kirsch, Vogel u.a. 2011a), sollte der Beweis erbracht werden, dass das Enzym auch *in vivo* die gezeigte Funktion erfüllt. Für ein Protein des Sekrets von *P. cochleariae*, welches mittels Proteomanalyse gefunden wurde, *Pc*To-like1, zeigte sich nach RNAi-vermittelter Herabregulierung einen Einfluss in der Zyklisierung von 8-Oxogeranial zu Chrysomelidial, ohne dass die *in silico* Analyse des Proteins zuvor eine solche Funktion vorhergesagt hätte (Arbeit von P. Rahfeld). Dieser Artikel ist chronologisch die älteste, weshalb hier auch die *in silico* off-target-Vorhersage etabliert worden ist.

4) **Systemische Analyse von Cu/Zn-SODs in *P. cochleariae*** (Manuskript 4)

Mittels RNAi sollte die genaue Art und Weise der Beteiligung von Cu/Zn-bindenden Superoxid-dismutasen (SOD) an der Immunantwort und anderen Mechanismen des oxidativen Stresses in den Larven von *P. cochleariae* untersucht werden. Da diese Enzyme in mehreren Geweben exprimiert werden, sollte anhand der Cu/Zn-SODs auch untersucht werden, wie systemisch RNAi in Blattkäfern wirkt. Die Eigenschaften der SOD und das Vorkommen der extrazellulären Variante im Sekret und in der Hämolymphe machten es ferner Möglich neue immunologische und xenobiotische Bioassays zu testen und die Resultate funktional zu validieren.

Das übergreifende Ziel dieser Arbeit ist die *in vivo* Identifizierung von Protein-Funktionen, die wie beschrieben wurde, auf allen Ebenen der Wehrbiochemie Anwendung findet. Anhand der durch vielfältige analytische Methoden charakterisierten „loss-of-function“ Phänotypen, kann eindeutig auf eine Funktion des Zieltranskriptes in den Larven zurückgeschlossen werden. Die hier erhobenen Daten sollen zum Verständnis der Wehrbiochemie in Blattkäferlarven beitragen und Modelle generieren, die auf andere Insekten mit vergleichbaren Mechanismen angewendet werden können.

2. Übersicht über die Manuskripte

Manuskript 1

Autoren:

Sindy Frick, Raimund Nagel, Axel Schmidt, René Roberto Bodemann (m. Gretscher), Peter Rahfeld, Gerhard Pauls, Wolfgang Brandt, Jonathan Gershenzon, Wilhelm Boland, Antje Burse

Titel:

Metal ions control product specificity of isoprenyl diphosphste synthases in the insect terpenoid pathway.

Status der Publikation:

Publiziert. PNAS; 25.02.2013 (vorab online); doi: 10.1073/pnas.1221489110

Zusammenfassung der Arbeit:

Im Manuskript 1 konnte gezeigt werden, dass sich das Produktspektrum der Isoprenyl-diphosphat-Synthase (*Pc*IDS1), eines Enzyms aus dem Fettkörper von *P. cochleariae*, in Abhängigkeit von verfügbaren Metall-Cofaktoren *in vitro* ändern lässt. Das stellt einen bislang unbekannten Mechanismus zur Wirkregulation von Enzymen dar und hat weitreichende Konsequenzen auf das geltende Verständnis von produktregulativen Möglichkeiten eines Gens. Durch die Anwendung von RNAi auf *PcIDS1* konnte nachgewiesen werden, dass das Enzym *in vivo* für die Produktion der Chrysomelidial-Vorstufe 8-hydroxygeraniol-8-o-*β*-d-glucosid verantwortlich ist, was sich durch eine zunehmende Reduktion des Gesamtgehaltes an Chysomelidial pro Larve über die Zeit zeigte, welche bei Kontrollbehandlungen nicht auftragt. Schließlich produzierten die Larven gar kein Wehrsekret mehr, was auch mit einer Abnahme des Glucosids in der Hämolymphe und im Fettkörper der Larve einhergeht.

Anteil der beteiligten Autoren:

S.F., A.S., J.G., W. Boland und A.B. entwarfen die Studie; S.F., R.N., R.R.B., P.R. und G.P. führten die Forschung durch; J.G., W. Boland und A.B. steuerten neue Reagenzien und Analysemethoden bei; S.F., R.N., A.S., R.R.B., P.R., G.P., W. Brandt. und A.B. analysierten die Messwerte. S.F., A.S., J.G., W. Boland und A.B. schrieben das Manuskript.

Manuskript 2

Autoren: Stock, M., Gretscher, R.R., Groth, M., Eiserloh, S., Boland, W., Burse, A.

Titel:

Putative sugar transporters of the mustard leaf beetle *Phaedon cochleariae*: their phylogeny and role for nutrient supply in larval defensive glands.

Status der Publikation:

Publiziert. PLOSone; 31.12.2013; doi: 10.1371/journal.pone.0084461

(*Anm. d. Autors:* In der Gutachter Version war der Artikel noch nicht veröffentlicht. Beide Artikel entsprechen sich inhaltlich exakt.)

Zusammenfassung der Arbeit:

Die Wehrdrüsenzelle von *P. cochleariae* ist eine polyploide Fabrik, deren Aufgabe in der Proteinbiosynthese und dem anschließenden Transport der produzierten Proteine, sowie glycosidisch gebundener Vorstufen in das Reservoir besteht. Dort findet dann die finale Biosynthese zum Wehrsekret statt. Für die Proteinsynthese und auch für den über ABC-Transporter vermittelten Weitertransport der Glucoside wird Energie in Form von ATP benötigt, welches in Mitochondrien durch Zellatmung gewonnen wird. Die hierfür benötigte Glukose wird in Insekten aus Trehalose gewonnen, die über Zucker-Transporter aus der Hämolymphe importiert wird.

In dieser Arbeit wird die Transkriptom-weite Analyse solcher Transporter unter phylogenetischen Gesichtspunkten beschrieben. Eine funktionale Validierung einzelner Transporter wurde mittels RNAi durchgeführt, wobei bei zwei Transportern eine Verminderung der Sekretmenge nachweisbar war. Weitergehende Analysen deckte ein metabolisches Netzwerk auf, welches das Herabregulieren einzelner Transporter durch das Heraufregulieren anderer zu kompensieren scheint.

Anteil der beteiligten Autoren:

A.B., M.S. und R.R.G. entwarfen und planten die Studie. M.S., R.R.G., A.B., M.G. und S.E. führten die Experimente durch. M.S., R.R.G., M.G. und A.B. analysierten die erhobenen Daten. M.G. and W.B. steuerten Reagenzien, Methoden und Analysen bei. M.S., A.B. und R.R.G. schrieben das Manuskrtipt.

Manuskript 3

Autoren:

René Roberto Bodemann (m. Gretscher), Peter Rahfeld, Magdalena Stock, Maritta Kunert, Natalie Wielsch, Marco Groth, Sindy Frick, Wilhelm Boland, Antje Burse

Titel:

Precise RNAi-mediated silencing of metabolically active proteins in the defence secretions of juvenile leaf beetles.

Status der Publikation:

Publiziert. Proceedings of the Royal Society B; 08.08.2012 (vorab online), Ausgabe 279, Seiten 4126-4134; doi: 10.1098/rspb.2012.1342

Zusammenfassung der Arbeit:

In dieser Arbeit fand erstmals RNAi Anwendung auf die Enzymatik des Wehrsekretes bei Larven zweier Blattkäferarten. Beim Silencen der Salicyl-Alkohol-Oxidase von *Chrysomela populi* (*Cpop*SAO) konnte *in vivo* dessen zuvor *in vitro* postulierte Funktion nachgewiesen werden. Die Entdeckung des Proteins *Pc*To-like1 in *Phaedon cochleariae* stellt den ersten Nachweis eines Proteins dieser Familie im Zusammenhang mit der immer noch ungeklärten Zyklisierung von Monoterpenen in Tieren dar (Beitrag von P. Rahfeld). Durch die Anwendung von RNAi in diesem Fall konnte die Zyklisierung zum Chysomelidial in *Phaedon cochleariae* inhibiert werden. Beide Enzyme konnten mithilfe der RNAi-Methodik als Teil der Abwehrbiochemie identifiziert werden und eine Reihe von neu etablierten Kontrollen sicherte die Ergebnisse ab.

Anteil der beteiligten Autoren:

R.R.B. und P.R. trugen im gleichen Maße zu dieser Publikation bei.

R.R.B., P.R., M.S., M.K., N.W., W.B. und A.B. entwarfen die Studie. R.R.B. etablierte RNAi für Blattkäfer und führte die RNAi- und Kontrollbehandlungen von *Cpop*SAO durch, validierte die Off-Target-Vorhersage, erhob die zugehörigen Daten, mit Ausnahme der Off-Target-Vorhersage und analysierte die gemessenen Daten. Er bereitete die Proben für die LC-MS^E-Analyse vor und trug zur Interpretation der dabei erhobenen Messwerte bei. Er unterstützte die Etablierung der Off-Target-Vorhersage. P.R. identifizierte *Pc*To-like1 und führte RNAi und Kontrollbehandlungen durch, erhob die dazugehörigen Daten und analysierte die Messwerte. S.F., M.S. und M.G. generierten die Transcriptom-Datenbanken. M.S. etablierte die Off-Target-Vorhersage und führte diese durch,

ferner trug sie zur Interpretation der LC-MS^E-Daten bei. M.K. entwarf die GC/MS Messungen, synthetisierte 8-Oxogeranial und Chrysomelidial und trug zur Interpretation der Messwerte bei.

N.W. führte die LC/MS^E-Analyse durch und erhob die zugehörigen Daten, zu deren Interpretation sie ferner beitrug. W.B. und A.B. trugen substanziell zur Interpretation aller Messwerte bei.

R.R.B., P.R. und A.B. schrieben das Manuskript und alle Autoren beteiligten sich intensiv an dessen Überarbeitungen.

Manuskript 4

Autoren:

René R. Gretscher, Magdalena Stock, Anja Strauß, Sindy Frick, Wilhelm Boland and Antje Burse.

Titel:

Extracellular Superoxide-dismutases take an active part in fitness, oxidative stress and pathogen resistance in juvenile *Phaedon cochleariae* (Coleoptera: Chrysomelidae: Chrysomelina).

Status der Publikation:

in Vorbereitung, zur Veröffentlichung bei PLOSone.

Zusammenfassung der Arbeit:

Extrazelluläre Cu/Zn-Superoxid-Dismutasen sind in Insekten so gut wie nicht erforscht. In *P. cochleariae* finden sich gleich drei dieser Isozyme, die in unterschiedlichen Geweben exprimiert werden nebst einer zellulären SOD. Diese vier SODs wurden mit RNAi ausgeschaltet. Mittels Fitnessanalysen, künstlicher Induktion von oxidativem Stress, sowie durch die Infektion mit Gram (+) und (-) Bakterien und dem Pilz *Metarhizium anisopliae*, wurde die Funktion der *Pc*SODs in der Antwort auf diese Faktoren identifiziert. Diese Arbeit beschreibt zum ersten Mal eine zentrale Rolle von extrazellulären SODs in der Immunantwort in Insekten, eine Rolle, die zuvor nur von zellulären SODs bekannt war.

Anteil der beteiligten Autoren:

R.R.G., A.S., W.B. und A.B. entwarfen die Studie und entwickelten die Experimente. R.R.G. und A.S. führten die Forschung durch, analysierten die erhobenen Daten und trugen zusammen mit A.B., M.S. und S.F. zu ihrer Interpretation bei. M.S., R.R.G., S.F. und A.S. identifizierten die *PcSOD* Sequenzen und M.S. führte die *in silico* off-target-Vorhersage für alle RNAi-Ziele durch. R.R.G. und A.B. schrieben das Manuskript.

3. Manuskipte

Manuskript 1: (Frick, Nagel u.a. 2013)

Metal ions control product specificity of isoprenyl diphosphate synthases in the insect terpenoid pathway

Sindy Frick[a], Raimund Nagel[b], Axel Schmidt[b], René R. Bodemann[a], Peter Rahfeld[a], Gerhard Pauls[a], Wolfgang Brandt[c], Jonathan Gershenzon[b], Wilhelm Boland[a], and Antje Burse[a,1]

Departments of [a]Bioorganic Chemistry and [b]Biochemistry, Max Planck Institute for Chemical Ecology, Beutenberg Campus, D-07745 Jena, Germany; and [c]Department of Bioorganic Chemistry, Leibniz Institute of Plant Biochemistry, D-06120 Halle/Saale, Germany

Edited by Jerrold Meinwald, Cornell University, Ithaca, NY, and approved January 29, 2013 (received for review December 12, 2012)

Isoprenyl diphosphate synthases (IDSs) produce the ubiquitous branched-chain diphosphates of different lengths that are precursors of all major classes of terpenes. Typically, individual short-chain IDSs (scIDSs) make the C_{10}, C_{15}, and C_{20} isoprenyl diphosphates separately. Here, we report that the product length synthesized by a single scIDS shifts depending on the divalent metal cofactor present. This previously undescribed mechanism of carbon chain-length determination was discovered for a scIDS from juvenile horseradish leaf beetles, *Phaedon cochleariae*. The recombinant enzyme *P. cochleariae* isoprenyl diphosphate synthase 1 (*Pc*IDS1) yields 96% C_{10}-geranyl diphosphate (GDP) and only 4% C_{15}-farnesyl diphosphate (FDP) in the presence of Co^{2+} or Mn^{2+} as a cofactor, whereas it yields only 18% C_{10} GDP but 82% C_{15} FDP in the presence of Mg^{2+}. In reaction with Co^{2+}, *Pc*IDS1 has a K_m of 11.6 μM for dimethylallyl diphosphate as a cosubstrate and 24.3 μM for GDP. However, with Mg^{2+}, *Pc*IDS1 has a K_m of 1.18 μM for GDP, suggesting that this substrate is favored by the enzyme under such conditions. RNAi targeting *Pc*IDS1 revealed the participation of this enzyme in the de novo synthesis of defensive monoterpenoids in the beetle larvae. As an FDP synthase, *Pc*IDS1 could be associated with the formation of sesquiterpenes, such as juvenile hormones. Detection of Co^{2+}, Mn^{2+}, or Mg^{2+} in the beetle larvae suggests flux control into C_{10} vs. C_{15} isoprenoids could be accomplished by these ions in vivo. The dependence of product chain length of scIDSs on metal cofactor identity introduces an additional regulation for these branch point enzymes of terpene metabolism.

cobalt | kinetic | prenyltransferase | secretions | silencing

Terpenes are an extensive group of natural products serving essential biological functions in Eukaryota, Bacteria, and Archaea. The more than 55,000 terpenes identified thus far are crucial components of intracellular signal-transduction pathways, electron transport chains, and membranes, or they can function as hormones, photosynthetic pigments, and semiochemicals (1, 2). Despite their structural diversity, terpenes are derived from the universal linear C_{10}, C_{15}, C_{20}, and larger diphosphate intermediates whose synthesis is catalyzed by isoprenyl diphosphate synthases (IDSs), also known as prenyltransferases (3). Depending on the stereochemistry of the double bond of the reaction product, these enzymes are classified as either *trans*-IDSs or *cis*-IDSs (4, 5).

Here, we focus on *trans*-IDSs, which can be further divided into enzymes producing short-chain (C_{10}–C_{20}), medium-chain (C_{25}–C_{35}), and long-chain (C_{40}–C_{50}) IDS products (6). Short-chain IDSs (scIDSs) are named for their main end products. Geranyl diphosphate synthases (GDPSs; EC 2.5.1.1) catalyze the alkylation of the homoallylic isopentenyl diphosphate (C_5-IDP) by the allylic dimethylallyl diphosphate (C_5-DMADP) resulting in geranyl diphosphate (GDP), the ubiquitous C_{10}-building block of many monoterpenes. Farnesyl diphosphate synthases (FDPSs; EC 2.5.1.10) form farnesyl diphosphate (FDP), the C_{15} precursor of sesquiterpenes, and geranylgeranyl diphosphate synthases (GGDPSs; EC 2.5.1.29) produce geranylgeranyl diphosphate (GGDP), the C_{20} backbone of diterpenes.

Whereas FDPSs and GGDPSs occur nearly ubiquitously in plants, animals, fungi, and bacteria, GDPSs have mainly been described in plants and insects to date (7). In plants, they participate in the biosynthesis of defenses against herbivores and pathogens, as well as in the formation of attractants for pollinators and seed-dispersing animals (1). Most plant GDPSs make GDP as a single product (8). However, occasionally, the enzymes are bifunctional and also produce FDP [*Pb*GDPS from the orchid *Phalaenopsis bellina* (9)] or GGDP [*Pa*IDS1 from the spruce *Picea abies* (10)] in addition to GDP. So far, only a few GDPSs have been characterized in insects (7). Strikingly, most of them have the ability to form multiple products.

The GDPSs cloned from the bark beetle *Ips pini*, for example, displayed prenyltransferase and terpene synthase activity in succession (11), resulting in the formation of precursors for the de novo synthesis of monoterpenoid aggregation pheromones such as ipsdienol, which coordinates the colonization of coniferous trees (12). Bifunctionality was also observed from the scIDSs characterized from different aphid species (13–17). Here, the recombinant proteins generated both GDP and FDP in parallel, and hence may be involved in the biosynthesis of either aphid sex pheromones or the sesquiterpene (*E*)-β-farnesene, the most common component of alarm pheromones. How nature accomplishes mixed-product formation by scIDSs in insects as well as in plants is still poorly understood.

Generally, catalysis by scIDSs follows a sequential mechanism called "head-to-tail alkylation." During chain elongation, the allylic cosubstrate (DMADP or GDP) undergoes coupling with IDP through electrophilic alkylation at its carbon-carbon double bond (18, 19). The reaction depends for activation on a trinuclear metal cluster, usually containing Mg^{2+} or Mn^{2+} (20). Based on earlier studies describing the role of metal cofactors for scIDS catalysis, we tested the product composition of a unique scIDS discovered from juvenile horseradish leaf beetles, *Phaedon cochleariae*, in the presence of different metal ions. To our surprise, we found that the enzyme *P. cochleariae* isoprenyl diphosphate synthase 1 (*Pc*IDS1) possesses an unusual product regulation mechanism not previously described for scIDSs. It alters the chain length of its products depending on the cofactor: The protein yields C_{10}-GDP in the presence of Co^{2+} or Mn^{2+}, whereas it produces the longer C_{15}-FDP in the presence of Mg^{2+}. GDP is needed for the de novo synthesis of the cyclopentanoid monoterpene iridoids, defensive compounds that are produced during the entire larval stage of *P. cochleariae* (21, 22) (Fig. 1). On the

Author contributions: S.F., A.S., J.G., W. Boland, and A.B. designed research; S.F., R.N., R.R.B., P.R., and G.P. performed research; J.G., W. Boland, and A.B. contributed new reagents/analytic tools; S.F., R.N., A.S., R.R.B., P.R., G.P., W. Brandt, and A.B. analyzed data; and S.F., A.S., J.G., W. Boland, and A.B. wrote the paper.

The authors declare no conflict of interest.

This article is a PNAS Direct Submission.

Data deposition: The *Pc*IDS1 sequence reported in this paper has been deposited in the GenBank database (accession no. KC109782) and the *Pc*IDS1 model has been deposited in the Protein Model DataBase (ID code PM0078683).

[1]To whom correspondence should be addressed. E-mail: aburse@ice.mpg.de.

This article contains supporting information online at www.pnas.org/lookup/suppl/doi:10.1073/pnas.1221489110/-/DCSupplemental.

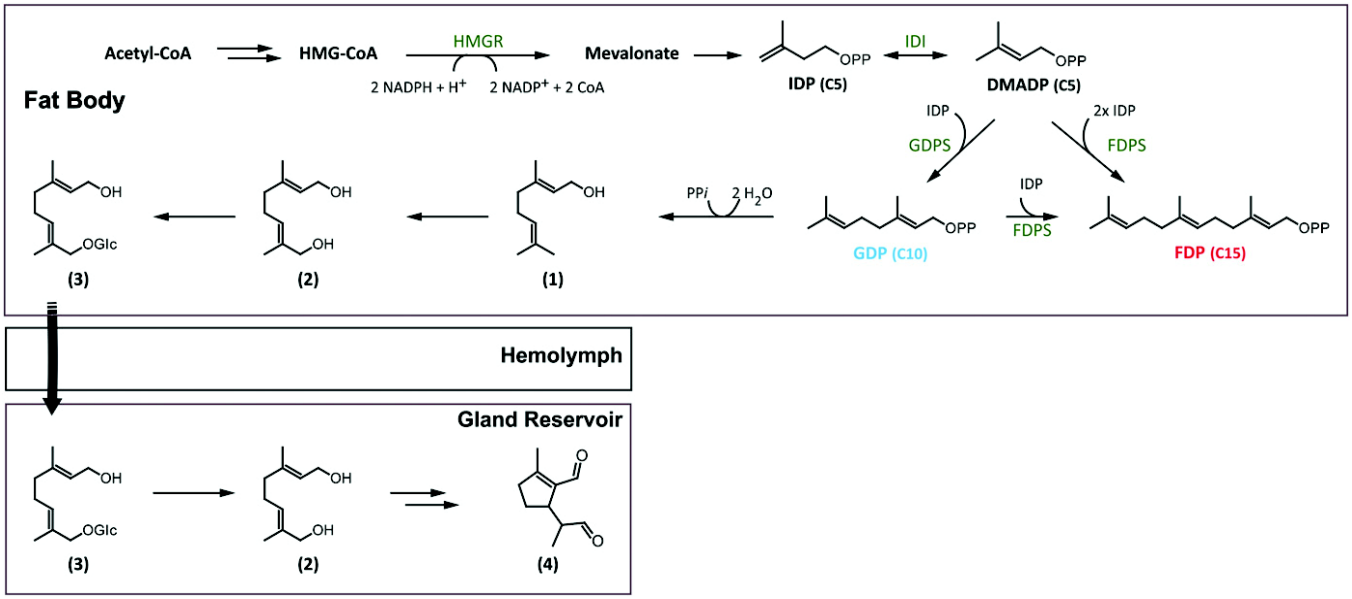

Fig. 1. Biosynthesis of iridoid monoterpene defenses in juvenile *P. cochleariae*: (1) geraniol, (2) 8-hydroxygeraniol, (3) 8-hydroxygeraniol-glucoside, (4) chrysomelidial. HMGR, 3-hydroxy-3-methyl-glutaryl-CoA reductase; IDI, isopentenyl diphosphate isomerase.

other hand, FDP serves as precursor for various primary metabolites and juvenile required hormone. The identification of Co^{2+}, Mn^{2+}, and Mg^{2+} in the juvenile beetles supports the notion that these organisms may control the product specificity of scIDSs by means of changes in local concentrations of these metal ions. Hence, the direction of flux at a branch point in terpene metabolism between defense and primary metabolism is regulated by an unprecedented IDS control mechanism.

Results

Identification and Tissue Distribution of a scIDS in Juvenile *P. cochleariae*. The use of degenerate primers allowed the amplification of a cDNA that encodes a protein of 430 aa (49.3 kDa, pI of 8.63) referred to here as *Pc*IDS1. ClustalW alignments revealed a high amino acid sequence identity of *Pc*IDS1 in relation to other functionally characterized insect scIDSs and showed all the conserved regions known for prenyltransferases (3, 23) (Fig. S1). The sequence also contains an RxxS motif (R_{67}–S_{70}), which could be the cleavage site for a mitochondrial targeting sequence already known from other identified scIDSs (11, 24).

Quantitative real-time assays revealed that *Pc*IDS1 transcripts are generally present in all analyzed larval tissues (Fig. S2*A*). However, the highest transcript abundance was observed in fat body tissue, which had a 5.6-fold higher transcript level compared with gut tissue. The transcript abundance was also reflected in protein level, because *Pc*IDS1 was detectable in all tested tissues, with the strongest signal derived from fat body tissue (Fig. S2*B*). Additionally, overall scIDS activity was determined in all crude extracts of the different larval tissues (Fig. 2*A*). In contrast to the trace amounts of FDP produced by extracts of every tissue tested, GDP-forming activity followed a different pattern. Compared with gut tissue, GDP formation was 141-fold higher in fat body tissue. Our results are consistent with recent findings on the distribution of the pathway to the iridoid defense compounds in *P. cochleariae* larvae. The early steps leading to the formation of the intermediate 8-hydroxygeraniol-glucoside are most likely localized in the fat body tissue. The glucoside is then transferred from there via the hemolymph into the defense glands, where the later steps in formation of chrysomelidial are located (25) (Fig. 1).

***Pc*IDS1 Is Involved in the Production of Defensive Monoterpenoids in Juvenile *P. cochleariae*.** RNAi experiments were performed with *P. cochleariae* to demonstrate the in vivo relevance of *Pc*IDS1. There were no significant differences in the relative growth rate between insects injected with a *PcIDS1*-dsRNA probe or with a control *Gfp* dsRNA probe and noninjected controls (NICs) (Fig. S3). However, transcript quantification 5 d after injection confirmed a significant *PcIDS1* mRNA reduction in fat body tissue (by 95%; $P < 0.001$) in comparison to *PcIDS1* mRNA levels in *Gfp*-treated larvae and NICs (Fig. 2*B*). Accordingly, 5 d after injection, the relative weight of defensive secretions decreased (by 52%; $P < 0.001$) in larvae challenged by *PcIDS1* dsRNA. This reduction continued until by day 13, a defenseless phenotype appeared that lacked secretions. The *Gfp* controls and NICs, on the other hand, produced unaltered amounts of defensive secretions (Fig. 2*C*). Detailed analyses of the relative amount of chrysomelidial per larva revealed a significant decline of this iridoid (by 78%; $P < 0.001$) in *PcIDS1*-treated larvae compared with the *Gfp* group and NICs after 5 d; this decline proceeded until there was a complete loss of secretions (Fig. 2*F*).

To determine if the chrysomelidial reduction is correlated with a decrease of the precursor, 8-hydroxygeraniol-glucoside, we analyzed the hemolymph and fat body tissue of larvae treated with *PcIDS1* dsRNA, *Gfp* dsRNA, and NICs. Seven days after *PcIDS1*-dsRNA injection, the level of precursor in the hemolymph was significantly reduced (by 89%; $P < 0.001$) compared with corresponding *Gfp* controls and NICs. This effect continued further with a reduction of 97% on day 11 (Fig. 2*E*). A similar effect was observed in the fat body tissue, where the amount of 8-hydroxygeraniol-glucoside was diminished (by 64.5 ± 14.08%) after 7 d. In addition to the reduction of chrysomelidial and 8-hydroxygeraniol-glucoside, we observed a significant loss of the overall scIDS activity (by 93%; $P < 0.001$) in the fat body tissue of *PcIDS1*-silenced larvae 7 d after injection compared with *Gfp* controls and NICs (Fig. 2*D*).

Recombinant *Pc*IDS1 Shows Metal Cofactor-Dependent Product Formation. Our results suggest that *Pc*IDS1 is involved in the biosynthesis of the monoterpenoid precursors needed for formation of the defensive compound chrysomelidial. Next, *Pc*IDS1 was expressed in *Escherichia coli* after truncation of the signal sequence at the 5′-end of the coding region, and the enzymatic activity of the purified recombinant protein was studied in vitro.

Like other scIDS proteins, *Pc*IDS1 was inactive without adding divalent metal cations, such as Mg^{2+} or Mn^{2+}. As recent

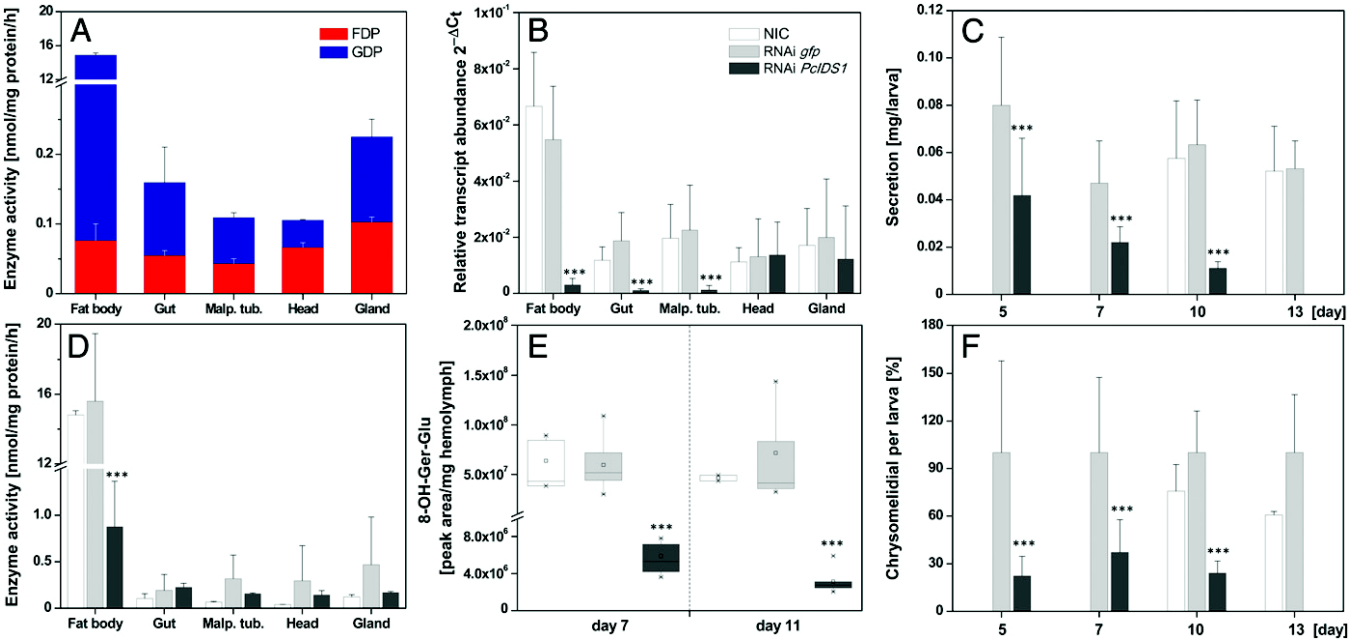

Fig. 2. Silencing *Pc*IDS1 in juvenile *P. cochleariae* by RNAi. (*A*) scIDS activity in tissue extracts of NICs: 10 µg of protein was incubated with 50 µM IDP, 50 µM DMADP, and 10 mM Mg^{2+} for 60 min ($n = 3$). (*B*) Relative transcript abundance ($2^{\Delta Ct}$) of *Pc*IDS1 in different larval tissues 5 d after dsRNA injection ($n = 3$, ±SD). (*C*) Relative weight of larval secretions observed at different time points after dsRNA injection ($n = 3$, ±SD). (*D*) scIDS activity in tissues extracts 7 d after dsRNA injection. Ten micrograms of protein was incubated with 50 µM IDP, 50 µM DMADP, and 10 mM Mg^{2+} for 60 min ($n = 3$, ±SD). (*E*) Amount of 8-hydroxygeraniol-glucoside (8-OH-Ger-Glu) in hemolymph by HPLC analyses after dsRNA injection ($n = 3$, ±SD). (*F*) GC-MS analyses of chrysomelidial after dsRNA injection ($n = 3$, ±SD). Malp. tub., Malpighian tubules. ***, $p < 0.001$.

studies show, scIDS activity can be modulated by these metal ion cofactors (7, 15, 16, 26, 27); we therefore tested *Pc*IDS1 activity with IDP and two different allylic substrates, DMADP and GDP, in the presence of five different divalent cations. Each ion was tested separately at comparable concentration ranges.

In our assays with DMADP, the maximum overall enzyme activity for each cation was observed at 5 mM for Mg^{2+}, 0.5 mM for Co^{2+} and Mn^{2+}, and 0.1 mM for Ni^{2+} and Zn^{2+} (Fig. 3*A*, Fig. S4*A*, and Table S1). *Pc*IDS1 was far more active with Co^{2+} as an additive than with any other tested metal ion. Intriguingly, not only the overall enzyme activity but the product specificity varied considerably according to the different ions. In the presence of Co^{2+} or Mn^{2+}, with DMADP as a cosubstrate, *Pc*IDS1 produced about 96% GDP and only 4% FDP. In contrast, with Mg^{2+} as an additive, *Pc*IDS1 produced 18% GDP and 82% FDP.

Moreover, the optimal ion concentration changed depending on the allylic substrates. After GDP was substituted for DMADP, leading to the production of FDP, we observed *Pc*IDS1 being most active by addition of 0.5 mM Mg^{2+} compared with any other tested cofactor (Fig. 3*B*, Fig. S4*B*, and Table S1). Overall, Mg^{2+}, Mn^{2+}, and Co^{2+} represent the cofactors most favored in *Pc*IDS1 catalysis. Because Co^{2+} and Mg^{2+} resulted in the highest levels of *Pc*IDS1 activity, we used these cofactors in the following experiments.

In a first approach with DMADP, a constant Co^{2+} concentration of 0.5 mM was complemented with an ascending concentration of Mg^{2+} in a range of 0.001–10 mM (Fig. 4*A*). *Pc*IDS1 formed mainly GDP and only minor amounts of FDP, suggesting that Co^{2+} is the dominant metal ion independent of the tested Mg^{2+} concentration.

In a second approach with DMADP, we measured the enzyme activity with Mg^{2+} constant at 5 mM and an ascending concentration of Co^{2+} in the range of 0.001–10 mM (Fig. 4*B*). At Co^{2+} concentrations lower than 0.05 mM, FDP was the main product, accompanied by a 50% reduction in enzyme activity. However, if Co^{2+} concentrations exceeded 0.1 mM, *Pc*IDS1 activity clearly increased. Simultaneously, a shift from FDP to the reduced chain length of GDP was observed. Even if Mg^{2+} was 100-fold more abundant in the mixture, the enzyme definitely showed a preference for Co^{2+}.

With GDP as a cosubstrate, a constant 0.5 mM Co^{2+}, and an ascending Mg^{2+} concentration, *Pc*IDS1 displayed low FDP-forming activity (Fig. 4*C*). If Mg^{2+} is constant at 5 mM and Co^{2+} concentrations vary, we observed high FDP production only at Co^{2+} concentrations below 0.1 mM. However, as soon as the Co^{2+} concentration ascends, the FDP-forming activity decreases dramatically (Fig. 4*D*). Our findings indicate that the Mg^{2+}-catalyzed activity of *Pc*IDS1 is abolished as soon as Co^{2+} reaches its optimal concentration.

To determine the conformational state of *Pc*IDS1 quaternary structure, size exclusion chromatography was performed. Fig. S5 shows the relative retention volumes of the apoprotein without adding cofactors and *Pc*IDS1 in presence of Co^{2+} (0.5 mM) or Mg^{2+} (5 mM). Surprisingly, we found an obvious difference in the elution volume among the apoprotein (without divalent metal), the *Pc*IDS1-Mg^{2+} complex, and the *Pc*IDS1-Co^{2+} complex. The apoprotein eluted from the column at a retention volume of 76.36 mL (corresponding to 74.6 kDa), whereas *Pc*IDs1-Mg^{2+} and *Pc*IDS1-Co^{2+} eluted at 73.65 mL (corresponding to 93.8 kDa) and 74.46 mL (corresponding to 87.6 kDa), respectively. Given the calculated monomeric mass of 45.8 kDa, this indicates on one hand that the enzyme is always present as a dimer regardless of added cofactor. On the other hand, the difference in the elution volume reflects a change in the hydrodynamic volume of the protein caused by the divalent metal. In the case of Mg^{2+}, the dimeric protein possesses the largest volume, most likely due to a more relaxed conformation. With Co^{2+}, *Pc*IDS1 seems to have a more compact conformation, which may be responsible for the change in product spectrum. As a control, we also analyzed the metal influence on the standard proteins and observed no obvious difference in the elution volume with addition of various amounts of Mg^{2+} or Co^{2+}.

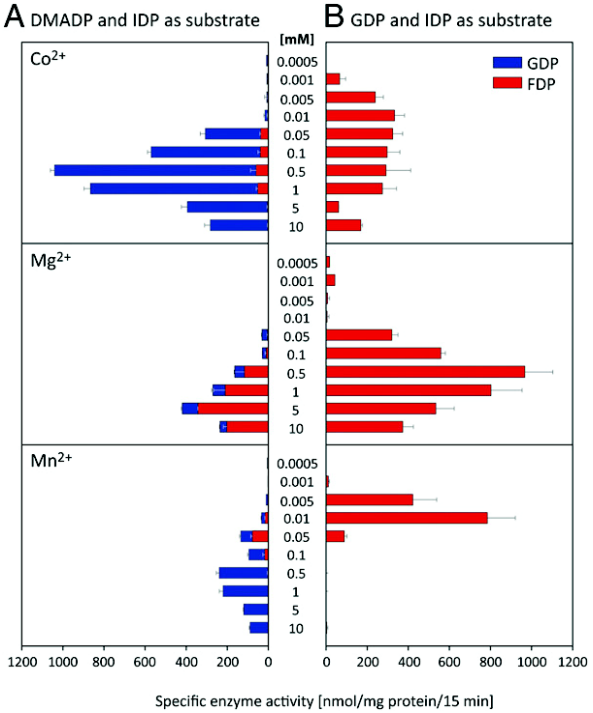

Fig. 3. Effect of metal cofactors on enzyme activity and product formation of *Pc*IDS1. (*A*) Different concentrations of Co^{2+}, Mg^{2+}, and Mn^{2+} were added to *Pc*IDS1 and incubated with 50 μM IDP and 50 μM DMADP ($n = 3$, ±SD). (*B*) Different concentrations of Co^{2+}, Mg^{2+}, and Mn^{2+} were added to *Pc*IDS1 and incubated with 50 μM IDP and 50 μM GDP ($n = 3$, ±SD).

Kinetic Analyses of Purified *Pc*IDS1. All kinetic parameters measured for *Pc*IDS1 are displayed in Table 1. In combination with Co^{2+} and fixed IDP, *Pc*IDS1 has a K_m of 11.6 μM for DMADP (Fig. S6*A*) and a K_m of 24.3 μM for GDP (Fig. S6*E*), suggesting that DMADP is the preferred substrate compared with GDP. Significant differences in the V_{max} were not observed. With Co^{2+} and DMADP fixed at 50 μM, *Pc*IDS1 has a K_m of 0.8 μM for IDP and substrate inhibition at higher concentrations with a K_i of 46.6 μM (Fig. S6*B*). No inhibitory effect of IDP was observed with GDP fixed at 50 μM (Fig. S6*F*).

In combination with Mg^{2+} and fixed IDP, *Pc*IDS1 displayed atypical kinetics for DMADP that resulted in a biphasic curve (Fig. S6*C*). In the first part of the curve from 0.1 to 100 μM DMADP, the reaction seems to follow a Michaelis–Menten kinetic. However, the curve displays a different slope as soon as the DMADP concentration exceeds 50 μM. The K_m for GDP was 1.2 μM with a slight substrate inhibition (Fig. S6*G*). With Mg^{2+} and DMADP fixed at 50 μM, *Pc*IDS1 has a K_m of 11.8 μM for IDP with a slight substrate inhibition (Fig. S6*D*), and with GDP fixed at 50 μM, the K_m of IDP was 7.1 μM (Fig. S6*H*). Analyses of the calculated V_{max} show that Mn^{2+} gave generally lower reaction velocities than did Co^{2+}.

The kinetic parameters substantiate our previous observations that *Pc*IDS1 has a preference for Co^{2+} with DMADP as an allylic cosubstrate giving the C_{10} product GDP. If Mg^{2+} is the metal cofactor, GDP is the favored cosubstrate affording the C_{15} product FDP.

Metal Cofactors Identified in *P. cochleariae* Larvae Have Different Affinities in the Enzyme Complex. Inductively coupled plasma-MS analysis of *P. cochleariae* larvae showed an overall concentration of Co^{2+} in the fat body tissue at ≥0.24 μg/g of dry weight (DW) or 4 nmol/g of DW, and an overall concentration of Mn^{2+} at ≥16.6 μg/g of DW or 0.3 μmol/g of DW, whereas Mg^{2+} was found at a concentration of 2,223 μg/g of DW or 91 μmol/g of DW in the fat body (Table S2).

Quantum mechanical calculations revealed reaction energies of about 40 kcal/mol lower for the formation of complexes containing Co^{2+} or Mn^{2+} compared with those containing Mg^{2+} for association with the diphosphate of DP^{3-} or the aspartate residues of the enzyme (mimicked by propionic acid anions) (Tables S3 and S4). In all cases, the affinity of the metal cations for the diphosphate was more than 200 kcal/mol higher than for the aspartate residues. Based on these gas phase calculations, the deduced minimum equilibrium constant for formation of the diphosphate metal complex is at least 10^{28}-fold higher for Co^{2+} or Mn^{2+} than for Mg^{2+}, which suggests that *Pc*IDS1 may have a considerably higher affinity for Co^{2+} or Mn^{2+} than for Mg^{2+}, although the magnitude of this difference may be reduced somewhat by solvation effects not considered here. Hence, the low concentrations of Co^{2+} or Mn^{2+} in the larval tissue in comparison to Mg^{2+} may be compensated for by their greater complex formation ability with diphosphate. On the other hand, if one compares the affinities of either the metal ion-complexed diphosphate with the aspartate (assuming the metal cations are delivered to the binding site together with the substrate) or, alternatively, the metal-complexed aspartates with the diphosphate (Tables S5 and S6), in both cases, the affinities for Co^{2+} or Mn^{2+} are lower than the affinity for Mg^{2+} in nice agreement with the measured lower $K_{m\,(GDP)}$ (higher affinity) ($Mg^{2+} = 1.18$ μM, $Co^{2+} = 24.3$ μM) and might be an explanation for the experimental differences in product specificity with different divalent metal ions. Note, one order of magnitude in K_m represents 1.4 kcal/mol (ΔG) in interaction energies.

Discussion

Understanding the mechanism of chain-length determination of scIDSs has been a major challenge for researchers of terpene biosynthetic enzymes, and much has been learned about active site features that restrict the length of the enzyme products. The determination of product carbon length by the identity of the metal cofactor apparently provides an alternative mechanism to the regulation of product formation by scIDS. Given that plants possess a number of genes encoding IDSs [e.g., at least 10 in *Arabidopsis thaliana* (8)], whereas insects possess only a few [e.g., 3 in *Bombyx mori* (28)], insects may compensate for this disparity by generating different chain-length products in other ways. In our case, the metal ion-mediated product differences enable the *P. cochleariae* beetles to supply precursors for two terpene pathways, one for monoterpene metabolism (synthesis of chemical defenses) and one for sesquiterpene metabolism (juvenile hormone formation), using only a single enzyme. Instead of "inventing" a new IDS, insects appear to use different cofactors to add an additional product to an enzyme's repertoire, thereby lowering metabolic costs. Such a regulation mechanism may allow faster adaptation to developmental or environmental changes that insects may face, such as metamorphosis or host plant shifts. Due to differences in metal ion identity and concentration, shifts in overall scIDS activity have previously been observed for enzymes from plants [e.g., *Abies grandis* (29)] and for enzymes from insects [e.g., *Myzus persicae* (15), *Choristoneura fumiferana* (30)], but without alterations in product chain length. However, Sen et al. (26) report cofactor-dependent changes of product chain length in crude homogenates of the *corpora allata* of the lepidopteran *Manduca sexta*. The product ratios formed during the coupling of DMADP with IDP by means of scIDS activity showed that FDP formation was stimulated by adding Mg^{2+}, whereas GDP formation increased in the presence of Mn^{2+}. Taken together with our results, these findings should motivate researchers to test alternative cofactors with scIDSs in the future.

*Pc*IDS1 produces mainly GDP (95%) in the presence of Co^{2+} (or Mn^{2+}) with IDP and DMADP as substrates and produces only minor amounts of FDP (4%). In contrast, with Mg^{2+}, the predominant product was FDP (82%); only minor amounts of GDP (18%) were produced. Our kinetic data for *Pc*IDS1 support the observation that the regulation of product distribution by these metal cofactors is biochemically relevant. Comparisons

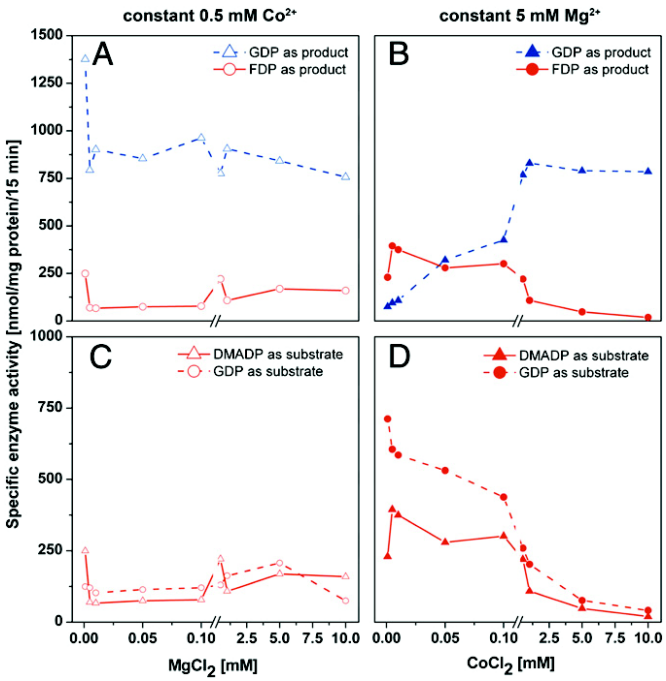

Fig. 4. Effect of mixtures of divalent metal ion cofactors on enzyme activity and product formation of *Pc*IDS1. (*A*) Constant 0.5 mM Co^{2+} with an ascending Mg^{2+} concentration in a range of 0.001 mM up to 10 mM with 50 μM IDP or 50 μM DMADP ($n = 2$). (*B*) Constant 5 mM Mg^{2+} with an ascending Co^{2+} concentration from 0.001 mM up to 10 mM with 50 μM IDP or 50 μM DMADP ($n = 2$). (*C*) FDP formation at constant 0.5 mM Co^{2+} with an ascending Mg^{2+} concentration with 50 μM GDP or 50 μM DMADP ($n = 2$). (*D*) FDP formation at constant 5 mM Mg^{2+} with an ascending Co^{2+} concentration with 50 μM GDP or 50 μM DMADP ($n = 2$).

with kinetic data available from plant GDPSs in the presence of DMADP revealed that the $K_{m(DMADP)}$ of *Pc*IDS1 (11.6 μM) with Co^{2+} corresponds to the K_m of the enzyme from *Anthirrhium majus* (24.1 μM) (31) or *Anthirrhium grandis* (16.7 μM) (29). $K_{m(DMADP)}$ values from insect scIDSs have so far been determined only for the bifunctional GDPSs of *M. persicae* *Mp*IPPS1-S (28.6 μM) (17) and *Mp*IPPS2-S (24.2 μM) (17), as well as *Aphis gossypii* (39.2 μM) (14), and for the FDPS from *Drosophila melanogaster* *Dm*FPPS-1b (33.5 μM) (32). The K_m of *Pc*IDS1 is found within the range of literature values. The combination of DMADP with Mg^{2+} did not allow a K_m calculation due to the biphasic progression of the kinetic curve. Although DMADP reacts initially with IDP to form GDP, in later catalytic cycles, the GDP formed can compete with another molecule of DMADP at the allylic binding site of *Pc*IDS1. If GDP is the preferred allylic substrate in combination with Mg^{2+}, it can lead to the formation of FDP.

The K_m values of *Pc*IDS1 for GDP, which are 24.3 μM and 1.1 μM in the presence of Co^{2+} and Mg^{2+}, respectively, are in the range of K_m values for previously described insect scIDSs, such as those of *A. gossypii* (12.6 μM) (14), *D. melanogaster* FPPS-1b (7 μM) (32), *M. sexta* (0.8 μM) (27), and *M. persicae* (*Mp*IPPS1-S, 25.4 μM; *Mp*IPPS2-S, 15.4 μM) (17). The difference in the *Pc*IDS1 K_m values for different metal cofactors suggests that the enzyme favors GDP as a substrate with Mg^{2+}. The alteration of IDS product specificity by metal ions has so far been described only for long-chain IDSs from microbes. In the presence of Co^{2+} or Mn^{2+}, octaprenyl-, solanesyl-, and decaprenyl-diphosphate synthases gave a variety of polyprenyl products whose chains were longer by up to two isoprene units than those of the products formed in the presence of Mg^{2+} (33–35).

IDS structure elucidation in combination with mutagenesis studies has suggested that product chain length is determined by the size of the hydrophobic pocket in the active center. In particular, the amino acids in the vicinity of the conserved first and second aspartate-rich regions (FARM and SARM motifs, respectively) form a steric hindrance that terminates chain elongation (3, 23, 36, 37). The van der Waals radii of Co^{2+} and Mn^{2+} are 1.73 Å and 1.9 Å, respectively, both of which are larger than that of Mg^{2+} at 0.96 Å (38). These differences may lead to conformational changes of *Pc*IDS1 or to rearrangements of substrate position in the enzymes that influence chain-length elongation. First hints toward conformational changes were obtained by size exclusion chromatography that revealed differences in the quaternary structure due to complex formation with different metal ions. Further homology modeling in combination with site-directed amino acid mutagenesis is needed to explain more fully how changes in cofactors influence the chain-length determination mechanism for *Pc*IDS1.

Mg^{2+} and Mn^{2+} are well-known cofactors for scIDS activity; however, in our biochemical characterization, *Pc*IDS1 showed the highest GDP synthase activity in the presence of Co^{2+}. Despite its rare occurrence in nature, Co^{2+} plays a role as a cofactor in a number of proteins (e.g., methionine aminopeptidase, glucose isomerase) (39). To balance the need for cobalt with its intrinsic toxicity, nature has evolved trafficking systems to maintain metal homeostasis (40). For example, in the transcriptome from *P. cochleariae*, we have identified a transport protein that shows high similarity to the cobalt uptake protein Cot 1 of *Saccharomyces cerevisiae* (41). This finding and the calculated high affinity of Co^{2+} to *Pc*IDS1 underline the possibility that Co^{2+} is an available as well as biologically relevant cofactor for this enzyme despite its low concentration in the larvae.

Using an RNAi approach, we were able to show that the *Pc*IDS1-catalyzed formation of GDP is involved in the production of monoterpenoid defensive compounds in *P. cochleariae* larvae. However, we could not detect a phenotype arising from the loss of formation of the alternate product, FDP. In insects, FDP is the essential precursor for the synthesis of juvenile hormones (42), and it is localized in the *corpora allata* complex found in the head posterior to the brain. Given that RNAi efficiency can differ from tissue to tissue as well as from gene to gene (43), the lack of a phenotype caused by low FDP levels might be attributed to ineffective silencing in the larval head. However, even more important may be the existence of additional prenyltransferases. Aphids, coleopterans, and lepidopterans are known to possess up to three scIDSs, and we are currently searching for additional scIDSs in *P. cochleariae*, which, like many other

Table 1. Kinetic constants for *P. cochleariae* *Pc*IDS1 depend on the identity of both the metal cofactor and allylic substrate

	Co^{2+}				Mg^{2+}			
Fixed substrate	$IDP_{(15\ \mu M)}$	$IDP_{(50\ \mu M)}$	$DMADP_{(50\ \mu M)}$	$GDP_{(50\ \mu M)}$	$IDP_{(50\ \mu M)}$	$IDP_{(50\ \mu M)}$	$DMADP_{(50\ \mu M)}$	$GDP_{(50\ \mu M)}$
Substrate	DMADP	GDP	IDP	IDP	DMADP	GDP	IDP	IDP
$K_{m\ (substrate)}$, μM	11.60	24.31	0.84	1.46	~1103	1.19	11.79	7.08
V_{max}, μmol·min^{-1}·mg^{-1} of protein	0.44	0.41	0.67	0.23	~2.39	0.12	0.17	0.20
$K_{I\ (substrate)}$, μM	n.d.	n.d.	46.62	n.d.	n.d.	1,047	572.7	322.1

n.d., not detectable.

enzymes of this class, may make more than one product. Our work shows that enzymes with an intrinsic promiscuity may also use exogenous factors, such as metal cofactors, to regulate product synthesis. It also serves as a reminder that neither substrate specificity nor product profiles can always be predicted by sequence similarity. Instead, rigorous biochemical testing is needed to establish enzyme function, especially among enzymes of terpene metabolism.

Materials and Methods

A scIDS from *P. cochleariae* was isolated with a degenerated PCR approach and RACE amplification. For further biochemical characterization, heterologous expression in *E. coli* Bl21 star (DE3) and protein purification were performed by affinity chromatography with Ni-nitrilotriacetric acid agarose columns. RNAi techniques were used to determine in vivo relevance, followed by quantitative real-time PCR, the quantification of 8-hydroxygeraniol via liquid chromatography (LC)-tandem MS (MS/MS), the relative quantification of chrysomelidial with GC-MS, and *Pc*IDS1 activity measurements determined by LC-MS/MS. Kinetic analyses and product determination were realized by LC-MS/MS, and calculations were performed with GraphPad Prism (GraphPad Software). Details of beetle rearing, reagents, protein purification/sequencing, antibody production, RNAi techniques, LC-MS/MS, GC-MS, quantitative PCR, sequence analyses, and other methods used in this study are described in *SI Materials and Methods*.

ACKNOWLEDGMENTS. We thank Dr. Dirk Merten for the element analysis and Angelika Berg and Dr. Maritta Kunert for technical assistance. We thank Prof. Jacques M. Pasteels for helpful discussions on aspects of this work and Emily Wheeler for critically reading of the manuscript. This work has been supported by the Deutsche Forschungsgemeinschaft (Grant BU 1862/2-1) and the Max Planck Society.

1. Gershenzon J, Dudareva N (2007) The function of terpene natural products in the natural world. *Nat Chem Biol* 3(7):408–414.
2. Pichersky E, Noel JP, Dudareva N (2006) Biosynthesis of plant volatiles: Nature's diversity and ingenuity. *Science* 311(5762):808–811.
3. Wang KC, Ohnuma S (2000) Isoprenyl diphosphate synthases. *Biochim Biophys Acta* 1529(1-3):33–48.
4. Kharel Y, Koyama T (2003) Molecular analysis of cis-prenyl chain elongating enzymes. *Nat Prod Rep* 20(1):111–118.
5. Liang PH (2009) Reaction kinetics, catalytic mechanisms, conformational changes, and inhibitor design for prenyltransferases. *Biochemistry* 48(28):6562–6570.
6. Gershenzon J, Kreis J (1999) Biochemistry of terpenoids: Monoterpenes, sesquiterpenes, diterpenes, sterols, cardiac glycosides, and steroid saponins. *Biochemistry of Plant Secondary Metabolism*, ed Wink M (Sheffield Academic, Sheffield, UK), pp 222–299.
7. Vandermoten S, Haubruge E, Cusson M (2009) New insights into short-chain prenyltransferases: Structural features, evolutionary history and potential for selective inhibition. *Cell Mol Life Sci* 66(23):3685–3695.
8. Tholl D, Lee S (2011) Terpene specialized metabolism in *Arabidopsis thaliana*. *The Arabidopsis Book*, ed Last R (American Society of Plant Biologists, Rockville, MD), Vol 9, pp e0143.
9. Hsiao YY, et al. (2008) A novel homodimeric geranyl diphosphate synthase from the orchid Phalaenopsis bellina lacking a DD(X)2-4D motif. *Plant J* 55(5):719–733.
10. Schmidt A, et al. (2010) A bifunctional geranyl and geranylgeranyl diphosphate synthase is involved in terpene oleoresin formation in *Picea abies*. *Plant Physiol* 152(2):639–655.
11. Gilg AB, Bearfield JC, Tittiger C, Welch WH, Blomquist GJ (2005) Isolation and functional expression of an animal geranyl diphosphate synthase and its role in bark beetle pheromone biosynthesis. *Proc Natl Acad Sci USA* 102(28):9760–9765.
12. Blomquist GJ, et al. (2010) Pheromone production in bark beetles. *Insect Biochem Mol Biol* 40(10):699–712.
13. Lewis MJ, Prosser IM, Mohib A, Field LM (2008) Cloning and characterisation of a prenyltransferase from the aphid *Myzus persicae* with potential involvement in alarm pheromone biosynthesis. *Insect Mol Biol* 17(4):437–443.
14. Ma G-Y, Sun XF, Zhang YL, Li ZX, Shen ZR (2010) Molecular cloning and characterization of a prenyltransferase from the cotton aphid, *Aphis gossypii*. *Insect Biochem Mol Biol* 40(7):552–561.
15. Vandermoten S, et al. (2008) Characterization of a novel aphid prenyltransferase displaying dual geranyl/farnesyl diphosphate synthase activity. *FEBS Lett* 582(13): 1928–1934.
16. Vandermoten S, et al. (2009) Structural features conferring dual geranyl/farnesyl diphosphate synthase activity to an aphid prenyltransferase. *Insect Biochem Mol Biol* 39(10):707–716.
17. Zhang Y-L, Li Z-X (2012) Functional analysis and molecular docking identify two active short-chain prenyltransferases in the green peach aphid, *Myzus persicae*. *Arch Insect Biochem Physiol* 81(2):63–76.
18. Oldfield E, Lin FY (2012) Terpene biosynthesis: Modularity rules. *Angew Chem Int Ed Engl* 51(5):1124–1137.
19. Brandt W, et al. (2009) Molecular and structural basis of metabolic diversity mediated by prenyldiphosphate converting enzymes. *Phytochemistry* 70(15-16):1758–1775.
20. Aaron JA, Christianson DW (2010) Trinuclear metal clusters in catalysis by terpenoid synthases. *Pure Appl Chem* 82(8):1585–1597.
21. Pasteels JM, Braekman JC, Daloze D, Ottinger R (1982) Chemical defence in chrysomelid larvae and adults. *Tetrahedron* 38(13):1891–1897.
22. Termonia A, Hsiao TH, Pasteels JM, Milinkovitch MC (2001) Feeding specialization and host-derived chemical defense in Chrysomeline leaf beetles did not lead to an evolutionary dead end. *Proc Natl Acad Sci USA* 98(7):3909–3914.
23. Tarshis LC, Proteau PJ, Kellogg BA, Sacchettini JC, Poulter CD (1996) Regulation of product chain length by isoprenyl diphosphate synthases. *Proc Natl Acad Sci USA* 93(26):15018–15023.
24. von Heijne G (1990) The signal peptide. *J Membr Biol* 115(3):195–201.
25. Burse A, et al. (2008) Implication of HMGR in homeostasis of sequestered and *de novo* produced precursors of the iridoid biosynthesis in leaf beetle larvae. *Insect Biochem Mol Biol* 38(1):76–88.
26. Sen SE, Brown DC, Sperry AE, Hitchcock JR (2007) Prenyltransferase of larval and adult M. sexta corpora allata. *Insect Biochem Mol Biol* 37(1):29–40.
27. Sen SE, Sperry AE (2002) Partial purification of a farnesyl diphosphate synthase from whole-body Manduca sexta. *Insect Biochem Mol Biol* 32(8):889–899.
28. Kaneko Y, Kinjoh T, Kiuchi M, Hiruma K (2011) Stage-specific regulation of juvenile hormone biosynthesis by ecdysteroid in *Bombyx mori*. *Mol Cell Endocrinol* 335(2): 204–210.
29. Tholl D, Croteau R, Gershenzon J (2001) Partial purification and characterization of the short-chain prenyltransferases, geranyl diphosphate synthase and farnesyl diphosphate synthase, from Abies grandis (grand fir). *Arch Biochem Biophys* 386(2):233–242.
30. Sen SE, et al. (2007) Purification, properties and heteromeric association of type-1 and type-2 lepidopteran farnesyl diphosphate synthases. *Insect Biochem Mol Biol* 37(8): 819–828.
31. Tholl D, et al. (2004) Formation of monoterpenes in *Antirrhinum majus* and *Clarkia breweri* flowers involves heterodimeric geranyl diphosphate synthases. *Plant Cell* 16(4):977–992.
32. Sen SE, Trobaugh C, Béliveau C, Richard T, Cusson M (2007) Cloning, expression and characterization of a dipteran farnesyl diphosphate synthase. *Insect Biochem Mol Biol* 37(11):1198–1206.
33. Ohnuma S, Koyama T, Ogura K (1992) Chain length distribution of the products formed in solanesyl diphosphate synthase reaction. *J Biochem* 112(6):743–749.
34. Ohnuma S, Koyama T, Ogura K (1993) Alteration of the product specificities of prenyltransferases by metal ions. *Biochem Biophys Res Commun* 192(2):407–412.
35. Fujii H, et al. (1980) Variable product specificity of solanesyl pyrophosphate synthetase. *Biochem Biophys Res Commun* 96(4):1648–1653.
36. Chen AJ, Kroon PA, Poulter CD (1994) Isoprenyl diphosphate synthases: Protein sequence comparisons, a phylogenetic tree, and predictions of secondary structure. *Protein Sci* 3(4):600–607.
37. Szkopińska A, Płochocka D (2005) Farnesyl diphosphate synthase; regulation of product specificity. *Acta Biochim Pol* 52(1):45–55.
38. Heuts JPA, Schipper E, Piet P, German AL (1995) Molecular mechanics calculations on cobalt phthalocyanine dimers. *Theochem-J Mol Struct* 333(1-2):39–47.
39. Kobayashi M, Shimizu S (1999) Cobalt proteins. *Eur J Biochem* 261(1):1–9.
40. Okamoto S, Eltis LD (2011) The biological occurrence and trafficking of cobalt. *Metallomics* 3(10):963–970.
41. Conklin DS, McMaster JA, Culbertson MR, Kung C (1992) COT1, a gene involved in cobalt accumulation in Saccharomyces cerevisiae. *Mol Cell Biol* 12(9):3678–3688.
42. Bellés X, Martín D, Piulachs MD (2005) The mevalonate pathway and the synthesis of juvenile hormone in insects. *Annu Rev Entomol* 50:181–199.
43. Terenius O, et al. (2011) RNA interference in Lepidoptera: An overview of successful and unsuccessful studies and implications for experimental design. *J Insect Physiol* 57(2):231–245.

Supporting Information

Frick et al. 10.1073/pnas.1221489110

SI Materials and Methods

Beetle Rearing and Secretion Collection. *Phaedon cochleariae* (F.) was laboratory-reared as continuous cultures (York chamber, 15 °C and 16-h/8-h light/dark period) on leaves of *Brassica rapa* spp. Larval secretion was collected in glass capillaries (inner diameter = 0.28 mm, outer diameter = 0.78 mm, length = 100 mm; Hirschmann Laborgeraete, Eberstadt, Germany). Sealed capillaries containing samples were stored at −20 °C until needed. Secretions were weighed in the sealed capillaries on an ultramicrobalance (Mettler–Toledo) three times; the weight of empty capillaries was subtracted, and the final weight was averaged.

Isolation and Cloning of a cDNA encoding the *Phaedon cochleariae* isoprenyl diphosphate synthase 1 (*Pc*IDS1). Tissue samples from the head, gut, fat body, Malpighian tubules, and defensive glands were taken from third-instar larvae dissected in Ringer's solution (1) and directly transferred in liquid nitrogen-cooled reaction tubes. Total RNA was extracted with the RNeasy Micro Kit (Qiagen) according to the manufacturer's instructions. Complete removal of DNA was achieved using the RNase-free DNase Set (Qiagen). The quality of the RNA was evaluated by measuring the 260:280-nm absorbance ratio, and the integrity of 18S and 28S ribosomal RNA bands was assessed by electrophoresis on RNA 6000 Nano labchips (Agilent Technologies). RNA concentrations were determined from absorbance values at a wavelength of 260 nm. First-strand cDNA was subsequently transcribed from total RNA using SuperScript III reverse transcriptase (Life Technologies). Up to 1 μg of total RNA was reverse-transcribed according to the manufacturer's instructions using oligo(dT)$_{12–18}$ primer. Degenerated primers were designed against the highly conserved regions of previously identified short-chain isoprenyl diphosphate synthases (scIDSs) from *Myzus persicae*, *Aphis gossypii*, *Agrotis ipsilon*, and *Anthonomus grandis*. PCR amplification using Taq DNA Polymerase (Promega) of a 686-bp core fragment was performed with the primer pair FWD_211_geranyl diphosphate synthase (GDPS) (5′-TTC ATG G(AC)(ACT)(GT)(GT)(GC)TTCCC(AGC)GA-3′) and REV_903_GDPS (5′-GAAGTCAT(CT)(CT)TGA(AC)(CT)TTG-3′). The following cycling profile was carried out in an Eppendorf thermal cycler: 3 min at 94 °C; 35 cycles of 30 s at 94 °C, 30 s at 45 °C, and 1 min at 72 °C; and a final 10-min extension at 72 °C. PCR products were purified using QiaEx II (Qiagen), ligated into pCR2.1-TOPO vector (Life Technologies), and sequenced. To obtain full-length cDNA sequence of *P. cochleariae* isoprenyl diphosphate synthase (IDS), a BD SMART RACE cDNA Amplification Kit (BD Biosciences) was used. For amplification of the 5′-end, site sequence-specific reverse primers were designed as followed: RACE_5_214_Rev (5′-CCCTAGGATGCCGGCCAATCTCACG-3′) and nested primer RACE_5_140_Rev (5′-GTGGACAGGCCCCTGGTCTTCTTGC-3′). The sequence-specific primers for the 3′-end site were RACE_3_447_FWD (5′-GACCAACATGGGCCAATCTTTAGACGC-3′) and nested primer RACE_3_483_FWD (5′-GAAGGATGGGAGGCCCATATTGAGCC-3′). The 5′ and 3′ RACE products were cloned and sequenced. The resulting assembled cDNA sequence contained a 1,290-bp open-reading frame that encodes an IDS similar protein of 430 aa referred to here as *P. cochleariae* isoprenyl diphosphate synthase 1 (*Pc*IDS1). This sequence of *Pc*IDS1was registered at GenBank (accession no. KC109782).

Functional Expression and Purification of Recombinant *Pc*IDS1. The entire encoding sequence of *Pc*IDS1 lacking the predicted signal peptide (based on analysis with SignalP 4.1 (2), available at the prediction servers of the Center for Biological Sequence Analysis, Technical University of Denmark, Lyngby, Denmark) was amplified with the following primers that included the start and stop codons for translation in an *Escherichia coli*-based heterologous expression system: *Pc*IDS1-forward (5′-CACCAGGGCCCTCTCCACGATC-3′) and *Pc*IDS1-reverse (5′-CTATGCATCCCTCTTGTAAATCTTCTT-3′). Template cDNA was synthesized by RT from RNA of whole-body *P. cochleariae* larvae, except for the gut tissue. PCR was performed using an Expand High Fidelity PCR system (Roche Applied Science). PCR was performed for 3 min at 94 °C for denaturation, followed by 10 cycles of 15 s at 94 °C, 30 s at 55 °C, and 90 s at 72 °C; 20 cycles of 15 s at 94 °C, 30 s at 55 °C, and 90 s plus 5 s of elongation for each cycle at 72 °C; and a final extension for 7 min at 72 °C. The resulting cDNA fragment was purified with the Zymoclean Gel DNA Recovery Kit (Zymo) and cloned in the expression vector pET100/D-TOPO (Invitrogen), which has a 6 × His-tag on the N terminus. Plasmids were transferred into the strain *E. coli* TOP10F (Life Technologies) and sequenced. Positive constructs were then transferred into different expression strains, including BL21(DE3) star (Invitrogen), BL21(DE3) pLysS (Life Technologies), and Rosetta (DE3; Novagen), but strain BL21(DE3) star produced the highest amount of soluble and active protein of long and short *Pc*IDS1. Bacterial precultures of 20 mL were grown over 3 d at 18 °C under continuous rotation on LB with 50 μg/mL carbenicillin. Afterward, the cells were pelleted and used to inoculate the 200-mL expression culture. There, we used the Overnight Express Autoinduction System 1 (Novagen) and let them grow over 2 d at 18 °C under continuous rotation to stationary phase according to the manufacturer's recommendations. Bacterial pellets were resuspended in 2 mL of assay buffer containing 25 mM 3-(*N*-morpholino)-2-hydroxypropanesulfonic acid (MOPSO; pH 7.3), 10% (vol/vol) glycerol, and 150 mM NaCl. The suspension was sonicated using a Sonopuls HD2070 (Bandelin) for 4 min, cycle 2, at 60% power. The overexpressed His-tagged proteins were subsequently column-purified by affinity chromatography with Ni-nitrilotriacetic acid agarose columns (Qiagen) using a stepwise imidazole gradient from 10 to 500 mM. The purity of the recombinant proteins was evaluated by SDS/PAGE gel electrophoresis, followed by colloidal Coomassie staining (Roti-Blue Colloidal Coomassie Staining; Carl Roth). The purified *Pc*IDS1 migrated at ~45.8 kDa (399 aa). Fractions that contained the highest amount of pure recombinant protein were pooled and desalted in assay buffer with a PD-10 Desalting column (Amersham Biosciences) to remove the imidazole.

To see if the affinity tag influenced the enzyme activity, the fusion protein *Pc*IDS1 was subsequently cleaved using the highly specific serine protease EnterokinaseMax (Life Technologies) according to the manufacturer's instructions. After purification and removal of the affinity tag, cleavage was checked by SDS/PAGE and Western blotting using the anti-His antibody. The fusion protein and the cleaved protein were tested for their enzyme activity. Because cleavage of the tag altered neither the activity nor the product profile, the truncated His-tagged fusion protein *Pc*IDS1 was used in all following experiments.

To determine the conformational state of the *Pc*IDS1 quaternary structure, size exclusion chromatography was performed. The protein was added to running buffer [25 mM MOPSO (pH 7.3), 10% (vol/vol) glycerol, and 150 mM NaCl] in the presence of either 5 mM $MgCl_2$ or 0.5 mM $CoCl_2$ and incubated for 10

min at 4 °C. To confirm the overall conformation of the protein with the different metal cofactors, an aliquot of each solution was separated on a SuperdexHiLoad 16/60 200 prep grade (GE Healthcare) column at a flow rate of 1 mL/min. The retention volume of *Pc*IDS1 was detected via its absorption at 280 nm. To calibrated the column, we used cytochrome *c* from horse heart (12.4 kDa), carbonic anhydrase from bovine erythrocytes (29 kDa), BSA (66 kDa), alcohol dehydrogenase from yeast (150 kDa), and β-amylase from sweet potato (200 kDa) in the presence of 10 mM $CoCl_2$ or 10 mM $MgCl_2$. The molecular weight for *Pc*IDS1 was calculated by the formula received from the corresponding standard curve. Without cofactor, $y = -27.133x + 128.38$ ($R^2 = 0.9925$); with Co^{2+}, $y = -27.133x + 128.21$ ($R^2 = 0.9927$); and with Mg^{2+}, $y = -27.122x + 128.26$ ($R^2 = 0.9921$).

Prenyltransferase Assay and Product Distribution Analyses. For kinetic analyses, enzyme assays of *Pc*IDS1 were carried out in a final volume of 200 μL containing 25 mM MOPSO (pH 7.3), 10% (vol/vol) glycerol, 150 mM NaCl, and 5 mM Mg^{2+} or 1 mM Co^{2+}, respectively. As substrates and countersubstrates, isopentenyl diphosphate (IDP), dimethylallyl diphosphate, and geranyl diphosphate (GDP; Sigma–Aldrich) were used. The countersubstrate concentration was kept constant at 50 μM; different experimental conditions are mentioned separately. The analyzed substrate ranged from 0.1 μM up to 100 μM. The reaction was heated to 30 °C and initiated by adding 0.2 μg of protein for Co^{2+} assays or 2 μg of protein for Mg^{2+} assays of the recombinant protein, and it was then incubated further at 30 °C. The water phase was analyzed by direct injection of 1 μL into the HPLC system at different time points from the same reaction mixture to identify the linear reaction velocity for every parameter. Calculation of the kinetic parameters was performed with GraphPad Prism version 5.04 (GraphPad Software) using the built-in enzyme kinetics module.

The pH optimum for the catalytic activity of *Pc*IDS1 was determined to be 7.0–7.5 in the presence of Mg^{2+} or Co^{2+}. However, the enzyme activity was quite stable over a broad range, from pH 4 to pH 8. Even the temperature optimum was not delimited to a narrow range. Acceptable activity with Mg^{2+} or Co^{2+} was measured from 15 °C up to 45 °C, whereas the optimum resided at 28 °C to 32 °C.

Activity testing of purified full-length *Pc*IDS1 in the presence of Mg^{2+} or Co^{2+} showed only about 5% of the activity in both cases in comparison to its truncated form, which lacks the predicted signal sequence.

For enzyme assay from larvae material, the samples were obtained by macerating different tissues with a 2-mL Potter–Elvehjem grinder with a Teflon pestle for 2 min at 4 °C with 300 μL of assay buffer. The suspension was centrifuged at 20,000 × *g*, and the protein concentration of the supernatant was determined. Ten micrograms of protein was used for standard assays and incubated at 30 °C for 60 min. The assays were stopped by adding 500 μL of chloroform and by mixing for 20 s, followed by centrifugation for 5 min at 5,000 × *g*. Subsequently, the water phase was transferred to a glass vial and measured directly by injecting 1 μL into the HPLC system. Protein concentrations were measured according to Bradford and Williams (3) and Bradford (4), using the Coomassie Plus Protein Assay Kit (Thermo Scientific Pierce) with BSA as a standard.

Liquid Chromatography-Tandem MS Method for *Pc*IDS1 Assay Product Determination. Analysis of isoprenoid diphosphates (IDS) was performed according to a modified method (5) on an Agilent 1260 HPLC system (Agilent Technologies) coupled to an API 5000 triple-quadrupole mass spectrometer (AB Sciex Instruments). For separation, a ZORBAX Extended C-18 column (1.8 μm, 50 mm × 4.6 mm; Agilent Technologies) was used. The mobile phase consisted of 5 mM ammonium bicarbonate in water as solvent A and acetonitrile as solvent B, with the flow rate set at 1.2 mL/min and the column temperature kept at 20 °C. Separation was achieved by using a gradient starting at 0% B, increasing to 90% B in 3 min and 100% B in 3.1 min (1-min hold), followed by a change to 0% B in 0.5 min (2.5-min hold) before the next injection. The injection volume for samples and standards [GDP and farnesyl diphosphate (FDP) from Sigma–Aldrich] was 1 μL; autosampler temperature was either 30 °C for assays without or 4 °C for assays with chloroform extraction. The mass spectrometer was used in the negative electrospray ionization (EI) mode. Optimal settings were determined using standards. Levels of ion source gases 1 and 2 were set at 60 and 70 psi, respectively, with a temperature of 700 °C. Curtain gas was set at 30 psi and collision gas was set at 7 psi, with all gases being nitrogen. Ion spray voltage was maintained at −4,200 V. Multiple-reaction monitoring (MRM) was used to monitor analyte parent ion-to-product ion formation: *m/z* 312.9/79 for GDP and *m/z* 380.9/79 for (*E,E*)-FDP. *Cisoid* products like neryl-diphosphate, (*Z,E*)-FDP, or (*Z,Z*)-FDP were not detected. Detection of GDP was omitted when used as substrate. Data analysis was performed using Analyst Software 1.6 Build 3773 (AB Sciex).

***Pc*IDS1 Antibody Production and Immunoblot Analysis.** For synthesis of polyclonal antibodies, a 16-aa peptide (HDLFFKIMKKIYKRDA) from the N-terminal end of the protein was used. The antibody was affinity-purified with 3 mg epoxy-immobilized antigen that was used for immunization (Davids Biotechnologie).

For immunoblot analysis, crude protein from different larval tissue was extracted in assay buffer as described above. Equal amounts of 5 μg of total protein of each tissue were separated by SDS/PAGE using any-KD acrylamide gels (BIO-RAD). Afterward, the proteins were transferred electrophoretically onto nitrocellulose membranes (BIO-RAD). Membranes were blocked with TBST [20 mM Tris (pH 7.5), 150 mM NaCl, 0.1% (vol/vol) Tween 20] and 10% nonfat milk, followed by incubation with 1:100 of the polyclonal anti-*Pc*IDS1 antibody at 16 °C overnight. After washing with blocking solution and a subsequent incubation with anti-rabbit HRP-conjugated secondary antibody, a final TBST washing was carried out. Signal detection was achieved by enhanced chemiluminescence (Thermo Scientific) and Amersham Hyperfilm ECL (GE Healthcare).

Sequence Comparison and Homology Modeling. Sequence similarity searches were performed using the alignment tool BLAST (6). Nucleotide sequences of different organisms were downloaded from the National Center for Biotechnology Information. To determine the degree of similarity between the members of insect scIDS and full-length *Pc*IDS1, sequence analysis was performed using the ClustalW tool (Lasergene 10 Core Suite; DNASTAR).

The 3D structure of truncated *Pc*IDS1 was modeled using the molecular modeling software YASARA (7). YASARA identified 15 templates based on alignment scores and low E-values suitable for homology modeling. Altogether, 32 models were automatically created and subsequently refined. The model based on the X-ray structure of FDP synthase from *Homo sapiens* deposited in the protein database (1zw5; see www.rcsb.org) (8, 9) appeared to be the most useful one. The structure of the model of *Pc*IDS1 has been deposited at the Protein Model DataBase (http://mi.caspur.it/PMDB/main.php) (10) and has been assigned the ID code PM0078683 for free download. The Mg^{2+} and the ligand binding position of IDP were automatically imported from the template's X-ray structure. The artificial cocrystallized zoledronic acid, [1-hydroxy-2-(1H-imidazol-1-yl)ethane-1,1-diyl]bis(phosphonic acid), was manually replaced by GDP. This model was then refined with the md-refinement tool of YASARA (7). The quality of the final model was checked with PROSA II (11) and PROCHECK (12). The graphical analysis with PROSA II showed one small loop (10 aa) area in positive energy range out-

side the active site. A combined energy z-score of −9.83 clearly indicated a native-like folded structure. Analysis of the calculated model with PROCHECK evaluated the consistency of all stereochemical parameters, such as the Ramachandran plot quality (92.3% of the backbone dihedral angles in most favored areas).

To investigate influences by the replacement of Mg^{2+} with Co^{2+}, the TRIPOS force field was used first (13). Thus, the atom types of Mg^{2+} were modified to Co^{2+}, and short molecular dynamics simulations (10 ps, 300 K) with subsequent energy minimization of GDP in the active site were performed. The Co^{2+} and the interacting side chains of all remaining amino acids except this ligand were kept fixed because the TRIPOS force field is not suitable for protein structure refinement. To estimate the interaction energies of different ions with the diphosphate moiety and aspartate side chains, density functional theory (DFT) B3LYP 6-311G++ calculations were performed using Gaussian 03 (14).

Tissue-Specific Expression of *Pc*IDS1. Quantitative real-time PCR was used for relative quantification (15). cDNA was synthesized from DNA-digested RNA and purified from three larvae per biological replicate using the RNAqueous Micro Kit (Life Technologies). Three biological replicates were analyzed twice. If technical replicates had a difference in the quantification cycle value greater than 1, the assay was repeated. Reference genes [*Pc*RPL8 (EMBL: AFQ22729.1) and *Pc*RPS3 (GenBank: KC109783)] were chosen. Real-time PCR data were acquired on an Mx3000P Real-Time PCR system (Agilent) using Brilliant III SYBR Green qPCR Master Mix (Agilent) according to the manufacturer's instructions. These analyses were performed following the minimum information for publication of quantitative real-time PCR experiments guidelines (16, 17).

RNAi in *P. cochleariae* Larvae. dsRNA was synthesized using the Megascript RNAi kit (Life Technologies) with altering of the elution buffer to 3.5 mM Tris·HCl, 1 mM NaCl, 50 nM Na_2HPO_4, 20 nM KH_2PO_4, 3 mM KCl, and 0.3 mM EDTA (pH 7.0). Off-target prediction was performed for highly specific silencing according to Bodemann et al. (18). The ORFs of full-length *PcIDS1* and *Gfp* were analyzed for off-target prediction by dicing the sequences *in silico* (19) and using the resulting putative 21-nt siRNAs for a BLASTn search linked to our transcriptome database of *P. cochleariae*. No putative off-target effects with other transcripts are predicted with the chosen dsRNA sequences on a critical value of at least 20 continuous nucleotides that have to be identical. The dsRNA synthesis templates with opposite T7-promotor sites were amplified out of sequenced plasmid pIB/V5-His (Life Technologies) containing full-length *PcIDS1* for 850 bp of *PcIDS1* using IDS1_FWD_T7_RNA (5′-TAATACGACTCACTATAGGGAGATCAAGCCAGTCTCCT-3′) as forward primer and IDS1_REV_T7_RNA (5′-TAATACGACTCACTATAGGGAGACTAAGCATCCCTCTTG-3′) as reverse primer and pCR3.1/CT-GFP-TOPO (Life Technologies) for 720 bp of *Gfp* (for primer, see ref. 18), respectively. The concentration of dsRNA was adjusted to 2 μg/μL, and for all injections, 250 nL (500 ng) of dsRNA solution was used.

Late first-instar larvae of *P. cochleariae* were used for injections. These were collected 5 d after hatching and were put in an incubator set to 16 h of light at 14 °C and 8 h of darkness at 12 °C for slow larval development after treatment. A Nano2000 injector (WPI) on a three-axis micromanipulator was used for injecting ice-chilled larvae parasagittal between the pro- and mesothorax.

Relative Quantification of 8-Hydroxygeraniol-Glucoside in *P. cochleariae* Fat Body and Hemolymph. Analysis was done on an Agilent 1260 HPLC system (Agilent Technologies) coupled to an API 5000 triple-quadrupole mass spectrometer (AB Sciex Instruments). For separation, a ZORBAX Eclipse XDB-C-18 column (1.8 μm, 50 mm × 4.6 mm; Agilent Technologies) was used. The mobile phase consisted of 20 mM ammonium formate in water as solvent A and acetonitrile as solvent B, with the flow rate set at 1.0 mL/min and the column temperature kept at 20 °C. Separation was achieved by using a gradient starting at 10% solvent B, increasing to 95% solvent B in 5 min (1-min hold), followed by a change to 10% solvent B in 1 min (1-min hold) before the next injection. Injection volume for samples and standards was 5 μL; the autosampler temperature was 4 °C. The mass spectrometer was used in negative EI mode. Optimal settings were determined using a standard. Ion source gases 1 and 2 were set at 70 psi, with a temperature of 700 °C. Curtain gas was set at 25 psi and collision gas was set at 6 psi, with all gases being nitrogen. Ion spray voltage was maintained at −3000 V. The monitored MRM transition was *m/z* 377.3/331.2. Data analysis was performed using Analyst Software 1.6 Build 3773 (AB Sciex).

Relative Quantification of Chrysomelidial in Defense Secretions of *P. cochleariae*. Secretions were collected and weighed in pulled-out glass capillaries from different instar stages of treated larvae, and they were then diluted 1:200 (wt/vol) in ethyl acetate supplemented with 100 μg/mL methyl benzoate as an internal standard. One microliter was subjected to GC-EI-MS analysis [ThermoQuest Finnigan ITQ GC-MS 2000 (quadrupole) equipped with Phenomenex ZB-5-W/Guardian-column, 25 m (10-m Guardian precolumn) × 0.25 mm, film thickness of 0.25 μm]. Substances were separated splitless using helium as a carrier (1.5 mL/min). Conditions were set as follows: 50 °C (2 min), 20 °C/min to 130 °C, 40 °C/min to 200 °C, 20 °C/min to 220 °C, and 40 °C/min to 300 °C (1 min). Inlet temperature was 220 °C, and transfer line temperature was 280 °C. Chrysomelidial was identified according to Oldham et al. (20). The peak areas were obtained using the Interactive Chemical Information System algorithm that is implemented in the Xcalibur bundle (version 2.0.7; Thermo Scientific). The relative amount of chrysomelidial per larva has been calculated with the following equation, in which *mChry* is the relative amount of chrysomelidial per larva, *AoChry* is the peak area of chrysomelidial, *AoMB* is the peak area of methyl benzoate, and *mSec* is the average mass of secretion per larva:

$$mChry = \left(\frac{AoChry}{AoMB} * dilution\right) * mSec.$$

Fitness Measurements. The development of larval weight was documented using five replicates of three larvae. Larval weight was measured per replicate on an ultramicrobalance in a 24-h ± 3-h period. In accordance with the method used by Kuehnle and Mueller (21), the relative growth rate was calculated using the weight of freshly emerged pupae as the final larval developmental stage.

1. Discher S, et al. (2009) A versatile transport network for sequestering and excreting plant glycosides in leaf beetles provides an evolutionary flexible defense strategy. *ChemBioChem* 10(13):2223–2229.
2. Petersen TN, Brunak S, von Heijne G, Nielsen H (2011) SignalP 4.0: Discriminating signal peptides from transmembrane regions. *Nat Methods* 8(10):785–786.
3. Bradford MM, Williams WL (1976) New, rapid, sensitive method for protein determination. *Fed Proc* 35(3):274.
4. Bradford MM (1976) A rapid and sensitive method for the quantitation of microgram quantities of protein utilizing the principle of protein-dye binding. *Anal Biochem* 72(1-2):248–254.
5. Nagel R, Gershenzon J, Schmidt A (2012) Nonradioactive assay for detecting isoprenyl diphosphate synthase activity in crude plant extracts using liquid chromatography coupled with tandem mass spectrometry. *Anal Biochem* 422(1):33–38.

6. Altschul SF, Lipman DJ (1990) Protein database searches for multiple alignments. *Proc Natl Acad Sci USA* 87(14):5509–5513.
7. Krieger E, et al. (2009) Improving physical realism, stereochemistry, and side-chain accuracy in homology modeling: Four approaches that performed well in CASP8. *Proteins* 77(Suppl 9):114–122.
8. Kavanagh KL, Dunford JE, Bunkoczi G, Russell RG, Oppermann U (2006) The crystal structure of human geranylgeranyl pyrophosphate synthase reveals a novel hexameric arrangement and inhibitory product binding. *J Biol Chem* 281(31):22004–22012.
9. Kavanagh KL, et al. (2006) The molecular mechanism of nitrogen-containing bisphosphonates as antiosteoporosis drugs. *Proc Natl Acad Sci USA* 103(20): 7829–7834.
10. Castrignanò T, De Meo PD, Cozzetto D, Talamo IG, Tramontano A (2006) The PMDB Protein Model Database. *Nucleic Acids Res* 34:D306–D309.
11. Sippl MJ (1990) Calculation of conformational ensembles from potentials of mean force. An approach to the knowledge-based prediction of local structures in globular proteins. *J Mol Biol* 213(4):859–883.
12. Laskowski RA, MacArthur MW, Moss DS, Thornton JM (1993) PROCHECK—A program to check the stereochemical quality of protein structures. *J Appl Cryst* 26(2):283–291.
13. Clark M, Cramer RD, Van Opdenbosch N (1989) Validation of the General Purpose Tripos 5.2 Force Field. *J Comp Chem* 10(8):982–1012.
14. Frisch MJ, et al. (2004) Gaussian 03, Revision C.02. (Gaussian, Wallingford CT).
15. Livak KJ, Schmittgen TD (2001) Analysis of relative gene expression data using real-time quantitative PCR and the $2^{(-\Delta\Delta C(T))}$ Method. *Methods* 25(4):402–408.
16. Bustin SA, et al. (2010) MIQE précis: Practical implementation of minimum standard guidelines for fluorescence-based quantitative real-time PCR experiments. *BMC Mol Biol* 11:74–78.
17. Bustin SA, Johnson G, Agrawal SG (2012) [MIQE—Guidelines for developing robust real-time PCR assays]. *Mycoses* 55(Suppl 2):30–34. German.
18. Bodemann RR, et al. (2012) Precise RNAi-mediated silencing of metabolically active proteins in the defence secretions of juvenile leaf beetles. *Proc Biol Sci* 279(1745):4126–4134.
19. Naito Y, et al. (2005) dsCheck: Highly sensitive off-target search software for double-stranded RNA-mediated RNA interference. *Nucleic Acids Res* 33(Web Server issue): W589-91.
20. Oldham NJ, Veith M, Boland W, Dettner K (1996) Iridoid monoterpene biosynthesis in insects—Evidence for a *de novo* pathway occurring in the defensive glands of *Phaedon armoraciae* (Chrysomelidae) leaf beetle larvae. *Naturwissenschaften* 83(10): 470–473.
21. Kuehnle A, Mueller C (2011) Responses of an oligophagous beetle species to rearing for several generations on alternative host-plant species. *Ecol Entomol* 36(2):125–134.

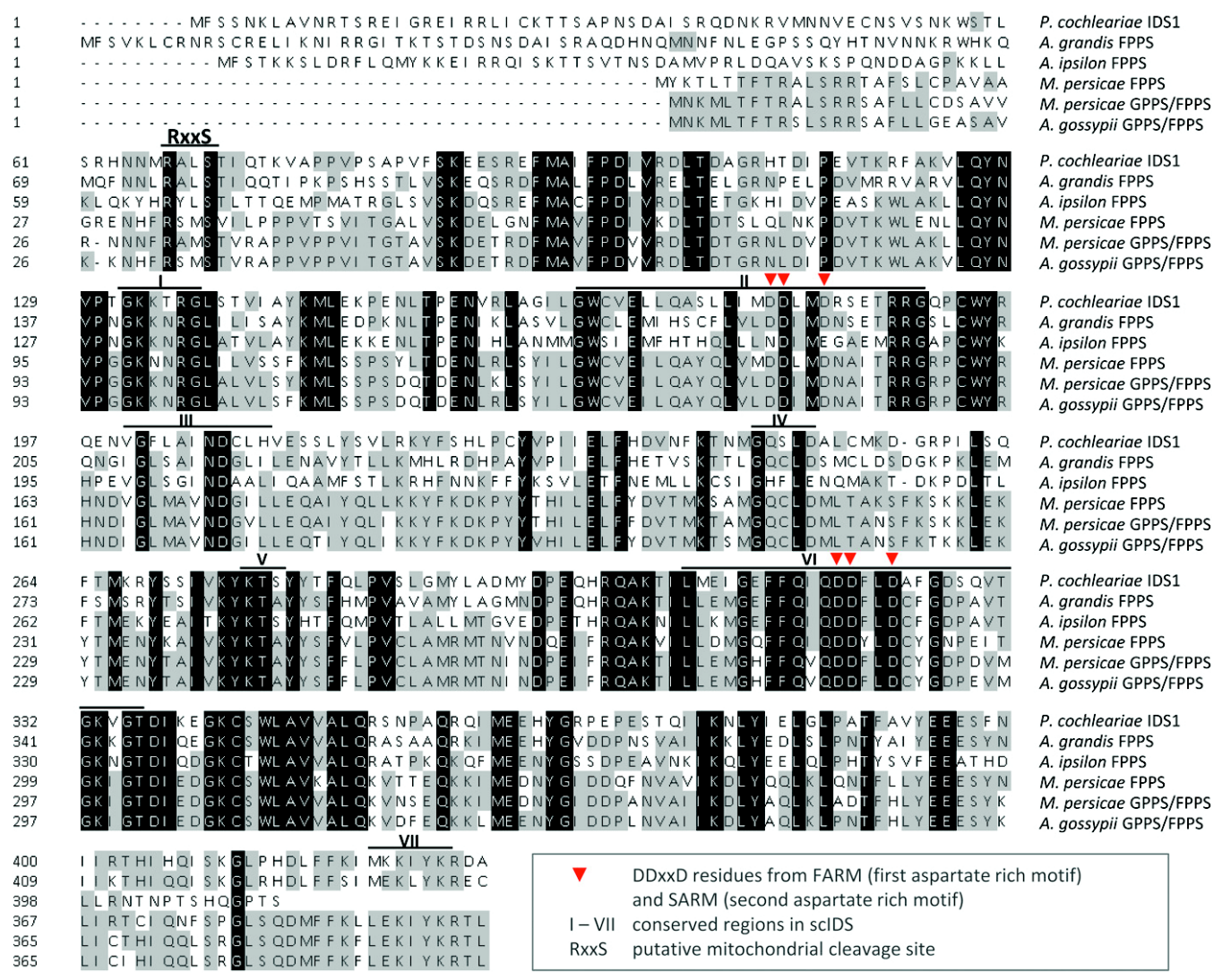

Fig. S1. Amino acid alignment (ClustalW) of full-length *Pc*IDS1 from *P. cochleariae* with other insect scIDSs. Sequence identity to other farnesyl diphosphate synthases (FDPSs): *Anthonomus grandis* (54.1%) (GenBank: AAX78434), *Myzus persicae* (45.4%) (GenBank: ABY19313), and *Agrotis ipsilon* (45.2%) (GenBank CAA08918). Sequence identity to bifunctional FDPSs/GDPSs: *Aphis gossypii* (48.6%) (EMBL: ACT79808) and *M. persicae* (48.4%) (EMBL: ABY19312). (Residues in black are identical in all sequences; gray residues are >50% identical in aligned sequences.)

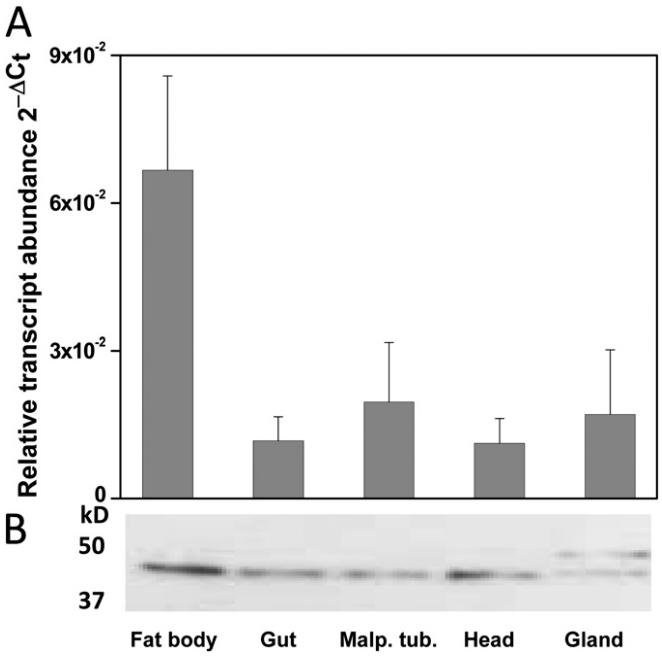

Fig. S2. (*A*) Relative transcript abundance ($2^{\Delta Ct}$) of *PcIDS1* in different larval tissues. (*B*) Western blot analyses of 5 μg of protein per lane probed with sequence-specific antibodies against *Pc*IDS1, followed by ECL detection. Malp. tub, Malpighian tubules.

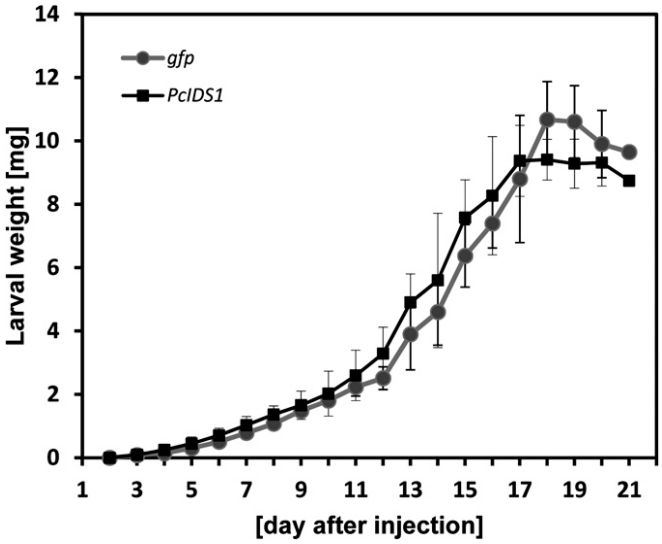

Fig. S3. Relative growth rate of RNAi-induced larvae from *P. cochleariae*. The development of larval weight was documented and measured in a 24-h ± 3-h period. No significant differences in the relative growth rate were observed between *Gfp*- and *PcIDS1*-injected larvae. The final larval developmental stage was the weight of freshly emerged pupae (n = 15, ±SD).

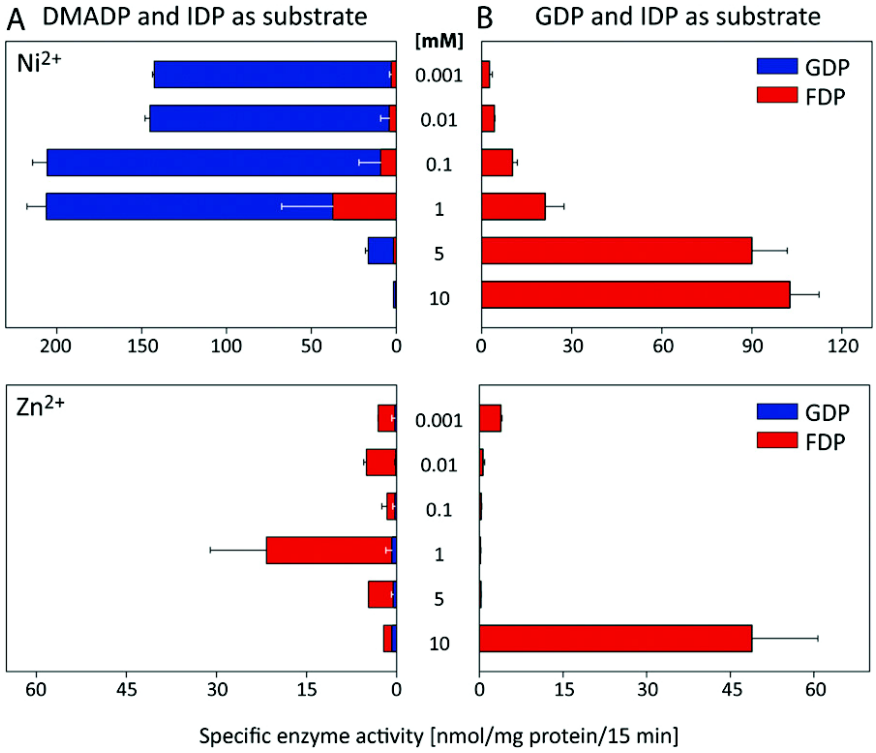

Fig. S4. Effect of metal cofactors regarding product formation and enzyme activity of *Pc*IDS1. (*A*) Different concentrations of Ni^{2+} and Zn^{2+} were added to *Pc*IDS1 and incubated with 50 μM IDP and 50 μM dimethylallyl diphosphate (DMADP; $n = 3$, ±SD). (*B*) Different concentrations of Ni^{2+} and Zn^{2+} were added to *Pc*IDS1 and incubated with 50 μM IDP and 50 μM GDP ($n = 3$, ±SD).

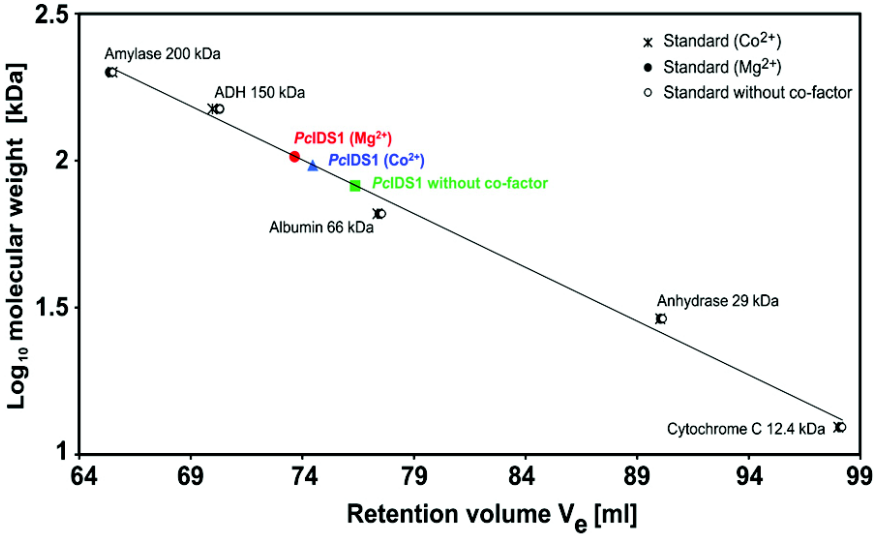

	Elution volume			MW log10			calc. MW (kDa)		
	No co-factor	Co^{2+}	Mg^{2+}	No co-factor	Co^{2+}	Mg^{2+}	No co-factor	Co^{2+}	Mg^{2+}
*Pc*IDS1	76.3	74.4	73.6	1.91	1.98	2.01	74.6	87.6	93.8
Amylase	65.5	65.4	65.3	2.31	2.31	2.31	207.5	204.9	208.5
ADH	70.3	69.9	70.2	2.14	2.14	2.13	138.1	140.1	137.2
Albumin	77.5	77.3	77.4	1.87	1.87	1.87	74.5	74.8	74.7
Anhydrase	90.1	90.0	90.0	1.40	1.40	1.40	25.6	25.5	25.6
Cytochrome C	98.1	98.0	98.0	1.11	1.11	1.11	12.9	12.9	12.9

Fig. S5. Analytical size exclusion chromatography of *Pc*IDS1. The plot shows the relative retention volumes of the protein molecular weight standards and the calculated standard curve by linear regression dependent on the divalent ions. The relative retention volumes of the apoprotein *Pc*IDS1 are shown by the green rectangle. The shifts of the retention volume dependent on the divalent metal cofactor are represented by the red dot in the presence of Mg^{2+} and the blue triangle in the presence of Co^{2+}.

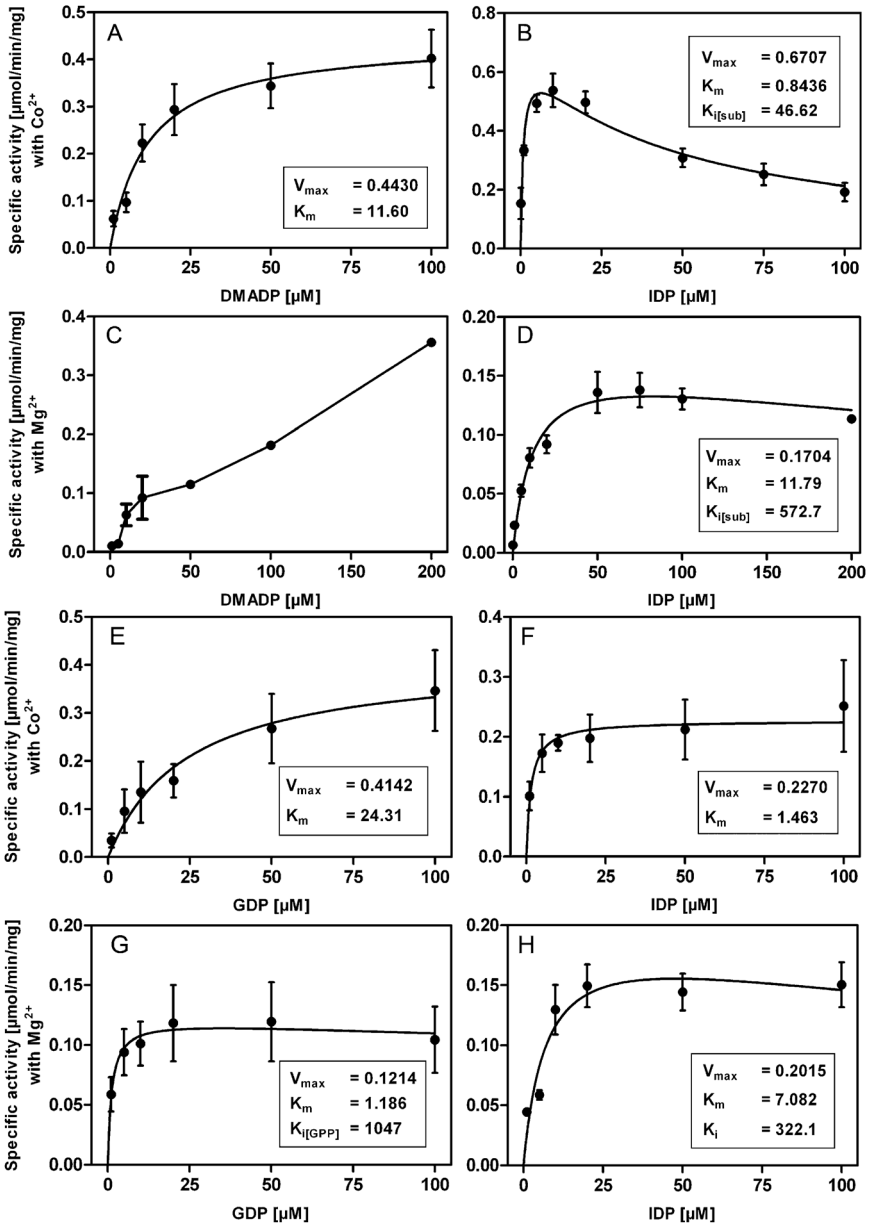

Fig. S6. Kinetic analyses of *Pc*IDS1 with nonlinear regression and built-in function calculated with GraphPad Prism version 5.04. (*A*) Calculation according to the Michaelis–Menten kinetic of $K_{m(DMADP)}$ with Co^{2+} and 15 µM IDP. (*B*) Calculation with substrate inhibition of $K_{m(IDP)}$ with Co^{2+} and 50 µM dimethylallyl diphosphate (DMADP). (*C*) Enzyme activity data with variable DMADP in the presence of Mg^{2+} and 50 µM IDP. (*D*) Calculation with substrate inhibition of $K_{m(IDP)}$with Mg^{2+} and 50 µM DMADP. (*E*) Calculation according to the Michaelis–Menten kinetic of $K_{m(GDP)}$ with Co^{2+} and 50 µM IDP as countersubstrate. (*F*) Calculation according to the Michaelis–Menten kinetic of $K_{m(IDP)}$ with Co^{2+} and 50 µM GDP as countersubstrate. (*G*) Calculation with substrate inhibition of $K_{m(GDP)}$ with Mg^{2+} and 50 µM IDP as countersubstrate. (*H*) Calculation with substrate inhibition of $K_{m(IDP)}$ with Mg^{2+} and 50 µM GDP as countersubstrate.

Table S1. Enzyme activity of *Pc*IDS1 with different metal cofactors

Substrate	Ion	Optimal cofactor concentration, mM	Total activity, nmol/mg of protein per 15 min (±SD)	GDP activity, % of total activity
DMADP	Co^{2+}	0.5	1,022.33 (±72.2)	95.9
	Mg^{2+}	5	418.85 (±6.2)	18.3
	Mn^{2+}	0.5	239.66 (±16.2)	98.8
	Ni^{2+}	0.1	206.8 (±41.3)	81.9
	Zn^{2+}	0.1	21.69 (±24.1)	96.3
GDP	Co^{2+}	0.01	333.56 (±48.13)	
	Mg^{2+}	0.5	967.25 (±136.4)	
	Mn^{2+}	0.01	785.07 (±136.5)	
	Ni^{2+}	0.001	102.68 (±9.6)	
	Zn^{2+}	0.001	48.90 (±11.8)	

DMADP, dimethylallyl diphosphate.

Table S2. ICP-OES and ICP-MS analyses of fat body and gut tissue of *P. cochleariae* larvae

		Fat body 1		Fat body 2		Gut	
Element	Method	DW, µg/g (±SD)	DW, µmol/g	DW, µg/g (±SD)	DW, µmol/g	DW, µg/g (±SD)	DW, µmol/g
Ca	ICP-OES	753.2 (±0.3)	18.7	788 (±16)	19.6	893 (±12)	22.2
Co	ICP-MS	0.243 (±0.005)	0.0041	0.198 (±0.005)	0.0033	0.297 (±0.001)	0.005
Cu	ICP-MS	14.09 (±0.07)	0.221	14.9 (±0.2)	0.234	12.88 (±0.03)	0.203
Fe	ICP-MS	41.7 (±0.1)	0.746	41.8 (±0.5)	0.748	92.6 (±0.04)	1.658
K	ICP-OES	12,075 (±274)	308.8	12,112 (±71)	309.8	18,299 (±4)	468
Mg	ICP-OES	2,223 (±41)	91.4	2,255.5 (±0.5)	92.8	2,205.2 (±0.4)	90.7
Mn	ICP-MS	16.51 (±0.04)	0.301	16.706 (±0.002)	0.304	47.3 (±0.4)	0.861
Na	ICP-OES	462 (±11)	20.1	463 (±5)	20.1	499.2 (±0.4)	21.7
Ni	ICP-MS	0.36 (±0.01)	0.0061	0.3598 (±0.0007)	0.0061	0.88 (±0.08)	0.0149
Zn	ICP-MS	62.3 (±0.3)	0.952	62.66 (±0.02)	0.958	141.1 (±0.03)	2.158

DW, dry weight; ICP-MS, inductively coupled plasma mass spectrometry; ICP-OES, inductively coupled plasma optical emission spectrometry.

Table S3. Energies of the compounds and resulting reaction energies for the formation of diphosphate metal complexes in kilocalories per mole calculated with density functional theory (DFT) B3LYP 6-311G++ (d.p)

	Products energy	Educts energy			
X	X-DP^{3-}	X	DP^{3-}	Reaction energy	Δ to Mg^{2+}
Mg^{2+}	−885,175.2	−125,023.7	−759,218.5	−933.0	0
Co^{2+}	−16,277,257.6	−867,059.6	−759,218.5	−979.6	−46.6
Mn^{2+}	−1,481,820.2	−721,619.3	−759,218.5	−982.4	−49.4

X, metal cation.

Table S4. Energies of the compounds and resulting reaction energies for the formation of propionic acid metal complexes in kilocalories per mole calculated with DFT B3LYP 6-311G++ (d.p)

	Products energy	Educts energy			
X	$X(CH_3CH_2COO^-)_2$	X	$(CH_3CH_2COO^-)_2$	Reaction energy	Δ to Mg^{2+}
Mg^{2+}	−461,861.2	−125,023.7	−336,166.4	−671.1	0
Co^{2+}	−1,203,933.8	−867,059.6	−336,166.4	−712.6	−41.5
Mn^{2+}	−1,058,498.3	−721,619.3	−336,166.4	−707.8	−36.7

X, metal cation.

Table S5. Energies of the compounds and resulting reaction energies for the formation of metal complexes with both propionic acid and diphosphate using the metal cation diphosphate complex as educt in kilocalories per mole calculated with DFT B3LYP 6-311G++ (d.p)

	Products energy	Educts energy			
X	$CH_3CH_2COO^- \times (P_2O_7H_3)^-$	$X\ (P_2O_7H_3)^-$	$CH_3CH_2COO^-$	Reaction energy	Δ to Mg^{2+}
Mg^{2+}	−1,054,033.6	−885,711.5	−168,083.2	−238.9	0
Co^{2+}	−1,796,098.5	−1,627,782.5	−168,083.2	−232.8	6.1
Mn^{2+}	−1,650,660.9	−1,482,341.6	−168,083.2	−236.1	2.8

X, metal cation.

Table S6. Energies of the compounds and resulting reaction energies for the formation of metal complexes with both propionic acid and diphosphate using the metal cation propionic acid complex as educt in kilocalories per mole calculated with DFT B3LYP 6-311G++ (d.p)

	Products energy	Educts energy			
X	$CH_3CH_2COO^- \times (P_2O_7H_3)^-$	$(P_2O_7H_3)^-$	$CH_3CH_2COO^-\ X$	Reaction energy	Δ to Mg^{2+}
Mg^{2+}	−1,054,033.6	−760,331.1	−293,532.0	−170.5	0
Co^{2+}	−1,796,098.5	−760,331.1	−1,035,599.4	−168.0	2.5
Mn^{2+}	−1,650,660.9	−760,331.1	−890,171.2	−158.6	11.9

X, metal cation.

Manuskript 2: (Stock, Gretscher u.a. 2013)

Da dieses Paper zum Zeitpunkt des Druckes der vorliegenden Belegversion der Dissertation bereits publiziert vorliegt, wurde hier nicht wie in der Gutachter-Version das vorläufige Manuskript eingebunden, sondern die publizierte Version. Beide unterscheiden sich lediglich in ihrem Layout, nicht aber in ihrem Inhalt. (Anm. d. Autors)

Da das Ergänzungsmaterial dieser Arbeit sehr umfangreich ist, wurde in dieser Version lediglich die Abbildung S9 angehängt, die für die Diskussion der Ergebnisse wichtig ist. Die weiteren Anhänge finden Sie auf der beiliegenden CD.

OPEN ACCESS Freely available online

PLOS ONE

Putative Sugar Transporters of the Mustard Leaf Beetle *Phaedon cochleariae*: Their Phylogeny and Role for Nutrient Supply in Larval Defensive Glands

Magdalena Stock[1], René R. Gretscher[1], Marco Groth[2], Simone Eiserloh[1], Wilhelm Boland[1], Antje Burse[1]*

1 Department of Bioorganic Chemistry, Max Planck Institute for Chemical Ecology, Jena, Thuringia, Germany, **2** Genome Analysis Group, Leibniz Institute for Age Research – Fritz Lipmann Institute, Jena, Thuringia, Germany

Abstract

Background: Phytophagous insects have emerged successfully on the planet also because of the development of diverse and often astonishing defensive strategies against their enemies. The larvae of the mustard leaf beetle *Phaedon cochleariae*, for example, secrete deterrents from specialized defensive glands on their back. The secretion process involves ATP-binding cassette transporters. Therefore, sugar as one of the major energy sources to fuel the ATP synthesis for the cellular metabolism and transport processes, has to be present in the defensive glands. However, the role of sugar transporters for the production of defensive secretions was not addressed until now.

Results: To identify sugar transporters in *P. cochleariae*, a transcript catalogue was created by Illumina sequencing of cDNA libraries. A total of 68,667 transcripts were identified and 68 proteins were annotated as either members of the solute carrier 2 (SLC2) family or trehalose transporters. Phylogenetic analyses revealed an extension of the mammalian GLUT6/8 class in insects as well as one group of transporters exhibiting distinctive conserved motifs only present in the insect order Coleoptera. RNA-seq data of samples derived from the defensive glands revealed six transcripts encoding sugar transporters with more than 3,000 counts. Two of them are exclusively expressed in the glandular tissue. Reduction in secretions production was accomplished by silencing two of four selected transporters. RNA-seq experiments of transporter-silenced larvae showed the down-regulation of the silenced transporter but concurrently the up-regulation of other SLC2 transporters suggesting an adaptive system to maintain sugar homeostasis in the defensive glands.

Conclusion: We provide the first comprehensive phylogenetic study of the SLC2 family in a phytophagous beetle species. RNAi and RNA-seq experiments underline the importance of SLC2 transporters in defensive glands to achieve a chemical defense for successful competitive interaction in natural ecosystems.

Citation: Stock M, Gretscher RR, Groth M, Eiserloh S, Boland W, et al. (2013) Putative Sugar Transporters of the Mustard Leaf Beetle *Phaedon cochleariae*: Their Phylogeny and Role for Nutrient Supply in Larval Defensive Glands. PLoS ONE 8(12): e84461. doi:10.1371/journal.pone.0084461

Editor: Claude Wicker-Thomas, CNRS, France

Received September 26, 2013; **Accepted** November 22, 2013; **Published** December 31, 2013

Funding: The authors' work was funded by the Max Planck Society (http://www.mpg.de/en) and the Deutsche Forschungsgemeinschaft (grand number BU1862/2-1; http://www.dfg.de/en/index.jsp). The funders had no role in study design, data collection and analysis, decision to publish, or preparation of the manuscript.

Competing Interests: The authors have declared that no competing interests exist.

* E-mail: aburse@ice.mpg.de

Introduction

Sugar sweetens our life. Glucose is one of the major energy sources and an important substrate for both protein and lipid synthesis. Its catabolism fuels cellular respiration for ATP production. For glucose absorption in the mammalian small intestine two pathways are known: the passive, paracellular absorption which bats rely on for more than 70% of their total sugar uptake [1] and the transporter-mediated transcellular pathways which non-flying mammals use preferentially. They take up glucose from interstitial fluid by a passive, facilitative transport process driven by the downward concentration gradient across the plasma membrane [2]. Exclusively in the epithelial cell brush border of the small intestine and the kidney proximal convoluted tubules, glucose is absorbed or reabsorbed against its electrochemical gradient by a secondary active transport mechanism which uses the sodium concentration gradient established by Na^+/K^+/ATP pumps [3]. Unlike glucose in mammals, the major blood (hemolymph) sugar of insects is often the disaccharide trehalose (α-D-glucopyranosyl-α-D-glucopyranoside) [4–6]. It is synthesized from glucose phosphates in fat body tissue and serves as a source of carbohydrates for various tissues including flight muscles [7,8], intestinal tract [9], fat body [10] or ovaries [11]. Besides trehalose absorption, the absorption of other sugars, such as fructose, glucose, and galactose, has been shown for different insect tissues [12–17]. Only few examples of sugar transport proteins from insects have been functionally characterized to date [17–23]. Except for SCRT, which was classified as a member of family 49 of solute carriers (SLCs) [17], they all belong to the SLC2 family of glucose and polyol transporters [24–27]. In principle, SLC2 proteins are integral membrane proteins exhibiting a predicted twelve transmembrane domain topology. The so-called 'sugar transport signatures' that signify substrate binding and catalytic activity are also conserved in the SLC2 family. Usually, the expression of these proteins is tissue-specific and

responds to metabolic and hormonal regulation. Each of the transporters possesses different affinities for sugars [28].

Although beetles (Coleoptera) represent one of the most diversified lineages on earth with about 350,000 species described and total numbers probably an order of magnitude higher, SLC2 sugar transporters of beetles have not been in the focus of researchers so far. In particular, Chrysomelidae (leaf beetles) constitute, together with the Cerambycidae (longhorn beetles) and the Curculionoidea (weevils), the largest beetle radiation, namely "Phytophaga", which represent about 40% of all known species [29]. Among phytophagous beetles are many pests such as the mustard leaf beetle *Phaedon cochleariae* which causes yield losses on cruciferous crops in Europe [30]. This species is adapted to use host plants' leaves as its food source for the duration of its life [31,32]. Due to its life in an exposed environment, it has to be protected against both the noxious effect of plant secondary metabolites and the attacks by its predators and parasitoids.

When it comes to producing defensive compounds to repel their omnipresent enemies, insect in general are very innovative [33]. To circumvent auto-intoxicative effects, these natural products frequently are processed in exocrine glands [34–36]. *P. cochleariae* is known to produce defensive compounds in such glands, herein further referred to as defensive glands, in the larval as well as in the adult stage [37–41]. The juvenile beetles possess nine pairs of these glands on their back and release deterrent secretions upon disturbance [42,43]. Each of these glands is composed of several secretory cells which are attached to a large reservoir. The anti-predatory effect of the secretions can be attributed to cyclopentanoid monoterpenes (iridoids) which are synthesized within the reservoir by few enzymatic reactions from a pre-toxin which is made in the fat body and from there transferred into the defensive glands [44,45]. Previously it has been shown that defensive gland cells possess ATP-binding cassette (ABC) transporters which are crucial for the shuttling of pre-toxins into the reservoir [46]. Because ATP is used for the cellular metabolism and transport process into the defensive glands, sugars need to be delivered by transporters to drive ATP production in this tissue. Although defensive secretions from phytophagous insects are key players in trophic interactions found in terrestrial food webs [47], their production pathways are often not fully understood. Sugar transporters may be essential components to fuel energy in insect defensive glands, however, nothing is known about their *in vivo* relevance for deterrent production.

Here we focus on a first catalogue of putative members of the SLC2 family as well as trehalose transporters for a phytophagous leaf beetle species. By means of a *de novo*-assembled transcriptome created from the mRNA of *P. cochleariae*, we have performed comprehensive and statistically supported phylogenetic analyses of the identified sequences together with their orthologs selected from other insects and other Metazoa including the known human glucose transporter (GLUT) isoforms. Our data revealed an enormous expansion of the GLUT6/8 sister group in insects and a clade of sequences unique for beetles. Subsequent next generation sequencing-based expression studies revealed putative SLC2 transcripts highly expressed in the defensive glands of juvenile *P. cochleariae*. Single silencing of selected SLC2-candidates by RNA interference (RNAi) resulted only in two cases in a reduced production of defensive secretions. However, in two other cases silencing did not affect deterrent production suggesting an adaptive backup system which stabilizes the sugar level in the defensive glands. To prove the observed homeostasis, we subsequently sequenced the mRNA of silenced larvae to study the differential expression of putative SLC2 transporters not only on phenotypic but also on a transcriptional level.

Materials and Methods

Beetles

P. cochleariae (F.) was lab-reared on *Brassica rapa chinensis* in a light/dark cycle of 16 h light and 8 h darkness, 14°C±1°C in light and 12°C±1°C in darkness.

RNA Isolation, Library Construction and Sequencing

Total RNA was isolated from tissue samples from *P. cochleariae* larvae as described by Bodemann *et al.* [48]. Up to 5 µg of total RNA was then used for library preparation using TruSeq™ RNA Sample Prep Kit according to manufacturer's description. RNA sequencing (RNA-seq) was done using Illumina next-generation sequencing technique [49] on a HiSeq2000 (Illumina, Inc., San Diego, California USA) in 50 bp single-read mode (two or three samples multiplexed in one lane). Pooled total RNAs from the different tissues (such as defensive glands, gut, fat body, Malpighian tubules, and head) from larval *P. cochleariae* were used for paired-end sequencing. Therefore, the fragmentation step during library preparation of the pooled total RNAs was shortened to four minutes (seven minutes for all the remaining samples) to obtain longer fragments. This library was sequenced using a GAIIx (Illumina, Inc., San Diego, California USA) in 150 bp paired-end mode in one sample per lane. All reads were extracted in FastQ format using CASAVA v1.7 (HiSeq) and v1.8 (GAIIx) (Illumina, Inc., San Diego, California USA) for further analysis.

Subsequently to the RNAi experiments (described below), additional sequencing was carried out. Four samples of glandular tissue (one sample of *gfp* dsRNA-injected larvae and three samples of larvae injected with dsRNA of three highly abundant sugar transporters) – two biological replicates each, have been prepared as mentioned above and sequenced on a HiSeq2500 (Illumina, Inc., San Diego, California USA) in 50 bp single-read mode (multiplexed in one lane). All reads were extracted in FastQ format using bcl2fastq v.1.8.3 (Illumina, Inc., San Diego, California USA). The raw sequence data are listed in Table 1 and are stored in the Sequence Read Archive at NCBI (cDNA library 1: SRA100673; cDNA libraries 2: SRA106118, SRA106122, SRA106161; cDNA libraries 3: SRA108012, SRA108036; cDNA libraries 4: SRA108037, SRA108041; cDNA libraries 5: SRA109958, SRA109964; cDNA libraries 6: SRA109966, SRA109967). The corresponding BioProject for *P. cochleariae* can be accessed at NCBI homepage (BioProject ID: PRJNA210148).

Transcriptome *de novo* Assembly

The paired-end reads were assembled using Trinity, a RNA-seq *de novo* assembly software [50,51] with default parameters, minimal contig length of 300 bp and paired fragment length of 500 bp. Afterwards, the *de novo* assembled transcripts were reassembled using the TGI Clustering tools (TGICL), a software program to cluster large EST datasets [52]. The clustering step is performed by NCBI's megablast [53] and the resulting clusters are then assembled using CAP3 assembly program [54] with following parameters: minimum overlap length of 100 bp and sequence similarity of 90 percent.

Pfam Analysis

The *de novo* transcripts were translated into their possible protein sequences (all six reading frames) by applying the transeq script which is part of the EMBOSS package (http://imed.med.ucm.es/EMBOSS/). Thereafter, the script pfam-scan.pl (downloaded from the ftp://ftp.sanger.ac.uk/pub/databases/Pfam/Tools/site) was used with showing overlapping hits within clan member families in addition to default parameters to search the protein

Table 1. Overview of the raw sequence data.

cDNA library	Tissues for RNA isolation	Total number of reads	Sequencing mode	Remarks
1	gut, fat body, glands, Malpighian tubules	46,030,279	GAIIx 2×150 bp	–
2	glands (3 replicates)	101,383,127	50 bp, HiSeq2000	–
3	glands (2 replicates)	33,013,829	50 bp, HiSeq2500	dsRNA-*gfp* injected
4	glands (2 replicates)	50,926,062	50 bp, HiSeq2500	dsRNA-*Pcsut1* injected
5	glands (2 replicates)	59,678,392	50 bp, HiSeq2500	dsRNA-*Pcsut2* injected
6	glands (2 replicates)	53,204,574	50 bp, HiSeq2500	dsRNA-*Pcsut6* injected

The table exhibits the RNA derived specimens, number of reads, sequencing technology and sequencing mode.
doi:10.1371/journal.pone.0084461.t001

sequences against the Pfam-A database which consists of high quality protein families based on profile HMMs and clans. A clan is a collection of Pfam-A entries which are related by similarity of sequence, structure or profile-HMM [55,56].

Identification of SLC2 Sequences and Trehalose Transporters

The SLC2 sequences and trehalose transporters were identified by searching the Pfam results for Sugar_tr hits. Sugar (and other) transporters are part of the major facilitator superfamily [25] which is believed to function primarily in the uptake of sugars. All identified sugar transporters were searched *via* BLASTp with an E-value smaller than 1e-3 against the Swiss-Prot protein database (ftp://ftp.ncbi.nlm.nih.gov/blast/db/). Swiss-Prot is a high quality and manually annotated and reviewed, non-redundant protein sequence database [57,58]. For each sugar transporter the top ten hits were inspected, and sequences homologous to known SLC2 or trehalose transporters were identified. SLC2 and trehalose transporters of full-length transcripts or those having a coding sequence of at least 900 bp of length were chosen for further analysis. All studied sugar transporter transcripts are stored in the GenBank database at NCBI as either mRNA (accession numbers: KF803259–KF803269) or Transcriptome Shotgun Assembly (TSA) sequences. This TSA project has been deposited at DDBJ/EMBL/GenBank under the accession GAPU00000000. The version described in this paper is the first version, GAPU01000000. All those sugar transporters were then observed by applying TMHMM [59] and Memsat2 [60] to predict their 12 transmembrane (TM) domains.

Calculation of Phylogenetic Trees

Phylogenetic trees were calculated for identified SLC2 encoding sequences (see above). Amino acid sequences in multi-FASTA format were aligned using Probalign version 1.4 [61] with default parameters or MAFFT version 7.023b with following settings: –maxiterate 1000 and –localpair. Thereafter, phylogenetic trees were calculated using MrBayes [62,63] version 3.2.1 and RAxML [64] version 7.2.8 which use different methods. Namely, MrBayes uses Bayesian inference of phylogeny, and RAxML uses maximum likelihood estimation. Applying MrBayes the following settings were used: number of generations was set to 300,000, samplefreq and printfreq were set to 100, the number of runs was set to 2, and the type to calculate the consensus tree was set to allcompat. Applying RAxML the following parameters were used: the model of substitution was PROTGAMMAJTT (GAMMA model of rate heterogeneity), and 1000 rapid bootstrap inferences were done.

Table 2. Characterized trehalose as well as glucose/fructose transporters.

	Description	NCBI accession	Organism
AaSUT_XP_001664193	sugar transporter	XP_001664193.1	*Aedes aegypti*
AgTRET1_BAF96742	trehalose transporter AgTRET1	BAF96742.1	*Anopheles gambia*
AmTRET1_NP_001107211	trehalose transporter 1	NP_001107211.1	*Apis mellifera*
ApTret1like_XP_001950697	fac trehalose transporter Tret1-like	XP_001950697.1	*Acyrthosiphon pisum*
BmTRET1_NP_001108344	fac trehalose transporter Tret1	NP_001108344.1	*Bombyx mori*
DmTRET1–1A	trehalose transporter 1–1, isoform A	NP_610693.1	*Drosophila melanogaster*
DmTRET1–1B	trehalose transporter 1–1, isoform B	NP_725068.1	*Drosophila melanogaster*
DmTRET1–2	trehalose transporter 1–2, isoform A	NP_610694.1	*Drosophila melanogaster*
NlHT1_ABM01870	fac hexose transporter 1	ABM01870.1	*Nilaparvata lugens*
NlSUT1	sugar transporter 1	BAI83415.1	*Nilaparvata lugens*
NlSUT6	sugar transporter 6	BAI83420.1	*Nilaparvata lugens*
NlSUT8	sugar transporter 8	BAI83422.1	*Nilaparvata lugens*
PvTRET1_A5LGM7	fac trehalose transporter Tret1	A5LGM7.1	*Polypedilum vanderplanki*
SiGLUT8	glucose transporter 8	AAX92638.1	*Solenopsis invicta*

They are listed with their description, accession number and organism. Those transporters were added to *P. cochleariae*'s chosen sequences to calculate phylogenetic trees.
doi:10.1371/journal.pone.0084461.t002

Table 3. Number of assembled transcripts and average length after assembly and reassembly showing the usefulness of reassembling.

	Number of transcripts	Sum_length	25th_pc	75th_pc	Ave_length
After Trinity assembly	107323	85,475,541 bp	379 bp	841 bp	796 bp
After reassembly with TGICL	68667	63,815,627 bp	383 bp	1037 bp	929 bp

doi:10.1371/journal.pone.0084461.t003

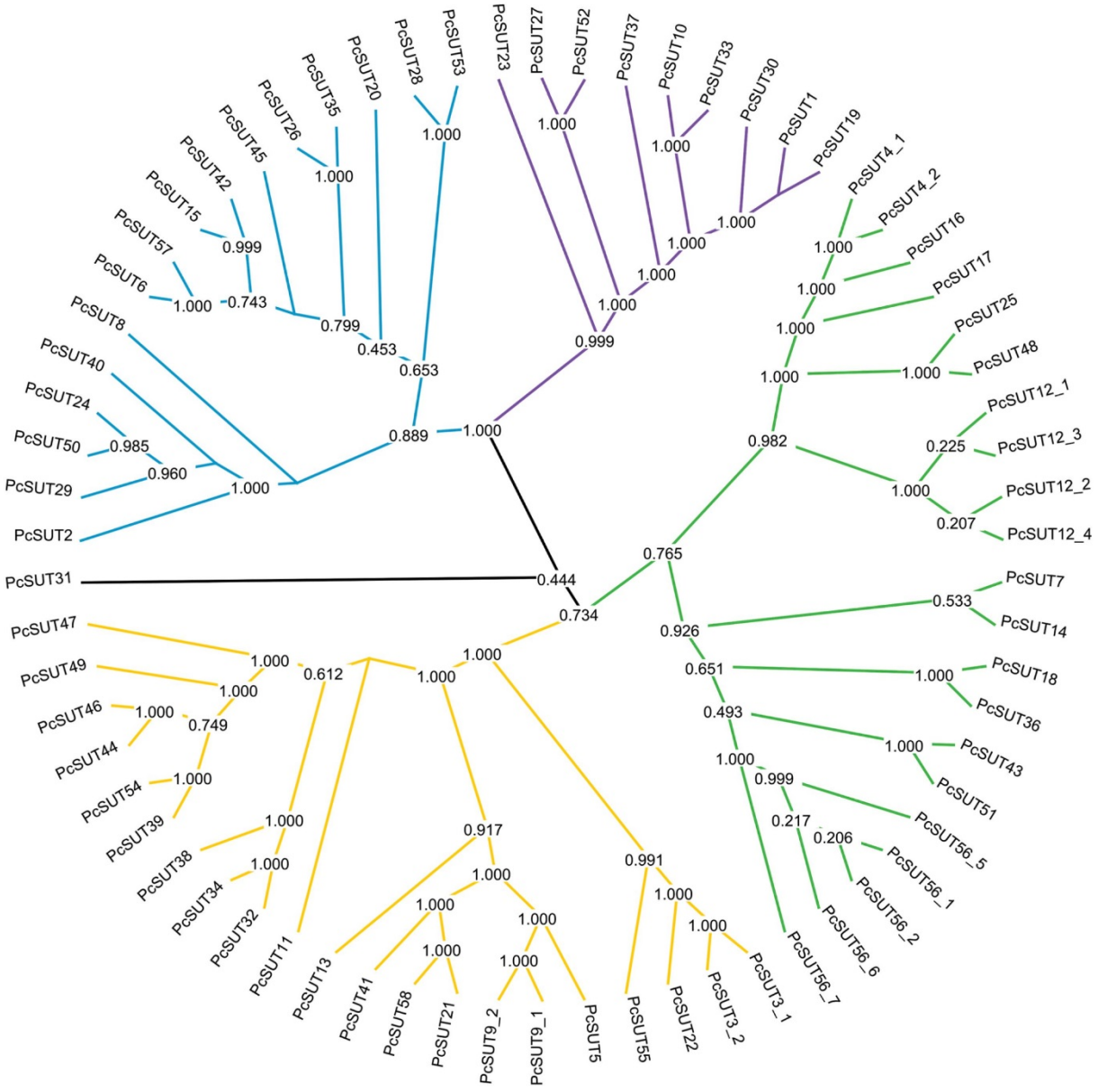

Figure 1. Phylogenetic tree of the 68 chosen sugar transporters derived from *P. cochleariae*. This circular phylogram shows the main 4 groups of chosen sugar transporters. Tree was calculated using MrBayes.
doi:10.1371/journal.pone.0084461.g001

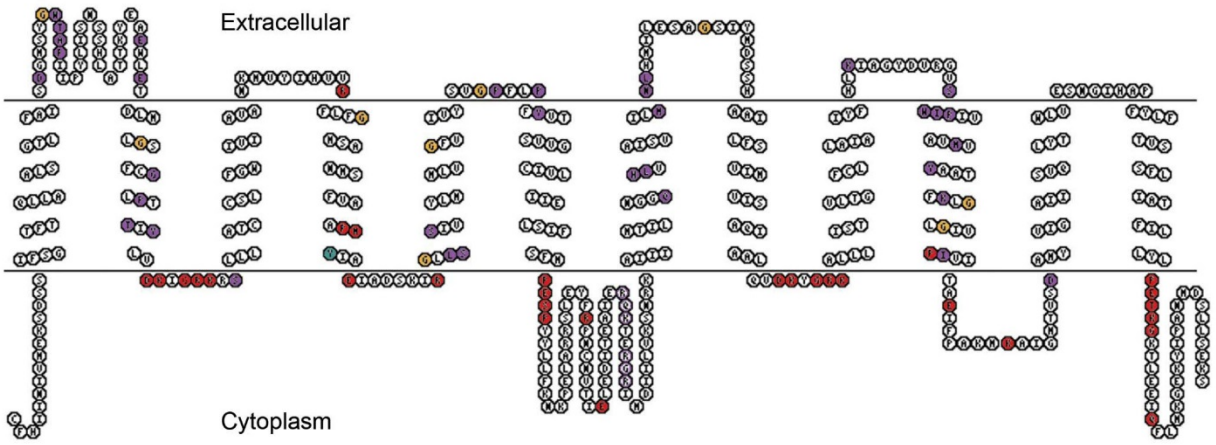

Figure 2. Schematic model for the structure of the putative SLC2 transporters derived from *P. cochleariae* by means of *Pc*SUT1. All 4 groups show the known and conserved facilitated sugar transporter motifs, such as DRxGRR/K in the second loop, PESPR/K in the sixth loop, E/DRxGRR/K in loop 8, and PETK/RGK/R in the carboxy terminal [2,15,18,76,86]. Furthermore, there are conserved amino acids, such as E and R in loop 4 and 10 (red). Those are needed for the glucose transport activity. Conserved tyrosines (turquois), such as the PMY motif mentioned by Chen *et al.* [15], can be found in our sequences in TMD 4. Additionally, conserved glycines (yellowish) in TMD 1, 2, 4, 5, 7, 8, and 10 as well as in loop 2 and 7 are present, characteristic for the mammalian glucose transporter family. The purple branch exhibits a GWTAP motif in loop 1, a PFYV motif in loop 5, and a VILMNLH motif in TMD 10 (purple colored amino acids).
doi:10.1371/journal.pone.0084461.g002

For every calculation of the phylogenetic tree only conserved parts were taken into account. Thus, the N-terminus, the loop between TM6 and TM7 as well as the C-terminus were excluded from calculating the phylogenetic tree.

First of all, the trees were calculated only for the chosen sequences derived from *P. cochleariae* to divide these into groups with respect to their sequence similarities. Second, sequences originating from other insects (*Nilaparvata lugens*, *Solenopsis invicta*, *Acyrthosiphon pisum*, *Polypedilum vanderplanki*, *Bombyx mori*) that have been functionally characterized were added to these sequences (see Table 2) [15,18,19,22]. Trees were re-calculated to identify sequences of *P. cochleariae* that are homologous to the characterized sequences. Third, the human GLUTs as well as other homologous sugar transporters from other Metazoa were selected. The chosen sequences derived from *P. cochleariae* were added to this selection and phylogenetic trees were calculated again to investigate the organisms' distribution in the trees. Furthermore, we calculated trees for one specific branch (which separated from the others with bootstrap percentage of 100%). For this, orthologous sequences derived from other beetles namely *Dendroctonus ponderosae* [65] and *Tribolium castaneum* were adjoined.

Gene Expression Profiling and Real-time PCR Validation of Putative Sugar Transporters in the Defensive Glands

Three replicates of the cDNA of *P. cochleariae*'s glands were prepared and sequenced as described above. All short reads of three replicates of glandular tissue were mapped onto the reassembled transcripts using Bowtie, an ultrafast short read aligner [66] with –best and –strata options. Bioconductor is an open source, open development software project to provide tools for the analysis and comprehension of high-throughput genomic data. It is based primarily on the R programming language [67]. The mapping results in bowtie format were loaded into R statistics using the ShortRead package [68] which is part of the Bioconductor package. For estimation of variance-mean dependence in count data, the DESeq package was used which is also part of the Bioconductor package (release 2.11) [69,70]. After analyzing the transcripts with DESeq, the sequences encoding the sugar transporters were selected and sorted regarding the number of sequence counts, beginning with the most abundant reads present in the glands. Furthermore, we normalized the normalized counts to the standards used for quantitative real-time PCR (*Pcrpl6* and *Pcrps3*) by first calculating the normalization factor [71]. The normalized counts were then divided by this normalization factor to get fold changes comparable to the values resulting from quantitative real-time PCR experiments.

Real-time PCR was employed for relative quantification [71]. RNA was isolated as described above. Up to 5 µg of the RNA was reverse transcribed at 50°C for 60 min using SuperScript III and Oligo(dT)$_{12–18}$ primer (life technologies, Darmstadt, Germany). Two technical replicates were performed from three biological replicates each. Technical replicates with a Cq difference of >1 were repeated. To normalize the PCRs for the amount of cDNA template added to the reactions, *Pcrpl6* and *Pcrps3* were chosen for *P. cochleariae* as reference genes. Primers were designed using primer3PLUS: http://www.bioinformatics.nl/cgi-bin/primer3plus/primer3plus.cgi (see Table S1 for primer sequences). Quantitative real-time PCR data were acquired on the CFX96 Touch Real-Time PCR Detection System (Bio-Rad Laboratories GmbH, Munich, Germany) using SYBR Premix Ex Taq II (Tli RNase H Plus) (Takara Bio Inc., Otsu, Japan). Running conditions: 3′ 94°C, 40 cycles [30″ 94°C; 30″ 60°C], melting curve with 1°C increase 60–95°C. These assays were performed following the MIQE-guidelines [72].

RNA Interference in *P. cochleariae* Larvae

The open reading frames encoding putative transporters of four highly abundant transcripts (*Pcsut1*, *Pcsut2*, *Pcsut5* and *Pcsut6*) were cloned into T7-promotor site lacking TOPO-plasmids pIBV5/HIS (life technologies, Darmstadt, Germany). Plasmids were sequenced prior to further processing. For double stranded RNA (dsRNA) production, sequences of these targets were analyzed *in silico* to avoid sequenced related off-target effects according to [48]. Unique parts of the sequences were amplified with opposing T7-

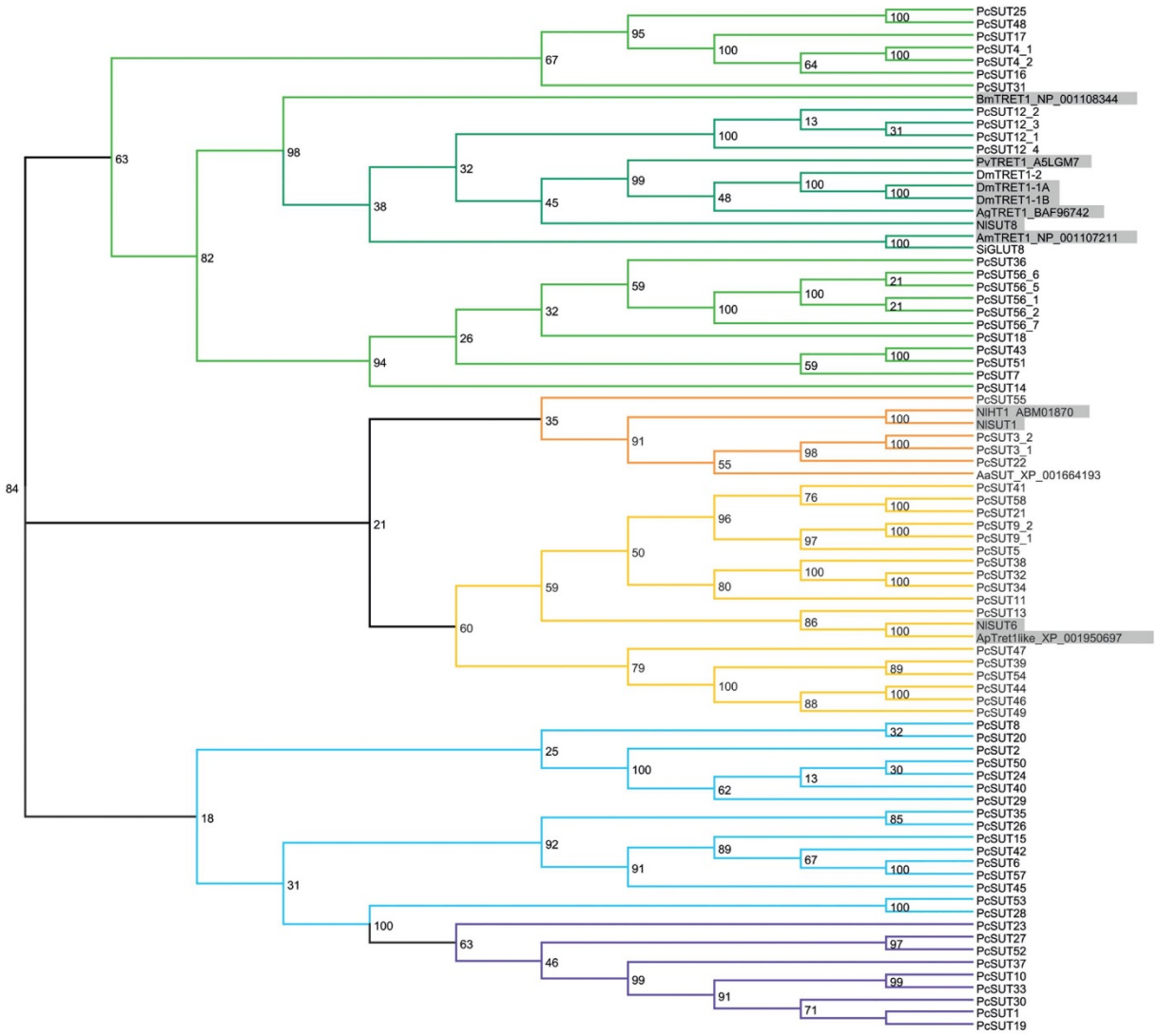

Figure 3. Phylogenetic tree of 68 chosen SLC2 transporters derived from *P. cochleariae* and chosen sugar transporters that have been functionally annotated in various insects (see Table 2). This tree was calculated by applying RAxML. The functionally characterized glucose/fructose transporters as well as trehalose transporters from insects are shaded in grey.
doi:10.1371/journal.pone.0084461.g003

promotor sequences attached to the 5′-end of each forward and reverse primer. The *gfp* sequence was amplified from pcDNA3.1/CT-GFP-TOPO (life technologies, Darmstadt, Germany) accordingly. The amplicons were subject to *in vitro* transcription assays according to instructions from the Ambion MEGAscript RNAi kit (life technologies, Darmstadt, Germany). The resulting dsRNA was eluted from silica membranes after nuclease digestion three times with 50 µl of injection buffer (3.5 mM Tris-HCl, 1 mM NaCl, 50 nM Na_2HPO_4, 20 nM KH_2PO_4, 3 mM KCl, 0.3 mM EDTA, pH 7.0). The concentration of dsRNA was calculated with $A_{260} = 1 = 45$ mg/ml and adjusted to 2 µg/µl. The quality of dsRNA was checked by TBE-agarose-electrophoresis.

P. cochleariae second instars with 4 mm body length, 0.5–0.7 mg body weight were injected with 0.4 µg of dsRNA about five days after hatching. Injections were accomplished with ice-chilled larvae using a Nano2010 injector (WPI, Sarasota, FL, USA) driven by a three-axis micromanipulator. The larvae were injected dorso-central between the pro- and mesothorax.

According to [45,73], we calculated the relative growth rate (RGR) of six biological replicates of each group of five larvae by RGR = [(final weight − weight of neonate larva)/(weight of neonate larva ×developmental time [days])]. Each replicate group was weighed each 24 or 48 h±3 h and data were compared statistically.

GC/MS Analysis of Low-molecular-weight Compounds in Defense Secretions

Larval secretions were collected in glass capillaries (i.d.: 0.28 mm, o.d.: 0.78 mm, length 100 mm; Hirschmann, Eberstadt, Germany). Secretions were weighed in the sealed capillaries on an ultra-microbalance (Mettler-Toledo, Gießen, Germany) three times; the weight of the capillaries was subtracted and the final

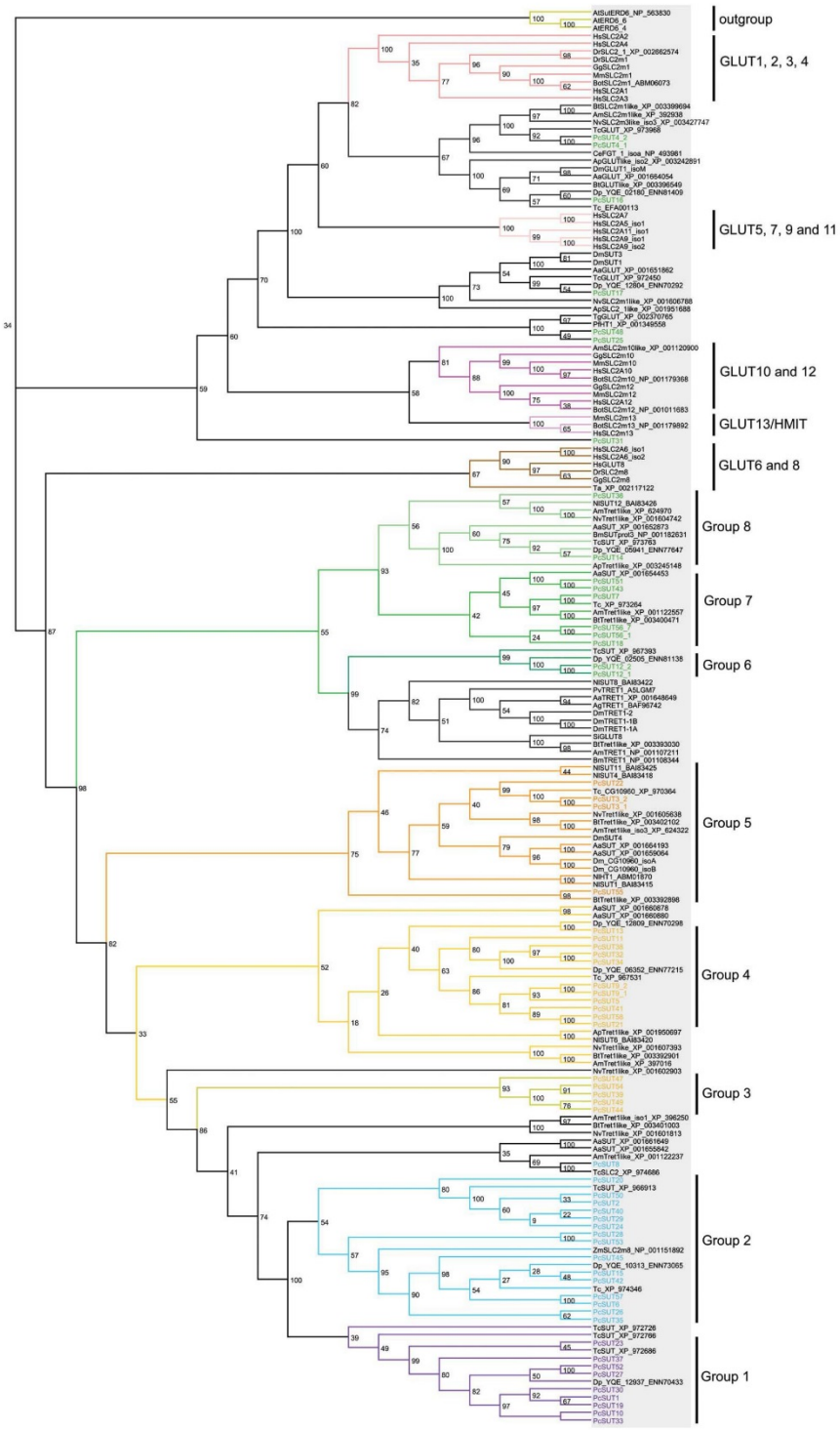

Figure 4. Phylogenetic tree of the *P. cochleariae* sequences and homologous sequences derived from the tree of life calculated using RAxML. Highlighted sequences regard to *P. cochleariae* and most similar sequences. Especially the green branch has to be subdivided into various subbranches, presenting all homologous sequences belonging to Metazoa. The tree significantly shows that the sugars (glucose) and trehalose transporters build up a huge tree in insects. Figure S5 shows the phylogeny of the selected organisms from the tree of life.
doi:10.1371/journal.pone.0084461.g004

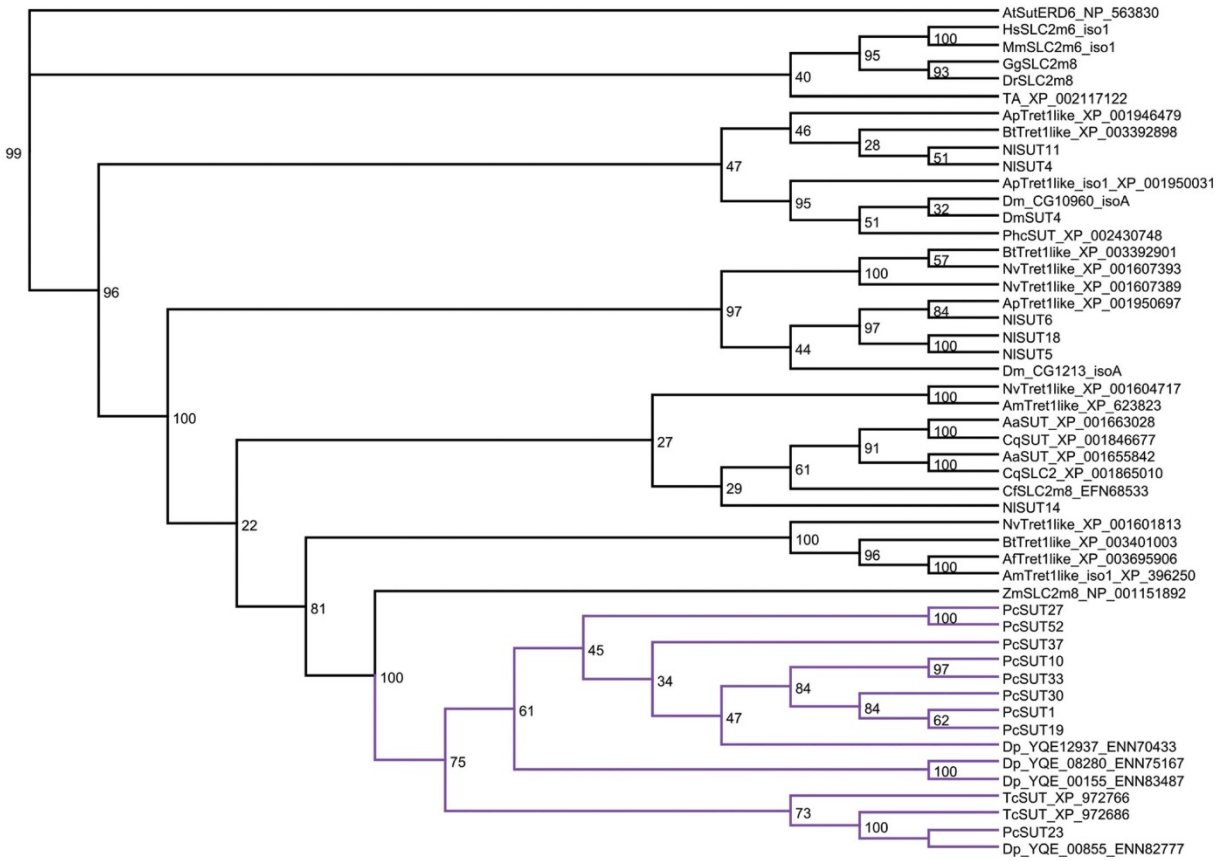

Figure 5. The phylogenetic tree of the nine sequences derived from *P. cochleariae* belonging to the purple branch (see Figure 3 and 4, Figure S4) and homologous sequences derived from the whole tree of life, especially from *Dendroctonus ponderosae* (Dc) as well as from *Tribolium castaneum* (Tc), was calculated using RaxML. Indicated in purple, it can be seen that the beetles' sequences build up a separate branch.
doi:10.1371/journal.pone.0084461.g005

weight was averaged. Sealed capillaries containing samples were stored at −80°C until needed.

According to [48] secretions of *P. cochleariae* were diluted in 1:200 (w/v) ethylacetate, supplemented with 100 µg/ml methylbenzoate as internal standard. Of each diluted secretion, 1 µl was subjected to GC/EIMS analysis (ThermoQuest Finnigan Trace GC/MS 2000, Frankenhorst, Germany) equipped with Phenomenex (Aschaffenburg, Germany) ZB–5–W/Guardian–column, 25 m. Substances were separated using helium as a carrier (1.5 ml/min). The column temperatures were set as followed: 50°C (2 min), 10°C min^{-1} to 80°C, 5°C mi^{-1} to 200°C, 30°C min^{-1} to 300°C (1 min). Inlet temperature was 220°C and transfer line was 280°C. Chrysomelidial was identified according to [36]. Peak areas of GC-chromatograms were obtained using the ICIS-algorithm (Xcalibur bundle vers. 2.0.7, Thermo Scientific).

Analysis of Differentially Expressed Genes in Glandular Tissue of RNAi Silenced *P. cochleariae* Larvae

The short reads (sequenced in 50 bp single-mode) from the glandular tissue (4 samples) of the RNAi-silenced *P. cochleariae* larvae have been mapped onto the studied sugar transporters of *P. cochleariae*'s transcriptome using bowtie [66]. The mappings results for the sugar transporters transcripts were subjected to DESeq statistical analysis by reading them into R statistics software, and transcript counts were normalized to the effective library size. Afterwards, the negative binomial testing was carried out to identify differentially expressed transcripts. All those sugar transporters were stringently determined as differentially expressed when having an adjusted p-value smaller than 0.1. Additionally, the normalized counts were stabilized according their variance as outlined in the DESeq package tutorial and heatmaps were generated [70].

Results

Identification of Sequences Encoding Putative Members of the SLC2 Family and Trehalose Transporters in the Transcript Catalogue of *Phaedon Cochleariae*

In order to predict sugar transporters in the larvae of *P. cochleariae* with special emphasis on the defensive glands, we performed a comprehensive analysis of transcriptomic data. For this purpose, cDNA libraries prepared from different tissues of juvenile *P. cochleariae* have been sequenced by using the Illumina technique. In addition to the sequencing of cDNA derived from a tissue pool in 150 bp paired-end mode, three biological replicates of the RNA of *P. cochleariae*'s defensive glands were extracted, processed and each sequenced in 50 bp single-read modes. The raw sequence data (in the following called reads) are listed in

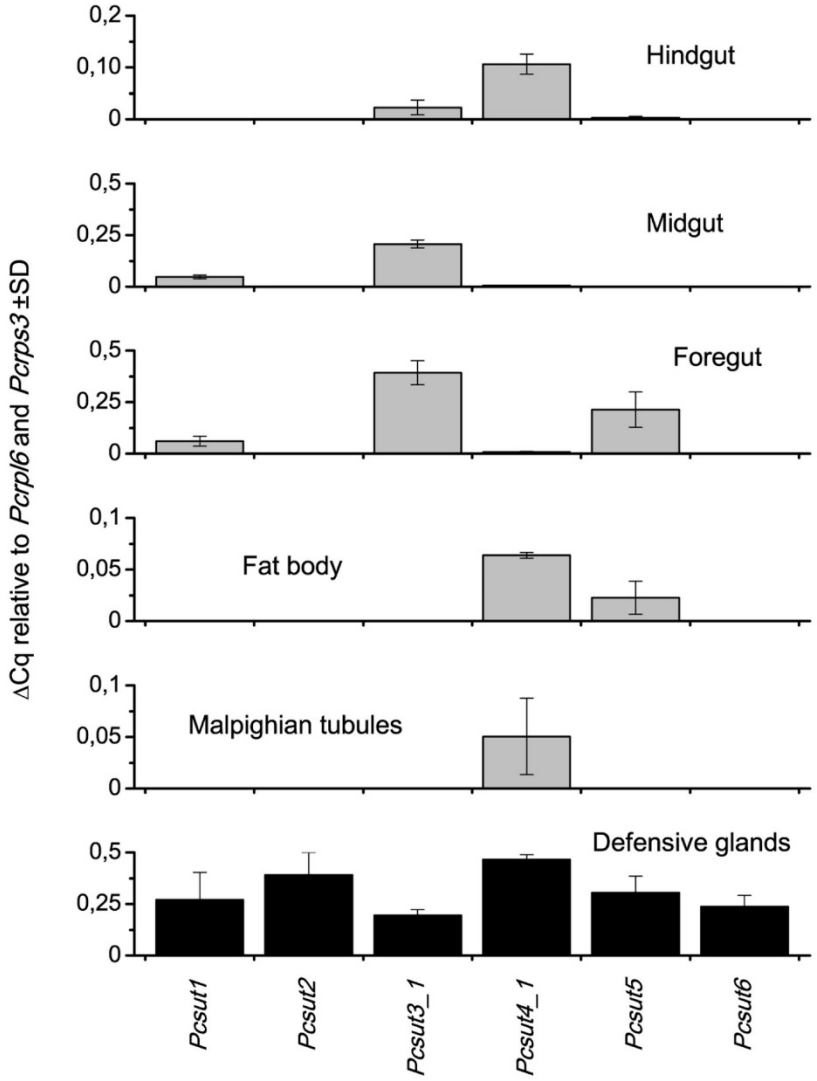

Figure 6. Distribution of mRNA levels of putative SLC2 transporters in various tissues of juvenile *P. cochleariae* by using quantitative real-time PCR.
doi:10.1371/journal.pone.0084461.g006

Table 1. The sequencing of the tissue pool resulted in 46,030,279 read pairs. The *de novo* assembly of those reads by using the Trinity software [50] resulted in 107,323 transcripts with an average sequence length of 796 bp. Reassembly by applying the TGI Clustering tool [52,74] reduced the number of transcripts to 68,667 with an average length of 929 bp (Table 3).

These 68,667 transcripts were then translated into possible protein sequences. The sequences encoding putative sugar transporters were identified by searching the Protein family database (Pfam) [55]. All sequences possessing a Sugar_tr domain (Sugar (and other) transporter family, PF00083) were selected. As a result, a total of 207 sugar transporters could be identified. Those hits were searched via BLASTp with an E-value threshold of 1e-3 against the Swiss-Prot protein database [58]. 68 predicted proteins were annotated as either SLC2 or trehalose transporters (Table S2, Figure S1). These sequences were given temporary designations as numbered series in the form of *Pc*SUTxx (Table S3). According to previous studies, transcripts with a minimum coding sequence length of 900 bp have been chosen for further phylogenetic analyses [20]. The prediction of putative transmembrane (TM) α-helices for those sequences by applying TMHMM [59] as well as Memsat2 [60] revealed that most of our sequences possess 12 TM regions (Table S3, columns 7 and 8). In total, Memsat2 was able to predict those 12 TM regions for 40 of all chosen 68 sequences, whereas TMHMM predicted these for just 33 of all 68 sequences.

Phylogenetic Analyses of Putative Sugar Transporter Sequences

The phylogenetic relationships of our selected 68 transporter sequences were analyzed by applying Probalign (as well as MAFFT [75] for the more complex multiple sequence alignments) for calculating the multiple alignments followed by calculating the phylogenetic trees. Two different methods namely MrBayes and

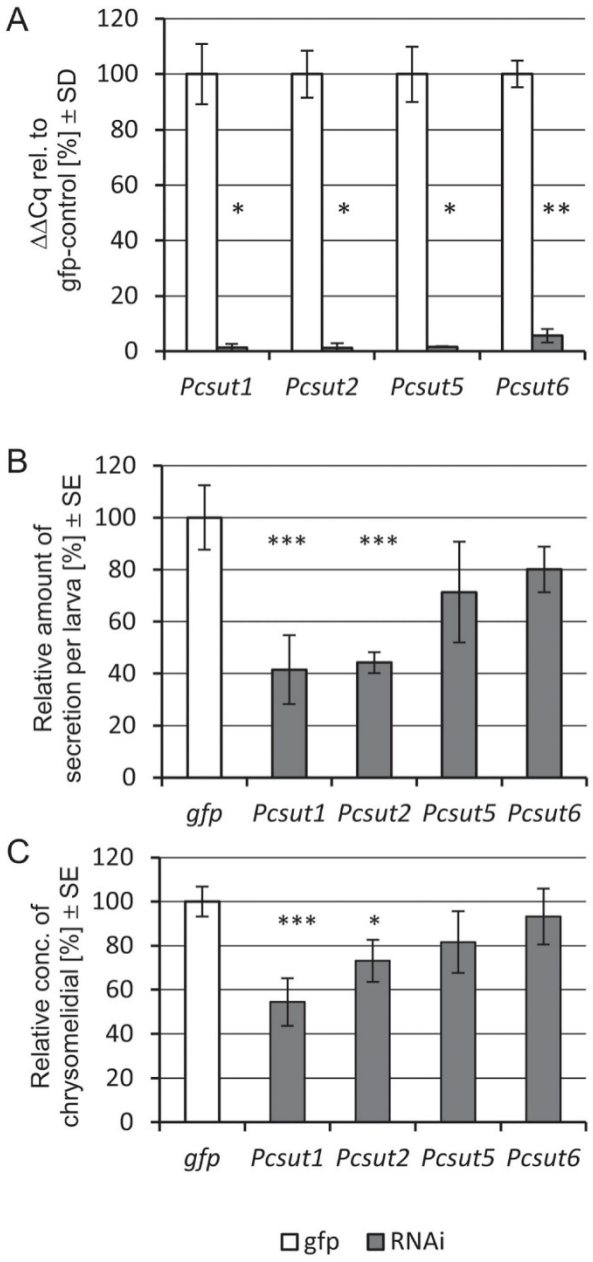

Figure 7. RNAi effects on transcript levels, amounts of defense secretions and chrysomelidial concentrations 10 days post RNAi induction in juvenile *P. cochleariae*. A, Relative expression of chosen transporters in glandular tissue, normalized internally to *Pcrpl6* and *Pcrps3* and externally to *gfp*-control, n = 5. B, Amounts of secretions produced by individual larvae were weighted and normalized to the control treatments. n = 5. C, Secretions samples of RNAi induced larvae were analyzed using GC/MS; Amounts of chrysomelidial were normalized to internal standard (methylbenzoate), values were calculated against control. n = 5. Asterisks indicate level of significance (T-test, 2-tailed; p-value< = 0.05 = *, < = 0.01 = **, < = 0.001 = ***).
doi:10.1371/journal.pone.0084461.g007

RAxML have been applied. In our case, we could show that both programs resulted in a division of the predicted transporters into at least 4 groups (Figure 1). Especially the purple branch is well supported by a bootstrap value of 100% (Figure S2).

In general, all 4 groups possess the conserved facilitated sugar transporter motifs important for transport activity and ligand binding, namely DRxGRR/K in the second loop, PESPR/K in the sixth loop, E/DRxGRR/K in loop 8, and PETK/RGK/R in the carboxy terminus (Figure 2, red colored amino acids) [2,15,18,22,76]. Additionally, conserved tryptophanes in TM domain (TMD) 4, 10 and 11, and loop 10 [77,78], and conserved tyrosines (turquois colored amino acids in TMD 4), such as the PMY [76], can be found. Furthermore, conserved glycines (yellow colored amino acids) in TMD 1, 2, 4, 5, 7, 8, and 10 as well as in loop 2 and 7 are present, characteristic for the mammalian glucose transporter family [76].

Besides the general conserved amino acid residues, we observed branch specific differences particularly for the purple branch (Figure 2, purple colored amino acids). The conserved motif QQLSG [2] which is present in all branches but substituted with QHXXG in the purple branch is important for the putative substrate binding. In addition, this purple branch exhibits several conserved motifs not present in other branches and not reported from any other transporter of the SLC2 family until now, such as a GWTAP motif in loop 1 (instead of GWTSP), a PFLPFY motif in loop 5, a VILMNLH motif in TMD 7, and a SWIP motif followed by a conserved methionine and tyrosine in TMD 10 (Figure S3, multiple sequence alignment).

By comparing the sequences of chosen sugar transporters to sugar transporters of other insect species that have been functionally characterized [15,18,19,22], we could show that these sequences fall exclusively into the green and yellow branch and not into the purple or blue branch (Figure 3, Figure S4). The functionally proven trehalose transporters such as TRET1 from *Polypedilum vanderplanki*, *Anopheles gambiae*, *Apis mellifera*, *Drosophila melanogaster* and *Bombyx mori* build up a subbranch within the green branch together with *Pc*SUT12_1–4 (with bootstrap percentage of 98%). The GLUT8 of *Solenopsis invicta* also belongs to this group. Therefore, we suggest (in agreement with Kanamori *et al.* [18]), that this fire ant GLUT8 is probably a TRET1 ortholog. The functionally characterized glucose and glucose/fructose transporters from *Nilaparvata lugens* and *Acyrthosiphon pisum* cluster in the yellow branch. However, functional analysis of *P. cochleariae*'s transcripts is required to confirm substrate spectra of the transporters clustering into different branches.

To study phylogeny of sugar transporters in a larger context, we selected the *P. cochleariae* sequences and its homologs from selected Metazoa from various branches of the tree of life (Figure S5), including the human SLC2 isoforms (GLUT1–12, H^+-*myo*-inositol transporter (HMIT)), for cladistic analyses by MrBayes and RAxML. Generally, Figure 4 displays that the sugar (glucose) and trehalose transporters build up a huge branch in insects, and the mammalian sugar porters form a separate branch. In accordance with the published phylogenetic analyses by Wilson-O'Brien *et al.* [79], the mammalian GLUTs isoforms segregate into five distinct classes, also showing that the mammalian GLUTs are separate from their insect orthologs. Some insect sequences also cluster into the mammalian clades, e.g. the class I clade (GLUT1, 2, 3, 4) also contains insect sequences branching at the base with strong support (with bootstrap percentage of 100%). *Pc*SUT31 clusters together with mammalian HMIT. The class II (GLUT5, 7, 9, 11) and the GLUT10/12 clade contain only vertebrate sequences. According to Wilson-O'Brien *et al.* [79], class II genes were most likely to arise after the divergence of this

Table 4. Differential expression analysis using DESeq package.

Differentially expressed transcripts with padj<0.1 after dsRNA injection of *Pcsut1*:						
Seq_Id	**baseMeanA**	**baseMeanB**	**foldChange**	**log_2FoldChange**	**pval**	**padj**
PcSUT1	4804.953616	240.8731589	0.050130174	−4.31817696	1.26E-16	7.31E-15
Differentially expressed transcripts with padj<0.1 after dsRNA injection of *Pcsut2*:						
Seq_Id	**baseMeanA**	**baseMeanB**	**foldChange**	**log_2FoldChange**	**pval**	**padj**
PcSUT2	8428.420254	2031.419654	0.241020214	−2.052773946	4.15E-08	2.49E-06
PcSUT25	22.79115587	394.3587471	17.30314817	4.112962644	0.003061159	0.091834771
Differentially expressed transcripts with padj<0.1 after dsRNA injection of *Pcsut6*:						
Seq_Id	**baseMeanA**	**baseMeanB**	**foldChange**	**log_2FoldChange**	**pval**	**Padj**
PcSUT6	3380.778995	95.65776606	0.028294593	−5.143329799	4.20E-14	2.56E-12
PcSUT25	22.79115587	995.628527	43.68486322	5.449061568	0.000272434	0.008309243

baseMeanA: mean of normalized counts value of ds*gfp*-injected samples. baseMeanB: mean of normalized counts values of dsRNA-*gfp*-injected, dsRNA-*Pcsut1*-injected, dsRNA-*Pcsut2*-injected, dsRNA-*Pcsut6*-injected samples. Fold-change: baseMeanA compared to baseMeanB. Log_2fold-change: logarithm (to base 2) of fold-change values. Pval: p-value for the statistical significance of this change. Padj: p-value adjusted for multiple testing with Benjamini-Hochberg procedure which controls false discovery rate.

doi:10.1371/journal.pone.0084461.t004

phylum, whereas the GLUT10/12 clade might has been lost in invertebrates secondarily. The majority of the tested insect sequences form a huge sister group of the GLUT6/8 class with strong support (100% bootstrap), suggesting an expansion of this class in insects. On inspection of the insect sequences, especially the green branch is remarkably large and can be subdivided into various subbranches. In addition to the five mammalian SCL2 classes, we suggest eight more classes in insects (each separated from the others with bootstrap percentages of at least 80%).

The bootstrap values of the tree of life support the notion that the purple branch may be restricted to the insect order Coleoptera. For deeper analysis of this branch, we have calculated trees with the sequences of this purple branch and its homologs/orthologs in insects. The MrBayes tree as well as the RAxML tree (Figure 5 and Figure S6) shows that only sequences derived from beetles such as *Dendroctonus ponderosae*, *Tribolium castaneum*, and *P. cochleariae* belong to this purple branch. Whereas, looking at Figure 3 and 4, all other sequences derived from *P. cochleariae* show homologies to Diptera, Apocrita and other insect orders. According to our cladistic analyses, the purple branch of the phylogenetic trees seems to be the most interesting. All changed and additionally conserved motifs together with the motif QH lead to the hypothesis that the sequences belonging to the purple branch may provide a new class of sugar transporters in insects, especially in the order Coleoptera, not before described. However, their biological function remains to be elucidated.

Expression Profiles of SLC2 and Trehalose Transporter Transcripts in the Defensive Glands of Immature *P. cochleariae*

The Illumina short reads derived from the glandular tissue sequenced using HiSeq2000 in 50 bp single-read mode (two or three samples multiplexed in one lane) resulted in 34,918,295 reads with length of 50 bp as well as 36,598,828 and 29,866,004 short reads, respectively. Those short reads have been mapped onto our transcriptome. 82.62% to 84.90% of all short reads could be mapped, whereas 14.28% to 16.31% of the reads failed to align (Table S4).

The mapping results were taken as input for R statistics. DESeq, belonging to the Bioconductor package, was applied to analyze the mapping results. The counts of transcripts are listed in Table S3 (columns 3 to 5). All observed putative sugar transporters of SCL2 and trehalose transporters could be identified in the glandular tissue, although most of them at a very low level. Interestingly, the six most abundant transcripts (inclusive isoforms) with more than 3,000 normalized counts are spread among all four major phylogenetic subtrees as highlighted in Figure S7. Therefore, no specific branch is particularly overrepresented in the defensive glands. As previously demonstrated in literature [80], evaluation of the RNA-seq data (standardized values shown in Table S5) with quantitative real-time PCR data shows also in our experiments the comparability of the two methods (Figure S8). Subsequently, the six transcripts have been analyzed regarding the distribution of their transcript levels in different larval tissues. Two sugar transporters namely *Pc*SUT2 and *Pc*SUT6, clustering into the blue branch, are exclusively expressed in defensive glands (Figure 6). The other four tested candidates were found to be also expressed in at least one more tissue.

Silencing of Putative Sugar Transporters in Immature *P. cochleariae* by RNAi

RNA interference (RNAi) was carried out, besides for *Pcsut2* and *Pcsut6*, also for *Pcsut1* (highly expressed in defensive glands and gut) and *Pcsut5* (highly expressed in defensive glands, fat body and gut) to get deeper insights into their biological function for the development of *P. cochleariae* larvae and the production of defensive secretions *in vivo*. Early second instars were injected with either dsRNA identical to a unique part of one of these transporters sequences or with dsRNA of *gfp*. As confirmed by quantitative real-time PCR, transcription of all targets was successfully silenced in the defensive glands 10 days after injection (Figure 7A). By monitoring the development of treated larvae, significant weight reduction was observed neither for the larvae nor the pupae by

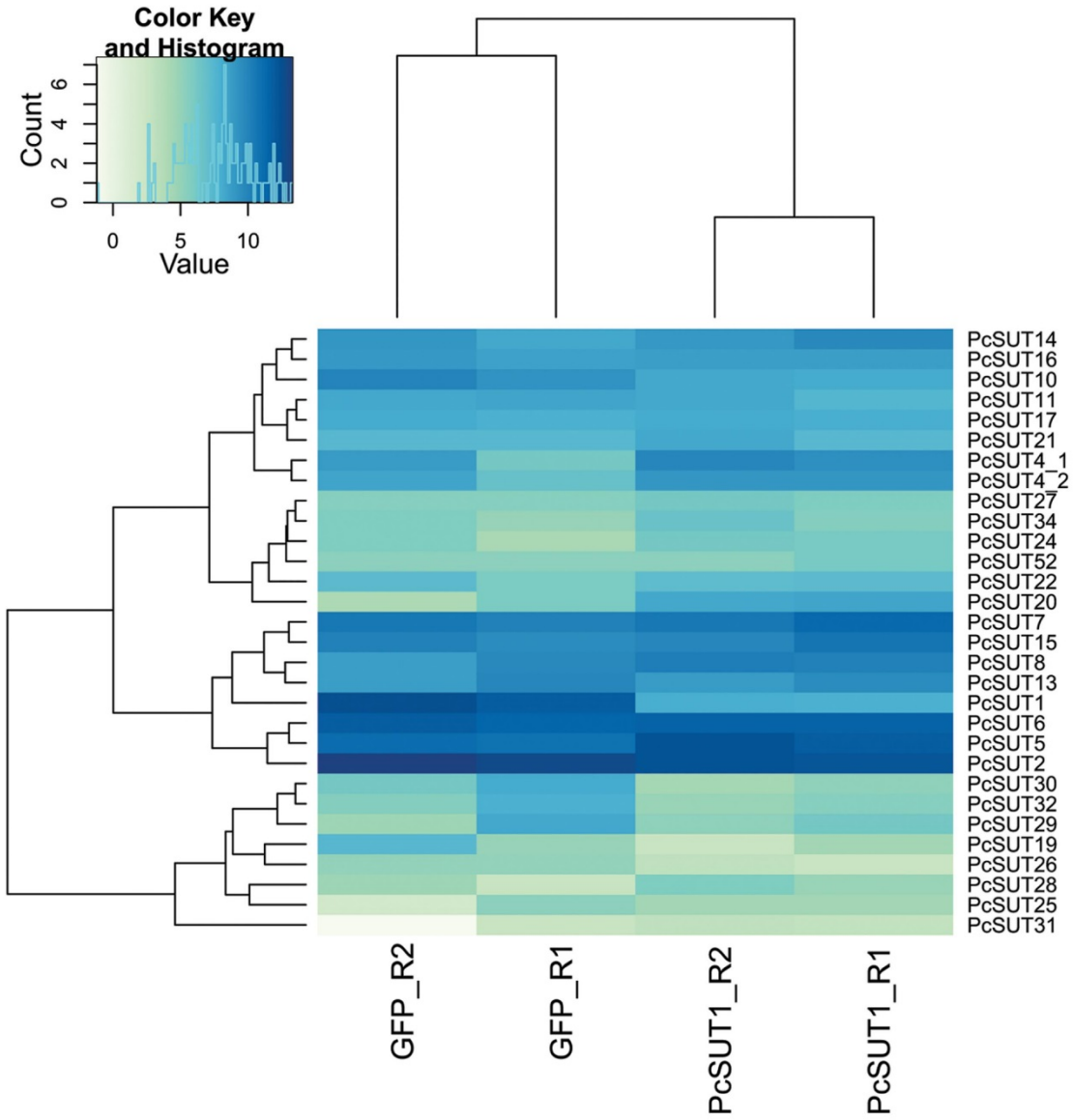

Figure 8. Heatmap of the variance stabilization transformed data (vsd) of ds*Pcsut1*-injected *vs.* ds*gfp*-injected samples. Samples derived from glandular tissue. For this, the transcript counts of the sugar transporters of each sample after dsRNA-injection have been normalized to the effective library size and the variance over all samples has been stabilized by applying the DESeq package. For each heatmap, the 30 most abundant sugar transporter transcripts are shown. Ds*gfp*-injected samples are the same in each heatmap.
doi:10.1371/journal.pone.0084461.g008

transporter silencing (Figure S9). To screen for the function of the transporters for the synthesis of secretions, GC/MS analysis was carried out for quantification of the amount of chrysomelidial relatively to the *gfp*-controls. Here, we could observe decreases in the amount of chrysomelidial by silencing *Pcsut1* ($p = 0.008$) and *Pcsut2* ($p = 0.001$) and also in the amount of secretions produced by targeting *Pcsut1* ($p = 0.007$) and *Pcsut2* ($p = 0.03$) (Figure 7B and 7C). Knocking down of neither *Pcsut5* nor *Pcsut6* resulted in alterations of the phenotype. We assume that *Pc*SUT1 and *Pc*SUT2 seem to be important for the production of defensive secretions. Their substrate selectivity, however, needs to be further studied *in vitro*.

In contrast to the silencing effect of the ABC transporter in the defensive glands which caused a total loss of defensive secretions [46], RNAi targeting SLC2 transporters could not shut down the production of defensive exudates completely. This may be due to the turn-over rate of the integral-membrane proteins which may diminish the silencing effect or other transporters may be expressed to take over the function to achieve homeostasis in the tissue. To test the latter hypothesis, we have gathered RNA-seq data from larvae silenced in *Pcsut2* or *Pcsut6* (as examples for SLC2 members exclusively expressed in glands) or *Pcsut1* (as example highly expressed in defensive glands and gut) and analyzed differential expression of SLC2 transporters in comparison to *gfp*-treated larvae.

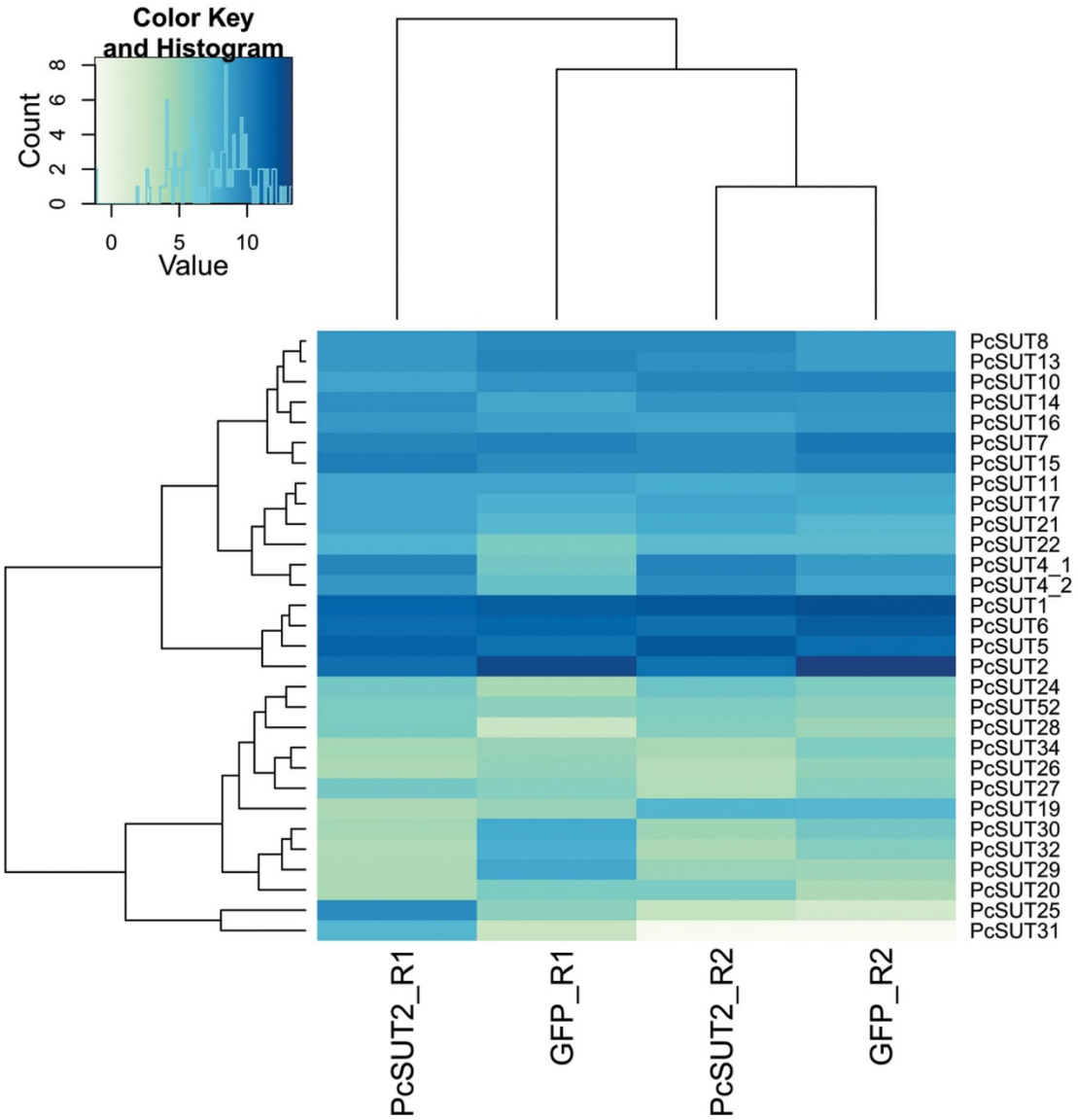

Figure 9. Heatmap of the variance stabilization transformed data (vsd) of ds*Pcsut2*-injected *versus* ds*gfp*-injected samples. Samples derived from glandular tissue. For further explanation see Figure 8.
doi:10.1371/journal.pone.0084461.g009

Analysis of Differentially Expressed Genes in the Glandular Tissue of RNAi-silenced *P. cochleariae* Larvae

Ten days after *Pcsut1*, *Pcsut2* and *Pcsut6*-silencing and ds*gfp*-injection, glandular tissues were dissected and two biological replicates for each treatment were sequenced. The normalized counts of all sugar transporters of all samples are listed in Table S6. The $\log_2$ fold-changes of the silenced transporters (ds*gfp*-injected samples as control) and adjusted p-values were determined using the DESeq package (see Table 4). In Figure S10 all sugar transporters exhibiting significantly different transcription levels are colored red (MA plot showing $\log_2$ fold-changes *vs.* mean values). In all samples (prepared in RNA-seq and quantitative real-time PCR experiments), we observed varying transcript levels of SCL2 transporters owing to the individual biological variance and diversity despite similar developmental stage or living conditions.

Pcsut1 knocking-down led to a significant decrease of its own transcript level (Table S6: adjusted p-value (padj) = 7.31E-15). Figure 8 exhibits a heatmap of the 30 most abundant sugar transporters. Besides *Pcsut1*, three more sugar transporters were co-silenced, namely *Pcsut10*, *Pcsut30* and *Pcsut32*. Those were not determined as differentially expressed, but have a $\log_2$ fold-change smaller −2 (Figure S10A, lower right quadrant). In contrast, *Pcsut4*, *Pcsut5*, *Pcsut20*, and *Pcsut22* were up-regulated ($\log_2$ fold-change of 1) suggesting counter-regulation to the silencing effect to ensure sugar homeostasis in the defensive glands. This up-regulation, however, did not fully compensate the silencing effect

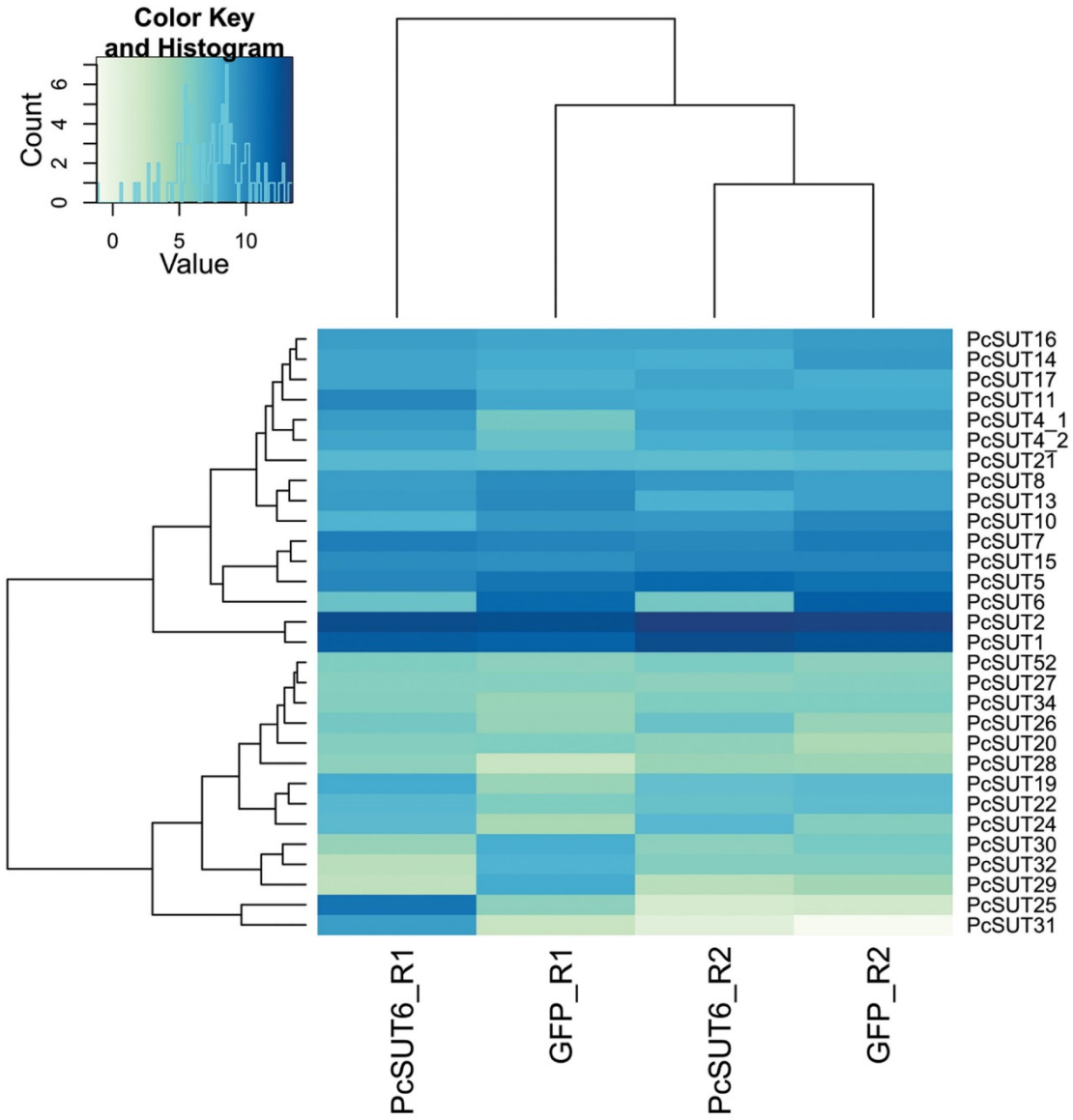

Figure 10. Heatmap of the variance stabilization transformed data (vsd) of ds*Pcsut6*-injected *vs.* ds*gfp*-injected samples. Samples derived from glandular tissue. For further explanation see Figure 8.
doi:10.1371/journal.pone.0084461.g010

of *Pcsut1* indicated by the decrease in the production of defensive secretions (as shown before).

The samples prepared after dsRNA-injection of *Pcsut2* showed, on the one hand, a significant down-regulation of *Pcsut2* itself (padj = 2.49E-06), but also a decrease of *Pcsut6*, *Pcsut26*, *Pcsut30*, *Pcsut32* and *Pcsut34* ($\log_2$ fold-change of −1, Figure S10B lower right section). On the other hand, *Pcsut4*, *Pcsut5*, *Pcsut14*, *Pcsut17*, *Pcsut21*, *Pcsut24* and *Pcsut28* were up-regulated (Figure 9). Additionally, the transcript level of *Pcsut25* was determined as significantly higher in the silenced samples than in the ds*gfp*-injected samples (padj = 0.092) (Table 4). But also here, the counter-regulated transporters did not compensate the silencing effect completely.

In the samples with *Pcsut6* silenced *via* dsRNA-injection, *Pcsut6* was drastically reduced (padj = 2.56E-12). Furthermore, *Pcsut13*, *Pcsut29*, *Pcsut30* and *Pcsut32* were also down-regulated ($\log_2$ fold-change of −1, Figure S10C). To establish the sugar homeostasis in this sample, *Pcsut1*, *Pcsut17*, *Pcsut24* and *Pcsut26* were transcribed at a higher level ($\log_2$ fold-change of 1) compared to the ds*gfp*-injected samples. Especially *Pcsut25* was significantly higher expressed (padj = 0.008) (Figure 10, Table 4).

Discussion

Sugars play an important role in all species' metabolism. Transporters of the SLC2 family are key elements involved in the adaptive response to sugar demand that have important physiological implications to cell survival and growth. They are expressed

in a tissue-specific manner with different affinity, specificity and capacity for substrate transport [81]. Recent phylogenetic analyses of genomic data available from sequenced insects suggest a remarkable expansion of the SLC2 family in insects compared to mammals [18,20,23,26,79]. Beetles, however, have not yet been addressed. Here we present the first comprehensive phylogenetic analysis of members of the SLC2 sugar transporter family identified in a leaf beetle species.

Phylogenetic Analyses

We created a transcript catalogue of juveniles of *P. cochleariae* in which we annotated 68 sequences as SLC2 transporters. The phylogenetic analyses of putative sugar transporters were performed with MrBayes and RAxML. MrBayes, on the one hand, is a program for Bayesian inference and model choice across a large space of phylogenetic and evolutionary models. On the other hand, RAxML is a maximum likelihood phylogeny estimation. In our case, we were able to show that both programs result in a division of the predicted transporters into 4 main groups. However, there are some differences in the results of the calculations with the two methods. For example, *Pc*SUT8 belongs to the green branch of the phylogenetic tree showing *P. cochleariae*'s sequences as well as the functionally characterized sequences of the other insects calculated by MrBayes; RAxML sorted it into the blue branch (Figure 3, Figure S4). Comparing these trees with the trees showing only sequences of *P. cochleariae* as well as with the trees which also include the sugar transporter sequences of mammals and other organisms, it can be seen that *Pc*SUT8 always belongs to the blue branch. To conclude, we propose that RAxML results in more stable trees when adding or deleting homologous sequences. This fact might be strengthened by Douady *et al.* [82] who concluded that the more conservative use of bootstrap percentages (as used by RAxML) might be less prone to supporting strongly a false phylogenetic hypothesis.

The mammalian GLUT proteins are well-studied, and phylogenetic studies have been carried out. In addition to the five distinct classes of mammalian GLUTs [79], we propose eight more groups of transporters including the trehalose transporters in the Insecta. The tree including mammalian GLUTs as well as homologous sequences of other organisms including insects shows that many transporters belonging to the SLC2 family derived from *P. cochleariae* and other insects constitute a huge subtree separate from the well-studied mammalian GLUTs. We suggest that the orange branch within this insect clade constitutes the fructose/glucose transporters. This suggestion is supported by, on the one hand, *Ap*ST3 from the pea aphid *A. pisum* which acts in the gut as a low-affinity uniporter for fructose and glucose [23], and on the other hand, *Nl*HT1 (*Nl*ST1) and *Nl*ST6 from the brown planthopper *N. lugens* which function as glucose and glucose/fructose transporters, respectively, in the gut [20,22]. The green branch within the huge insect clade most likely contains trehalose transporters including the transporter TRET1 from the sleeping chironomid *P. vanderplanki* and its orthologs from *A. gambiae*, *B. mori*, *A. mellifera* and *D. melanogaster* [18,19] and a proton-dependent transporter participating in trehalose reabsorption in Malpighian tubules of *N. lugens* [21]. Kinetic parameters show different affinities for trehalose among the TRET1 orthologs which mirror the trehalose:glucose ratio in the hemolymph of each species [18]. No functional assumptions can be made regarding all other subbranches, especially concerning the purple one which seems the most interesting to the study of beetles.

The large number of SLC2 transporters may result from gene duplications as has been suggested for *A. pisum*, whose genome contains a conspicuous number of genes encoding predicted sugar transporters [23]. While such an idea still needs experimental proof, it may contribute to the reflection on how insects are able to adapt to extreme dietary conditions and to the testing of substrates not yet in the focus for SLC2 members such as plant derived glucosides, for example, present in large amounts in the diet of phytophagous insects.

Interestingly, the mammalian GLUT6/8 form a sister group of the expanded insect clade. In accordance with the literature [76,79] we see that GLUT6 and 8 are more closely related to sugar transporters present in invertebrate species than to other mammalian GLUTs. Mueckler *et al.* [27] stated that the primary physiological substrate for mammalian GLUT6 and 8 have not been definitely identified. Therefore, knowledge of substrate selectivity of the SLC2 members in the insect clade may also contribute to a deeper understanding of the function of GLUT 6 and 8 in mammals.

Membrane Protein Topology

Membrane proteins, such as sugar transporters, seem to have a restricted range of folds than their water-soluble counterparts, making them more amenable to structural predictions [83]. α-Helical membrane proteins contain one or more transmembrane helices which consist predominantly of hydrophobic amino acids. In our study of sugar transporters, 12 TM helices are stated [26]. To predict the TM domains of *P. cochleariae*'s sugar transporters, TMHMM as well as Memsat2 were used. For 40 of 68 sequences, Memsat2 was able to predict all 12 TM domains. TMHMM predicted those 12 TM domains for just 33 sequences. But, for three sequences Memsat2 failed to predict at least 10 TM helices and proposed 1 (twice) and 2 (once) TM helices. For those three sequences, TMHMM predicted 10 (once) and 12 (twice) TM helices. This leads us to the conclusion that neither of these prediction methods is perfect, but applying both gives us the required information. Furthermore, Cuthbertson *et al.* [83] suggested that optimal prediction is obtained by the method that best reflects the biological and physical principles governing membrane protein architecture.

RNAi and Subsequent RNA-seq

After silencing *Pcsut1* and *Pcsut2*, phenotypic analyses revealed a reduction of defensive exudates in the larvae. Silencing of *Pcsut5* and *Pcsut6* did not result in a changed phenotype. By combining the RNAi experiments (silencing *Pcsut1*, *Pcsut2* and *Pcsut6*) with subsequent mRNA isolation and RNA sequencing, we could show the down-regulation as well as up-regulation of sugar transporters in the defensive glands. Silenced and induced sequences belong to separate branches in the phylogenetic trees which also suggest that insect transporters belonging to different clades can have comparable substrate preference. Anyhow, a direct correlation of counter-acting transporters was difficult to identify. All predicted off-targets according to Bodemann *et al.* [48] were excluded in the transporter sequences used for RNAi. Nevertheless, co-silencing effects could not be avoided. These effects could not be predicted most likely because of metabolic co-silencing which was already observed for two hexokinases in *T. castaneum* [84].

Homeostasis may not only be achieved by the induced expression of transporters but, for example, also by the induced trafficking of transport proteins within a cell. This trafficking is known, for example, from the mammalian GLUT4. The protein is hormonally induced to translocate from intra-cellular membranes to the plasma membrane for the absorption of excessive glucose from the blood [85]. In insects, however, an analogous phenomenon is not known and was not addressed in our analyses. In general, sugar homeostasis is not very well understood in insects,

and the role of SLC2 members in this process has not been addressed to date. By transporter silencing in the defensive glands of the mustard leaf beetle larvae, we conclude that there is a complex network of SLC2 transporters in which several transporters compensate the function of the silenced ones. We demonstrate clearly the potential of SLC2 transporters to respond adaptively to nutrient demand. This response may have paramount ecological implications for the survival of phytophagous beetles in plant-insect interactions.

Supporting Information

Figure S1 Bar plot showing the molecular functions assigned to the *Pc*SUTs. First, BLASTx was performed to annotate the studied sugar transporters of *P. cochleariae*. Thereafter, BLAST2GO was applied to those BLAST hits. The assigned molecular functions are displayed.
(EPS)

Figure S2 Phylogenetic tree of the 68 chosen sugar transporters derived from *P. cochleariae*. The phylogenetic tree was calculated with RAxML showing the main 4 groups. The purple subbranch is separated from the other branches with a bootstrap value of 100%.
(EPS)

Figure S3 Multiple sequence alignment of the 68 chosen sugar transporters derived from *P. cochleariae*. The multiple sequence alignment was calculated using Probalign. The purple-branch-specific amino acids are framed.
(TIF)

Figure S4 Phylogenetic tree of *Pc*SUTs derived from *P. cochleariae* and functionally characterized sugar transporters of other insects listed in Table 2 calculated with MrBayes.
(EPS)

Figure S5 Phylogenetic tree showing the selected organisms from the tree of life.
(EPS)

Figure S6 The phylogenetic tree of the nine sequences derived from *P. cochleariae* belonging to the purple branch (see Figure 3 and 4, Figure S4) and homologous sequences derived from the whole tree of life, especially from *Dendroctonus ponderosae* (Dc) as well as from *Tribolium castaneum* (Tc), was calculated using MrBayes. Indicated in purple, it can be seen that the beetles' sequences build up a separate branch.
(EPS)

Figure S7 Phylogenetic *tree* of the 68 chosen sugar transporters derived from *P. cochleariae*. The six most abundant glandular sugar transporters are circled and not branch-specific, but distributed all over the tree.
(EPS)

Figure S8 Relative mRNA levels of putative SLC2 transporters in the defensive glands of juvenile *P. cochleariae* determined by carrying out RNA-seq (A) and quantitative real-time PCR (B) experiments. The corresponding fold-changes of the RNA-seq samples are listed in Table S5.
(TIF)

Figure S9 RNAi effects on the development of the larvae from *P. cochleariae*. A, The development of larval weight was documented and measured in a 24 or 48 h±3 h period. B, In neither the relative growth rate nor in the weight of freshly emerged pupae significant differences could be observed between ds*gfp*- and ds*Pcsut1*-, ds*Pcsut2*-, ds*Pcsut5*-, ds*Pcsut6*-injected larvae, n = 30.
(TIF)

Figure S10 MvA-Plot showing normalized mean values *versus* $\log_2$fold-changes. The fold-changes (log-transformed) were computed for the comparison of ds*gfp*-injected and ds*Pcsut1*-injected samples. The transcript levels are significant at 10% FDR (padj< = 0.1, padj: p-value adjusted for multiple testing with the Benjamini-Hochberg procedure which controls false discovery rate (FDR)). The differentially expressed transporters, the ones colored red, are listed in Table 4. (A) MvA-Plot of the comparison of ds*Pcsut1*-injected and ds*gfp*-injected samples. *Pcsut1*'s transcript level was significantly reduced by RNAi (red dot in the lower right quadrant). (B) MvA-Plot of the comparison of ds*Pcsut2*-injected and ds*gfp*-injected samples. *Pcsut2*'s transcript level was significantly reduced by RNAi (red dot in the lower right area). Additionally, the expression of *Pcsut25* was significantly induced (red dot in the upper right part). (C) MvA-Plot of the comparison of ds*Pcsut6*-injected and ds*gfp*-injected samples. *Pcsut6*'s transcript level was significantly reduced by RNAi (red dot in the lower right area). Additionally, the expression of *Pcsut25* was significantly induced (red dot in the upper right part).
(TIF)

Table S1 Primer sets used in quantitative real-time PCR and RNAi experiments.
(XLSX)

Table S2 BLAST2GO results for all identified sugar transporters. Table shows sequence description, sequence length, minimal e-value of BLAST search, mean similarity to all 5 hits for each query sequence respectively, the number of assigned gene ontology (GO) categories as well as assigned GO categories.
(XLSX)

Table S3 Prediction of 12 transmembrane regions using TMHMM as well as Memsat2. Furthermore, the counts of each replicate as well as sequence length and coding region's length are listed.
(XLSX)

Table S4 The short reads of glandular tissues were mapped onto the transcriptome using bowtie. The short reads of the three replicates of RNA derived from the glandular tissue were mapped onto the transcriptome by applying bowtie. The percentages of aligned reads and of reads that did not align or were suppressed (due to option m) are listed. Furthermore, the numbers of reads that have been mapped are shown.
(XLSX)

Table S5 *Pcsut* counts normalized to the effective library size, relatively to *Pcrps3* and *Pcrpl6* according to Livak and Schmittgen [71]. Samples were derived from glandular tissue from juvenile *P. cochleariae*.
(XLSX)

Table S6 Counts normalized to the effective library size of all sugar transporters after dsRNA-injection. dsRNA targeting *Pcsut1*, *Pcsut2* and *Pcsut6* as well as dsRNA targeting *gfp* were injected. Samples were derived from glandular tissue from juvenile *P. cochleariae*.
(XLSX)

Acknowledgments

We sincerely thank Dr. Maritta Kunert and Angelika Berg for technical assistance. We are grateful for Dr. Lydia Gramzow's advices regarding the calculation of phylogenetic trees. Furthermore, we thank Andreas Petzold, Anja Strauß, Sindy Frick and Peter Rahfeld for all of their encouragement and fruitful discussions and Melinda Palmer-Kolb for critical reading of the manuscript.

Author Contributions

Conceived and designed the experiments: AB MS RRG. Performed the experiments: MS RRG AB MG SE. Analyzed the data: MS RRG MG AB. Contributed reagents/materials/analysis tools: MG WB. Wrote the paper: MS AB RRG.

References

1. Caviedes-Vidal E, Karasov WH, Chediack JG, Fasulo V, Cruz-Neto AP, et al. (2008) Paracellular absorption: A bat breaks the mammal paradigm. Plos One 3.
2. Augustin R (2010) The protein family of glucose transport facilitators: It's not only about glucose after all. Iubmb Life 62: 315–333.
3. Wright EM, Loo DDF, Hirayama BA (2011) Biology of human sodium glucose transporters. Physiol Rev 91: 733–794.
4. Elbein AD, Pan YT, Pastuszak I, Carroll D (2003) New insights on trehalose: a multifunctional molecule. Glycobiology 13: 17R–27R.
5. Becker A, Schloder P, Steele JE, Wegener G (1996) The regulation of trehalose metabolism in insects. Experientia 52: 433–439.
6. Thompson SN (2003) Trehalose - The insect 'blood' sugar. In: Simpson SJ, editor. Advances in Insect Physiology, Vol 31. London: Academic Press Ltd-Elsevier Science Ltd. 205–285.
7. Wegener G, Macho C, Schloder P, Kamp G, Ando O (2010) Long-term effects of the trehalase inhibitor trehazolin on trehalase activity in locust flight muscle. J Exp Biol 213: 3852–3857.
8. Candy DJ, Becker A, Wegener G (1997) Coordination and integration of metabolism in insect flight. Comp Biochem Physiol B Biochem Mol Biol 117: 497–512.
9. Silva MCP, Terra WR, Ferreira C (2010) The catalytic and other residues essential for the activity of the midgut trehalase from *Spodoptera frugiperda*. Insect Biochem Mol Biol 40: 733–741.
10. Bounias M, Bahjou A, Gourdoux L, Moreau R (1993) Molecular activation of a trehalase purified from the fat body of a coleopteran insect (*Tenebrio molitor*), by an endogenous insulin-like peptide. Biochem Mol Biol Int 31: 249–266.
11. Shimada S, Yamashita O (1979) Trehalose absorption related with trehalase in developing ovaries of the silkworm, *Bombyx mori*. J Comp Physiol 131: 333–339.
12. Bifano TD, Alegria TGP, Terra WR (2010) Transporters involved in glucose and water absorption in the *Dysdercus peruvianus* (Hemiptera: Pyrrhocoridae) anterior midgut. Comp Biochem Physiol B Biochem Mol Biol 157: 1–9.
13. Caccia S, Casartelli M, Grimaldi A, Losa E, de Eguileor M, et al. (2007) Unexpected similarity of intestinal sugar absorption by SGLT1 and apical GLUT2 in an insect (*Aphidius ervi*, Hymenoptera) and mammals. Am J Physiol Regul Integr Comp Physiol 292: R2284–R2291.
14. Giordana B, Milani A, Grimaldi A, Farneti R, Casartelli M, et al. (2003) Absorption of sugars and amino acids by the epidermis of *Aphidius ervi* larvae. J Insect Physiol 49: 1115–1124.
15. Chen ME, Holmes SP, Pietrantonio PV (2006) Glucose transporter 8 (GLUT8) from the red imported fire ant, *Solenopsis invicta* Buren (Hymenoptera : Formicidae). Arch Insect Biochem Physiol 62: 55–72.
16. Pascual I, Berjon A, Lostao MP, Barber A (2006) Transport of D-galactose by the gastrointestinal tract of the locust, *Locusta migratoria*. Comp Biochem Physiol B Biochem Mol Biol 143: 20–26.
17. Meyer H, Vitavska O, Wieczorek H (2011) Identification of an animal sucrose transporter. J Cell Sci 124: 1984–1991.
18. Kanamori Y, Saito A, Hagiwara-Komoda Y, Tanaka D, Mitsumasu K, et al. (2010) The trehalose transporter 1 gene sequence is conserved in insects and encodes proteins with different kinetic properties involved in trehalose import into peripheral tissues. Insect Biochem Mol Biol 40: 30–37.
19. Kikawada T, Saito A, Kanamori Y, Nakahara Y, ichi Iwata K, et al. (2007) Trehalose transporter 1, a facilitated and high-capacity trehalose transporter, allows exogenous trehalose uptake into cells. Proc Natl Acad Sci U S A 104: 11585–11590.
20. Kikuta S, Kikawada T, Hagiwara-Komoda Y, Nakashima N, Noda H (2010) Sugar transporter genes of the brown planthopper, *Nilaparvata lugens*: A facilitated glucose/fructose transporter. Insect Biochem Mol Biol 40: 805–813.
21. Kikuta S, Hagiwara-Komoda Y, Noda H, Kikawada T (2012) A novel member of the trehalose transporter family functions as an H^+-dependent trehalose transporter in the reabsorption of trehalose in Malpighian tubules. Front Physiol 3: 290–290.
22. Price DRG, Wilkinson HS, Gatehouse JA (2007) Functional expression and characterisation of a gut facilitative glucose transporter, NlHT1, from the phloem-feeding insect *Nilaparvata lugens* (rice brown planthopper). Insect Biochem Mol Biol 37: 1138–1148.
23. Price DRG, Tibbles K, Shigenobu S, Smertenko A, Russell CW, et al. (2010) Sugar transporters of the major facilitator superfamily in aphids; from gene prediction to functional characterization. Insect Mol Biol 19: 97–112.
24. Thorens B, Mueckler M (2010) Glucose transporters in the 21st Century. Am J Physiol Endocrinol Metab 298: E141–E145.
25. Pao SS, Paulsen IT, Saier MH (1998) Major facilitator superfamily. Microbiol Mol Biol Rev 62: 1–34.
26. Joost HG, Thorens B (2001) The extended GLUT-family of sugar/polyol transport facilitators: nomenclature, sequence characteristics, and potential function of its novel members. Mol Membr Biol 18: 247–256.
27. Mueckler M, Thorens B (2013) The SLC2 (GLUT) family of membrane transporters. Mol Aspects Med 34: 121–138.
28. Manolescu AR, Witkowska K, Kinnaird A, Cessford T, Cheeseman C (2007) Facilitated hexose transporters: New perspectives on form and function. Physiology 22: 234–240.
29. Gomez-Zurita J, Hunt T, Kopliku F, Vogler AP (2007) Recalibrated tree of leaf beetles (Chrysomelidae) indicates independent diversification of angiosperms and their insect herbivores. Plos One 2.
30. Uddin MM, Ulrichs C, Tokuhisa JG, Mewis I (2009) Impact of glucosinolate structure on the performance of the crucifer pest *Phaedon cochleariae* (F.). J Appl Bot Food Qual 82: 108–113.
31. Tremmel M, Mueller C (2013) The consequences of alternating diet on performance and food preferences of a specialist leaf beetle. J Insect Physiol 59: 840–847.
32. Termonia A, Hsiao TH, Pasteels JM, Milinkovitch MC (2001) Feeding specialization and host-derived chemical defense in Chrysomeline leaf beetles did not lead to an evolutionary dead end. Proc Natl Acad Sci USA 98: 3909–3914.
33. Whitman DW, Blum MS, Alsop DW (1990) Allomones: chemicals for defense. 289–351 p.
34. Noirot C, Quennedey A (1974) Fine-structure of insect epidermal glands. Annu Rev Entomol 19: 61–80.
35. Noirot C, Quennedey A (1991) Glands, gland-cells, glandular units - some comments on terminology and classification. Annales De La Societe Entomologique De France 27: 123–128.
36. Quennedey A (1998) Insect epidermal gland cells: Ultrastructure and morphogenesis; Harrison FWLM, editor. 177–207 p.
37. Laurent P, Braekman JC, Daloze D, Pasteels J (2003) Biosynthesis of defensive compounds from beetles and ants. Eur J Org Chem: 2733–2743.
38. Laurent P, Braekman JC, Daloze S (2005) Insect chemical defense. In: Schulz S, editor. Chemistry of Pheromones and Other Semiochemicals II. Schulz, S. ed: Springer, Berlin/Heidelberg. 167–229.
39. Pasteels JM, Braekman JC, Daloze D, Ottinger R (1982) Chemical defence in chrysomelid larvae and adults. Tetrahedron 38: 1891–1897.
40. Pasteels JM, Rowell-Rahier M, Brackman J-C, Daloze D (1994) Chemical defence of adult leaf beetles updated. In: Jolivet PH, Cox ML, Petitpierre E, editors. Novel aspects of the biology of Chrysomelidea. Dordrecht: Kluwer Academic Publishers. 289–301.
41. Deroe C, Pasteels JM (1982) Distribution of adult defense glands in chrysomelids (Coleoptera: Chrysomelidae) and its significance in the evolution of defense mechanisms within the family. J Chem Ecol 8: 67–82.
42. Pasteels JM, Rowell-Rahier M (1989) Defensive glands and secretions as taxonomical tools in the Chrysomelidae. Entomography 6: 423–432.
43. Renner K (1970) Über die ausstülpbaren Hautblasen der Larven von *Gastroidea viridula* De Geer und ihre ökologische Bedeutung (Coleoptera: Chrysomelidae). Beiträge zur Entomologie 20: 527–533.
44. Burse A, Schmidt A, Frick S, Kuhn J, Gershenzon J, et al. (2007) Iridoid biosynthesis in Chrysomelina larvae: Fat body produces early terpenoid precursors. Insect Biochem Mol Biol 37: 255–265.
45. Frick S, Nagel R, Schmidt A, Bodemann RR, Rahfeld P, et al. (2013) Metal ions control product specificity of isoprenyl diphosphate synthases in the insect terpenoid pathway. Proc Natl Acad Sci U S A 110: 4194–4199.
46. Strauss AS, Peters S, Boland W, Burse A (2013) ABC transporter functions as a pacemaker for sequestration of plant glucosides in leaf beetles. eLife: DOI:10.7554/eLife.01096.
47. Ibanez S, Gallet C, Després L (2012) Plant insecticidal toxins in ecological networks. Toxins 4: 228–243.
48. Bodemann RR, Rahfeld P, Stock M, Kunert M, Wielsch N, et al. (2012) Precise RNAi-mediated silencing of metabolically active proteins in the defence secretions of juvenile leaf beetles. Proc R Soc B 279: 4126–4134.
49. Bentley DR, Balasubramanian S, Swerdlow HP, Smith GP, Milton J, et al. (2008) Accurate whole human genome sequencing using reversible terminator chemistry. Nature 456: 53–59.
50. Grabherr MG, Haas BJ, Yassour M, Levin JZ, Thompson DA, et al. (2011) Full-length transcriptome assembly from RNA-Seq data without a reference genome. Nat Biotechnol 29: 644–652.

51. Haas BJ, Papanicolaou A, Yassour M, Grabherr M, Blood PD, et al. (2013) De novo transcript sequence reconstruction from RNA-seq using the Trinity platform for reference generation and analysis. Nat Protoc 8: 1494–1512.
52. Pertea G, Huang X, Liang F, Antonescu V, Sultana R, et al. (2003) TIGR Gene Indices clustering tools (TGICL): a software system for fast clustering of large EST datasets. Bioinformatics 19: 651–652.
53. Zhang Z, Schwartz S, Wagner L, Miller W (2000) A greedy algorithm for aligning DNA sequences. J Comput Biol 7: 203–214.
54. Huang X, Madan A (1999) CAP3: A DNA sequence assembly program. Genome Res 9: 868–877.
55. Punta M, Coggill PC, Eberhardt RY, Mistry J, Tate J, et al. (2012) The Pfam protein families database. Nucleic Acids Res 40: D290–D301.
56. Finn RD, Tate J, Mistry J, Coggill PC, Sammut SJ, et al. (2008) The Pfam protein families database. Nucleic Acids Res 36: D281–D288.
57. Boeckmann B, Bairoch A, Apweiler R, Blatter MC, Estreicher A, et al. (2003) The SWISS-PROT protein knowledgebase and its supplement TrEMBL in 2003. Nucleic Acids Res 31: 365–370.
58. O'Donovan C, Martin MJ, Gattiker A, Gasteiger E, Bairoch A, et al. (2002) High-quality protein knowledge resource: SWISS-PROT and TrEMBL.. Brief Bioinform 3: 275–284.
59. Krogh A, Larsson B, von Heijne G, Sonnhammer EL (2001) Predicting transmembrane protein topology with a hidden Markov model: application to complete genomes. J Mol Biol 305: 567–580.
60. Jones DT, Taylor WR, Thornton JM (1994) A model recognition approach to the prediction of all-helical membrane protein structure and topology. Biochemistry 33: 3038–3049.
61. Roshan U, Livesay DR (2006) Probalign: multiple sequence alignment using partition function posterior probabilities. Bioinformatics 22: 2715–2721.
62. Ronquist F, Teslenko M, van der Mark P, Ayres DL, Darling A, et al. (2012) MrBayes 3.2: efficient Bayesian phylogenetic inference and model choice across a large model space. Syst Biol 61: 539–542.
63. Huelsenbeck JP, Ronquist F (2001) MRBAYES: Bayesian inference of phylogenetic trees. Bioinformatics 17: 754–755.
64. Stamatakis A (2006) RAxML-VI-HPC: maximum likelihood-based phylogenetic analyses with thousands of taxa and mixed models. Bioinformatics 22: 2688–2690.
65. Keeling CI, Henderson H, Li M, Yuen M, Clark EL, et al. (2012) Transcriptome and full-length cDNA resources for the mountain pine beetle, *Dendroctonus ponderosae* Hopkins, a major insect pest of pine forests. Insect Biochem Mol Biol 42: 525–536.
66. Langmead B (2010) Aligning short sequencing reads with Bowtie. Curr Protoc Bioinformatics Chapter 11: Unit 11.17.
67. Gentleman RC, Carey VJ, Bates DM, Bolstad B, Dettling M, et al. (2004) Bioconductor: open software development for computational biology and bioinformatics. Genome Biol 5: R80.
68. Morgan M, Anders S, Lawrence M, Aboyoun P, Pagès H, et al. (2009) ShortRead: a bioconductor package for input, quality assessment and exploration of high-throughput sequence data. Bioinformatics 25: 2607–2608.
69. Anders S, Huber W (2010) Differential expression analysis for sequence count data. Genome Biol 11: R106.
70. Anders S, McCarthy DJ, Chen Y, Okoniewski M, Smyth GK, et al. (2013) Count-based differential expression analysis of RNA sequencing data using R and Bioconductor. Nat Protoc 8: 1765–1786.
71. Livak KJ, Schmittgen TD (2001) Analysis of relative gene expression data using real-time quantitative PCR and the $2^{-\Delta\Delta CT}$ method. Methods 25: 402–408.
72. Bustin SA, Benes V, Garson JA, Hellemans J, Huggett J, et al. (2009) The MIQE Guidelines: Minimum Information for Publication of Quantitative Real-Time PCR Experiments. Clin Chem 55: 611–622.
73. Kuhnle A, Muller C (2009) Differing acceptance of familiar and unfamiliar plant species by an oligophagous beetle. Entomol Exp Appl 131: 189–199.
74. Quackenbush J, Liang F, Holt I, Pertea G, Upton J (2000) The TIGR gene indices: reconstruction and representation of expressed gene sequences. Nucleic Acids Res 28: 141–145.
75. Katoh K, Misawa K, Kuma K, Miyata T (2002) MAFFT: a novel method for rapid multiple sequence alignment based on fast Fourier transform. Nucleic Acids Res 30: 3059–3066.
76. Zhao F–Q, Keating AF (2007) Functional properties and genomics of glucose transporters. Curr Genomics 8: 113–128.
77. Garcia JC, Strube M, Leingang K, Keller K, Mueckler MM (1992) Amino acid substitutions at tryptophan 388 and tryptophan 412 of the HepG2 (Glut1) glucose transporter inhibit transport activity and targeting to the plasma membrane in *Xenopus* oocytes. J Biol Chem 267: 7770–7776.
78. Schuermann A, Keller K, Monden I, Brown FM, Wandel S, et al. (1993) Glucose transport activity and photolabelling with 3-[^{125}I]iodo-4-azidophenethylamido-7-*O*-succinyldeacetyl (IAPS)-forskolin of two mutants at tryptophan-388 and −412 of the glucose transporter GLUT1: dissociation of the binding domains of forskolin and glucose. Biochem J 290: 497–501.
79. Wilson-O'Brien AL, Patron N, Rogers S (2010) Evolutionary ancestry and novel functions of the mammalian glucose transporter (GLUT) family. BMC Evol Biol 10.
80. Petzold A, Reichwald K, Groth M, Taudien S, Hartmann N, et al. (2013) The transcript catalogue of the short-lived fish *Nothobranchius furzeri* provides insights into age-dependent changes of mRNA levels. BMC Genomics 14: 185.
81. Cura AJ, Carruthers A (2012) Role of monosaccharide transport proteins in carbohydrate assimilation, distribution, metabolism, and homeostasis. Compr Physiol 2: 863–914.
82. Douady CJ, Delsuc F, Boucher Y, Doolittle WF, Douzery EJP (2003) Comparison of Bayesian and maximum likelihood bootstrap measures of phylogenetic reliability. Mol Biol Evol 20: 248–254.
83. Cuthbertson JM, Doyle DA, Sansom MS (2005) Transmembrane helix prediction: a comparative evaluation and analysis. Protein Eng Des Sel 18: 295–308.
84. Fraga A, Ribeiro L, Lobato M, Santos V, Silva JR, et al. (2013) Glycogen and glucose metabolism are essential for early embryonic development of the red flour beetle *Tribolium castaneum*. Plos One 8.
85. Leto D, Saltiel AR (2012) Regulation of glucose transport by insulin: traffic control of GLUT4. Nat Rev Mol Cell Biol 13: 383–396.
86. Price DRG, Karley AJ, Ashford DA, Isaacs HV, Pownall ME, et al. (2007) Molecular characterisation of a candidate gut sucrase in the pea aphid, *Acyrthosiphon pisum*. Insect Biochem Mol Biol 37: 307–317.

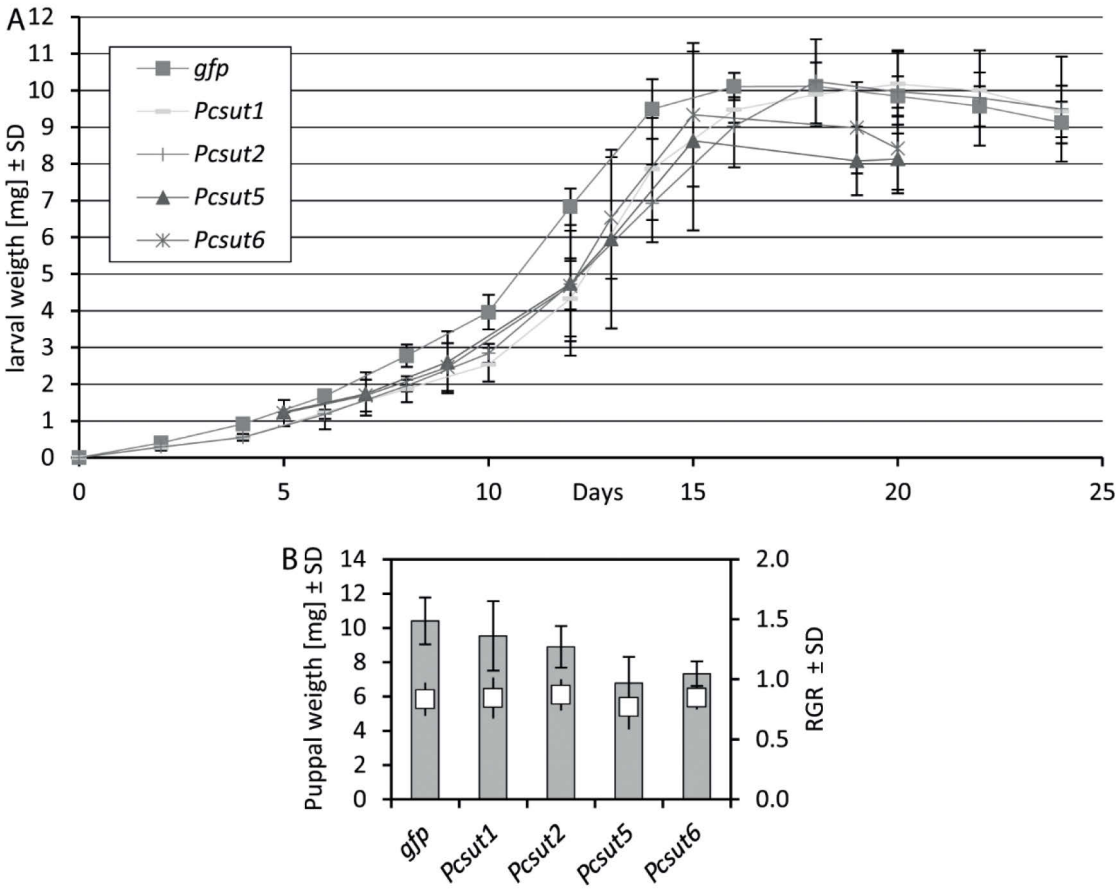

Figure S9 RNAi effects on the development of the larvae from *P. cochleariae*.

A, The development of larval weight was documented and measured in a 24 or 48 h period. B, In neither the relative growth rate nor in the weight of freshly emerged pupae significant differences could be observed between ds*gfp*- and ds*Pcsut1*-, ds*Pcsut2*-, ds*Pcsut5*-, ds*Pcsut6*-injected larvae, n =30.

Manuskript 3: (Bodemann, Rahfeld u.a. 2012)

PROCEEDINGS OF THE ROYAL SOCIETY B

Proc. R. Soc. B (2012) **279**, 4126–4134
doi:10.1098/rspb.2012.1342
Published online 8 August 2012

Precise RNAi-mediated silencing of metabolically active proteins in the defence secretions of juvenile leaf beetles

René Roberto Bodemann[1,†], Peter Rahfeld[1,†], Magdalena Stock[1], Maritta Kunert[1], Natalie Wielsch[1], Marco Groth[2], Sindy Frick[1], Wilhelm Boland[1] and Antje Burse[1,*]

[1]*Max Planck Institute for Chemical Ecology, Beutenberg Campus, Hans-Knoell-Str. 8, 07745 Jena, Germany*
[2]*Leibniz Institute for Age Research – Fritz Lipmann Institute, Beutenbergstr. 11, 07745 Jena, Germany*

Allomones are widely used by insects to impede predation. Frequently these chemical stimuli are released from specialized glands. The larvae of Chrysomelina leaf beetles produce allomones in gland reservoirs into which the required precursors and also the enzymes are secreted from attached gland cells. Hence, the reservoirs can be considered as closed bio-reactors for producing defensive secretions. We used RNA interference (RNAi) to analyse *in vivo* functions of proteins in biosynthetic pathways occurring in insect secretions. After a salicyl alcohol oxidase was silenced in juveniles of the poplar leaf beetles, *Chrysomela populi*, the precursor salicyl alcohol increased to 98 per cent, while salicyl aldehyde was reduced to 2 per cent within 5 days. By analogy, we have silenced a novel protein annotated as a member of the juvenile hormone-binding protein superfamily in the juvenile defensive glands of the related mustard leaf beetle, *Phaedon cochleariae*. The protein is associated with the cyclization of 8-oxogeranial to iridoids (methylcyclopentanoid monoterpenes) in the larval exudates made clear by the accumulation of the acylic precursor 5 days after RNAi triggering. A similar cyclization reaction produces the secologanin part of indole alkaloids in plants.

Keywords: RNAi; insects; leaf beetle; secretome; salicyl alcohol oxidase; monoterpene cyclization

1. INTRODUCTION

Insects are extraordinarily inventive when it comes to producing defensive compounds for repelling their enemies. To circumvent auto-intoxicative effects, these natural products frequently originate in the epidermis-derived exocrine glands [1]. The gland cells produce secretions that are fortified with defensive compounds [2,3]. It has been demonstrated that insects convert either intrinsic precursors or food-derived compounds into biologically active allelochemicals [4–7]. The precursors can be activated in the defensive glands or in the secretions. Immature leaf beetles of the subtribe Chrysomelina, for example, produce their deterrents in biphasic secretions, and store them in nine unique pairs of impermeable reservoirs in their backs [8,9]. The larval exudates containing salicyl aldehyde (**3**) have been of particular interest [10,11]. The hydrophobic aldehyde forms an organic layer, accounting for 15 per cent of the total discharge volume, while the aqueous phase constitutes 85 per cent [12]. The latter contains the precursor salicyl alcohol (**2**) and a flavine-dependent salicyl alcohol oxidase (SAO); the SAO uses molecular oxygen as an electron acceptor for alcohol oxidation, yielding the aldehyde and hydrogen peroxide [12–14] (figure 1). Salicyl aldehyde is considered as a potent repellent against generalist predators [11,15] and as an antimicrobial agent [16]. The larvae feed on salicaceous plants and sequester the secondary metabolite salicin (**1**) [17–19]. After shuttling salicin to the defensive glands, the glucoside is cleaved by a β-glucosidase into **2** and glucose for further metabolism [20] (figure 1). According to phylogenetic analyses, the synthesis of **3** from sequestered precursors has evolved from the de novo production of defensive iridoids (methylcyclopentanoid monoterpenes containing an iridane skeleton) [21]. Also the last steps of the iridoid pathway in the secretions are thought to be similar to those found in sequestering species [20] (figure 1). At first, the sugar moiety is cleaved from 8-hydroxygeraniol-8-*O*-β-D-glucoside (**4**), and an oxygen-dependent oxidase converts the aglucone into 8-oxogeranial (**6**) [20,22–24]. A subsequent cyclization reaction yields iridoids (**7**) [25].

Despite the many current genome- and transcriptome-sequencing projects, up to now it has only been shown for SAO sequences to be entangled in allomone production in the defensive secretions of the leaf beetle species *Chrysomela tremulae*, *Chrysomela populi*, *Chrysomela lapponica* and *Phratora vitellinae* [13,14,26]. To demonstrate the *in vivo* relevance of a target sequence, gene silencing by RNA interference (RNAi) is a suitable method. RNAi is an endogenous mechanism, derived from an anti-viral immune response [27], and can be found virtually in all eukaryotic species. It can be triggered artificially by double-stranded RNA (dsRNA), whose nucleotide sequence is identical to that of the target gene [28]. The

* Author for correspondence (aburse@ice.mpg.de).
†These authors contributed equally to the study.

Electronic supplementary material is available at http://dx.doi.org/10.1098/rspb.2012.1342 or via http://rspb.royalsocietypublishing.org.

Received 12 June 2012
Accepted 17 July 2012

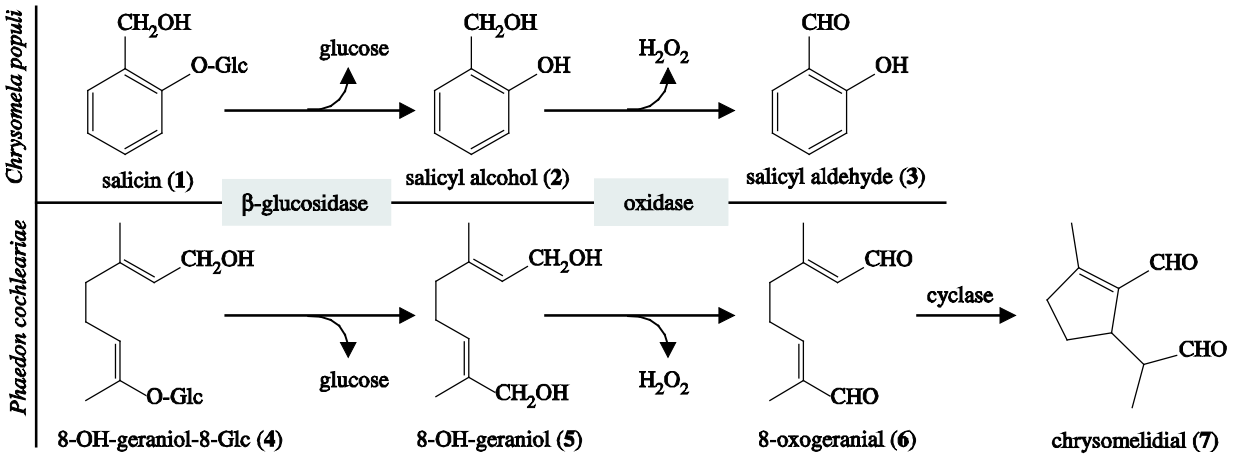

Figure 1. Enzymatic reactions in the defensive secretions of juvenile *C. populi* and *P. cochleariae* adapted from Michalski *et al.* [14]. Glc, Glucose.

RNAi effect is attended by decreased transcript and protein levels, and consequently by loss-of-function phenotypes. In addition to embryogenesis, pattern formation, reproduction and behaviour, RNAi allows biosynthetic pathways in insects to be successfully analysed [29–31].

Here, we describe how RNAi can be used to target the biosynthesis of discrete components in the defensive discharges of juvenile Chrysomelina. We first validated this technique by silencing the known *SAO* sequence in the sequestering species *C. populi* (*CpopSAO*). After knocking down the SAO, the alcohol precursor of **3** accumulated in the gland. This showed that we are able to interrupt the deterrent biosynthesis *in vivo*. Next, we extended the method to the related de novo iridoid-producing species, *P. cochleariae*. In the secretions of its larvae C_{10}-precursors are converted to the methylcyclopentanoid monoterpene chrysomelidial. Particularly, the cyclization mechanism is of importance because it occurs not only in insects but also in plants. Here, the cyclization leads ultimately to secologanin, one of the building blocks for more than 2500 indole alkaloids that have been isolated mainly from three plant families [32]. Although an enzyme with cyclase activity for secologanin biosynthesis has long been predicted, a corresponding sequence has yet to be published. In the *P. cochleariae* secretome, we identified a novel protein which is involved in the cyclization reaction of the monoterpenoid 8-oxogeranial to chrysomelidial.

2. MATERIAL AND METHODS

See electronic supplementary material for complete secretome analyses by data-independent liquid chromatography/mass spectrometry detection (LC/MS^E), cloning procedures, detailed quantitative real-time PCR procedure (qPCR), all primer sequences and accession numbers.

(a) *Beetle rearing and secretion analyses*

Chrysomela populi (L.) was collected near Dornburg, Germany (latitude 51.015, longitude 11.64), on *Populus maximowiczii* × *Populus nigra*. In the laboratory, beetles were kept in a 16 L : 8 D cycle, 18 ± 2°C in light and 13 ± 2°C in darkness. *Phaedon cochleariae* (F.) was laboratory-reared on *Brassica oleracea* convar. *capitata* var. *alba* (Gloria F1) in 16 L : 8 D cycle conditions and 15 ± 2°C. According to [33], we obtained the relative growth rate (RGR) of six biological replicates of each group of five larvae by RGR = [(final weight − weight of neonate larva)/(weight of neonate larva × developmental time (days))]. Each replicate group was weighed every 24 ± 3 h and data were compared with two-tailed *t*-test. Larval secretions were collected in glass capillaries (inner diameter, 0.28 mm; outer diameter, 0.78 mm, length 100 mm; Hirschmann, Eberstadt, Germany). Sealed capillaries containing samples were stored at −20°C until needed. Secretions were weighed in the sealed capillaries on an ultra-microbalance (Mettler-Toledo, Greifensee, Switzerland) three times; the weight of the capillaries was subtracted and the final weight was averaged.

(b) *Production of double-stranded RNA*

Sequenced plasmids pIB-*CpopSAO* (GeneBank: HQ245 154.1) and pIB-*PcTo-like* (GeneBank: JQ728549) were used to amplify a 1.5 kb *CpopSAO* fragment and a 450 bp *PcTo-like* fragment, respectively. The *gfp* sequence was amplified from pcDNA3.1/CT- GFP-TOPO (Life Technology, Darmstadt, Germany). The amplicons were subject to *in vitro* transcription assays according to instructions from the Ambion MEGAscript RNAi kit (Life Technologies, Darmstadt, Germany). The resulting dsRNA was eluted after nuclease digestion three times with 50 µl of injection buffer (3.5 mM Tris–HCl, 1 mM NaCl, 50 nM Na_2HPO_4, 20 nM KH_2PO_4, 3 mM KCl, 0.3 mM EDTA, pH 7.0). The concentration of dsRNA was calculated with A = 1 = 45 mg ml^{-1} and adjusted to 1 µg $µl^{-1}$. The quality of dsRNA was checked by TBE-agarose-electrophoresis.

(c) *Injection of double-stranded RNA*

First instar of *C. populi* with 5 mm body length was injected with 0.1–3 µg of dsRNA approximately 10 days after hatching. *Phaedon cochleariae* second instar with 4 mm body length was injected with 0.3 µg of dsRNA approximately 5 days after hatching. Injections were accomplished with ice-chilled larvae using a Nano2000 injector (WPI, Sarasota, FL, USA) directed by a three-axis micromanipulator. The larvae were injected parasagittally between the pro- and mesothorax.

(d) *Off-target prediction*

According to the mechanism of RNAi [28], the top and bottom strands of dsRNAs of *CpopSAO*, *PcTo-like* and *gfp* were diced *in silico* into all possible 21 bp fragments [34]. The resulting siRNAs were subjected to BLASTn

(stand-alone NCBI-BLAST) [35] by invoking BLASTALL v. 2.2.21 (parameters: -p blastn -e 1e-1 -G 7 -T -b 80 -v 80) searching against our in-house transcriptome databases of *C. populi* and *P. cochleariae*. Hits less than 20 nts in length were ignored and hits more than or equal to 20 nts were considered as putative off targets.

(e) CpopSAO *and* PcTo-like *transcript abundance*

Cq values of genes of interest from three biological replicates were normalized by *CpRPL45* and *CpActin* for *C. populi* and *PcRP-L8* and *PcRP-S18* for *P. cochleariae*, respectively. Real-time PCR data were acquired on an Mx3000P Real-Time PCR system using Brilliant II SYBR Green qPCR Master Mix (Agilent, Santa Clara, CA, USA).

(f) *Gas chromatographylmass spectrometry analysis of low-molecular-weight compounds in chrysomelid secretions*

Secretions of *C. populi* were diluted in 1 : 150 (w/v) ethyl acetate and secretions of *P. cochleariae* were diluted in 1 : 100 (w/v) dichloromethane. Of each diluted secretion, 1 µl was subjected to GC/EIMS analysis (ThermoQuest Finnigan Trace GC/MS 2000, Frankenhorst, Germany) equipped with Phenomenex (Aschaffenburg, Germany) ZB–5–W/Guardian–column, 25 m. Substances were separated using helium as a carrier (1.5 ml min^{-1}). Conditions for *C. populi* secretions: 50°C (1 min), 10°C per minute to 80°C, 60°C per minute to 280°C (1 min). Inlet temperature was 220°C, transfer line was 280°C. Substances were identified according to standard substances **2** and **3**. Conditions for *P. cochleariae* secretions: 50°C (2 min), 10°C per minute to 80°C, 5°C per minute to 200°C, 30°C per minute to 300°C (1 min). Inlet temperature was 220°C and transfer line was 280°C. Substances were identified according to [36] and the reference compounds 8-oxogeranial and chrysomelidial. The synthesis of 8-oxogeranial and chrysomelidial was carried out as in [25,37], respectively. Peak areas from GC-chromatograms were obtained using an ICIS-algorithm (XCALIBUR BUNDLE v. 2.0.7, Thermo Scientific).

(g) *Statistical analyses*

Two-tailed Student's *t*-tests for unequal variation were used to value the significance levels of transcript abundances and to weight differences comparing values of three different biological replicates from the non-injected control (NIC) group with those of either the RNAi group or the *gfp* control. Multi-dimensional ANOVA tests were carried out to validate significant differences in time series and between different RNAi treatments. The level of significance was reached at a *p*-value of 0.05. Calculations were done with R (http://www.r-project.org/).

3. RESULTS

(a) *Targeting the defensive glands of juvenile poplar leaf beetles by RNA interference*

Recently, a 1872-bp *CpopSAO* cDNA (Genbank/HQ245154.1) encoding a 69 kDa protein for conversion of **2** into **3** was identified from the larval defensive glands of *C. populi* [13,14] (figure 2*a*). It belongs to the glucose–methanol–choline (GMC) family of oxido-reductases [38]. Given that the expression of *CpopSAO* was detectable exclusively in glandular tissues (figure 2*b*), silencing this gene would affect only the process of glandular biosynthesis.

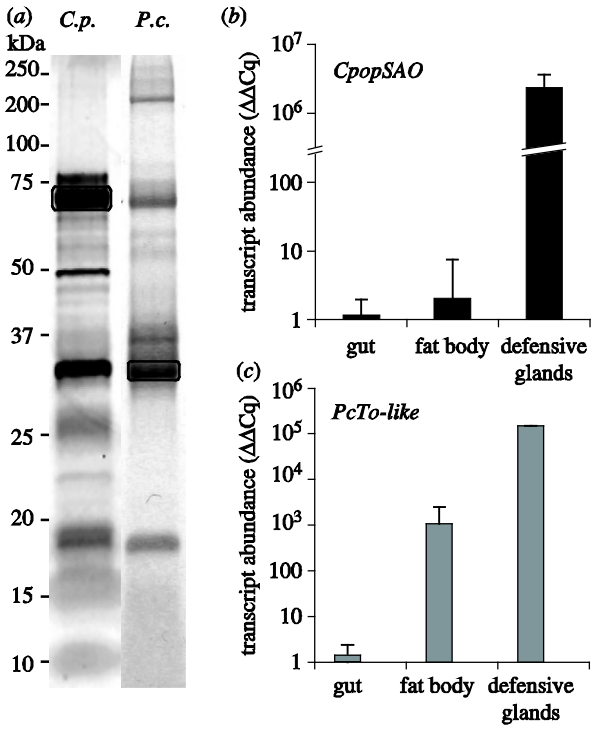

Figure 2. Protein and transcript abundance in juvenile leaf beetles. (*a*) Proteins in defensive exudates separated by one-dimensional SDS–PAGE. left: 1 mg secretions of *C. populi* (*C.p.*), silver stained, box marks *Cpop*SAO; right: 0.65 mg secretions of *P. cochleariae* (*P.c.*), Coomassie stained, box marks *Pc*To-like. (*b*) Expression pattern of *CpopSAO* ±s.d. in different *C. populi* tissues, $n = 3$. (*c*) Expression pattern of *PcTo-like* ±s.d. in different *P. cochleariae* tissues, $n = 2$. Both *y*-axes are in $\log_{10}$ scale.

To induce RNAi in *C. populi* larvae, we injected 1.0 µg of 1.5 kb *CpopSAO* dsRNA into late first instar. A 719-bp dsRNA fragment of *gfp* served as a control for effects caused by dsRNA; although the RNAi machinery will be induced, genes should not be silenced. Furthermore, we included an NIC group in our experiments. By monitoring the developmental traits and the secretion production in *C. populi* and comparing the results with those from control groups, we found that silencing *CpopSAO* did not influence either growth rate or pupae weight (see the electronic supplementary material, figure S1*a*). But the larvae treated with *CpopSAO* dsRNA produced slightly more secretions than did the larvae of the control groups (see the electronic supplementary material, figure S1*b*), which might be owing to the different osmotic characteristics between **2** and **3** [12]. Because we did not detect significant differences between NIC and *gfp* controls in any experiments delineated below, we continue showing only the data of the *gfp* controls.

Transcript abundance was measured in glandular tissue using qPCR after 1, 3 and 12 days. Comparing tissue from these samples to tissue from the *gfp* controls, we noticed significant reductions to 7.6 per cent mRNA level ($p = 0.002$) just 24 h after injection. After day 3, the transcript level was diminished to 1.6 per cent ($p = 0.004$), and after day 12, to 0.5 per cent (figure 3*a*).

In accordance with the literature, SAO corresponds to the dominant band at 70 kDa in the secretions of

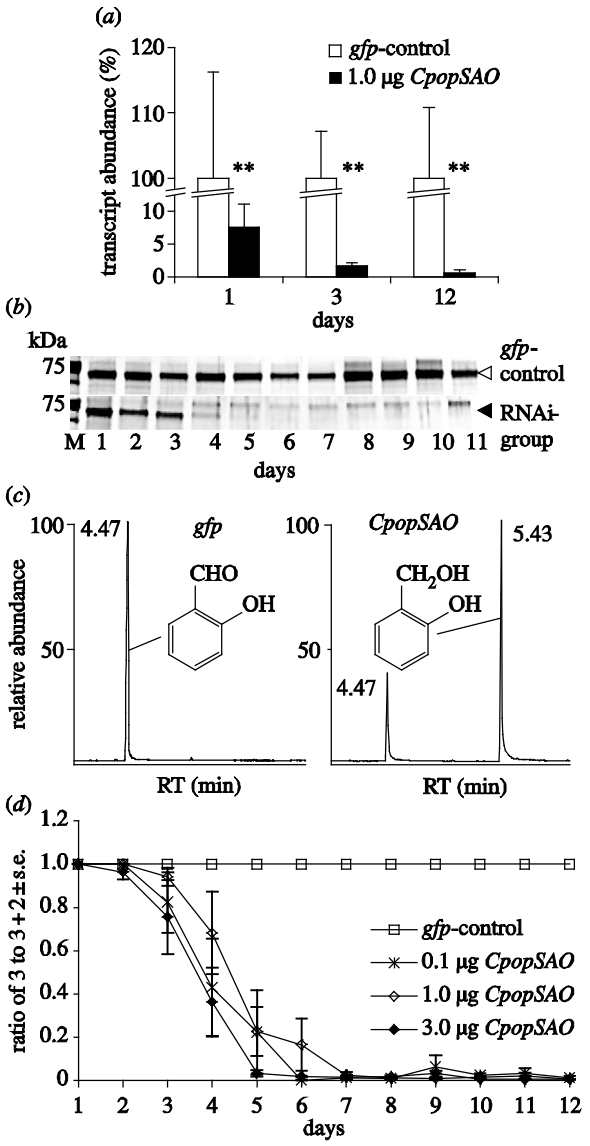

Figure 3. RNAi effects in juvenile *C. populi*. (*a*) White bars: transcript abundance of *CpopSAO* after injecting 1.0 µg *gfp* dsRNA, $n = 3 \pm$ s.d.. Black bars: transcript abundance of *CpopSAO* after injecting 1.0 µg *CpopSAO* dsRNA, $n = 3$. 100% = ΔCq of *gfp* control. Asterisks indicate level of significance: $^{**}p < 0.01$ (*b*) *Cpop*SAO protein abundance in defence secretions was monitored over time. A total of 0.85 mg secretions per lane was separated on silver-stained SDS gels. The 70-kDa band corresponds to *Cpop*SAO. Secretions originating from control treatment with 1 µg dsRNA of *gfp* (white arrowhead) and RNAi treatment with 1 µg dsRNA of *CpopSAO* (black arrowhead) are shown. (*c*) GC-chromatogram of secretions on day 5 after treatment; left: injecting 1.0 µg *gfp* dsRNA resulted in the production of **3**, right: injecting 1.0 µg *CpopSAO* dsRNA resulted in the production of **2** and **3**. (*d*) GC-chromatogram peak-area-based plot of secretions after dsRNA injection of *gfp* and different amounts of *CpopSAO* ($n = 5$).

C. populi (figure 2*a*) [12,14]. The composition of the secretome after dsRNA treatment was monitored in a time series in silver-stained one-dimensional SDS gels. Owing to the silencing effect, the quantity of *Cpop*SAO was apparently reduced just 2 days after dsRNA injection and the protein was barely visible after day 5 (figure 3*b*).

The effects on the biosynthesis of **3** in the defensive secretions were determined by GC/MS analysis. For these experiments, 0.1, 1.0 and 3.0 µg of *CpopSAO* dsRNA were injected into larvae from the same clutch. As in the protein reduction, we detected **2** in the defensive secretions just 2 days after the injection of 3.0 µg *CpopSAO* dsRNA (figure 3*c*). Compound **2** was not detectable in *gfp* control secretions. In addition, no unexpected chemical compound arose owing to the dsRNA treatments. By setting the peak area of **3** in ratio equalling the sum of the main peak areas, a diagram of the RNAi-dependent reduction of **3** can be plotted (figure 3*d*). We have tested dsRNA amounts ranging from 0.1 to 3.0 µg. After RNAi induction, significantly less aldehyde was observed for the 3.0 µg *CpopSAO* group ($p = 0.015$) on the 4th day and for all tested *CpopSAO* groups on the 5th day (0.1 µg, $p = 0.016$; 1 µg, $p = 0.002$; 3 µg, $p = \ll 0.001$). Biological variation prevented us from observing dose-dependent RNAi effects in these experiments; the amount of **2** did not differ significantly between the RNAi samples.

(b) *Off-target prediction and validation for* CpopSAO

Owing to strong sequence identities, co-silencing non-target genes can cause unintended side-effects [39,40]. Therefore, we performed off-target predictions for the desired dsRNA sequences of *CpopSAO* and *gfp*. Predicted off-target genes were validated by qPCR using cDNA derived from successful RNAi experiments. Because of a lack of genome sequences, the potential silencing effects of targeting the nucleus where fragments of the long dsRNA may bind to non-transcribed regulatory sequences [41] or introns [42] could be neither predicted nor validated.

For *gfp* dsRNA, no critical candidates were detected in the transcriptome library of *C. populi*. Off-target analyses in the *C. populi* sequence library, however, identified 25–21 bp contiguous regions of *CpopSAO* dsRNA that were identical to sequences of eight unique transcripts (see the electronic supplementary material, table ST2 for putative off-target hits). Three of them encode putative proteins having the GMC-oxidoreductase motif in the C-terminal region (*Cp*GMClike I-III) and five were annotated as hypothetical proteins (*Cp*COMP3092; *Cp*COMP6024; *Cp*COMP36289; *Cp*COMP38777; *Cp*COMP51471).

CpopSAO shares with *CpGMClike-I* two similar regions spanning 22 and 25 nucleotides (nts) each; these regions are interrupted by one mismatch (22/1 and 25/1) and, with *CpGMClike-III*, one similar sequence stretch without mismatch (24/0). *CpGMClike-II* and the five remaining transcripts possess sequence regions of 22/0 to 20/0 nts identical to *CpopSAO*. In all tissues, all putative off-target genes exhibited generally low expression levels with relative Cq values median less than 2×10^{-3}. qPCR assays were carried out for all eight targets 12 days after larvae were treated with 1.0 µg 1500-bp *CpopSAO* dsRNA; only for the *CpGMClike-I* and *CpGMClike-II* did these treatments reveal significant differences of transcript level in the gut tissue ($p = 0.049$; $p = 0.032$). No other tested transcripts showed changes of mRNA abundance in the examined tissues

(see the electronic supplementary material, figure S2). Since *C. populi* larvae transport the plant-derived precursor into the defensive glands for final transformation, we assume that the off-target effects on the putative GMC-oxidoreductases in gut tissue of unknown function do not distort the RNAi effects observed in the secretions.

(c) *Identification of unknown proteins in the defence-related secretome of* Phaedon cochleariae

After successfully introducing the 'lack-of-function approach' to the defensive secretions of *C. populi* by silencing an enzyme for which we had a clear expectation of the resulting phenotype, we used the method to identify proteins in unknown secretions. For this reason, we chose the larval exudates from the related de novo iridoid-producing species *P. cochleariae*. We assigned to the abundant 35-kDa band a putative protein whose deduced sequence contains 243 amino acids and a 22 amino acid signal peptide; the existence of such a sequence suggests that the mature protein is secreted (figure 2*a*). It possesses a conserved domain (pfam06585) characteristic for the juvenile hormone-binding protein (JHBP) superfamily. Sequence comparisons using the BLAST algorithm [35] revealed that the *P. cochleariae* amino acid sequence shares only very limited identity with functionally characterized insect proteins, for example, 12 per cent identity with the JHBP from *Bombyx mori* [43] and 16 per cent with the takeout (To) 1 from *Epiphyas postvittana* [44] (figure 2*a*). Higher identities up to 25 per cent were found only with insect proteins not yet fully characterized in their functions, such as those with the To-like protein (NP_001191952) from *Acyrtosyphon pisum* or the JHBP-like (XP_001359416) from *Drosophila pseudoobscura pseudoobscura*. None of the mentioned insect species is known to produce cyclic monoterpenoids.

The JHBP superfamily combines both the To protein family and the JHBP family. There are two major differences between the families: one is the number of disulphide bonds (To proteins have one and JHBPs have two) and the second are the conserved C-terminal sequence motives that are only present in To proteins. *In silico* analyses predicted in the *P. cochleariae* sequence seven N-glycosylation sites and only one disulphide bond. Along with identifying the two To-specific motives [45] (figure 4) in the C-terminal region, we conclude that our protein can be attributed to the To family. Therefore, we named it *Pc*To-like.

Despite the generally low sequence similarity, most To proteins and JHBPs are classified as ligand-binding proteins for juvenile hormones or similar hydrophobic terpenoids [44,46–49]. Because the precursor of the cyclic iridoid is also a terpenoid, we hypothesize that the putative protein could be involved in the iridoid biosynthesis in the defensive secretions. The assumption that the putative protein has relevance in the defensive glands is corroborated by the high transcript level which has been detected mainly in the glandular tissue of juvenile mustard leaf beetles (figure 2*c*). Low mRNA levels were also detectable in the fat body tissue.

(d) *RNA interference effects in larvae of* Phaedon cochleariae

A total of 0.3 µg of dsRNA derived from a 450-bp fragment of the *PcTo-like* sequence was injected into second instars of *P. cochleariae*. Transcript quantification 5 days after dsRNA injection confirmed a significant reduction of the mRNA in glandular tissue ($p = 0.043$) down to 1.0 per cent ($\pm 0.9\%$) compared with mRNA levels in *gfp* injections (figure 5*a*).

Phenotypic analyses after injection of dsRNA on the composition of low-molecular-weight compounds in the secretions were carried out by using GC/MS. The quality of the metabolites in samples collected 1 and 2 days after *Pc*To-like RNAi induction did not vary from the quality of the metabolites in those collected from *gfp* controls. In both treatments, we detected only the end-product **7**. The first deviation in the composition of the secretions was measured 3 days after dsRNA injection. Only in samples triggered by *PcTo-like* RNAi did minor amounts of the postulated intermediate **6** in addition to **7** emerge. After 5 days, however, **6** clearly accumulated in addition to **7** owing to the RNAi effect (figure 4*b*). Therefore, we conclude that the *Pc*To-like has to be involved in the cyclization of monoterpene precursors into iridoids.

Off-target effects were predicted using the method described for *CpopSAO*, and predicted off-target effects were avoided from final dsRNA sequence by choosing the template for dsRNA outside of areas of predicted off-target effects.

4. DISCUSSION

The results of our larval RNAi experiments clearly demonstrate selective excision of a component in a biosynthetic pathway. To the best of our knowledge, RNAi has never been used to target enzymes in insect defensive secretions. Owing to the silencing of *Cpop*SAO, the chemical composition in the larval exudates of *C. populi* was massively altered, starting as early as 48 h after treatment. This shows a distinct function of this enzyme *in vivo*. Before, Kirsch *et al.* [13] showed activity only in *in vitro* assays. Evidently, RNAi is a valuable technique for identifying *in vivo* relevance for unknown proteins in defensive glands. Although insects contain a large number of exocrine glands in which bioactive compounds are produced, to date few studies have relied on RNAi to provide evidence for the *in vivo* function of enzymes in insect glands. One example is the production of sex pheromones in special glands of the silkmoth *Bombyx mori*. By injecting the pupae with dsRNA, Ohnishi *et al.* [50,51] were able to dissect the components of the biosynthetic pathway as well as assign a function to a transport protein within the glands of adults. Another RNAi target was the production of pheromone in jewel wasps, *Nasonia vitripennis*. Silencing an epoxide hydrolase in these insects resulted in pheromone reduction by 55 per cent and suppressed the targeted gene transcripts by 95 per cent [52]. Freshly emerged males were injected and 2 days later levels of transcript and pheromones were analysed. As our results demonstrate, RNAi effects are easily detectable in exocrine glands. In the secretions of immature *P. cochleariae*, we were able to assign *in vivo* relevance to a cDNA encoding a protein which is important for the cyclization of iridoids. The iridoid pathway in insects was already proposed by using deuterium labelled precursors by Weibel *et al.* [53]. In his work, the stereospecifity of the cyclization was analysed and allocated to an enzymatic conversion. However, to date JHBPs and

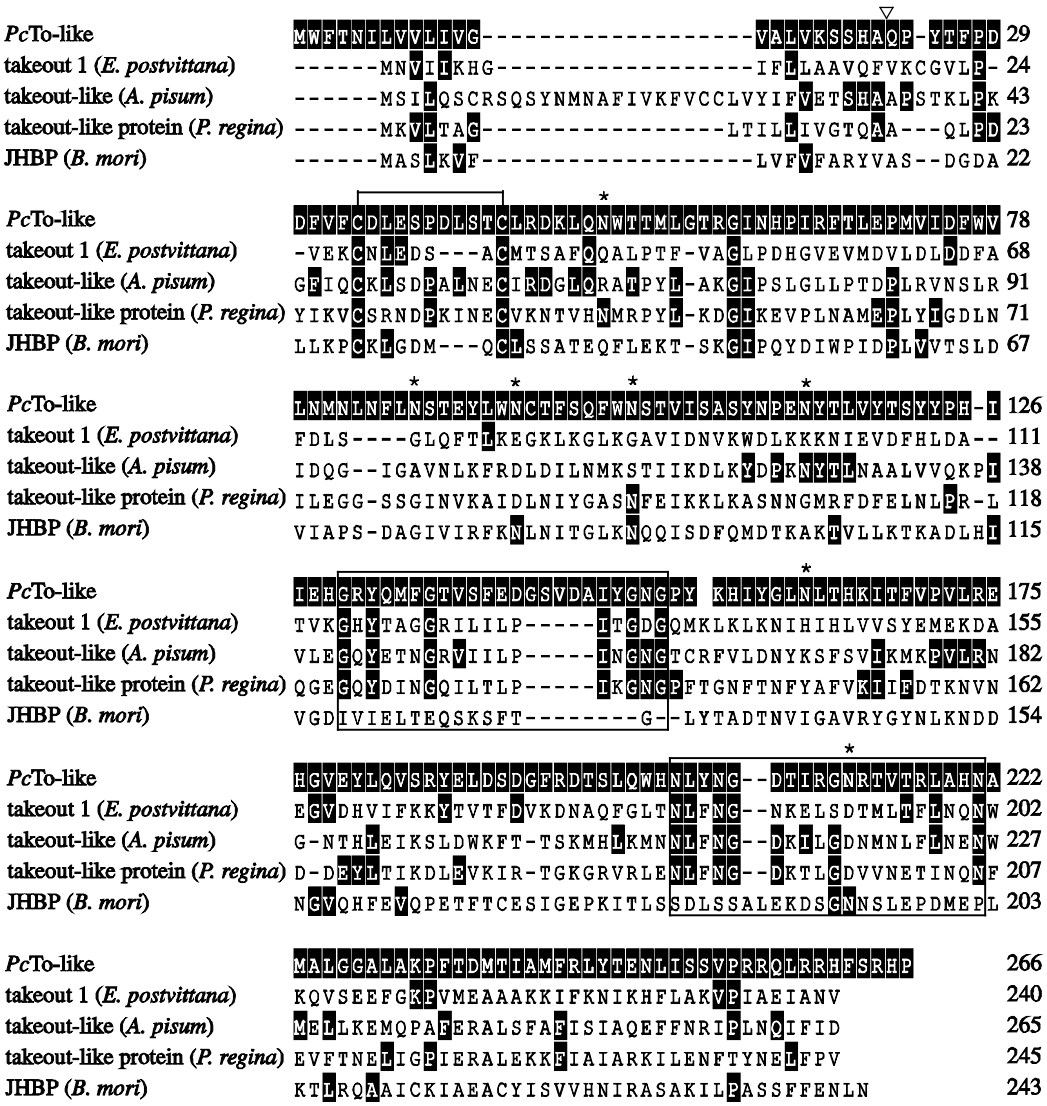

Figure 4. Amino acid alignments (ClustalW) of *Pc*To-like from *P. cochleariae* and other members from the To/JHBP family (*Epiphyas postvittana* To1: GeneBank: ACF39401; *Acyrthosiphon pisum* To-like: GeneBank: XP_001952685; *Phormia regina* To-like protein: GeneBank: BAD83405; *Bombyx mori* JHBP: GeneBank: AAF19267). Solid black shading depicts amino acids identical to *Pc*To-like sequence. White inverted triangles indicate the predicted signal peptide of *Pc*To-like. Asterisks mark the predicted N-glycosylation sites. Conserved cysteine residues that form disulphide bonds are marked with a bracket above the sequence. The two black boxes show the location of the To-typical motives.

To proteins have been established as being carriers of hydrophobic ligands [44,48]. Several lines of evidence indicate that JHBPs form complexes with juvenile hormones (JHs) which provide protection of the chemically labile JHs against nonspecific enzymatic degradation and/or adsorption to lipophilic surfaces during the delivery process from the production site to the target tissue [46,47,49]. Up to now only the crystal structure of To 1 from *E. postvittana* with ubiquinone provided direct evidence for ligand binding in To proteins [44]. Most of the putative To proteins await elucidation of their mode of action. Therefore, the actual mechanism how *Pc*To-like acts in the defensive exudates has to be analysed *in vitro* with purified recombinant protein. On-going experiments will reveal more functional enzymes in Chrysomelina and clarify the molecular machinery for the biosynthesis of deterrents in larval defence secretions.

To perform RNAi experiments, it is essential to ensure the specificity. Off-target effects can arise when siRNAs diced from long dsRNA fragments possess sufficient sequence similarity to non-target mRNA and thus triggering degradation of similar sequences [39]. For sequenced organisms, genome-scale off-target prediction programs are available [34]. These approaches are not suitable for organisms whose genomes have yet to be sequenced. In the last few years, several approaches have been used to detect off targets for those species, such as screening for target specificity by rapidly amplifying cDNA ends [54]. Another approach has used microarrays to compare the cDNAs from treated groups with those from non-treated groups; such comparisons offer proof of differentially expressed transcripts *via* qPCR [55]. Transcriptome sequences have rarely been used for approaches based on local alignment algorithms but represent an economical

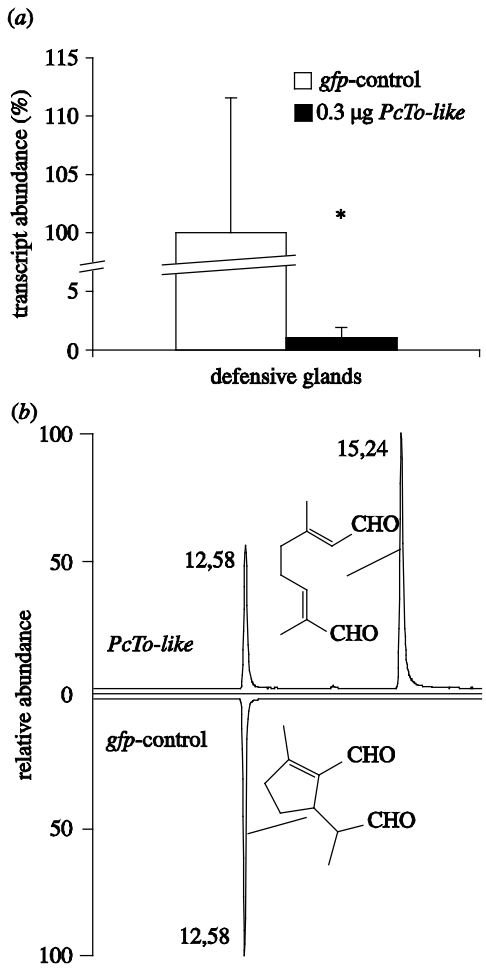

Figure 5. RNAi effects in juvenile *P. cochleariae*. (*a*) White bars: transcript abundance of *PcTo-like* after injecting 0.3 µg *gfp* dsRNA, $n = 3$ ±SD. Black bars: transcript abundance of *PcTo-like* after injecting 0.3 µg *PcTo-like* dsRNA, $n = 3$. 100% = ΔCq of *gfp*-control. Asterisks indicate level of significance: $*p < 0.05$. (*b*) GC-chromatogram of diluted secretions on day 5 after treatment, above: injecting 0.3 µg *PcTo-like* dsRNA resulted in the production of **6** and **7**; below: injecting 0.3 µg *gfp* dsRNA resulted in the production of **7**.

way to make off-target predictions [56]. In our case, we showed that *in silico* dicing of long dsRNA pieces to 21-bp fragments and subsequent BLASTn searches in our transcriptome libraries also lead to the identification of putative off-target transcripts. Subsequent qPCR analysis after successful RNAi induction revealed the co-silencing of predicted transcripts in *C. populi*. Two of eight mRNAs were significantly altered in gut tissue (see the electronic supplementary material, figure S2). But the observed off-target silencing could be assigned neither to the length of the fragments nor to the amount of pmol of the putative siRNAs (see the electronic supplementary material, table ST2). Furthermore, the composition and internal stability of the sequence fragments are supposed to have an impact on successful RNAi triggering [57] and could be included in the prediction. Although publications concerning off-target prediction have increased in the last 2 years, as yet no standard method is available. But as our results indicate, off-target validation is crucial for a realistic discussion of RNAi effects.

The authors would like to express their gratitude to Heiko Vogel for making available 454-sequences from *P. cochleariae*. We also gratefully acknowledge Angelika Berg, Kerstin Ploss, Gerhard Pauls and Antje Loele for technical assistance. We thank Gregor Bucher for helpful discussions on aspects of this work. Very special thanks are due to Prof. Jacques M. Pasteels and Emily Wheeler for their critical reading of the manuscript. This work was supported by the Deutsche Forschungsgemeinschaft (BU 1862/2-1) and the Max Planck Society.

R.R.B., P.R., M.S., M.K., N.W., W.B. and A.B. designed study. R.R.B. established RNAi in leaf beetles and performed RNAi treatments of *Cpop*SAO and its control treatments, performed off-target validation, collected all corresponding data except the off-target prediction and analysed output data. P.R. identified *PcTo-like*, performed RNAi treatments of *PcTo-like* and control treatments, collected all corresponding data and analysed output data. S.F., M.S. and M.G. generated transcriptome libraries. M.S. established and performed off-target prediction and contributed to interpretation of LC/MS^E output data. M.K. designed GC/MS assays, synthesized **6** and **7** and contributed to interpretation of output data. N.W. performed LC/MS^E analysis, collected and contributed to interpretation of output data. W.B. and A.B. contributed substantially to interpretation of all output data. R.R.B., P.R. and A.B. wrote first draft of the manuscript, and all authors contributed substantially to revisions.

REFERENCES

1 Quennedey, A. 1998 Insect epidermal gland cells: ultrastructure and morphogenesis. In *Microscopic anatomy of invertebrates, vol. 11A: insecta* (eds W. H. Harrison & M. Locke) pp. 177–207. New York: Wiley-Liss.

2 Dettner, K. 1987 Chemosystematics and evolution of beetle chemical defenses. *Annu. Rev. Entomol.* **32**, 17–48. (doi:10.1146/annurev.en.32.010187.000313)

3 Pasteels, J. M., Gregoire, J. C. & Rowell-Rahier, M. 1983 The chemical ecology of defense in arthropods. *Annu. Rev. Entomol.* **28**, 263–289. (doi:10.1146/annurev.en.28.010183.001403)

4 Burse, A., Frick, S., Discher, S., Tolzin-Banasch, K., Kirsch, R., Strauss, A., Kunert, M. & Boland, W. 2009 Always being well prepared for defense: the production of deterrents by juvenile Chrysomelina beetles (Chrysomelidae). *Phytochemistry* **70**, 1899–1909. (doi:10.1016/j.phytochem.2009.08.002)

5 Duffey, S. S. 1980 Sequestration of plant natural-products by insects. *Annu. Rev. Entomol.* **25**, 447–477. (doi:10.1146/annurev.en.25.010180.002311)

6 Opitz, S. E. W. & Mueller, C. 2009 Plant chemistry and insect sequestration. *Chemoecology* **19**, 117–154. (doi:10.1007/s00049-009-0018-6)

7 Laurent, P., Braekman, J. C., Daloze, D. & Pasteels, J. 2003 Biosynthesis of defensive compounds from beetles and ants. *Eur. J. Org. Chem.* 2733–2743. (doi:10.1002/ejoc.200300008)

8 Hinton, H. E. 1951 On a little-known protective device of some chrysomelid pupae (Coleoptera). *Proc. R. Entomol. Soc. A* **26**, 67–73. (doi:10.1111/j.1365-3032.1951.tb00123.x)

9 Pasteels, J. M. & Rowell-Rahier, M. 1989 Defensive glands and secretions as taxonomical tools in the Chrysomelidae. *Entomography* **6**, 423–432.

10 Pasteels, J. M., Daloze, D. & Rowell-Rahier, M. 1986 Chemical defense in chrysomelid eggs and neonate larvae. *Physiol. Entomol.* **11**, 29–37. (doi:10.1111/j.1365-3032.1986.tb00388.x)

11 Pasteels, J. M., Rowell-Rahier, M., Braekman, J. C. & Dupont, A. 1983 Salicin from host plant as precursor of salicyl aldehyde in defensive secretion of chrysomeline larvae. *Physiol. Entomol.* **8**, 307–314.
12 Brueckmann, M., Termonia, A., Pasteels, J. M. & Hartmann, T. 2002 Characterization of an extracellular salicyl alcohol oxidase from larval defensive secretions of *Chrysomela populi* and *Phratora vitellinae* (Chrysomelina). *Insect Biochem. Mol. Biol.* **32**, 1517–1523. (doi:10.1016/S0965-1748(02)00072-3)
13 Kirsch, R., Vogel, H., Muck, A., Reichwald, K., Pasteels, J. M. & Boland, W. 2011 Host plant shifts affect a major defense enzyme in *Chrysomela lapponica*. *Proc. Natl Acad. Sci. USA* **108**, 4897–4901. (doi:10.1073/pnas.1013846108)
14 Michalski, C., Mohagheghi, H., Nimtz, M., Pasteels, J. M. & Ober, D. 2008 Salicyl alcohol oxidase of the chemical defense secretion of two chrysomelid leaf beetles—molecular and functional characterization of two new members of the glucose–methanol–choline oxidoreductase gene family. *J. Biol. Chem.* **283**, 19 219–19 228. (doi:10.1074/jbc.M802236200)
15 Wallace, J. B. & Blum, M. S. 1969 Refined defensive mechanisms in *Chrysomela scripta*. *Ann. Entomol. Soc. Am.* **62**, 503–506.
16 Gross, J., Podsiadlowski, L. & Hilker, M. 2002 Antimicrobial activity of exocrine glandular secretion of *Chrysomela* larvae. *J. Chem. Ecol.* **28**, 317–331. (doi:10.1023/a:1017934124650)
17 Rowell-Rahier, M. & Pasteels, J. M. 1986 Economics of chemical defense in Chrysomelinae. *J. Chem. Ecol.* **12**, 1189–1203. (doi:10.1007/bf01639004)
18 Kuhn, J., Pettersson, E. M., Feld, B. K., Burse, A., Termonia, A., Pasteels, J. M. & Boland, W. 2004 Selective transport systems mediate sequestration of plant glucosides in leaf beetles: a molecular basis for adaptation and evolution. *Proc. Natl Acad. Sci. USA* **101**, 13 808–13 813. (doi:10.1073/pnas.0402576101)
19 Discher, S., Burse, A., Tolzin-Banasch, K., Heinemann, S. H., Pasteels, J. M. & Boland, W. 2009 A versatile transport network for sequestering and excreting plant glycosides in leaf beetles provides an evolutionary flexible defense strategy. *ChemBioChem* **10**, 2223–2229. (doi:10.1002/cbic.200900226)
20 Pasteels, J. M., Duffey, S. & Rowell-Rahier, M. 1990 Toxins in chrysomelid beetles possible evolutionary sequence from de novo synthesis to derivation from food-plant chemicals. *J. Chem. Ecol.* **16**, 211–222. (doi:10.1007/bf01021280)
21 Termonia, A., Hsiao, T. H., Pasteels, J. M. & Milinkovitch, M. C. 2001 Feeding specialization and host-derived chemical defense in Chrysomeline leaf beetles did not lead to an evolutionary dead end. *Proc. Natl Acad. Sci. USA* **98**, 3909–3914. (doi:10.1073/pnas.061034598)
22 Daloze, D. & Pasteels, J. M. 1994 Isolation of 8-hydroxygeraniol-8-O-beta-D-glucoside, a probable intermediate in biosynthesis of iridoid monoterpenes, from defensive secretions of *Plagiodera versicolora* and *Gastrophysa viridula* (Coleoptera, Chrysomelidae). *J. Chem. Ecol.* **20**, 2089–2097. (doi:10.1007/BF02066245)
23 Soetens, P., Pasteels, J. M. & Daloze, D. 1993 A simple method for *in vivo* testing of glandular enzymatic activity on potential precursors of larval defensive compounds in *Phratora* species (Coleoptera, Chrysomelinae). *Experientia* **49**, 1024–1026. (doi:10.1007/BF02125653)
24 Veith, M., Oldham, N. J., Dettner, K., Pasteels, J. M. & Boland, W. 1997 Biosynthesis of defensive allomones in leaf beetle larvae—stereochemistry of salicylalcohol oxidation in *Phratora vitellinae* and comparison of enzyme substrate and stereospecificity with alcohol oxidases from several iridoid producing leaf beetles. *J. Chem. Ecol.* **23**, 429–443. (doi:10.1023/B:JOEC.0000006369.26490.c6)
25 Veith, M., Lorenz, M., Boland, W., Simon, H. & Dettner, K. 1994 Biosynthesis of iridoid monoterpenes in insects—defensive secretions from larvae of leaf beetles (Coleoptera, Chrysomelidae). *Tetrahedron* **50**, 6859–6874. (doi:10.1016/S0040-4020(01)81338-7)
26 Kirsch, R., Vogel, H., Muck, A., Vilcinskas, A., Pasteels, J. M. & Boland, W. 2011 To be or not to be convergent in salicin-based defence in chrysomeline leaf beetle larvae: evidence from *Phratora vitellinae* salicyl alcohol oxidase. *Proc. R. Soc. B* **278**, 3225–3232. (doi:10.1098/rspb.2011.0175)
27 Ding, S.-W., Li, H., Lu, R., Li, F. & Li, W.-X. 2004 RNA silencing: a conserved antiviral immunity of plants and animals. *Virus Res.* **102**, 109–115. (doi:10.1016/j.virusres.2004.01.021)
28 Fire, A., Xu, S. Q., Montgomery, M. K., Kostas, S. A., Driver, S. E. & Mello, C. C. 1998 Potent and specific genetic interference by double-stranded RNA in *Caenorhabditis elegans*. *Nature* **391**, 806–811. (doi:10.1038/35888)
29 Belles, X. 2010 Beyond *Drosophila*: RNAi *in vivo* and functional genomics in insects. *Annu. Rev. Entomol.* **55**, 111–128. (doi:10.1146/annurev-ento-112408-085301)
30 Mito, T., Nakamura, T., Bando, T., Ohuchi, H. & Noji, S. 2011 The advent of RNA interference in entomology. *Entomol. Sci.* **14**, 1–8. (doi:10.1111/j.1479-8298.2010.00408.x)
31 Terenius, O. *et al.* 2011 RNA interference in Lepidoptera: an overview of successful and unsuccessful studies and implications for experimental design. *J. Insect Physiol.* **57**, 231–245. (doi:10.1016/j.jinsphys.2010.11.006)
32 Szabo, L. F. 2008 Rigorous biogenetic network for a group of indole alkaloids derived from strictosidine. *Molecules* **13**, 1875–1896. (doi:10.3390/molecules13081875)
33 Kuhnle, A. & Muller, C. 2011 Responses of an oligophagous beetle species to rearing for several generations on alternative host–plant species. *Ecol. Entomol.* **36**, 125–134. (doi:10.1111/j.1365-2311.2010.01256.x)
34 Naito, Y., Yamada, T., Matsumiya, T., Ui-Tei, K., Saigo, K. & Morishita, S. 2005 dsCheck: highly sensitive off-target search software for double-stranded RNA-mediated RNA interference. *Nucleic Acids Res.* **33**, W589–W591. (doi:10.1093/nar/gki419)
35 Altschul, S. F., Madden, T. L., Schaeffer, A. A., Zhang, J., Zhang, Z., Miller, W. & Lipman, D. J. 1997 Gapped BLAST and PSI-BLAST: a new generation of protein database search programs. *Nucleic Acids Res.* **25**, 3389–3402. (doi:10.1093/nar/25.17.3389)
36 Oldham, N. J., Veith, M., Boland, W. & Dettner, K. 1996 Iridoid monoterpene biosynthesis in insects—evidence for a de novo pathway occurring in the defensive glands of *Phaedon armoraciae* (Chrysomelidae) leaf beetle larvae. *Naturwissenschaften* **83**, 470–473. (doi:10.1007/BF01144016)
37 Uesato, S., Ogawa, Y., Doi, M. & Inouye, H. 1987 Biomimetic synthesis of (±)-chrysomelidial, (±)-dehydroiridoidal, and (±)-iridoidal. *J. Chem. Soc.-Chem. Commun.* 1020–1021. (doi:10.1039/c39870001020)
38 Cavener, D. R. 1992 GMC oxidoreductases: a newly defined family of homologous proteins with diverse catalytic activities. *J. Mol. Biol.* **223**, 811–814. (doi:10.1016/0022-2836(92)90992-s)
39 Jackson, A. L., Bartz, S. R., Schelter, J., Kobayashi, S. V., Burchard, J., Mao, M., Li, B., Cavet, G. & Linsley, P. S. 2003 Expression profiling reveals off-target gene

regulation by RNAi. *Nat. Biotechnol.* **21**, 635–637. (doi:10.1038/nbt831)

40 Seinen, E., Burgerhof, J. G. M., Jansen, R. C. & Sibon, O. C. M. 2011 RNAi-induced off-target effects in *Drosophila melanogaster*: frequencies and solutions. *Brief. Funct. Genom.* **10**, 206–214. (doi:10.1093/bfgp/elr017)

41 Morris, K. V., Chan, S. W. L., Jacobsen, S. E. & Looney, D. J. 2004 Small interfering RNA-induced transcriptional gene silencing in human cells. *Science* **305**, 1289–1292. (doi:10.1126/science.1101372)

42 Bosher, J. M., Dufourcq, P., Sookhareea, S. & Labouesse, M. 1999 RNA interference can target pre-mRNA: consequences for gene expression in a *Caenorhabditis elegans* operon. *Genetics* **153**, 1245–1256.

43 Vermunt, A. M. W., Kamimura, M., Hirai, M., Kiuchi, M. & Shiotsuki, T. 2001 The juvenile hormone binding protein of silkworm haemolymph: gene and functional analysis. *Insect Mol. Biol.* **10**, 147–154. (doi:10.1046/j.1365-2583.2001.00249.x)

44 Hamiaux, C., Stanley, D., Greenwood, D. R., Baker, E. N. & Newcomb, R. D. 2009 Crystal structure of *Epiphyas postvittana* takeout 1 with bound ubiquinone supports a role as ligand carriers for takeout proteins in insects. *J. Biol. Chem.* **284**, 3496–3503. (doi:10.1074/jbc.M807467200)

45 So, W. V., Sarov-Blat, L., Kotarski, C. K., McDonald, M. J., Allada, R. & Rosbash, M. 2000 Takeout, a novel *Drosophila* gene under circadian clock transcriptional regulation. *Mol. Cell. Biol.* **20**, 6935. (doi:10.1128/MCB.20.18.6935-6944.2000)

46 deKort, C. A. D. & Granger, N. A. 1996 Regulation of JH titers: the relevance of degradative enzymes and binding proteins. *Arch. Insect Biochem. Physiol.* **33**, 1–26. (doi:10.1002/(sici)1520-6327(1996)33:1<1::aid-arch1>3.0.co;2-2)

47 Prestwich, G. D., Wojtasek, H., Lentz, A. J. & Rabinovich, J. M. 1996 Biochemistry of proteins that bind and metabolize juvenile hormones. *Arch. Insect Biochem. Physiol.* **32**, 407–419. (doi:10.1002/(sici)1520-6327(1996)32:3/4<407::aid-arch13>3.0.co;2-g)

48 Suzuki, R., Fujimoto, Z., Shiotsuki, T., Tsuchiya, W., Momma, M., Tase, A., Miyazawa, M. & Yamazaki, T. 2011 Structural mechanism of JH delivery in hemolymph by JHBP of silkworm, *Bombyx mori*. *Sci. Rep.* **1**, 133. (doi:10.1038/srep00133)

49 Winiarska, B., Dwornik, A., Debski, J., Grzelak, K., Bystranowska, D., Zalewska, M., Dadlez, M., Ozyhar, A. & Kochman, M. 2011 N-linked glycosylation of *G. mellonella* juvenile hormone binding protein—Comparison of recombinant mutants expressed in *P. pastoris* cells with native protein. *Biochim. Biophys. Acta: Proteins Proteom.* **1814**, 610–621. (doi:10.1016/j.bbapap.2011.02.002)

50 Ohnishi, A., Hashimoto, K., Imai, K. & Matsumoto, S. 2009 Functional characterization of the *Bombyx mori* fatty acid transport protein (BmFATP) within the silkmoth pheromone gland. *J. Biol. Chem.* **284**, 5128–5136. (doi:10.1074/jbc.M806072200)

51 Ohnishi, A., Hull, J. J. & Matsumoto, S. 2006 Targeted disruption of genes in the *Bombyx mori* sex pheromone biosynthetic pathway. *Proc. Natl Acad. Sci. USA* **103**, 4398–4403. (doi:10.1073/pnas.0511270103)

52 Abdel-Latief, M., Garbe, L. A., Koch, M. & Ruther, J. 2008 An epoxide hydrolase involved in the biosynthesis of an insect sex attractant and its use to localize the production site. *Proc. Natl Acad. Sci. USA* **105**, 8914–8919. (doi:10.1073/pnas.0801559105)

53 Weibel, D. B., Oldham, N. J., Feld, B., Glombitza, G., Dettner, K. & Boland, W. 2001 Iridoid biosynthesis in staphylinid rove beetles (Coleoptera : Staphylinidae, Philonthinae). *Insect Biochem. Mol. Biol.* **31**, 583–591. (doi:10.1016/s0965-1748(00)00163-6)

54 Sabirzhanov, B., Sabirzhanova, I. B. & Keifer, J. 2011 Screening target specificity of siRNAs by rapid amplification of cDNA ends (RACE) for non-sequenced species. *J. Mol. Neurosci.* **44**, 68–75. (doi:10.1007/s12031-011-9514-6)

55 Lew-Tabor, A. E., Kurscheid, S., Barrero, R., Gondro, C., Moolhuijzen, P. M., Valle, M. R., Morgan, J. A. T., Covacin, C. & Bellgard, M. I. 2011 Gene expression evidence for off-target effects caused by RNA interference-mediated gene silencing of *Ubiquitin-63E* in the cattle tick *Rhipicephalus microplus*. *Int. J. Parasitol.* **41**, 1001–1014. (doi:10.1016/j.ijpara.2011.05.003)

56 Qiu, S., Adema, C. M. & Lane, T. 2005 A computational study of off-target effects of RNA interference. *Nucleic Acids Res.* **33**, 1834–1847. (doi:10.1093/nar/gki324)

57 Reynolds, A., Leake, D., Boese, Q., Scaringe, S., Marshall, W. S. & Khvorova, A. 2004 Rational siRNA design for RNA interference. *Nat. Biotechnol.* **22**, 326–330. (doi:10.1038/nbt936)

ELECTRONIC SUPPLEMENTARY MATERIAL

(I) Materials and Methods

All chemicals are purchased from Sigma-Aldrich (St. Louis, MO, USA), Carl Roth (Karlsruhe, Germany) or Serva (Heidelberg, Germany), if not stated other.

(a) Secretome analysis by LC-MS/MS and data processing. Larval secretions samples of *P. cochleariae* were separated by any-kD gradient gels (Bio-Rad Laboratories, Munich, Germany) in SDS-PAGE [1]. Protein bands of Coomassie Brilliant blue R250 stained gels were cut from the gel matrix and tryptic digestion was carried out as described by Shevchenko et al. [2]. Samples were separated using a nanoUPLC system (Waters, Manchester, UK). A mobile phase of 0.1% aqueous formic acid was used to concentrate and desalt the sample on a Symmetry C18 trap-column (20 x 0.18 mm, 5 µm particle size) at a flow rate of 15 µL/min. Subsequently, peptides were separated by in-line gradient elution onto a nanoAcquity C18 column (200 mm ×75 µm ID, C18 BEH 130 material, 1.7 µm particle size) at a flow rate of 0.350 µl/min using an increasing acetonitrile gradient from 1-95% B over 90 min (Buffers: A, 0.1% formic acid in water; B: 100% acetonitrile in 0.1% formic acid). The eluted peptides were transferred to the nanoelectrospray source of a Synapt HDMS tandem mass spectrometer (Waters, Manchester, UK) equipped with a metal-coated nanoelectrospray tip (Picotip, 50 ×0.36 mm, 10 µm internal diameter, New Objective, Woburn, USA). The source temperature was set to 80°C, cone gas flow 20 L/h, and the nanoelectrospray voltage was 3.2 kV. For all measurements, the mass spectrometer was operated in V-mode with a resolving power of at least 10,000 FWHM. All analyses were performed in positive ESI mode. A 650 fmol/µL human Glu-fibrinopeptide B in 0.1% formic acid/acetonitrile (1:1 v/v) was infused at a flow rate of 0.5 µL min-1 through the

reference NanoLockSpray source every 30 seconds to compensate for mass shifts in MS and MS/MS fragmentation mode.

LC-MS data were collected using data-independent LC-MS^E analysis [3]. Full scan LC-MS data were collected using alternating mode of acquisition: low energy (MS) and elevated energy (MS^E) mode over 1.5 sec intervals in the range m/z of 50-1700 with an interscan delay of 0.2 sec. In low energy mode, data were collected at constant collision energy of 4 eV set on the trap T-wave device and ramped during scan from 15 to 40 eV in elevated MS^E mode.

The continuum LC-MS^E data were processed by PLGS 2.5 software (Waters). Baseline-subtracted, smoothed, deisotoped, and lockmass-corrected spectra were aligned according to the ion accounting algorithm [4]. The processed data were searched against the *P. cochleariae* protein subdatabases constructed from in-house transcriptome-database by their translation from all six reading frames. In order to increase the complexity of the searched database it was appended with Swissprot database downloaded on 13 August, 2011. Automatic settings for precursor and product ion tolerance were used for database searching, with a maximum false positive rate of 4%. Ion accounting search parameter were: minimum of 1 peptide matches per protein, with a minimum of 5 consecutive fragment ions per peptide, and minimum number of product ion matches per protein, 7. The acquired data were searched with a fixed carbamidomethylation of cysteine, along with variable oxidation of methionine residues.

(**b**) **Cloning of *CpopSAO* and *PcTo-like*.** Tissue samples from beetles were collected as described by Burse et al. [5]. Total RNA was extracted from insect tissue with the RNAqueous Micro Kit (Ambion, Life Technologies) according to the manufacturers' instructions except that 1% (v/v) ExpressArt NucleoGuard (Amplification technologies, Hamburg, Germany) was added to the lysis buffer. For method establishment, the integrity of RNA purified this way, was validated by electrophoresis on RNA 6000 Nano labchips on a Bioanalyzer 2100 (Agilent

Technologies). No RNA degradation products were observed. A RNA-integrity number could not be determined, as insects 28S-RNA breaks up in the purification process and accumulates around the 18S-RNA [6]. In on-going experiments RNA integrity was evaluated by TBE-gels and measurement of 260:280 nm absorbance ratios. RNA concentrations were determined employing a NanoView (GE-Healthcare, Little Chalfont, UK). Up to 5 µg of the RNA was reverse transcribed at 50°C for 60 min. using SuperScript III and Oligo(dT)$_{12\text{-}18}$ primer (both, Invitrogen, Life Technologies).

Full length cDNA sequence of *CpopSAO* and *PcTo-like* were amplified by the high fidelity *Pfx*-Polymerase (Invitrogen, Life Technologies) (for Primers see supplemental table ST1). After purification with PCR-purification Kit (Roche, Basel, Switzerland) the resulting fragments were cloned into T7-promotor site free pIB/V5-HIS-TOPO vectors (Invitrogen, Life Technologies). Further, the pIB-CpopSAO and pIB-PcTo-like vectors, isolated from transformed *E. coli* TOP10 cells, were sequenced to confirm the presence of unaltered *CpopSAO* and *PcTo-like*. Functional allocations were performed with pfam-search (http://pfam.sanger.ac.uk/). The signal peptides were predicted using SignalP 3.0 [7] (http://www.cbs.dtu.dk/services/SignalP/), for N-glycosylation site prediction NetNGlyc 1.0 (http://www.cbs.dtu.dk/services/NetNGlyc/) was used.

(**b**) **Quantitative Real-time PCR.** Real-time PCR was employed for relative quantification [8]. Two technical replicates were performed from three biological replicates each. Technical replicates with a Cq difference of >1 were repeated. To normalize the PCRs for the amount of cDNA template added to the reactions, *CpRP-L45* and *CpActin* were chosen as reference genes in *C. populi* and *PcRP-L8* and *PcRP-S18* were chosen for *P. cochleariae*, respectively. Primers were designed using primer3PLUS:

http://www.bioinformatics.nl/cgi-bin/primer3plus/primer3plus.cgi (See supplemental table ST1 for primer sequences). Real-time PCR data were acquired on an Mx3000P Real-Time PCR system (Stratagene, Agilent Technologies) using Brilliant II SYBR Green qPCR Master Mix (Agilent Technologies). These assays were performed following the MIQE-guidelines [9].

References

1. Sambrook J., Russell D.W. 2001 *Molecular cloning: A laboratory manual*, Cold Spring Harbor Laboratory Press {a} , 10 Skyline Drive, Plainview, NY, 11803-2500, USA.
2. Shevchenko A., Tomas H., Havlis J., Olsen J.V., Mann M. 2006 In-gel digestion for mass spectrometric characterization of proteins and proteomes. *Nat. Prot.* **1**(6), 2856-2860. (doi:10.1038/nprot.2006.468).
3. Levin Y., Hradetzky E., Bahn S. 2011 Quantification of proteins using data-independent analysis (MSE) in simple and complex samples: A systematic evaluation. *Proteomics* **11**(16), 3273-3287. (doi:10.1002/pmic.201000661).
4. Li G.Z., Vissers J.P.C., Silva J.C., Golick D., Gorenstein M.V., Geromanos S.J. 2009 Database searching and accounting of multiplexed precursor and product ion spectra from the data independent analysis of simple and complex peptide mixtures. *Proteomics* **9**(6), 1696-1719. (doi:10.1002/pmic.200800564).
5. Burse A., Schmidt A., Frick S., Kuhn J., Gershenzon J., Boland W. 2007 Iridoid biosynthesis in Chrysomelina larvae: Fat body produces early terpenoid precursors. *Insect Biochem. Mol. Biol.* **37**(3), 255-265. (doi:10.1016/j.ibmb.2006.11.011).
6. Krupp G. 2005 Stringent RNA quality control using the Agilent 2100 bioanalyzer. In *www.Agilent.com/chem/labonachip* (01.02.2005 ed.
7. Bendtsen J.D., Nielsen H., von Heijne G., Brunak S. 2004 Improved prediction of signal peptides: SignalP 3.0. *J. Mol. Biol.* **340**(4), 783-795.
8. Livak K.J., Schmittgen T.D. 2001 Analysis of relative gene expression data using real-time quantitative PCR and the 2-DELTADELTACT method. *Methods (Orlando)* **25**(4), 402-408. (doi:10.1006/meth.2001.1262).
9. Bustin S.A., Benes V., Garson J.A., Hellemans J., Huggett J., Kubista M., Mueller R., Nolan T., Pfaffl M.W., Shipley G.L., et al. 2009 The MIQE Guidelines: Minimum Information for Publication of Quantitative Real-Time PCR Experiments. *Clin. Chem.* **55**(4), 611-622. (doi:10.1373/clinchem.2008.112797).

Table ST1

List of primers used for cloning, dsRNA synthesis and quantitative Real-Time PCR (qPCR)

Gene name used in this study		Cloning Primers
CpopSAO	fwd:	ATGTAGGAGTTAGTTTTATTATT
GeneBank: HQ245154.1	rev:	TCACATTCCGTAGTCTTTTT
PcTo-like	fwd:	GTAAAATCAAGTCATGCTCAACCATATAC
GeneBank: JQ728549	rev:	CTAAGGATGTCTGGAGAAATGTCTGCG
		Primers for dsRNA
CpopSAO	fwd:	TAATACGACTCACTATAGGGAACTTGATAATGAGTTGTCTGG
	rev:	TAATACGACTCACTATAGGGTTTTTGCATGGCAGGAGTTC
PcTo-like	fwd:	GTAATACGACTCACTATAGGGAGGGTTCTAAACATGAACCTGA ACTTTTTG
	rev:	GTAATACGACTCACTATAGGGAGACGAATAGTGTCACCATTGT ATAAGTTATG
gfp	fwd:	TAATACGACTCACTATAGGGAGATGGCTAGTAAGGGA
UniProtKB: P42212.1	rev:	TAATACGACTCACTATAGGGAGATTATTTGTAGAGTTC
		qPCR-primers
CpopSAO	fwd:	CCATGCAAAAATATAATCCAACGA
GeneBank: HQ245154.1	rev:	TACTTCTGATACCACATTCCCAA
CpRPL45	fwd:	CACTGGAATCCAAAGTGGAAACTG
GeneBank: JX 122918	rev:	CTGCCTTTCAACCCATGGTC
CpActin	fwd:	ACGTGGACATCAGGAAGGAC
GeneBank: JX122919	rev:	ACATCTGCTGGAAGGTGGAC
CpGMClike-I	fwd:	ACAATCAAACAGGGGTAATG
GeneBank: JX122924	rev:	CAAGGCTTTTTGTTAGCACT
CpGMClike-II	fwd:	TGACGTCTATGTTGTCTGGA
GeneBank: JX122922	rev:	CATCCAAAATCCAAAGGATA
CpGMClike-III	fwd:	TTTTTGCATAGTGGGAGTTT
GeneBank: JX122928	rev:	TTGAACTGAAATCGGCTAAT
Cp-comp3092	fwd:	ACTACTGCCGAGTGAAAAAG
GeneBank: JX122926	rev:	TGAACAATTGCATTGTGAAT
Cp-comp6204	fwd:	ATATCTTGCTTGGGAATTGA
GeneBank: JX122923	rev:	AGCGGAACCTGAAGATTTAT
Cp-comp36289	fwd:	TTGAAAACTGATTCTGTGGA
GeneBank: JX136676	rev:	TAGGAGTTGAAACCCAAAAA
Cp-comp38777	fwd:	TCATTGGGGAAAAATACAAC
GeneBank: JX122927	rev:	TGAAGGGGATAGGAATTATG
Cp-comp51471	fwd:	TGCAATATTGATTTCAAAGGT
GeneBank: JX122925	rev:	AATGATATCACCCCATGGTA
PcTo-like	fwd:	CTTACTACCCCCACATCATC
GeneBank: JQ728549	rev:	CTGGGACGAAGGTTATTTTGTG
PcRPL8	fwd:	CATGCCTGAAGGTACTATAGTGTG
GeneBank: JX122920	rev:	GCAATGACAGTGGCATAGTTACC
PcRPS18	fwd:	ATGCTCCGATGAAGAAGTCG
GeneBank: JX122921	rev:	GCCTATTCAAGAACCAGTCAGG

(II) Results

Table ST2

Off-target prediction for dsRNA sequence of *CpopSAO*. Putative siRNAs are labelled as length of sequence/mismatch.

Query id	Subject	% identity	mismatch	gap opening	Subject start	Subject end	putative siRNAs
CpopSAO dsRNA	CpGMClike-I	95.24	1	0	324	304	22/1
CpopSAO dsRNA	CpGMClike-I	95.24	1	0	325	305	25/1
		95.24	1	0	331	311	
		95.24	1	0	332	312	
		95.24	1	0	333	313	
		95.24	1	0	334	314	
		95.24	1	0	335	315	
CpopSAO dsRNA	CpGMClike-II	95.24	1	0	605	625	21/1
CpopSAO dsRNA	CpGMClike-III	100.00	0	0	822	841	24/0
		100.00	0	0	821	841	
		100.00	0	0	820	840	
		100.00	0	0	819	839	
		100.00	0	0	818	838	
		100.00	0	0	818	837	
CpopSAO dsRNA	CpCOMP3092	95.24	1	0	94	74	21/1
CpopSAO dsRNA	CpCOMP6204	95.24	1	0	1377	1357	22/1
		95.24	1	0	420	400	
CpopSAO dsRNA	CpCOMP36289	95.24	1	0	167	147	21/1
CpopSAO dsRNA	CpCOMP38777	100.00	0	0	295	275	22/0
		100.00	0	0	294	274	
CpopSAO dsRNA	CpCOMP38777	100.00	0	0	295	276	20/0
		100.00	0	0	293	274	
CpopSAO dsRNA	CpCOMP51471	100.00	0	0	231	212	20/0

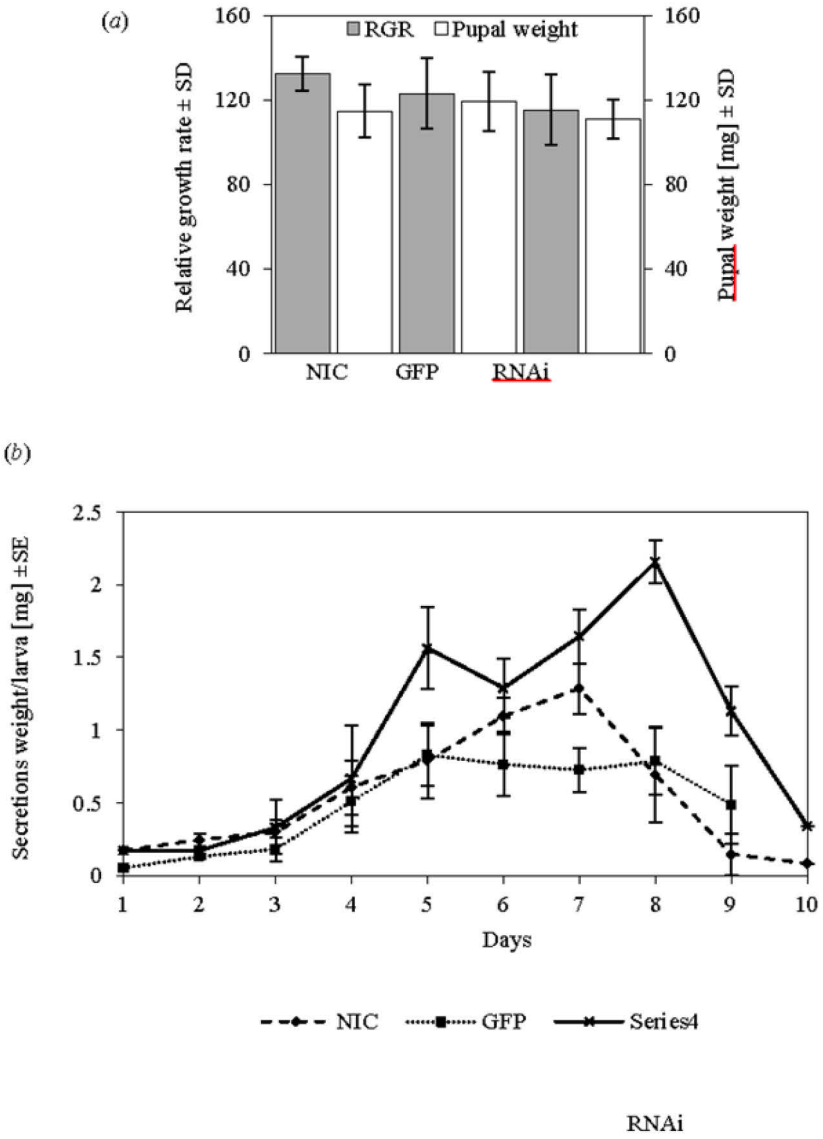

Figure S1

Developmental and metabolic effects of RNAi treatments. (*a*) Relative growth rate (RGR) and pupae weight of non-injected control (NIC), 1.0 µg dsRNA of *gfp*-treated groups (GFP), and 1.0 µg dsRNA of *CpopSAO*-treated groups (RNAi), n=6, (*b*) Produced secretions per day and larva, n=6.

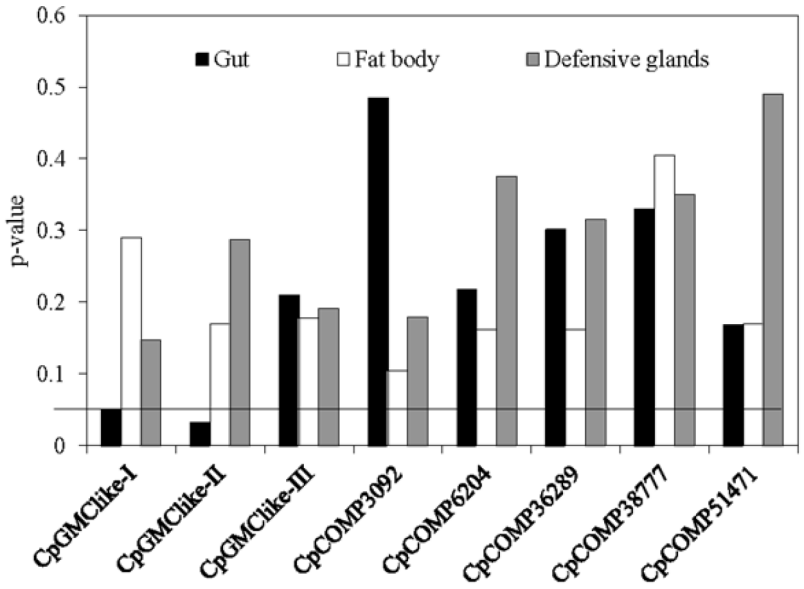

Figure S2

Significance of off-target-validation in *C. populi* larvae. Expression level was measured by qPCR 12 days after RNAi induction. Cq-values of off-target-genes were normalized using *CpRPL45* and *CpActin* and tested for significance by student's t-test; test compared expression levels between dsRNA injections of *gfp* and those of *CpopSAO*, respectively, n=3. Threshold line indicates p-value of 0.05, n=3.

Manuskript 4: (Gretscher, Stock u.a. tba)

Title:

Extracellular Superoxide-dismutases take an active part in fitness, oxidative stress and pathogen resistance in juvenile *Phaedon cochleariae* (Coleoptera: Chrysomelidae: Chrysomelina).

Authors & Affiliations:

René R. Gretscher[a], Magdalena Stock[a], Anja Strauß[a], Sindy Frick[a], Wilhlem Boland[a] and Antje Burse[a].

[a] Department of bioorganic chemistry, Max-Planck-Institute for chemical ecology, Hans-Knöll-Str. 8, 07745 Jena, Germany.

Abstract

Superoxide dismutases (SOD) protect cells and tissues from oxygen radicals (superoxides, $O2^{\cdot-}$) and their reactive derivatives. This kind of oxygen-species can be generated by oxidative metabolism, respiration, toxins and in immune response. Two general groups of SODs are described in eukaryotes, the cellular Cu/Zn containing SOD1 along with the mitochondrial Mn or Fe containing SOD2 and the extracellular Cu/Zn containing SOD3. The function of SOD3s in insect has only been speculated until to date. In the mustard leaf beetle *P. cochleariae* we identified one *SOD1* and three *SOD3* transcripts and discriminated their localization in the larval body by quantitative PCR. *Pc*SOD1 is located in each tissue tested, whereas *Pc*SOD3.1 is localized in the defensive secretions and the hemolymph, *Pc*SOD3.2 could be found exclusively expressed in the fat body, and *Pc*SOD3.3 in the Malpighian tubules respectively.

With RNA interference we were able to silence each of the four *PcSOD*s individually and tested their influence in life history traits, detoxification of artificial introduced superoxide stress and in immune response. So far no influence in lifespan regulation or fecundity could be observed. After application of 2.4 mM Menadione (2-Methylnaphthalene-1,4-dione) an earlier death of all *PcSOD*(-) groups could be observed, where after the application of 61µM Paraquat (1,1'-Dimethyl-4,4'-bipyridinium dichloride), all groups, including the controls, died simultaneously. The same could be observed with injection of 24.5 mM 3-nitropropeoic acid which exception of *Pc*SOD3.1. Upon infection with *Micrococcus luteus* and *Metharizium anisopliae*, larvae of the *PcSOD3.1*(-) group died earlier than all others.

We suggest a role of all *PcSODs* in the protection against oxidative stress and locate *Pc*SOD3.1 as needed for adequate immune response in *P. cochleariae*. This paper reports for the first time an active role of extracellular SODs in various stresses and contributes to the upraising elucidation of insect serum-proteins from non-model insects.

Acknowledgements

We like to thank our student assistants Christin Meißner, Toni Krause, Tim Baumeister, Anthea Wirges and Franziska Eberl for their versatile help on daily lab-work over the last three years. Further we would like to thank Andreas Weber from the greenhouse team for the supply of chinese cabbage. This work was supported by the Deutsche Forschungsgemeinschaft (BU 1862/2-1) and the Max Planck Society.

Author contributions

RRG, AS, WB and AB designed the study and developed the experiments. RRG and AS performed the research, analyzed output data and together with AB, MS and SF contributed to their interpretation. MS, RRG, SF and AS contributed the *PcSOD* sequences and MS performed *in silico* off-target-prediction for all RNAi targets. RRG and AB wrote the manuscript.

1. Introduction

Oxygen changes the world. It was acting as a selector for organisms which could sustain its reactive variants and those which are not able to tolerate the oxidative radicals coming forcefully through the presence of O_2 and UV-radiation. Superoxides ($O_2^{\cdot -}$), for example, are such reactive byproducts, generated also in organisms by respiration and oxidative enzymatic activities [1]. $O_2^{\cdot -}$), is able to mutate DNA, lipids, proteins as well as induce additional oxidative stress by Haber-Weiss-reactions [2]. The cytotoxic effects of $O_2^{\cdot -}$ are also due to downstream reactions with NO·, which yield $ONOO^-$ radicals and induces nitrogenic cytotoxicity [3]. Therefore, all oxygen-exposed organisms need protection accomplished by a conserved group of antioxidant enzymes in which superoxide dismutases (SOD, E.C. 1.15.1.1) have a pivotal position [4]. SODs are the only enzymes known, which are able to detoxify $O_2^{\cdot -}$ to O_2 and H_2O_2 by reducing and oxidizing their metal cofactors. H_2O_2 is then converted to H_2O and O_2 by a catalase or different peroxidases [5]. The non-enzymatically disproportionation of $O_2^{\cdot -}$ to O_2 and H_2O may also occur, but in case of reactions- pace, SODs work an order of magnitude faster [5]. SODs are classified according to their metal co-factors and localization. Class 1 Cu/Zn-binding SODs (SOD1) are the dominant isoforms in the cytosol of eukaryotes. Class 2 SODs (SOD2) contain Ni, Fe, Mn or Fe/Mn and can be found in prokaryotes, mitochondria or plastids. Class 3 Cu/Zn binding SODs (SOD3) are localized exclusively in the extracellular space of eukaryotes, defined by the presence of a coding sequence for a signal peptide (SP) which is cleaved during posttranslational processing [6].

Cellular and mitochondrial SOD isozymes are well characterized in insects with respect to oxidative stress resistance, life span regulation and general fitness [e.g. 7,8]. The first functional evidence of SOD3 in insects was published 2004 by Parker *et al.* [9] presented 2004, which were not predicted to exist in insects berfore. 2011 two studies were published almost at the same time with molecular evidence of SOD3s in the venom of parasitoid wasps [10] and in *D. melanogaster* [11]. Latter study was able to allocate the function of SOD3 in the protection from oxidative stress, induced by UV-radiation or xenobiotics and a role in life span regulation via stable knock-out lines, as in SOD1 deficient strains of *D. melanogaster* [8].

Since $O_2^{\cdot -}$ is documented to be one of the most abundant radicals produced as reactive oxygen species (ROS) in insect immune cascades [12,13,14], an SOD3 in the context of immune response can be supposed. The insect immune response reacts after recognition of a "non-self" intruder also by peptidoglycan recognition proteins (PGRP) or Gram negative binding proteins (GNBP) assumingly upstream of Toll- or immune deficiency (IMD)-pathway with a fast and localized immune response including melanin-encapsulation phagocytosis and production of antimicrobial peptides via NF-kappa B signaling [15,16,17]. Another way to activate NF-kappa B cascades are mitogen-activated protein kinases (MAPK) which are activated upon suppression of counteracting phosphorylases [18]. In insects, H_2O_2 production is described in context of NADPH oxidase (Nox) mediated signal cascades in immune response [e.g. 19,20]. Since this kind of oxidases acts via an one electron transfer from NADPH as a $O_2^{\cdot -}$ generator [21], SOD may work intermediately in this context to produce H_2O_2 signals [cf. 22,23]. $O_2^{\cdot -}$ as such has been shown to be an efficient toxin of *E. coli* in case of an inhibition of melanisation by phenylthiourea [24]. RNAi experiments showed, that *D. melanogaster* larvae, which were taken as a host by parasitoids were unable to kill the parasite in the formed melanoic capsule, if SOD1 is reduced [12]. On the other hand, SOD1s are down regulated by the hosts body, since the generated $O_2^{\cdot -}$ is needed for the back-reaction of semiquinones to quinones [25] in the process of melanin generation. Since in *Galleria mellonella* ROS have been detected to be raised in the haemolymph as well in connection with immune response and melanisation of pathogens [14], a function of SOD3 in immune resonse could be assumed either as a protection of the hosts tissue before getting poisoned by excesses of $O_2^{\cdot -}$, as an intermediate enzyme yielding more reactive radicals to kill pathogens or as the mediator between Nox and H_2O_2 signals.

The involvement of extracellular SOD3 isozymes in arthropod immune response is documented in crustaceans, which are the next related order to insects [26]. In crayfish, for example, a SOD3 attaches to β-integrin and heme-peroxidase and produces H_2O_2 which results in killing of microbial pathogens due to $HOCl^-$ poisoning, similarly to human myeloperoxidase [27]. Further, SOD3s in mangrove crab are expressed upon peptidoglycan or beta-glucan exposures [28].

SOD1, SOD2, SOD3 isozymes can be found in insects from publicly available sequences [e.g. 10,29], but extracellular variants are barely investigated in insects to date. In this study we identified SOD3 activity in secretions and hemolymph of most different leaf beetle species with regards of their climate, host plant and defense metabolism [30] (Fig. 1). Within the subtribe Chrysomelina, the larvae of all species defend themselves with a combination of repelling allomones in defense secretions [31]. This secretions are produced and stored in extracellular reservoirs, which are yielded by secretory gland cells attached to them [32]. The allomones are either produced by sequestering food derived plant alcohols, *de novo* produced iridoids from endogenous sources or by a combination of both [30]. In cases of disturbance the secretion is exhibited as droplets on the back of the larvae, which can be sucked in again, when the deflection is over. From those droplets volatiles evaporate, emitting olfactory signals, which repel various enemies [33]. Since SOD3 activity has been found in species having neither the mode of defense biosynthesis, nor the host plant in common, SOD3 activity represents a common feature, independently on species specificities.

We identified and heterologously expressed a SOD1 and three different extracellular isozymes of *Phaedon cochleariae*. By applying a combination of RNA interference (RNAi) mediated silencing [34] of all four Cu/Zn-SODs individually, we were able to allocate *in vivo* functionality to each isozyme. In accordance with [35], we emphasize that *in vivo* experiments with SODs outperform the *in vitro* assays for their biologically relevant answers. *In vitro* we can show the activity, but the relevance of each isozyme should be investigated in the organism itself. This study demonstrates for the first time the complex role of extracellular superoxide dismutases in insects, showing an involvement in $O_2^{\cdot-}$ detoxification, but also in innate immune response.

2. Materials and methods

Information on biological replicates and the speciesmen pooled within is given in the figure legends.

Statistical calculations are indicated in the figure legends; Excel (Microsoft, Redmond, WA, USA) and SPSS (IBM, Armonk, NJ, USA) have been used for the calculations.

For primers used in cloning and qPCR, please see supplemental table 1 (ST1)

For an overview of the sequences used for sequence alignments, not published before, see ST2.

2.1 Chemicals used

All chemicals are purchased from Serva (Heidelberg, Germany), Sigma-Aldrich (St. Louis, MO, USA) or Carl Roth (Karlsruhe, Germany), if not stated other.

2.2 Transcriptome work

The in house transcriptome-database of *P. cochleariae* and has been introduced before [36]. Sequences were either subjected to a BLAST approach [37] against the NCBI non-redundant database or analyzed using pfam [38] in order to find SOD related transcripts. SignalP [39] has been used to identify extracellular SODs (SOD3). *PcSOD1* (Accession), *PcSOD3.1* (GeneBank: JQ424878.1), *PcSOD3.2* (Accession), *PcSOD3.3* (Accession) were chosen for heterologous expression and functional characterization via RNAi. Further sequence analysis was performed using TargetP [40] and conserved domain prediction [41]. Cu/Zn-SOD sequences of *C. populi* (*Cp*), *C. lapponica* feeding either on *Birch spp.* (*Cl*B) or on *Salix spp.* (*Cl*S) and of *Gastrophysa veridula* (*Gv*) are derived from an in house transcriptome database; all are only *in silico* characterized and used for sequence alignment only. A complete list of sequences identified as SOD related protein is given in supplemental table 2 (ST2).

2.3 Quantitative PCR

cDNA from gut, Malpighian tubules, fat body and accessory defense glands, whole larvae or adults of *P. cochleariae* was used as a template for expression analysis of *PcSOD*s using a CFX96 qPCR system (biorad, Hercules, CA, USA) and Brilliant III SYBR green mastermix (Agilent, Santa Clara, CA, USA). Cq values of *PcSOD*s from three biological and two technical replicates were normalized by *PcRP-L6* (Accession) and *PcRP-S3* (Genebank: KC109783.1). Resulting data were analysed using qBASE PLUS software [42]. Assays were performed following the MIQE guidelines [43].

2.4 Cloning of Cu/Zn-*Pc*SODs

For generation of cDNA insects were dissected in 0.9% NaCl solution under an stereomicroscope (Zeiss, Jena, Germany), where fat body, gut and malpighian tubules were frozen directly on the wall of liquid nitrogen cooled reaction tubes. Defense glands were collected with a pipette in 200µl RNAlater (Qiagen, Hilden, Germany). Whole larvae and adults were placed alive in 2ml safe-lock reaction tubes (Eppendorf) containing 6-10 silica beads (Ø2mm) and poured with 200 µl lysis-buffer (kit see below). These samples were homogenized using a genogrinder2010 (Spex samplePrep, Metuchen, NJ, USA). All samples were stored until further processing at -80°C. RNA extraction and cDNA synthesis were performed according to [36] using the RNAqueous kit (Ambion, life technologies, Carlsbad, CA, USA), superscript III enzyme and oligo $dT_{(12\text{-}18)}$ primer (both Invitrogen, life technologies). Quality was assessed by TA gel electrophoresis, and the A_{260}/A_{280} value. Coding sequences of *PcSOD*s were amplified from a cDNA pool of all tissues using *Pfx*-Polymerase (Invitrogen, Life Technologies). The fragments were cloned into pIB/V5-HIS TOPO vectors (Invitrogen, life technologies), which is lacking T7-promotor sites, interfering with dsRNA synthesis. For that a part of each *PcSOD* coding region has been chosen, which results unique after off-target-prediction [36]. These fragments were amplified using PCR with primers containing both a 5' -T7-promotor-sequence. Also the unique part of the coding sequence of the green fluorescent protein from pcDNA3.1/CT- GFP-TOPO (Invitrogen, life technologies) was subjected to the described protocol and cloned into a pIB-vector. The cloning products were primarily amplified using *E. coli* TOP10F' cells (Invitrogen, life technologies) and sequenced, to confirm unaltered dsRNA templates.

2.5 dsRNA synthesis

Sequenced pIB-plasmids were used to re-amplify DNA templates via PCR. The amplicons were subjected to T7-polymerase based *in vitro* transcription reactions (MEGAscript RNAi kit (Ambion, life technologies) according to manufacturer's instructions. The resulting dsRNA was eluted after nuclease digestion three times with 50 µl hot injection buffer (3.5 mM Tris-HCl, 1 mM NaCl, 50 nM Na_2HPO_4, 20 nM KH_2PO_4, 3 mM KCl, 0.3 mM EDTA, pH 7.0). The resulting dsRNA was 238bp for *PcSOD1*, 193bp for PcSOD3.1, 508bp for PcSOD3.2 and 172bp for PcSOD3.3 respectively. gfp dsRNA has a length of 523bp. The concentration of dsRNA was measured spectrophotometrically, calculated with A_{260} = 1 = 45 mg/ml and adjusted to 2 µg/µl. The quality of dsRNA was checked by TBE-agarose-electrophoresis.

2.6 RNAi induction.

Second instars of *P. cochleariae* with three mm body length and >1.0 mg body weight were injected individually with 0.2 µg of dsRNA about five days after hatching. Injections were

accomplished with ice-chilled larvae using a Nano2010 injector (WPI, Sarasota, FL, USA) driven by a three-axis micromanipulator mounted to a stereomicroscope (Zeiss). The larvae were injected dorso-median between the pro- and mesothorax.

2.7 Heterologous expression of Cu/Zn-*Pc*SODs

For *in vitro* functional validation of *Pc*SODs, we used heterologous expressed 6xHIS-tagged proteins. The coding sequence of *PcSOD*s were amplified from sequenced pCR2.1 plasmids using primers, suitable for directional TOPO cloning and omitting the signal peptide-sequence on cases of *PcSOD3*s. pET100 vectors adding a N-terminal HIS-tag were chosen for producing r*Pc*SOD1, r*Pc*SOD3.1, r*Pc*SOD3.2 and r*Pc*SOD3.3. These proteins were purified from *E. coli* BL21(DE3)star cells (Invitrogen, Life technologies) according to [44] using the Calbiochem Autoinduction system 1 (Merck, Darmstadt, Germany). The elution from Ni-NTA resin (Qiagen) occurs with raising concentrations of imidazole to keep native protein folding. A negative control has been included with a recycled pET100-TOPO vector with no insert.

2.8 Xenobiotic application

Xenobiotics used:

Paraquat (1,1-dimethyl-4,4-bipyridinium chloride, PQ) is a herbicide known for its high toxicity [45] and it is used as an ROS-generator, for the simulation of ROS-stress in other pro- and eukaryotic systems [e.g. 46,47]. The bivalent PQ-ion (PQ^{2+}) takes up a free electron from the mitochondrial respiration chain, or any other reducing agent (like NADPH), overcoming the PQ-redox potential of -446mV, and forms its radical state PQ^{+1}. In the following autoxidation of PQ^{+1} a $O_2\cdot^-$ is generated and the PQ^{2+}-state is thus restored, ready for a new redox cycle [48] (See Fig. 8A) . If this $O_2\cdot^-$ is not dismuted via SOD, it subsequently induces Haber-Weiss and Fenton reactions by reacting with metal ions, yielding highly reactive hydroxyl-radicals which may cause severe damage. Resistances against PQ are only known from plants and only if it has either evolved a fast transport-mechanism of the molecule in secure areas (e.g. the vacuoles) or an advanced antioxidant system but not Cu/Zn-SODs or CATs [49].

Menadione (2-Methylnaphthalene-1,4-dione, MEN), redox potential -203 mV [50], is a quinone, which generates $O_2\cdot^-$ by one electron reduction, again using NADPH as electron source. Besides, MEN may produce other reactive oxygen species by two electron reduction and if further induces cell death by causing cytochrome C release from mitochondria [51]. The mechanism is still not fully understood but it is used both in studies addressing cell death and medicinal applications [e.g. 52] utilizing the cell signaling and necrosis related consequences or as a very powerful ROS generator to study antioxidant systems [e.g. 53]

3-nitropropanoic acid (3-NPA) is a known cytotoxin, which generates $O_2^{\cdot -}$ by irreversible blocking the succinate dehydrogenase of the complex II in the mitochondrial respiratory chain. Here it is responsible for an over-reduction of complex II, by hindering the electron-escape or the backflow from the ubiquinone-pool via ubisemiquinone. By utilizing the membrane potential $O_2^{\cdot -}$ are generated in the inner mitochondrial membrane, most likely associated with a switched fumarate-reductase function from the succinate oxidation activity of complex II [54].

RNAi was induced by injection of 200 ng dsRNA according to *PcSOD*s or *gfp* in early L2-instars of a 24h clutch. The groups were named after the origin of their elicitor or treatment: *PcSOD1*(-), *PcSOD3.1*(-), *PcSOD3.2*(-), *PcSOD3.3*(-), *gfp* and a sixth one stays untreated (NIC). Five days after this initial injection, 25 L3-larvae of each group were treated with either 20ng/mg Paraquat (61µM), 500ng/mg Menadione (2.4mM) or 3.5µg/mg 3-nitropropionic acid (24.5mM), based on the LD_{50}-value calculated by pilot experiments with wildtype larvae. PQ and 3-NPA were dissolved in ringer-solution [19], MEN was dissolved in 100% DMSO, which does not lead to higher mortality in the injected amount. The molarity is based on the fact that the larvae lose per average 81% of their weight after vacuum drying. The larvae were incubated at room temperature and the experiment was terminated when pupal stage has been reached successfully. The survival was determined and the time until the population is reduced to a defined strength has been calculated.

2.9 Microbial infection

Metarhizium anisopliae (DSM-1490, DSMZ, Braunschweig, Germany) was maintained on potato-dextrose-agar (Sigma, 2% glucose), and mycelia were used for subsequent propagation. Conidia were harvested from liquid culture (Potato-dextrose, 200 ml in 500 ml Erlenmeyer flask), which was incubated at room temperature for three weeks without shaking, after overnight agitation of cultures with a 10 cm magnetic stirring staff at 4°C. Mycelium was separated through filtrating the suspension through fine gauze. The supernatant, containing the conidia was centrifuged (10.000xg, 4°C, 10min.) and washed twice with 0.1 % aqueous tween20 solution. Concentration of conidia was adjusted to $1*10^6$ (Hemocytometer) and infection was performed according to [55]. RNAi has been induced as described before. All larvae of one group were submerged for 30 sec. in 1 ml of well mixed conidia suspension after swabbing the larvae on lab tissue, to get rid of defense secretions. The suspension was poured on filter paper and the larvae were air dried for 1 min. Only those larvae were assigned as killed by the fungus, which show mycelia growth out of the carcass after incubating the corps on humid sterile filter paper in a sealed petri dishes.

For bacterial infections, RNAi has been induced and $1*10^6$ cells of *Escherichia coli* K12 (NEB, Ipswich, MA, USA) or *Micrococcus luteus* (DSM 20030, DSMZ) in 100nl were injected in L3 larvae. Both bacterial species were maintained on LB-agar-plates and fresh bacteria were purified from

inoculated liquid LB cultures, agitating for four days at 37°C, 200 rpm. The cells were pelleted (5 min., 8.000 xg, 4°C) in 50 ml Falcon tubes and washed twice in Ringer solution [19] and adjusted to $1*10^{10}$ cells/ml. The experiment ended again with the death or the successful pupation of the speciesmen.

3. Results and discussion

3.1 Identification of Cu/Zn-SODs in *P. cochleariae*

Following the phenomenological identification of SOD activity in different Chrysomelina species (Fig. 1), we used the in-house transcriptome database of *P. cochleariae* to identify the molecular base of this common feature. Four Cu/Zn-SODs were identified along with the Mn-SOD, the copper-chaperone for SOD (CCS) and a multi-SOD-motif protein (MSMP) by pfam [38] and BLAST search [37]. The conserved domain prediction [41] revealed for all proteins the required number of active sites and binding motifs for the metal cofactors (Fig. 2). Analyis of the *in silico* translated amino acid sequence revealed signal peptides (SP) and their cleavage site for *PcSOD3.1*, *3.2* and *3.3* via SignalP [39] and a mitochondrial target sequence for *Pc*SOD2 via TargetP [40], (see supplemental table ST 2 for details). Other listings of antioxidant enzymes of insects are available [e.g. 29,56] and reveal a strong conserved variety of SOD genes including the uncharacterized MSMP variants (Rsod in *D. melanogaster*), to which the present study contributes without conflict in the quality, but *P. cochleariae* is the first insect described to have three SOD3 isozymes, (cf. Fig. S1 for ClustralW-alignment) [cf. 29,56]. We perfomed qPCR analysis to reveal localization of all *Pc*SODs. *Pc*SOD1 as the only cytosolic enzyme is distributed in all tissues in comparable amounts. *PcSOD3.1* is mostly expressed in defense gland-cells and in fat-body tissue. *PcSOD3.2* is almost solely expressed in fat-body tissue comparably in the amount of expression of *PcSOD3.1. PcSOD3.3* can be exclusively found in Malpighian tubules (Fig. 3*A*). We heterologously expressed all four SODs in *E. coli* and observed SOD activity in in-gel assays (Fig. 3*B*). As the zymogram of the heterologous r*Pc*SODs revealed, *Pc*SOD1 forms homotetramers (molecular weight of a recombinant monomer around 20.01 kDa), which is usually not known from other SOD1s, which are predicted as cytosolic dimers [cf. 57]. *Pc*SOD3.1 and *Pc*SOD3.2 buildup homodimers (monomers: 20.2 kDa and 20.67 kDa) and PcSOD3.3 is active as a monomer (20.08 kDa), which is also unusual for that kind of SODs with regards on non-insect SOD3s, but has been shown before in case of the venomous SOD3 of parasitoid wasps [10]. Since *Pc*SOD3.1 is the dominant SOD3 in hemolymph and secretion of *P. cochleariae*, the zymogram of Fig. 1 shows the natural size of *Pc*SOD3.1, which is around 50kDa and thus comparable to the recombinant variant.

With the analysis of *Pc*SODs and related proteins and the *in vitro* prove of activity, we contributed to the investigation of the molecular base of antioxidant enzymes in insects and lay the base for the following investigations.

3.2 Pioneering RNAi with *Pc*SOD3.1

In order to use RNAi to predict *in vivo* SOD function, we checked the efficiency of RNAi mediated silencing of *Pc*SOD3.1 as ageneral model of PcSOD-RNAi. This SOD is unique since it is channeled in the defense secretion of *P. cochleariae*, where a functional reduction can be followed easily without injuring the larva, subjecting collected secretions to SOD activity assays. However, the involvement of SOD in the defense biosynthesis could not be predicted and can be suspended. Most likely it could have assist the alcohol oxidase (AO), which is common in many species, oxidizing precursor alcohols to final aldehydes [58]. But first, it has been shown, that the AOs are producing directly H_2O_2 as a byproduct of oxidation, without superoxide intermediate, second, silencing of *Pc*SOD3.1 does not interfere with the amount of chrysomelidial produced, which is the final allomone of *P. cochleariae* (Fig.6D). The final prove is the occurrence of SOD activity in the defense secretions of birch-feeding *Chrysomela lapponica* (Fig. 1). This ecotype is special because it losses the active alcohol-oxidase due to a host-plant-shift [59]. If SOD would therefore cooperate in the alcohol oxidation, the selective pressure would vanish after loss of oxidase activity and the SOD would have been inactivated too.

RNAi has been proven to work fine with proteins of the defense secretion and fat body of *P. cochleariae* [36,44]. To follow the *Pc*SOD3.1-RNAi, we injected 200ng of a 193 bp dsRNA in each larva, which was synthesized according to the remaining *PcSOD3.1* open-reading-frame-sequence after off-target prediction. For control of the influence of the activation of the RNAi-machinery, we by default raised a control group injected with corresponding amounts of dsRNA according to the *gfp* nucleotide sequence, which has no counterpart in *P. cochleariae* transcriptome.

We observed a fast reduction of the transcript in the whole larvae compared to the control, which was significant 6h after injection (29.51% ± 7.9) and reaches a maximum reduction after 24h (1.04% ± 1.08) which was stable until pupation ten days later (0.63% ± 0.6) (Fig. 4A). The reduction of the transcript was stable even in adult beetles until their death, eight weeks after maturation (4.5% ± 7.4), but RNAi effects were not transmitted in the F1-generation (Fig. 4 C-E) [cf. 60].

Following the reduction of the transcript, both, the protein and the enzymatic function reduces rapidly (Fig. 4B, C). *Pc*SOD3.1 was not detectable anymore in defense secretome nine days after dsRNA injection, where the protein patterning of the remaining proteins compared to the controls, kept unchanged. SOD activity of the secretion was reduced to 5.74% ± 7.1 compared to *gfp*-control and stayed reduced more than 80% until prepupal stage.

These experiments show that RNAi is applicable for this enzyme and that we can work with a reduced SOD activity for the whole larval stage three days after RNAi induction.

3.3 Systemic RNAi on *Pc*SODs

We act on the assumption that the protein and the activity of *Pc*SOD1, *Pc*SOD3.2 and *Pc*SOD3.3 reduces comparable to that of *Pc*SOD3.1, since the transcript is reduced to a comparable amount ten days after injection. By comparing the transcript levels of the other *PcSOD* isozymes in cases of silencing of single ones; we observed no severe co-silencing or up-regulation (Fig. 5A). For example in case of *PcSOD3.2*(-) where the silencing of *PcSOD3.3* in the gut is even better than that of *PcSOD3.2*, we know, that both targets are expressed very basally in this tissue, and the divergence is caused by fault of qPCR, which does not discriminate well between such low expression levels. In case of *PcSOD1*(-) the overall upregulation of *Pc*SODs (*PcSOD3.1* in fat body (2.4x), *PcSOD3.2* in gut and fat body (2.31x and 3.73x) and *PcSOD3.3* in Malpighian tubules (3.79x) could not be explained by qPCR limit of detection, but is most likely caused by higher oxidative stress in the mentioned tissues. The missing higher expression of *PcSOD3.1* in defense glands indicates the isolation of this defense system from the rest of the body. A zymogram of hemolymph and secretions of RNAi induced groups also shows no additional SOD active bands but a clear reduction of SOD activity in case of *PcSOD3.1*(-) (Fig. 5B).

Since also an in-tube SOD detection assay only revealed significant reduced activity of the *Pc*SOD3.1(-)-group, it seems to be the responsible enzyme for the default SOD activity of hemolymph and secretions (Fig. 5B-C). For *Pc*SOD3.2 is equally strong expressed in fat body we assume, that this enzyme is not secreted in the hemolymph, but is probably bound to fat body cells which are suspended from SOD-detection assays. Since *Pc*SOD3.3 is also not detectable in free hemolymph, it also is most likely attached on the inner or outer surface of the Malpighian tubules, a SOD activity assay for this would need a tissue preparation, which has not been done, as it is true also for *Pc*SOD1 and *Pc*SOD3.2.

Here we have shown that the transcript of each Cu/Zn binding SOD can be reduced by the method we established for *Pc*SOD3.1. A functional reduction under default conditions can be observed in cases of *Pc*SOD3.1(-), and the loss of function of the other *Pc*SODs could be expected with regards on the transcript reduction and the results of the following chapters.

3.5 Mortality, life-span and fecundity

We induced RNAi as described in materials and methods and checked for an influence of the loss of SODs in mortality, weight gain in larval stage, defence chemistry and egg production per adults.

The silencing of *Pc*SODs does not interfere significantly with the development of larvae raised under optimal conditions and leads neither to a different pupal weight nor to a difference in the relative growth (Fig. S2). This observation is in accordance with [61] and contradicts to other papers,

showing an impact of SOD1 in life-span and fertility of *D. melanogaster* knockout mutants [e.g. 8]. That fore we incubated RNAi groups in an environment with stronger abiotic conditions (LD 14/10, 21°C ± 2, 70% humidity) and observed no differences in any groups so far. (Fig.6A). The time individuals of one group remain in one developmental stage differs in contrast a lot. For example all L3 larvae of *PcSOD1*(-) group have developed to prepupae at day 12, while the controls stays three more days in this state. *PcSOD3.2*(-) L3-larvae actually have fulfilled this step at day 17. At the transition from prepupae to adults, *PcSOD3.2*(-)-group needs even five days longer, than NIC. That implies, that at least this two SODs have an impact in holometabolic stage transitions.

We weighted the pupae as an indicator of fitness [62] (Fig. 6B), but observed no statistical variation among the samples. After maturation we counted the eggs produced per a pair of adults to observe changes in fecundity (Fig. 6E), but all groups laid comparable amounts of eggs. Additionally we checked the amount of chrysomelidial in the defense secretion, as an indicator of an RNAi-related derogation of the *de novo* synthesis of this defense allomone, but observed no significant differences among the populations (Fig. 6D).

3.6 Consequences of SOD-loss after exposure to xenobiotics

Different $O_2^{\cdot -}$ generating chemicals are described which induce oxidative stress *in vivo* (Fig. 7) and are introduced in chapter 2.8.

We induced RNAi as described by injection of dsRNA in L2-instars, five days ahead of xenobiotic treatment, to ensure maximal reduced SOD activity. Our experiments have shown, that PQ induces larval death independently of SOD-activity. All populations were reduced to 60% of their initial quantity, 7.7 to 11.25 days without observable differences (Fig. 8A). In case of MEN a clear SOD-dependency could be seen, where the populations of all RNAi groups were reduced to 50% 4.9 to 3.75 days ahead of the NIC group (Fig. 8B) between the SOD(-) groups no differences can be seen. In contrast, 3-NPA treatment leads to an early 50% reduced population in all groups but NIC and *PcSOD3.1*(-), but the final mortality is highest in case of *PcSOD1*(-) and *PcSOD3.3*(-), whereas the remaining *PcSOD3.1*(-) and -*3.2(-)* groups are similar to each other and intermediate compared to NIC (Fig. 8C).

Especially in case of MEN, which mechanistically mimics the DOPA-redox cycling during melanisation cascade in the encapsulation module of the insect immune response, the strong dependency of *P. cochleariae* survival to active *Pc*SODs could be observed. That MEN is active in the cytoplasm as well as in the extracellular space is shown by the lack of difference in the survival of *Pc*SOD1 and its extracellular counterparts. In case of 3-NPA the slightly smaller mortality rate of *Pc*SOD3.1(-) and *Pc*SOD3.2(-) groups indicates likely both enzymes as uninvolved in detoxification of exclusively intracellular produced $O_2^{\cdot -}$, whereas *Pc*SOD3.3 thus seems to have the function also to

detoxify cellular $O_2^{\cdot -}$. The unspecific killing of PQ indicates an additional toxic mechanism which is not based on $O_2^{\cdot -}$ production.

3.7 *Pc*SOD dependency in pathogen resistance

As introduced, $O_2^{\cdot -}$ and hydrogen peroxide play important roles on all levels of immune response, namely signaling, insect pathogen immobilization, killing, and phagocytosis. Besides the few examples from crustaceans, where extracellular SODs are described as active part of the immune response [27,28], most immune related SODs are identified as SOD1 [63,64].

We tested whether the deficiency in one *Pc*SOD alters developmental parameters or survival of *P. cochleariae* larvae exposed to pathogens by inoculation with bacteria (Gram(-) *E. coli* K12 and Gram(+) *M. luteus)* and with the entomopathogenic fungus *M. anisopliae*. Both bacteria are not known for entomopathogenic activity, but are established models for immune triggering in insect systems. However, after injection of $3*10^6$ cells of either *E. coli* or *M. luteus* in L3-larvae, *P. cochleariae* died within 48h (data not shown).

Again, L2-larvae of *P. cochleariae* were treated with dsRNA according to *PcSOD*s or *gfp*, or kept without initial injection. Developed L3-larvae larvae from five days later, were injected with bacteria or dipped into conidia solution. Hereafter they were kept in room temperature, to allow the pathogens to develop.

In case of inoculation by $1*10^6$ *E. coli* cells, we could not detect any difference on the survival, the mortality (Fig. 9A) or the pupal weight (Fig. 9D) between the groups. The observed mortality is coincident with other experiments under the same conditions (see Fig. 6A).

In a similar experiment, using $1*10^6$ of *M. luteus,* cells we could detect a reduced survival in *PcSOD3.1*(-) group. Surprisingly NIC, *gfp* and *PcSOD3.3*(-) groups build up an intermediate group suffering more from *M. luteus* treatment than *PcSOD1*(-) and *PcSOD3.2*(-) groups, but less than *PcSOD3.1*(-) (Fig. 9B). To date we have no explanation for that phenomenon. Further testing's with other Gram(+) bacteria are needed to see, whether that response is only related to *M. luteus*.

In a third experiment, using the entomopathogenic fungus *M. anisopliae*, we briefly submerged larvae of the previous introduced RNAi-groups in a $1*10^6$ conidia/ml suspension, which mimics the natural way of infection [cf. 55]. Here we could observe a fast increase in mortality of all groups, starting six days after inoculation (Fig. 9C). The survival of the *PcSOD3.1*(-) group starts to be reduced more intense than that of the other groups, nine days after inoculation and has been reduced to the end of the experiment, where mortality was 88.46%, followed by *PcSOD3.2*(-) (60%). Also the pupal weight was reduced to average 6.37 mg which was significantly less than the 9 mg of *gfp* control (Fig. 9D). The larvae of *PcSOD3.1*(-) suffer that fore during the whole larval phase from the fungal infection, and does not accumulates as many nutrition as each of the other groups, which intact *Pc*SOD3.1 enzyme.

Based on the reported data, we assume, two possible functions of *Pc*SOD3.1 from the hemolymph. First is could be intended to produce H_2O_2 which will fuel Fenton reactions, generating even more toxic HO· radicals, used to kill the intruders. Second $O_2^{\cdot-}$ is a signal intermediate, necessary transcriptional adaptations for an adequate immune response. An involvement in the phenoloxidase cascade leading to melanin capsules could be excluded by two examples. First, $O_2^{\cdot-}$ is needed to drive melanisation, it has been shown, that the addition of SOD to the enzymatic reaction *in vitro*, decreases the H_2O_2 production by 25%, what is due to the competition for $O_2^{\cdot-}$ between DOPA ((S)-2-Amino-3-(3,4-dihydroxyphenyl)propanoic acid) and SOD [65]. A SOD in the process of encapsulation is contra productive since it slows down melanisation [25]. Second, SOD3 is injected together with the egg of a parasitoid wasp in the host, where it is assumed to function exactly as described, by interfering with melanisation-cascade [cf. 10].

Since H_2O_2 signaling, which is involved in immune response, is working via nox-enzymes, active also in the outer cell membrane, the $O_2^{\cdot-}$ produces have to be converted in extracellular space to H_2O_2 to be active in the cytosol after reimport [22,23]. This path is often described to rely on spontaneous dismutation of $O_2^{\cdot-}$ but SODs works an order of magnitude faster yielding H_2O_2 and prohibit the depolarization of the membrane due to too much negative charges [66,67]. As far as annotated, insects possess only nox5 and duox1 genes, with exceptions in case of *Anopheles spp.* [68]. In contrast to other *nox* genes, *nox5* and *duox* proteins are usually activated via Ca^{2+} ions at an intracellular EF-binding site [69]. *nox5* genes in humans may be involved in cell migration and development of B- and T-lymphocytes. Further they are discribed as involved in regulation of cell growth and the fusion of sperm and oocyte [69]. H_2O_2 is an activator of Ca^{2+} channels and protein-kinase-C, which is discussed as an activator of Nox enzymes, enhancing the binding of Ca^{2+} through phosphorylation of residues at the EF-hands [20]. Another signal cascade, NF-kappa-B, initiate the production of antimicrobial peptides, but may be independent form H_2O_2-signaling, since the recognition of Gram(+) and Gram(-) bacteria via IMD- and Toll-receptors have a direct impact on NF-kappa-B-transcription factors without further intermediate signals [17]. Taking together, if the responsible SOD would not be available, the immune response may be activated anyway, but the production of antimicrobial radicals, or H_2O_2 for signaling man be interfered. Downstream reactions, dependent on H_2O_2 reaction with proteins in the cytosol or with metal ions, yielding more toxic radicals in the extracellular space, are prohibited and an effective immune response is prevented.

These results show the importance of the hemolymph *Pc*SOD3.1 in the functional immune response of juvenile *P. cochleariae* against entomopathogenic fungi and Gram(+) bacteria. A direct influence against Gram(-) bacteria or of the other *Pc*SODs could not be observed by this experiments, and needs further research. Since *Pc*SOD3.1 is also present in the defense secretion, the exact function there keeps enigmatic for the moment.

4. Conclusion

Extracellular Superoxide dismutases are versatile enzymes in *P. cochleariae*. Besides the protective function against artificial introduced stresses they play a role in the defense against entomopathogenic fungi and Gram(+) bacteria. This contributes to other insect immune studies, showing an influence of SOD1 in general in immune response against parasites [e.g. 12,19,70] or for bacteria and fungi [e.g. 64,71]. The function of insects SOD3s are either speculated or proven in *in vitro* assays [e.g. 10,11]. In crustacean SOD3 has been proposed to play an active role in immune-signaling by binding extracellularly, but membrane bound, to a peroxinectin, mediating cell adhesion and thus localize the hemocyte activity [27].

Liochev [72] reviewed ROS as "beneficial" substances, and collected evidence for a change of paradigm in the view on ROS. We also suggest in addition a change of view on extracellular SODs whose investigation and comparison to known reactions depending on SOD1 will certainly boost the ROS research. Further studies will reveal the distinct function of *Pc*SODs based on the observations reported here. They will address the differential expression upon infection with *PcSOD*-silenced larvae by using the RNAseq approach [73] and would clarify the involvement of *Pc*SODs in cellular immune signaling, as it has proposed mechanistically [23].

5. References

1. Nohl H (1994) Generation of Superoxide Radicals as by-Product of Cellular Respiration. Annales De Biologie Clinique 52: 199-204.
2. Boelsterli U, A. (2009) Mechanistic toxicology. the molecular basis of how chemicals disrupt biological target. 2 ed. Chippenham and Eastbourne.
3. Nappi AJ, Vass E, Frey F, Carton Y (2000) Nitric oxide involvement in Drosophila immunity. Nitric Oxide-Biology and Chemistry 4: 423-430.
4. Wolfe-Simon F, Grzebyk D, Schofield O, Falkowski PG (2005) The role and evolution of superoxide dismutases in algae. Journal of Phycology 41: 453-465.
5. McCord JM, Fridovich I (1969) Superoxide dismutase. An enzymic function for erythrocuprein (hemocuprein). J Biol Chem 244: 6049-6055.
6. Miller AF (2004) Superoxide dismutases: active sites that save, but a protein that kills. Current Opinion in Chemical Biology 8: 162-168.
7. Landis GN, Tower J (2005) Superoxide dismutase evolution and life span regulation. Mechanisms of Ageing and Development 126: 365-379.
8. Phillips JP, Campbell SD, Michaud D, Charbonneau M, Hilliker AJ (1989) Null mutation of copper/zinc superoxide dismutase in Drosophila confers hypersensitivity to paraquat and reduced longevity. Proc Natl Acad Sci U S A 86: 2761-2765.
9. Parker JD, Parker KM, Keller L (2004) Molecular phylogenetic evidence for an extracellular CuZn superoxide dismutase gene in insects. Insect Molecular Biology 13: 587-594.
10. Colinet D, Cazes D, Belghazi M, Gatti JL, Poirie M (2011) Extracellular superoxide dismutase in insects: characterization, function, and interspecific variation in parasitoid wasp venom. J Biol Chem 286: 40110-40121.
11. Jung I, Kim TY, Kim-Ha J (2011) Identification of Drosophila SOD3 and its protective role against phototoxic damage to cells. Febs Letters 585: 1973-1978.
12. Nappi AJ, Vass E, Frey F, Carton Y (1995) Superoxide anion generation in Drosophila during melanotic encapsulation of parasites. European Journal of Cell Biology 68: 450-456.
13. Nappi AJ, Christensen BM (2005) Melanogenesis and associated cytotoxic reactions: Applications to insect innate immunity. Insect Biochemistry and Molecular Biology 35: 443-459.
14. Dubovskii IM, Grizanova EV, Chertkova EA, Slepneva IA, Komarov DA, et al. (2010) Generation of reactive oxygen species and activity of antioxidants in hemolymph of the moth larvae Galleria mellonella (L.) (Lepidoptera: Piralidae) at development of the process of encapsulation. Journal of Evolutionary Biochemistry and Physiology 46: 35-43.
15. Hoffmann JA (2003) The immune response of Drosophila. Nature 426: 33-38.
16. Foley E, O'Farrell PH (2004) Functional dissection of an innate immune response by a genome-wide RNAi screen. Plos Biology 2: 1091-1106.
17. Ganesan S, Aggarwal K, Paquette N, Silverman N (2011) NF-kappa B/Rel Proteins and the Humoral Immune Responses of Drosophila melanogaster. In: Karin M, editor. Nf-Kb in Health and Disease. Berlin: Springer-Verlag Berlin. pp. 25-60.
18. Gunaratna RT, Jiang HB (2013) A comprehensive analysis of the Manduca sexta immunotranscriptome. Developmental and Comparative Immunology 39: 388-398.
19. Arbi M, Pouliliou S, Lampropoulou M, Marmaras VJ, Tsakas S (2011) Hydrogen peroxide is produced by E-coli challenged haemocytes and regulates phagocytosis, in the medfly Ceratitis capitata. The active role of superoxide dismutase. Developmental and Comparative Immunology 35: 865-871.
20. Jiang F, Zhang Y, Dusting GJ (2011) NADPH Oxidase-Mediated Redox Signaling: Roles in Cellular Stress Response, Stress Tolerance, and Tissue Repair. Pharmacological Reviews 63: 218-242.
21. Lambeth JD (2004) Nox enzymes and the biology of reactive oxygen. Nature Reviews Immunology 4: 181-189.
22. Rhee SG (2006) H2O2, a necessary evil for cell signaling. Science 312: 1882-1883.
23. Forman HJ, Maiorino M, Ursini F (2010) Signaling Functions of Reactive Oxygen Species. Biochemistry 49: 835-842.

24. Whitten MMA, Ratcliffe NA (1999) In vitro superoxide activity in the haemolymph of the West Indian leaf cockroach, Blaberus discoidalis. Journal of Insect Physiology 45: 667-675.
25. Winterbourn CC, French JK, Claridge RFC (1978) Superoxide-Dismutase as an Inhibitor of Reactions of Semi-Quinone Radicals. Febs Letters 94: 269-272.
26. Regier JC, Shultz JW, Kambic RE (2005) Pancrustacean phylogeny: hexapods are terrestrial crustaceans and maxillopods are not monophyletic. Proceedings of the Royal Society B-Biological Sciences 272: 395-401.
27. Johansson MW, Holmblad T, Thornqvist PO, Cammarata M, Parrinello N, et al. (1999) A cell-surface superoxide dismutase is a binding protein for peroxinectin, a cell-adhesive peroxidase in crayfish. Journal of Cell Science 112: 917-925.
28. Lin YC, Vaseeharan B, Chen JC (2008) Identification of the extracellular copper-zinc superoxide dismutase (ecCuZnSOD) gene of the mud crab Scylla serrata and its expression following beta-glucan and peptidoglycan injections. Molecular Immunology 45: 1346-1355.
29. Corona M, Robinson GE (2006) Genes of the antioxidant system of the honey bee: annotation and phylogeny. Insect Molecular Biology 15: 687-701.
30. Termonia A, Hsiao TH, Pasteels JM, Milinkovitch MC (2001) Feeding specialization and host-derived chemical defense in Chrysomeline leaf beetles did not lead to an evolutionary dead end. Proceedings of the National Academy of Sciences of the United States of America 98: 3909-3914.
31. Pasteels JM, Rowellrahier M, Braekman JC, Daloze D (1984) CHEMICAL DEFENSES IN LEAF BEETLES AND THEIR LARVAE - THE ECOLOGICAL, EVOLUTIONARY AND TAXONOMIC SIGNIFICANCE. Biochemical Systematics and Ecology 12: 395-406.
32. Quennedey A (1998) Insect epidermal gland cells: Ultrastructure and morphogenesis; Harrison FWLM, editor. 177-207 p.
33. Dettner K (1987) Chemosystematics and evolution of beetle chemical defenses. Annual Review of Entomology 32: 17-48.
34. Fire A, Xu SQ, Montgomery MK, Kostas SA, Driver SE, et al. (1998) Potent and specific genetic interference by double-stranded RNA in Caenorhabditis elegans. Nature 391: 806-811.
35. Liochev SI, Fridovich I (2007) The effects of superoxide dismutase on H2O2 formation. Free Radical Biology and Medicine 42: 1465-1469.
36. Bodemann RR, Rahfeld P, Stock M, Kunert M, Wielsch N, et al. (2012) Precise RNAi-mediated silencing of metabolically active proteins in the defence secretions of juvenile leaf beetles. Proceedings of the Royal Society B-Biological Sciences 279: 4126-4134.
37. Altschul SF, Madden TL, Schaeffer AA, Zhang J, Zhang Z, et al. (1997) Gapped BLAST and PSI-BLAST: A new generation of protein database search programs. Nucleic Acids Research 25: 3389-3402.
38. Punta M, Coggill PC, Eberhardt RY, Mistry J, Tate J, et al. (2012) The Pfam protein families database. Nucleic Acids Research 40: D290-D301.
39. Petersen TN, Brunak S, von Heijne G, Nielsen H (2011) SignalP 4.0: discriminating signal peptides from transmembrane regions. Nature Methods 8: 785-786.
40. Emanuelsson O, Nielsen H, Brunak S, von Heijne G (2000) Predicting subcellular localization of proteins based on their N-terminal amino acid sequence. Journal of Molecular Biology 300: 1005-1016.
41. Marchler-Bauer A, Lu S, Anderson JB, Chitsaz F, Derbyshire MK, et al. (2011) CDD: a Conserved Domain Database for the functional annotation of proteins. Nucleic Acids Research 39: D225-D229.
42. Hellemans J, Mortier G, De Paepe A, Speleman F, Vandesompele J (2007) qBase relative quantification framework and software for management and automated analysis of real-time quantitative PCR data. Genome Biology 8: 14.
43. Bustin SA, Benes V, Garson JA, Hellemans J, Huggett J, et al. (2009) The MIQE Guidelines: Minimum Information for Publication of Quantitative Real-Time PCR Experiments. Clinical Chemistry 55: 611-622.

44. Frick S, Nagel R, Schmidt A, Bodemann RR, Rahfeld P, et al. (2013) Metal ions control product specificity of isoprenyl diphosphate synthases in the insect terpenoid pathway. Proc Natl Acad Sci U S A 110: 4194-4199.
45. Homer RF, Mees GC, Tomlinson TE (1960) Mode of action of dipyridyl quaternary salts as herbicides. Journal of the Science of Food and Agriculture 11: 309-315.
46. Suntres ZE (2002) Role of antioxidants in paraquat toxicity. Toxicology 180: 65-77.
47. Park SY, Nair PMG, Choi J (2012) Characterization and expression of superoxide dismutase genes in Chironomus riparius (Diptera, Chironomidae) larvae as a potential biomarker of ecotoxicity. Comparative Biochemistry and Physiology C-Toxicology & Pharmacology 156: 187-194.
48. Bus JS, Gibson JE (1984) Paraquat: model for oxidant-initiated toxicity. Environ Health Perspect 55: 37-46.
49. Szigeti Z, Lehoczki E (2003) A review of physiological and biochemical aspects of resistance to atrazine and paraquat in Hungarian weeds. Pest Management Science 59: 451-458.
50. Thiboldeaux RL, Lindroth RL, Tracy JW (1994) Differential Toxicity of Juglone (5-Hydroxy-1,4-Naphthoquinone) and Related Naphthoquinones to Saturniid Moths. Journal of Chemical Ecology 20: 1631-1641.
51. Samali A, Nordgren H, Zhivotovsky B, Peterson E, Orrenius S (1999) A comparative study of apoptosis and necrosis in HepG2 cells: Oxidant-induced caspase inactivation leads to necrosis. Biochemical and Biophysical Research Communications 255: 6-11.
52. Monteiro JP, Martins AF, Nunes C, Morais CM, Lucio M, et al. (2013) A biophysical approach to menadione membrane interactions: Relevance for menadione-induced mitochondria dysfunction and related deleterious/therapeutic effects. Biochimica Et Biophysica Acta-Biomembranes 1828: 1899-1908.
53. Mittra B, Cortez M, Haydock A, Ramasamy G, Myler PJ, et al. (2013) Iron uptake controls the generation of Leishmania infective forms through regulation of ROS levels. Journal of Experimental Medicine 210: 401-416.
54. Bacsi A, Woodberry M, Widger W, Papaconstantinou J, Mitra S, et al. (2006) Localization of superoxide anion production to mitochondrial electron transport chain in 3-NPA-treated cells. Mitochondrion 6: 235-244.
55. Rostas M, Hilker M (2003) Indirect interactions between a phytopathogenic and an entomopathogenic fungus. Naturwissenschaften 90: 63-67.
56. Shi GQ, Yu QY, Zhang Z (2012) Annotation and evolution of the antioxidant genes in the silkworm, Bombyx mori. Arch Insect Biochem Physiol 79: 87-103.
57. Perry JJP, Shin DS, Getzoff ED, Tainer JA (2010) The structural biochemistry of the superoxide dismutases. Biochimica Et Biophysica Acta-Proteins and Proteomics 1804: 245-262.
58. Brueckmann M, Termonia A, Pasteels JM, Hartmann T (2002) Characterization of an extracellular salicyl alcohol oxidase from larval defensive secretions of Chrysomela populi and Phratora vitellinae (Chrysomelina). Insect Biochemistry and Molecular Biology 32: 1517-1523.
59. Kirsch R, Vogel H, Muck A, Reichwald K, Pasteels JM, et al. (2011) Host plant shifts affect a major defense enzyme in Chrysomela lapponica. Proceedings of the National Academy of Sciences of the United States of America 108: 4897-4901.
60. Bucher G, Scholten J, Klingler M (2002) Parental RNAi in Tribolium (Coleoptera). Current Biology 12: R85-R86.
61. Van Raamsdonk JM, Hekimi S (2012) Superoxide dismutase is dispensable for normal animal lifespan. Proceedings of the National Academy of Sciences of the United States of America 109: 5785-5790.
62. Kuhnle A, Müller C (2011) Responses of an oligophagous beetle species to rearing for several generations on alternative host-plant species. Ecological Entomology 36: 125-134.
63. Bergin D, Reeves EP, Renwick J, Wientjes FB, Kavanagh K (2005) Superoxide production in Galleria mellonella hemocytes: Identification of proteins homologous to the NADPH oxidase complex of human neutrophils. Infection and Immunity 73: 4161-4170.

64. Krishnan N, Chattopadhyay S, Kundu JK, Chaudhuri A (2002) Superoxide dismutase activity in haemocytes and haemolymph of Bombyx mori following bacterial infection. Current Science 83: 321-325.
65. Komarov DA, Slepneva IA, Glupov VV, Khramtsov VV (2005) Superoxide and hydrogen peroxide formation during enzymatic oxidation of DOPA by phenoloxidase. Free Radical Research 39: 853-858.
66. Fridovich I (1995) Superoxide radical and superoxide dismutases. Annu Rev Biochem 64: 97-112.
67. Rada BK, Geiszt M, Kaldi K, Timar C, Ligeti E (2004) Dual role of phagocytic NADPH oxidase in bacterial killing. Blood 104: 2947-2953.
68. Kawahara T, Quinn MT, Lambeth JD (2007) Molecular evolution of the reactive oxygen-generating NADPH oxidase (Nox/Duox) family of enzymes. Bmc Evolutionary Biology 7: 21.
69. Banfi B, Tirone F, Durussel I, Knisz J, Moskwa P, et al. (2004) Mechanism of Ca2+ activation of the NADPH oxidase 5 (NOX5). Journal of Biological Chemistry 279: 18583-18591.
70. Bahia AC, Oliveira JHM, Kubota MS, Araujo HRC, Lima JBP, et al. (2013) The Role of Reactive Oxygen Species in Anopheles aquasalis Response to Plasmodium vivax Infection. Plos One 8: 10.
71. Lozinskaya YL, Slepneva IA, Khramtsov VV, Glupov VV (2004) Changes of the antioxidant status and system of generation of free radicals in hemolymph of Galleria mellonella larvae at microsporidiosis. Journal of Evolutionary Biochemistry and Physiology 40: 119-125.
72. Liochev SI (2013) Reactive oxygen species and the free radical theory of aging. Free Radical Biology and Medicine 60: 1-4.
73. Stock M, Gretscher RR, Groth M, Eiserloh S, Boland W, et al. (2013) Putative sugar transporters of the mustard leaf beetle Phaedon cochleariae: their phylogeny and role for nutrient supply in larval defensive glands. PLOS one.
74. Brewer GJ (1967) Achromatic regions of tetrazolium stained starch gels: inherited electrophoretic variation. Am J Hum Genet 19: 674-680.

6. Figure captions

Figure 1: Detection of SOD activity in secretion and hemolymph of larvae of different leaf beetle species.
Each 1 µl hemolymph (left) and 0.3 µl secretion (right) was separated on native PAGE and functional stained for SOD activity (uncolored areas). Indicated phylogeny is taken from [30]

Figure 2: Sequence analysis of *Pc*SODs and related proteins.
Translated Amino acid sequences were analyzed by pfam [38] to obtain the protein-domains and graphics were annotated according to the significant pfam-A hits. SignalP [39] and TargetP [40] has been used to identify signal peptides or target sequences and the cleavage sites. Conserved domain search [41] has been used to identify all remaining annotated features. *Pc*MSMP was only available as a partial sequence.

Figure 3: Distribution and heterologous expression of Cu/Zn-binding *Pc*SODs.
A: qPCR analysis has been performed with gene specific primers and Cq values of the target genes were normalized afterwards with Cq values of *PcRP-L6* and *PcRP-S3* (ΔCq). n=3. Error bars indicate standard-deviation (SD). B: purified *Pc*SODs after heterologous expression in *E. coli* cells, left: elution fraction, stained with coomassie, right: functional staining of native-PAG after separation of the elution fractions.

Figure 4: RNAi effects on transcript, protein and SOD activity.
A: Transcript abundance of *PcSOD3.1* after injection with 200ng corresponding dsRNA or *gfp* as a control respectively. RNA from whole larvae has been used as template. ΔCq values of the RNAi group samples has been normalized to the ΔCq values of the gfp-injected samples (ΔΔCq). n=3. B: Coomassie stained SDS-PAGE with each 0.3 µl of defense secretions, 9 days after RNAi induction. NIC: Non-injected control, *gfp* and RNAi as in A. C: Time series of SOD-activity of defense secretion, measured in the microplate assay. Values of RNAi-group were normalized to *gfp*-control. D: Transcript abundance (see A) of female adult beetles eight weeks after maturation. n=5. L200: larvae injected with 200ng, L500: larvae injected with 500ng, P500: pupae injected with 500ng, P1K: pupae injected with 1µg dsRNA according to *gfp* (darker brown) or *PcSOD3.1* (green). E and F: qPCR results (ΔΔCq) of F1-generations of larvae, injected with 500ng dsRNA (E) or pupae injected with 4µg dsRNA (F), relative to gfp-control. n=3. Error bars represent the standard-deviation (SD) or standard error of the mean (SE) as indicated in the axis description.

Figure 5: RNAi effects after individual silencing of *PcSOD*s.
A: ΔΔCq values of PcSOD expression in different tissues of *P. cochleariae* larvae. Each 200ng dsRNA of each *PcSOD1* to *PcSOD3.3* or gfp has been used to induce RNAi. Tissue were dissected ten days after injection. Green: expression reduced, red: transcript increases. n=3. Bold boxes indicate tissue of predominant expression in wildtype. B: Zymogram of 0.3 µl secretions (left) and 1µl hemolymph (right) of groups indicated in C, samples from day ten after injection. C: SOD activity measured with in tube assays, left: defense secretions, right: hemolymph, ten days after injection. n=3.

Figure 6: Effects on the development, survival and fitness after silencing of *PcSOD*s.
A: Survival plot of *P. cochleariae* after injections of each 200ng of *PcSODs* or *gfp* or without injection, normalized to initial population strength. n=60. B: graphical representation of life stage development in each group. L1-L3: larval instars, PP: prepupal stage, P: pupal stage, Ad: Adults, each stage consists of six groups (colors see A). Marker indicates 50% of population in this state, line represents first and last turnover. C: freshly emerged pupae from A/B were weighted on the day of their occurrence. n>40. D: GC/MS analysis of secretion from day 6 after inoculation, amount of chrysomelidial was normalized to internal standard methylbenzoate. n=5. E: Eggs laid per couple in 24h, n=5.

Figure 7: Xenobiotics used for generation of oxidative stress.
Ed. from manufacturer's documentation with ChemBiodraw Ultra 12.0.

Figure 8: Resistance to artificial induced oxidative stress.
n=25 larvae were treated with 200ng of dsRNA according to *PcSOD*s or left without treatment, five days after this initial injection, xenobiotics were injected, yielding the noted concentrations in the larvae. For each treatment the scheme of the reaction, the survival analysis and the time is shown, which has passed before a certain strength of population has been reached. A: Paraquat, B: Menadione, C: 3-nitropropanoic acid.

Figure 9: Immunologic consequences of *Pc*SOD silencing.
For each assay n=30 larvae were treated with 200ng of dsRNA according to *PcSOD*s, *gfp* or left without treatment. Inoculation has been done five days later (Day 0). A: $1*10^6$ *E. coli*-cells/200nl were injected in each L3-larva and final mortality as well as the survival has been documented by calculating the percentage of the current population strength against the initial population size. B: $1*10^6$ *M. luteus*-cells/200nl were injected in each L3-larva and survival and mortality was documented as in A. C: After emptying of the defense reservoirs, larvae of one group were submerged at the same time in the same solution of *M. anisopliae* $1*10^6$ conidia/ml. survival and mortality was documented as in A. D: pupal weight of freshly emerged pupa from wildtype: only RNAi was induced, without further treatments and the three treatments A-C. Level of significance: *($p \leq 0.05$).

Figure S1: ClustralW alignment of Amino acid sequences of various insect and human Cu/Zn-SODs. SOD1 and SOD3 of different species (*Pl*: *Pacifastacus leniusculus*; *Ss*: *Scylla serrata*; *Lb*: *Leptopilina boulardi*; *Ln*: *Lasius niger*; *Nv*: *Nasonia vitripennis*; *Lh*: *Leptopilina heterotoma*; *Tc*: *Tribolium castaneum*; *Bm*: *Bombyx mori*; *Dm*: *Drosophila melanogaster*; *Md*: *Musca domestica*; *Hs*: *Homo sapiens*; *Mm*: *Mus musculus*), were downloaded from GeneBank and aligned to *Pc*SODs and those of other Chrysomelina from our in house database (*Cl*S, *Cl*B, *Cp*, *Gv* according to Fig. 1). Bootstrapping was performed as annotated in the figure.

Figure S2: Developmental parameters in unstressed *PcSOD* silenced larvae. n=30 larvae were treated with 200ng of dsRNA according to *PcSOD*s or *gfp*. A: All larvae were weighted every two days after RNAi induction, individually .Day 4: most larvae developed to L3-instars, day 10: most larvae are in prepupal stage. B: Pupal weight and relative growth rate of the introduced groups.

Table S1: Sequences of used primers. For amplification of cds, dsRNA template, qPCR analysis and pET100 inserts.

Table S2: Identification of SOD similar sequences in available in house databases. Species annotations according to Fig. 1. Classification has been done according to pfam identification [38] and Signal peptides [39].

7. Figures and tables

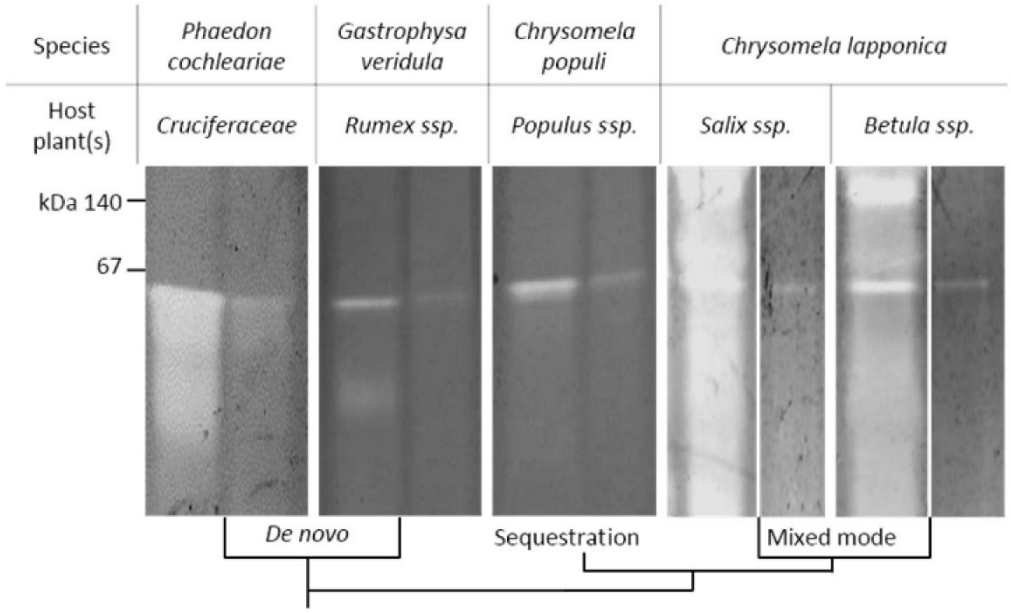

Figure 1.

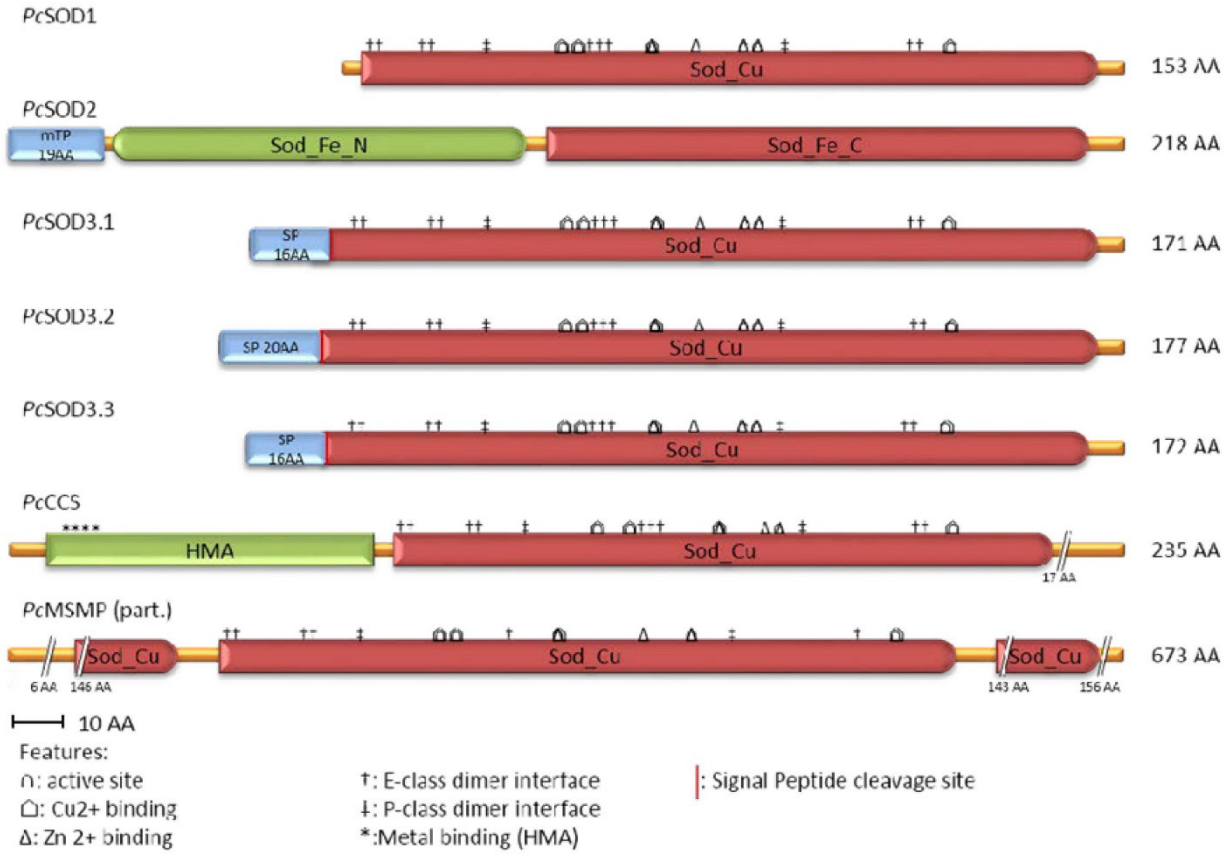

Figure 2.

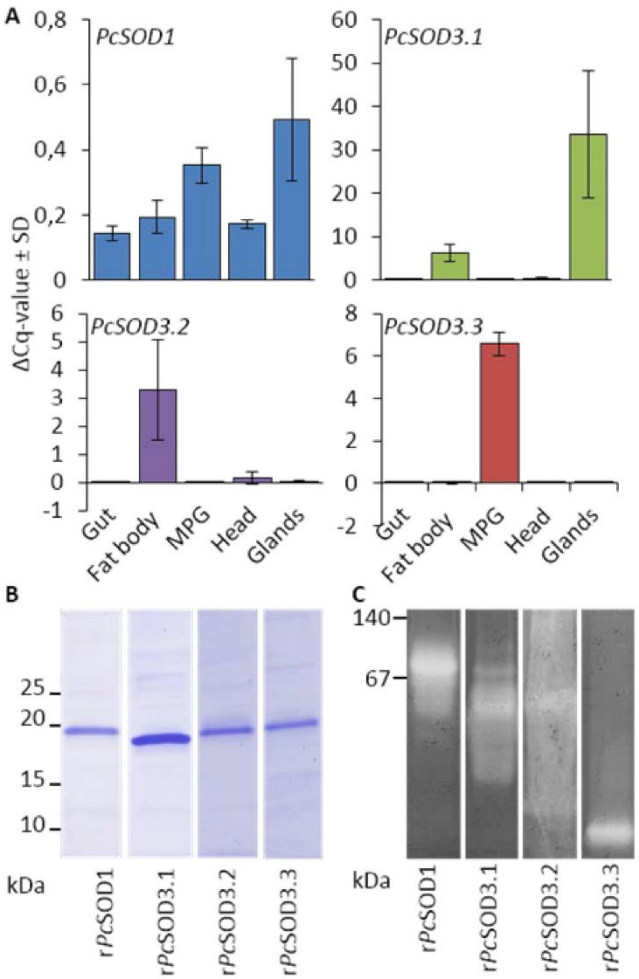
A
PcSOD1
PcSOD3.1
PcSOD3.2
PcSOD3.3
ΔCq-value ± SD
Gut
Fat body
MPG
Head
Glands
B
kDa
25
20
15
10
rPcSOD1
rPcSOD3.1
rPcSOD3.2
rPcSOD3.3
C
140
67
kDa
rPcSOD1
rPcSOD3.1
rPcSOD3.2
rPcSOD3.3

Figure 3.

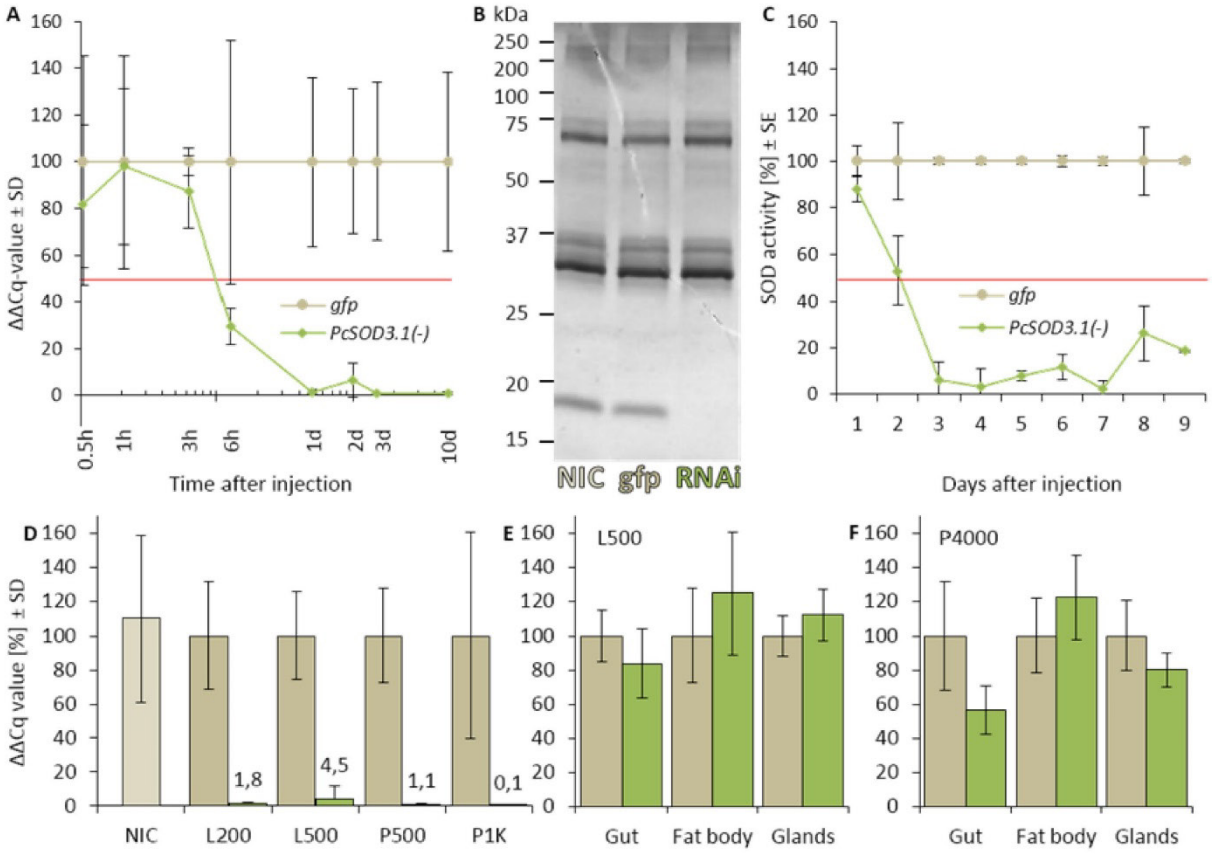
A
ΔΔCq-value ± SD
gfp
PcSOD3.1(-)
0.5h
1h
3h
6h
1d
2d
3d
10d
Time after injection
B kDa
250
200
100
75
50
37
25
20
15
NIC gfp RNAi
C
SOD activity [%] ± SE
gfp
PcSOD3.1(-)
Days after injection
D
ΔΔCq value [%] ± SD
1,8
4,5
1,1
0,1
NIC
L200
L500
P500
P1K
E
L500
Gut
Fat body
Glands
F
P4000
Gut
Fat body
Glands

Figure 4.

A

		PcSOD1	PcSOD3.1	PcSOD3.2	PcSOD3.3
PcSOD1(-)	Gut	6,01	55,31	261,07	77,90
	Fat body	6,57	236,28	373,94	127,01
	MPT	8,48	43,77	20,81	378,80
	Glands	0,44	110,40	65,53	64,00
PcSOD3.1(-)	Gut	97,29	1,62	189,30	26,75
	Fat body	85,82	0,07	108,55	16,60
	MPT	98,54	3,30	49,69	44,17
	Glands	87,59	0,65	177,77	136,40
PcSOD3.2(-)	Gut	56,73	124,12	33,98	15,22
	Fat body	81,29	24,75	1,90	196,13
	MPT	49,94	96,74	2,38	22,68
	Glands	43,98	99,04	19,61	63,66
PcSOD3.3(-)	Gut	111,42	11,89	61,20	7,24
	Fat body	113,01	270,69	472,66	123,16
	MPT	87,99	84,26	34,72	3,96
	Glands	62,77	54,83	431,77	53,26

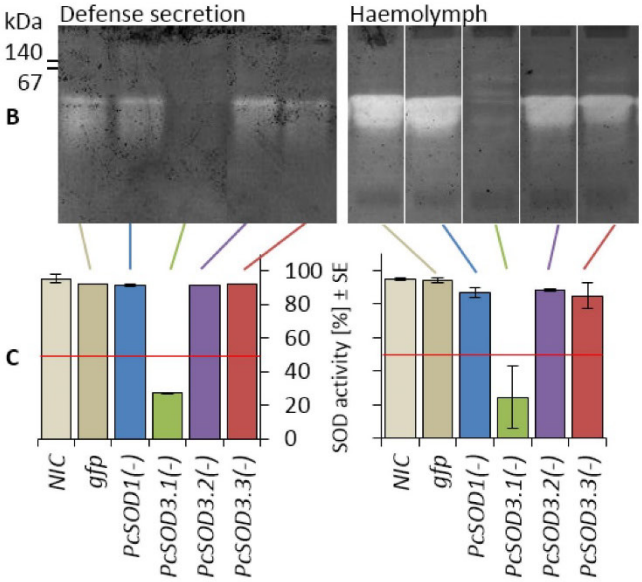

Figure 5.

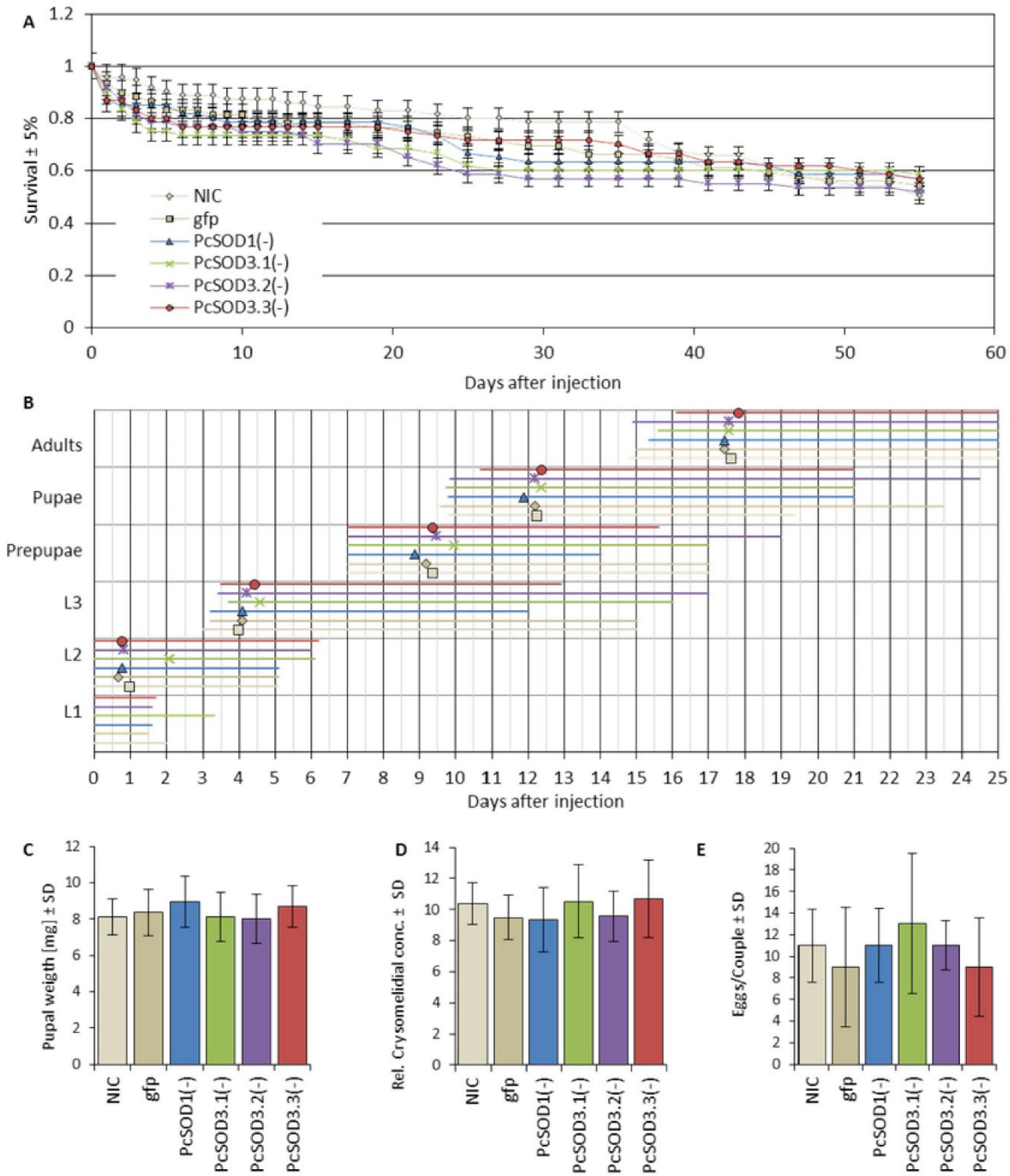

Figure 6.

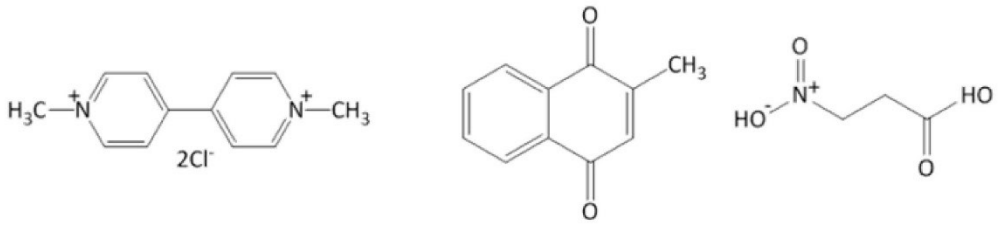

1,1'-Dimethyl-4,4'-bipyridinum dichloride (Paraquat, PQ) | 2-Methyl-1,4-napthoquinone (Menadione, MEN) | 3-nitropropanoic acid (3-NPA)

Figure 7.

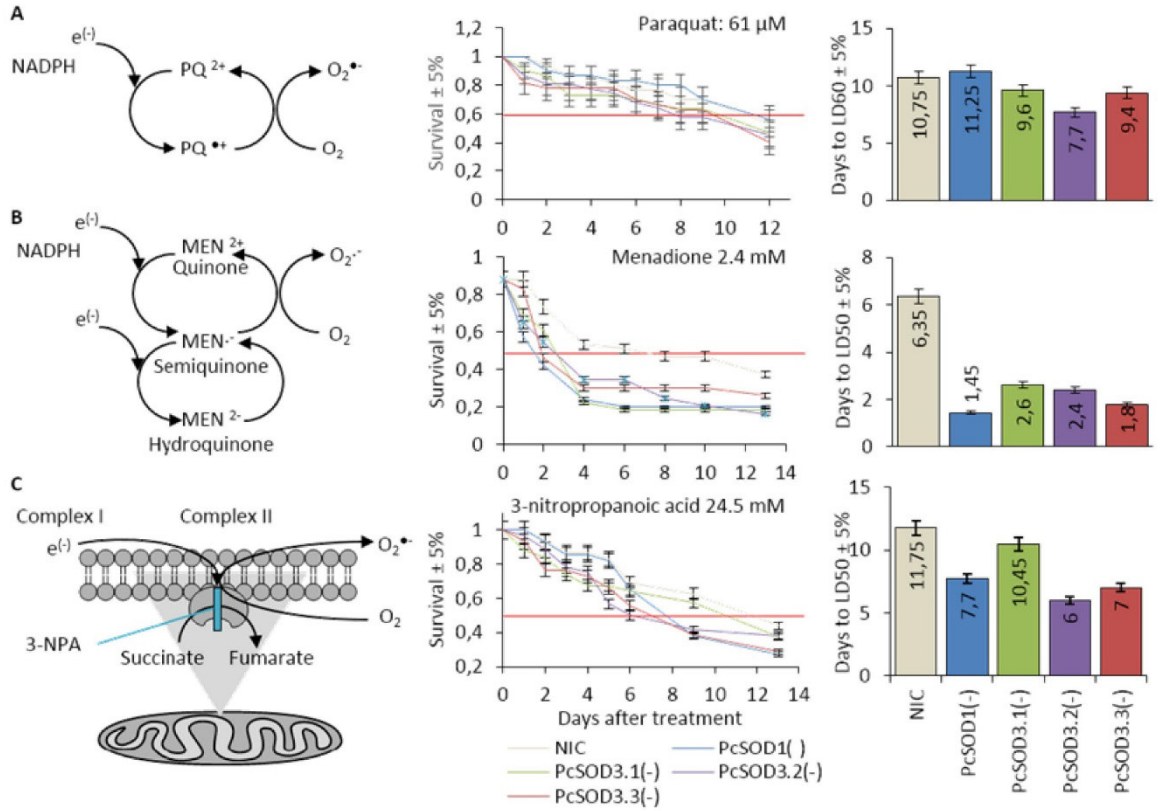
A
NADPH
e(-)
PQ 2+
PQ •+
O2•-
O2
B
NADPH
MEN 2+
Quinone
MEN·-
Semiquinone
MEN 2-
Hydroquinone
C
Complex I
Complex II
3-NPA
Succinate
Fumarate
Paraquat: 61 µM
Menadione 2.4 mM
3-nitropropanoic acid 24.5 mM
Survival ± 5%
Days after treatment
Days to LD60 ± 5%
Days to LD50 ± 5%
10,75
11,25
9,6
7,7
9,4
6,35
1,45
2,6
2,4
1,8
11,75
7,7
10,45
6
7
NIC
PcSOD1(-)
PcSOD3.1(-)
PcSOD3.2(-)
PcSOD3.3(-)

Figure 8.

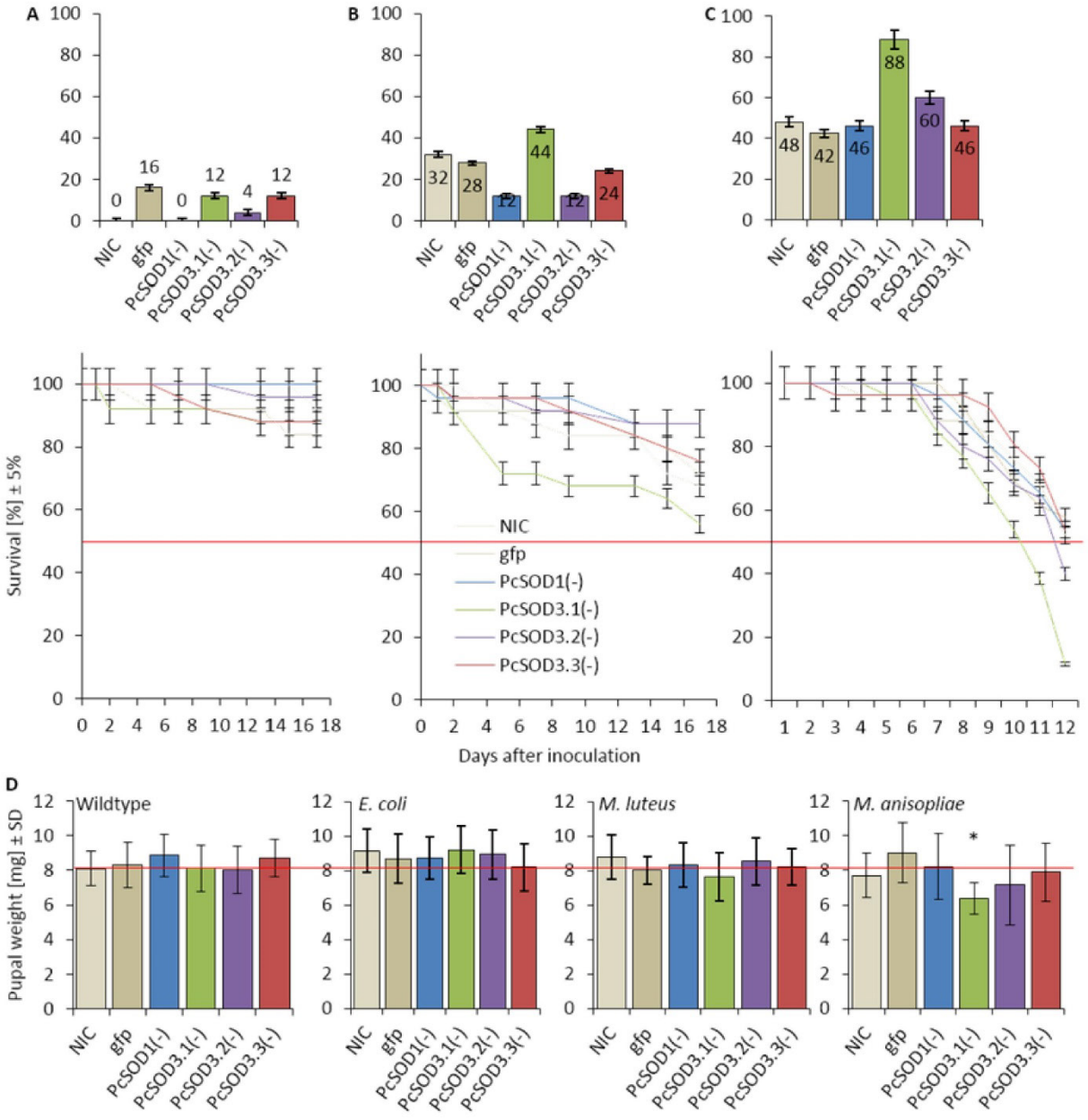
A
B
C
NIC
gfp
PcSOD1(-)
PcSOD3.1(-)
PcSOD3.2(-)
PcSOD3.3(-)
Survival [%] ± 5%
Days after inoculation
D
Wildtype
E. coli
M. luteus
M. anisopliae
Pupal weight [mg] ± SD

Figure 9.

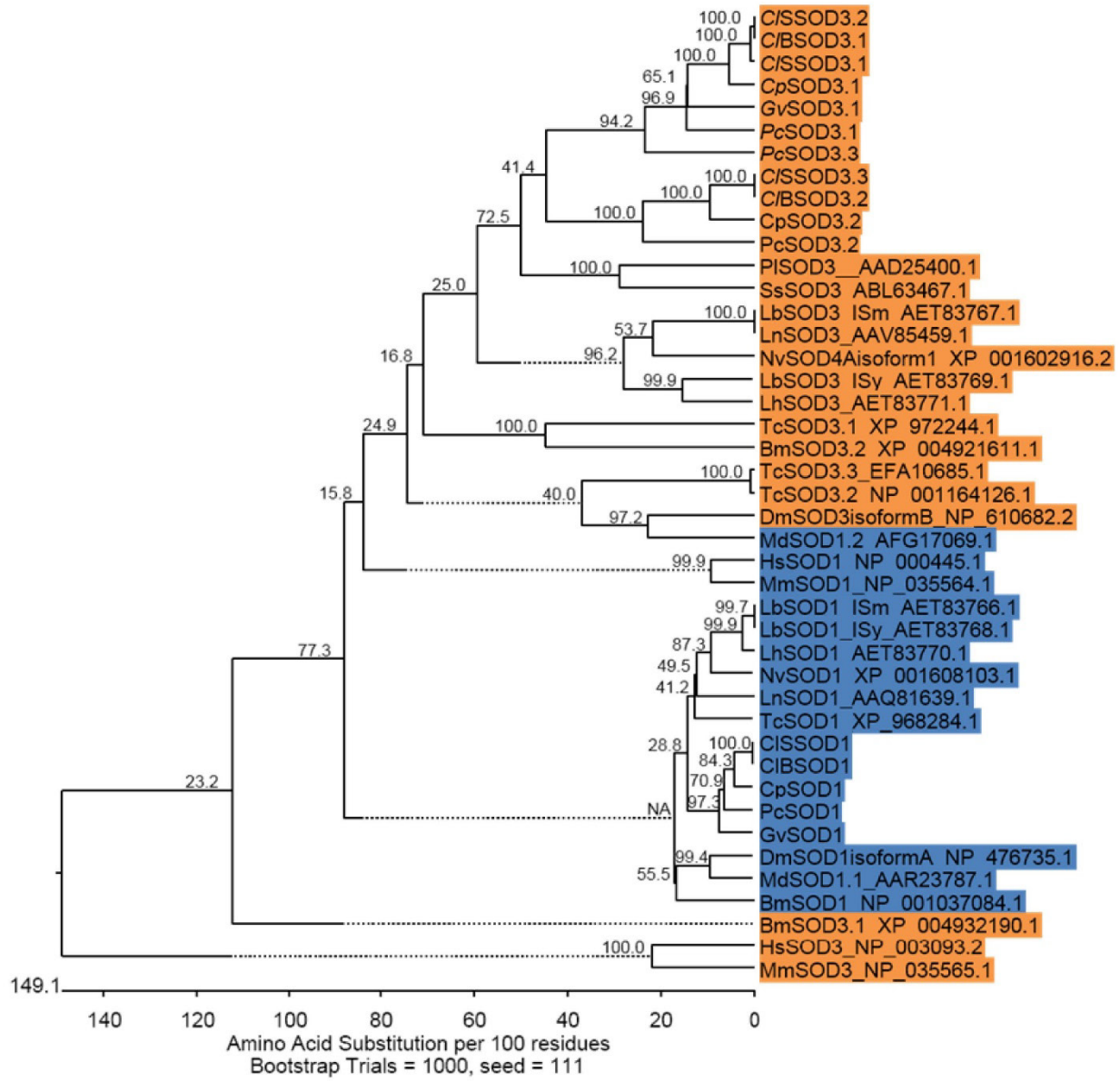
ClSSOD3.2
ClBSOD3.1
ClSSOD3.1
CpSOD3.1
GvSOD3.1
PcSOD3.1
PcSOD3.3
ClSSOD3.3
ClBSOD3.2
CpSOD3.2
PcSOD3.2
PlSOD3__AAD25400.1
SsSOD3_ABL63467.1
LbSOD3_ISm_AET83767.1
LnSOD3_AAV85459.1
NvSOD4Aisoform1_XP_001602916.2
LbSOD3_ISy_AET83769.1
LhSOD3_AET83771.1
TcSOD3.1_XP_972244.1
BmSOD3.2_XP_004921611.1
TcSOD3.3_EFA10685.1
TcSOD3.2_NP_001164126.1
DmSOD3isoformB_NP_610682.2
MdSOD1.2_AFG17069.1
HsSOD1_NP_000445.1
MmSOD1_NP_035564.1
LbSOD1_ISm_AET83766.1
LbSOD1_ISy_AET83768.1
LhSOD1_AET83770.1
NvSOD1_XP_001608103.1
LnSOD1_AAQ81639.1
TcSOD1_XP_968284.1
ClSSOD1
ClBSOD1
CpSOD1
PcSOD1
GvSOD1
DmSOD1isoformA_NP_476735.1
MdSOD1.1_AAR23787.1
BmSOD1_NP_001037084.1
BmSOD3.1_XP_004932190.1
HsSOD3_NP_003093.2
MmSOD3_NP_035565.1
149.1
140
120
100
80
60
40
20
0
Amino Acid Substitution per 100 residues
Bootstrap Trials = 1000, seed = 111

Figure S1.

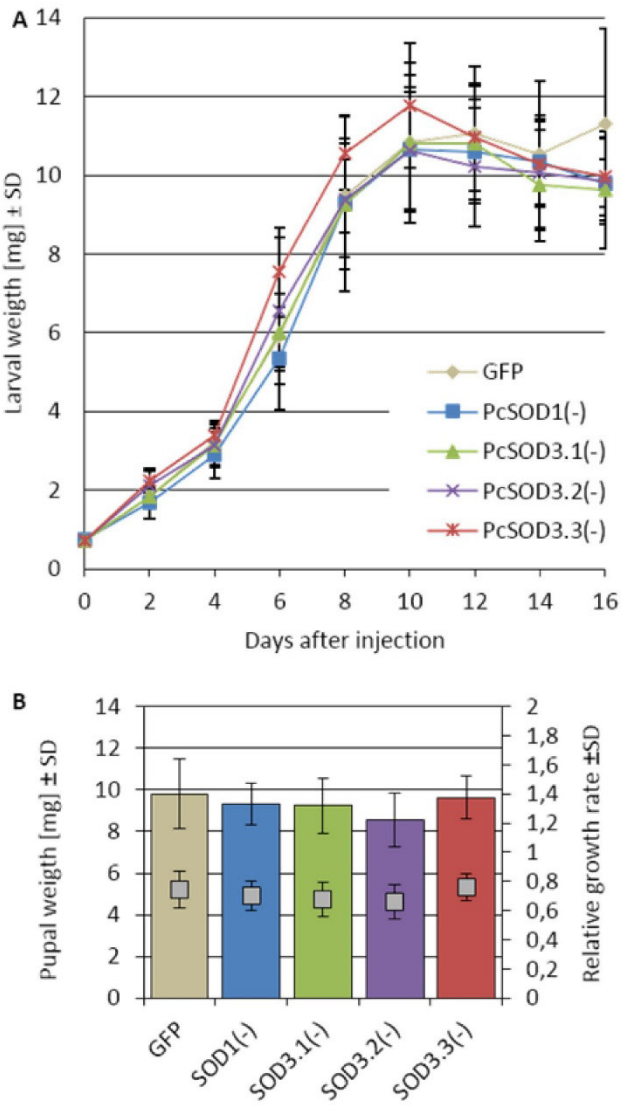
A
Larval weigth [mg] ± SD
Days after injection
GFP
PcSOD1(-)
PcSOD3.1(-)
PcSOD3.2(-)
PcSOD3.3(-)
B
Pupal weigth [mg] ± SD
Relative growth rate ±SD
GFP
SOD1(-)
SOD3.1(-)
SOD3.2(-)
SOD3.3(-)

Figure S2.

Primer type	Target	↔	Sequence	length
Coding sequence	*PcSOD1*	→	ATGCCTACAAAAGCAGTTTGCGTTCTC	462
		←	CTATATTTTTGCCAATCCAATGACTCCA	
	PcSOD3.1	→	GAGAAAAAATTTGATACTTCG	670
		←	TTTTCACTTATCTAAAATCGTTTAT	
	PcSOD3.2	→	ATGTTCAAGTTTGTAGTAGCCGTGGTTT	553
		←	CTCCCTAATCGTAGGTTATTCATTCTTCC	
	PcSOD3.3	→	ATGTTCGGATTTGCTATATTAGCAGCAC	519
		←	CTACTGATCTGTGAGGACTCCTATAACTC	
dsRNA template	*PcSOD1*	→	TAATACGACTCACTATAGGGAGACTCCAATGTGGC GAATA	243
		←	TAATACGACTCACTATAGGGAGATGCCTACAAAAG CAGTT	
	PcSOD3.1	→	TAATACGACTCACTATAGGGAGAACATCGTAGCCG ACGCA	193
		←	TAATACGACTCACTATAGGGAGACCGATGACCCCG CAA	
	PcSOD3.2	→	TAATACGACTCACTATAGGGAGAGACTCCGCAAGC TATAC	508
		←	TAATACGACTCACTATAGGGAGACAAGTTTGTAGT AGCCG	
	PcSOD3.3	→	TAATACGACTCACTATAGGGAGATCGCGCTCCTGC GTG	172
		←	TAATACGACTCACTATAGGGAGACATCGAGGCCGA CGAAT	
	gfp	→	TAATACGACTCACTATAGGGAGACCATGGCCAACA CTTGT	523
		←	TAATACGACTCACTATAGGGAGATAATCCCAGCAG CAGTT	
qPCR	*PcSOD1*	→	ATCATGATCTGGGCCACCATGC	77
		←	ACAACACCAACGGGTGCATTTCC	
	PcSOD3.1	→	AAACATCGTAGCCGACGCAACAG	89
		←	TGCCGATGATGTTGTGGTTGC	
	PcSOD3.2	→	TCAATGTGAGCGACGCCGAAAC	111
		←	TGGACCTTTCAATCCCCACAACG	
	PcSOD3.3	→	GCGCGATGCCGTATTCGTCGG	130
		←	ATTGGATCAGGATGTCTGGCA	
	PcRP-L6	→	CAAGACAGGATCAGACCTAGAC	126
		←	CACTCTCTTTCCTTTGTGGGAAC	
	PcRP-S3	→	AAGGCTGTGAAGTTGTGGTATCTGG	128
		←	ATGGCGGGTGGCAGTGTCTAC	
pET100 Insert	*PcSOD1*	→	CACCATGCCTACAAAAGCAGTTTGC	466
		←	CTATATTTTTGCCAATCCAATGACT	
	PcSOD3.1	→	CACCATGCGTAGCGCAGTCGTCTATCT	487
		←	AGCCAGAACGCGTATTTACTC	
	PcSOD3.2	→	CACCGATGTGCATTCAGCAACAGTT	478
		←	TCATTCTTCCAATACTTCGA	
	PcSOD3.3	→	CACCGCAGCGCAACGCAATCGTCT	475
		←	CTACTGATCTGTGAGGACTCCTA	

Table S1.

Name in this	Predicted as	Genbank	Pfam	Signal peptide

study		accession Nr.		
*Pc*SOD1	SOD1		SOD_Cu domain	Non
*Pc*SOD2	SOD2		Sod_Fe_N SOD_Fe_C	Non
*Pc*SOD3.1	SOD3	JQ424878.1	Sod_Cu	16AA
*Pc*SOD3.2	SOD3		Sod_Cu	20AA
*Pc*SOD3.3	SOD3		Sod_Cu	16AA
*Pc*CCS	Copper chaperone		HMA Sod_Cu	Non
*Pc*MSMP	rSOD		Sod_Cu (3x)	Non
*Cp*SOD1	SOD1		Sod_Cu	Non
*Cp*SOD3.1	SOD3		Sod_Cu	25AA
*Cp*SOD3.2	SOD3		Sod_Cu	20AA
*Cl*SSOD1	SOD1		Sod_Cu	Non
*Cl*SSOD3.1	SOD3		Sod_Cu	16AA
*Cl*SSOD3.2	SOD3		Sod_Cu	25AA
*Cl*SSOD3.3	SOD3		Sod_Cu	20AA
*Cl*BSOD1	SOD1		Sod_Cu	Non
*Cl*BSOD3.1	SOD3		Sod_Cu	25AA
*Cl*BSOD3.2	SOD3		Sod_Cu	20AA
*Gv*SOD1	SOD1		Sod_Cu	Non
*Gv*SOD3.1	SOD3		Sod_Cu	16AA

Table S2.

Supplemental Information

1 Additional material and methods

1.1 Beetle rearing and body-fluid collection.

P. cochleariae was incubated on *Brassica rapa pekinensis* from a local public supplier for stock rearing. For experiments adults were placed on *B. rapa pekinensis* "Cantonner Witkrop" (Quedlinburger Saatgut, Quedlinburg, Germany) from the institutes greenhouse. 24 h after the adults were sited back on regular Chinese cabbage where the eggs and the resulting larvae were fed on greenhouse plants. Stock and default rearing occurs in a Snider chamber (Snijders scientific, Tilburg, Netherlands) in a light/dark cycle of 16 h light and 8 h darkness (LD 16/8) and 13°C/11°C ± 1°C, 70% humidity. After microbial infection and during developmental experiments the speciesmen were incubated at LD 14/10, 21 ± 2°C, 70% humidity.

Larval secretions were soaked directly from the larval back in glass capillaries (i.d.: 0.28 mm, o.d.: 0.78 mm, length 100 mm; Hirschmann, Eberstadt, Germany), after softly anger them with scissors. Secretions were weighed in the sealed capillaries on an ultra-microbalance (Mettler-Toledo, Greifensee, Switzerland) three times; the weight of the capillaries was subtracted and the final weight was averaged. Sealed capillaries were stored at -20°C until needed. Hemolymph was collected in graduated 5µl glass capillaries (Hirschmann) after scissoring of one meta-thoracal legs at the coxa and also stored at -20°C after sealing.

1.2 Developmental parameters

Survival or mortality of different treatments has been measured by counting the speciesmen of an experimental group and compare the value with the initially larvae appointed to the experiment.

The weight of the pupae has been measured individually and directly on the day of their occurrence on a microbalance (Mettler-Toledo) as an indicator of success of the larval phase.

According to [62], we obtained the relative growth rate (RGR) by RGR = [(final weight – weight of neonate larva)/(weight of neonate larva × developmental time [days])]. Each replicate group was weighed each 24h ± 3h.

For comparison of fertility, five times one pair of at least seven days old adults of each group were placed in individual plastic cups on fresh food. After 24h they were removed again and the eggs laid in the food was further incubated until the larvae were hatching. These were counted and used for comparison. The same approach was repeated one and two weeks later.

1.3 GC-MS detection of chrysomelidial

Secretions were diluted in 1:400 (w/v) ethyl acetate which was supplemented with 10 µg/ml methyl benzoate as an internal standard. One µl was subjected to GC/MS analysis (ThermoQuest Finnigan Trace GC-MS 2000, Frankenhorst, Germany) equipped with Phenomenex ZB–5–

W/Guardian–column, 25 m. Substances were separated using helium as a carrier (1.5 ml/min); conditions: 50°C (2 min), 15°C min^{-1} to 180°C, 30°C min^{-1} to 300°C (1 min). Inlet temperature was 220°C; transfer line was 280°C. Peak areas from GC-chromatograms were obtained using an ICIS-algorithm (Xcalibur bundle vers. 2.0.7, Thermo Scientific). Peak-area of Chrysomelidial was normalized to Peak area of methyl benzoate.

1.4 Native polyacrylamid gel electrophoresis.

Hemolymph, secretions and heterologous purifications were diluted in 0.1 M potassium buffer, pH 6.4 and spiked with 100% (v/v) native sample buffer. The prepared samples were loaded on gradient mini-gels (anyKD, biorad) and run by the use of native running buffer (144g/l glycin, 30,2 g/l tris base) in a mini-tetracell vertical electrophoresis system (biorad) at 200 V for 60 min. Occasionally the run was extended for 60 min. to bring 67 kDa band in the middle of the gel to obtain better resolution. As a reference 10µl of a native molecular standard (GE Healthcare, Piscataway, NJ, USA) was loaded.

A functional stain for SOD activity was performed after the electrophoresis incubating each gels in 80 ml 50 mM Tris-HCl buffer pH 8.5, supplemented with 15mg $MgCl_2$, 10mg 3-(4,5-dimethylthiazol-2-yl)-2,5-diphenyltetrazolium bromide (MTT) and 3mg phenazine methosulfate (PMS) in daylight for 15 min., clear or pale areas on an purple background indicate SOD activity [74].

1.5 In tube SOD activity assay

Hemolymph and secretion were diluted 1:80 or 1:40 respectively with ringer solution [19] and 10µl of each dilution was subjected to microplate SOD detection assay (Sigma-Alrich) following the manufacturer's guidelines, detecting SOD activity in final 0.25mg hemolymph and 0.5mg defense secretion. The microplate reader was set for kinetic detection, A_{450nm}, 28°C, 60 min. Data were analyzed and an endpoint calculation of SOD activity was performed using the data from the last third of the log-slope of an uninhibited control-well.

1.6 Sequence alignments

Aminoacid sequences of previous identified and annotated Cu/Zn-SOD proteins from insects, crustaceans, mouse and human (For accession numbers see Fig. S1) have been downloaded from NCBI refseq database (Bethesda, MD, USA). ClustralW alignment, subsequent bootstrapping and generation of graphics were performed using MegAlign software, which is a part of DNASTAR (Madison, WI, USA) Lasergene 10 core suite package.

4. Rahmende Diskussion

4.1 Funktionale Identifizierung von Proteinen im Wehrsystem mittels RNAi

Wie anhand der für diese Dissertation zusammengefassten Arbeiten gezeigt werden konnte, ist es möglich mittels RNAi molekulare Grundlagen der Wehrbiochemie zu identifizieren und dank des funktionalen Nachweises *in vivo,* zu einem tieferen Verständnis der Zusammenhänge beizutragen.

*Pc*IDS1 zeigte *in vitro* eine Bifunktionalität als Produzent von Geranyl-Diphosphat (GDP), bzw. von Farnesyl-Diphosphat (FDP), wenn entweder Co^{2+} oder Mg^{2+} als Metall-Cofaktor verfügbar ist (Manuskript1, Fig. 3). Der in Manuskript 1 dargestellte RNAi-Phänotyp zeigt die Funktion dieses Enzyms in der Produktion von 8-HO-Geraniol-8-O-*β*-D-glucosid erstmals *in vivo*, da ohne dieses Enzym sowohl die Konzentration dieser Vorstufe in der Hämolymphe abnimmt (Manuskript 1, Fig. 2*E*), weniger Sekret produziert wird (Manuskript 1, Fig. 2*C*) und pro Larve weniger Chrysomelidial messbar ist (Manuskript 1, Fig. 2*F*). Durch die Analyse der Entwicklungsparameter der Larven konnte gezeigt werden, dass das Enzym keinen Einfluss auf die Entwicklung derselben hat (Manuskript 1, Fig. S3). Sollte *Pc*IDS1 für die Synthese von essentiellem FDP verantwortlich sein hätten sich dahingehend Einflüsse zeigen sollen, dass entweder das Gewicht oder die Entwicklungszeit gegenüber den Kontrollen verschoben gewesen wäre. Die Vermutung liegt daher nahe, dass noch eine weitere IDS im Körper vorhanden ist, die FDP synthetisiert, da die Mengen an essentiellem FDP, die benötigt werden um den Metabolismus in Gang zu halten nicht durch die verbleibende Enzymaktivität der *Pc*IDS1 erklärt werden können (Manuskript 1, Fig. 2*D*). Denkbar wäre auch, dass *Pc*IDS1 in einer noch unbekannten Kompartimentierung des Fettkörpers lokalisiert ist, die eine höhere Co^{2+} Konzentration im Vergleich zur Umgebung aufweist. Das Enzym könnte daher ausschließlich für die Synthese von GDP verantwortlich sein und nur potentielle Aktivität in der FDP-Synthese *in vitro* zeigen, nicht aber *in vivo*. Im Hinblick auf die Entwicklung der Larven ist es auch noch relevant, dass das mit FDP synthetisierte Juvenilhormon, welches der Steuerung der Entwicklung dient, in der *Corpora allata* im Gehirn der Insekten gebildet wird (Bellés, Martín u.a. 2005). Im Gewebe des Kopfes der Larven zeigte sich allerdings keine signifikante Reduktion des Transkripts nach der Behandlung mit dsRNA (Manuskript 1, Fig. 2*B*), wonach unverändert Juvenilhormon durch *Pc*IDS1 gebildet werden könnte.

Zusammengenommen sind die Informationen aus dem *in vitro* und dem RNAi Assay gleichsam bedeutend. Eine Aussage über die potentielle Aktivität des Enzyms wäre mit RNAi nicht möglich gewesen und ein *in vitro* Assay hätte die betonte Aktivität des Enzyms in der Wehrbiochemie nicht erkennen lassen können.

Dieses gilt im gleichen Maße für die Experimente im Manuskript 2, die *in vivo* zu einer kontextualen Differenzierung von *in silico* charakterisierten Zucker-Transportern führte. Transporter der „solute carriers (SLC) 2 family“, die auch als „Glucose und Polyol Transporter“

bezeichnet werden, befinden sich demnach in der Membran der Wehrdrüsenzelle wo sie für den Transport von Trehalose und auch anderen Zuckern verantwortlich sein können. Die getesteten Transporter waren in den Wehrdrüsenzellen hoch exprimiert, fanden sich aber mitunter auch in anderen Geweben (Manuskript 2, Fig. 6). Da mit der Injektion von dsRNA in den getesteten Fällen RNAi immer in mehreren Geweben ausgelöst wurde, war es gerade im Hinblick auf den Zucker-Stoffwechsel wichtig zu überprüfen, ob mit dem Herabregulieren eines Zucker-Transporters vielleicht die Versorgung des Organismus' mit Energieträgern gestört wird. Daher wurden Entwicklungsparameter ähnlich wie in Manuskript 1 erhoben, welche in keinem der getesteten Fälle zu einer Veränderung der Larval-Entwicklung oder des Puppen-Gewichts führte (Manuskript 2, Fig. S9). Eine Erklärung dafür könnte sich in einer metabolischen Co-Regulation finden, die durch die Heraufregulierung anderer Zucker-Transporter eine kontinuierliche Versorgung der Zellen mit Energieträgern gewährleistet. Selbst die Injektion mit dsRNA gegen vier verschiedene Transporter gleichzeitig führte nicht zu einer Veränderung der Entwicklungsparameter, obwohl auf Transkript-Ebene nachweisbar war, dass RNAi erfolgreich induziert wurde (Manuskript 2, Fig. 7*A*). Eine genauere Diskussion dieses Aspekts findet sich in Kap. 4.2.2)

Anders verhält es sich mit der Wehrchemie. Zwar wurden auch im Fall der RNAi auf *Pc*SUT1 und *Pc*SUT2 andere Transproter-Transkripte heraufreguliert, aber in diesen beiden Fällen wurde einerseits weniger Wehrsekret produziert und andererseits nahm die Menge an Chrysomelidial ab (Manuskript 2, Fig. 7*B*, *C*). Da sich in diesen beiden Fällen die larvalen Entwicklungsparameter auch nicht von denen der Kontrollen unterschieden, liegt es nahe anzunehmen, dass diese beiden Transporter eine für die Drüsenzellen exklusive Funktion in der Versorgung des Wehrdrüsengewebes mit Kohlenhydraten haben. In diesem Fall müssen *in vitro* Assays nach der RNAi-basierenden Identifizierung zeigen, was genau das Substratspektrum von *Pc*SUT1 und *Pc*SUT2 ist, um eine Aussage darüber treffen zu können was genau transportiert werden kann.

Die Anwendung von RNAi gegen das bereits *in vitro* charakterisierte Enzym *Cpop*SAO führte zur Bestätigung der vorhergesagten Rolle in der Wehrchemie *in vivo* (Manuskript 3, Fig. 3*c*,*d*). Da sich eine Reihe von Proteinen mittels LC-MS/MS in Sekreten von Blattkäferlarven und -adulten identifizieren lassen, die zum Teil unbekannt sind, könnte die in Manuskript 3 gezeigte Herangehensweise auch genutzt werden um unbekannte Proteine funktional zu charakterisieren. Am Beispiel des in der gleichen Arbeit von Peter Rahfeld bearbeiteten Proteins *Pc*To-like1 konnte bereits beispielhaft gezeigt werden, dass weder Sequenzvergleiche mit charakterisierten Transkripten anderer Arten, noch mittels funktionaler Vorhersage über die Aminosäuresequenz, die Position eines Proteins im Metabolismus sicher bestimmt werden kann. Denn dieses Protein, welches dem Transport von hydrophoben Stoffen im Insekt dienen soll, hat entscheidenden Einfluss

auf die Zyklisierungsreaktion von 8-Oxogeranial zu Chrysomelidial im Sekret von *P. cochleariae* (Manuskript 3, Fig. 5*b*).

Neben dem Potential der Methode in der Anwendung auf sekretorische Proteine, wurde in diesem Manuskript auch die Methode zur off-target-Vorhersage für nicht-Modellorganismen beschrieben, die in allen Arbeiten Anwendung findet und in Kap. 4.2.1 näher beschrieben wurde.

Schließlich wurden in Manuskript 4 Cu/Zn-SODs bearbeitet. SODs sind bekannt dafür, dass sie Superoxide mithilfe von Catalasen über Wasserstoffperoxid zu Wasser und O_2 abbauen. Diese Funktionalität wurde in den größeren Zusammenhang der Langlebigkeit verschiedener Organismen (Diaz-Albiter, Mitford u.a. 2011, Phillips, Campbell u.a. 1989), und menschlichen Krankheiten gestellt, die durch oxidativen Stress verursacht, oder verstärkt werden (z.B. Moretto und Colosio 2013). Eine aktive Rolle in Insekten wird lediglich der zellulären SOD in Hämozyten nachgesagt, die daran beteiligt ist, Pathogene abzutöten (Arbi, Pouliliou u.a. 2011). Heterolog exprimierte SODs in *P. cochleariae* zeigen alle *in vitro* Aktivität (Manuskript 4, Fig. 3*C*), und mit RNAi konnte nachgewiesen werden, dass alle vier Isozyme tatsächlich eine Rolle im Schutz vor reaktivem Sauerstoff spielen, der durch verschiedene Chemikalien ausgelöst wurde (Manuskript 4, Fig. 8). Interessanterweise konnte für eine der extrazellulären SODs (*Pc*SOD3.1) eine Rolle in der Abwehr von Gram positiven Bakterien und Pilzen zugeordnet werden (Manuskript 4, Fig. 9*B*, *C*). Ob vielleicht eine der *Pc*SODs auch eine Rolle in der Langlebigkeit der Tiere spielt, bleibt abzuwarten, denn diese Experimente sind noch nicht abgeschlossen (Stand 13.12.2013).

Alle diese Arbeiten beleuchten einen besonderen Teilaspekt der Anwendung von RNAi in Blattkäfern, sei es nun das Gewebe, in dem RNAi induziert wird, die Komplexität des metabolischen Netzwerkes in dem das Protein sitzt, oder die Analysen, die notwendig sind, die meist versteckten Phänotypen zu erkennen. Weitere Projekte, die RNAi nutzen sind bereits in Vorbereitung und im Kapitel 4.4.2 wird die Anwendung von RNAi auf einen ganz neuen Aspekt, der Ökologie von Blattkäfern, in Aussicht gestellt.

4.2 Parameter zur Validierung von RNAi-Effekten.

Wie aus Manuskript 4, Fig. 4*A* hervorgeht, beginnt die Reduktion des Transkripts bereits sechs Stunden nach der Injektion signifikant zu sein. Die Reduktion von *PcSOD3.1* in diesem Fall, ist stabil über das gesamte Zeit des Larvenstadiums und auch noch acht Wochen nach der Imaginalhäutung (Manuskript 4, Fig. 4*D*). In Manuskript 3, Fig. 3*a* wurde gezeigt, dass sich die Reduktion des Transkripts von *CpopSAO* tageweise ähnlich reduzieren lässt. Ausgehend von diesen beiden ausführlichen Analysen, wurden die Transkripte in Manuskript 1 und 2 nur noch an einzelnen Tagen überprüft und eine Reduktion ab Tag eins bis zum Ende des Larvenstadiums bei gleicher RNAi-Methodik vorausgesetzt. In den Manuskripten 1 und 4 konnte mit der Analyse der Expression in

verschiedenen Geweben bereits gezeigt werden, dass RNAi in Blattkäfern zur systemischen Reduktion des Trankripts fähig ist. *PcIDS1* wurde im Fettkörper, den Malpighischen Gefäßen und im Darm reduziert, nicht aber in den Wehrdrüsen oder dem Kopf (Manuskript 1, Fig. 2*B*) und *PcSOD3.1* wurde in Wehrdrüsen, Fettkörper, Malpighischen Gefäßen und dem Darm herabreguliert (Manuskript 4, Fig. 5*A*).

Untersuchungen des Transkripts in der F1-Generation von verschiedentlich induzierten Larven, Puppen und Imagines sollte Hinweise darauf geben, ob die Arbeit an Blattkäfern durch parentales RNAi erleichtert werden könnte (Bucher, Scholten u.a. 2002). Leider stellte sich für die getesteten Targets heraus, dass das Transkript in den Larven der nächsten Generation nicht signifikant reduziert worden war (Manuskript 4*D-F*)

Durch Verfolgen der sekretorischen Proteine *Cpop*SAO und *Pc*SOD3.1 in PA-Gel konnte die Verminderung des Proteins nachvollzogen werden. Wie in Manuskript 3 Fig. 3*b* anhand eines zeitlichen Verlaufes gezeigt ist, wird das Protein kontinuierlich weniger bis es selbst in der Silber-Färbung ab Tag sechs nicht mehr zu erkennen ist. In Manuskript 4, Fig. 4*B* ist exemplarisch das Sekret von *P. cochleariae* neun Tage nach der Injektion mit dsRNA aufgetragen, bei dem auch kein Protein des Zielgens mehr zu erkennen ist.

Der dritte Nachweis, dass RNAi erfolgreich induziert wurde ist schließlich die Verminderung der enzymatischen Aktivität oder der Transportrate. In Manuskript 1 konnte gezeigt werden, das spätestens ab Tag sieben nach der Injektion die Enzymaktivität signifikant reduziert ist (Manuskript 1, Fig. 2*D*), wobei sich Auswirkungen auf das Wehrsekret schon ab Tag fünf zeigen, hier also bereits eine verminderte Aktivität anzunehmen ist (Manuskript 1, Fig. 2*C*, *F*). Die Analysen der Auswirkungen der Anwendung von RNAi auf die Zuckertransporter in *P. cochleariae* sind absichtlich erst fast am Ende des Larvenstadiums gemacht worden, da Transportmoleküle einen langsameren Umsatz zu haben scheinen als Enzyme, wie anhand eines ABC Transporters in der Drüsenzelle gezeigt wurde (Strauss, Peters u.a. 2013), (Manuskript 2, Fig. 7*A*). Nichtsdestoweniger konnte auch hier in zwei Fällen eine Veränderung an den Konzentrationen von Chrysomelidial im Wehrsekret gezeigt werden, was auf die verminderte Zucker-Transportrate ohne *Pc*SUT1 und *Pc*SUT2 zurückzuführen ist. In Manuskript 3, Fig. 3*d*, konnte anhand der Reduktion des Salicylaldehyds zugunsten des Salicylalkohols die Verminderung der *Cpop*SAO-Aktivität mittels täglicher GC-Vermessung von Sekretproben nachvollzogen werden. Ein direkter Vergleich mit der funktionalen Reduktion von *Pc*SOD3.1 in Manuskript 4, Fig 4*C* zeigt, dass das Minimum an enzymatischer Aktivität bereits nach drei Tagen erreicht wird, wohingegen einen Minimum-Phänotyp bei *Cpop*SAO erst ca. 5 Tage nach RNAi-Induktion nachweisbar war. Diese Diskrepanz ergibt sich entweder aus der größeren Menge an *Cpop*SAO-Enzym im Sekret von *C. populi* oder aus einem Unterschied beider Arten im Hinblick auf die RNAi-Sensitivität.

RNAi kann mit unterschiedlichen Mitteln verfolgt und validiert werden, wobei das Transkript einen ersten Hinweis liefert, dass die dsRNA die Zielzellen erreicht hat. Viel entscheidender im Zusammenhang mit der funktionalen Identifizierung von Proteinen ist allerdings der Nachweis der verminderten jeweiligen Aktivität des Genprodukts. Wie in Manuskript 2 gezeigt werden konnte hängen beide Dinge nicht zwangsläufig zusammen, da metabolische Co-Regulation zu einem bewahren des Wildtyps bei vermindertem Transkript führen kann (s. Kap. 4.2.2).

4.2.1 Vermeidung von off-target-Effekten durch *in silico* Validierung der dsRNA

Im Vorausgang der Synthese von dsRNA für die spätere Injektion in die Tiere, muss sichergestellt sein, dass die gewählte Sequenz einzigartig im Ziel-Transkriptom ist, damit es nicht zur ungewollten Co-Regulierung von Transkripten kommt, die nicht Ziel der RNAi-Induktion waren (vgl. Kap. 1.1). Es konnte gezeigt werden, dass in einigen Fällen eine Übereinstimmung der im RISC eingebauten 21 nt übereinstimmende Sequenz von 11 nts ausreicht, um erfolgreich off-target-Effekte zu verursachen (Jackson, Bartz u.a. 2003). Die zitierte Studie untersuchte die Effekte im Zusammenhang mit siRNAs, wobei naturgemäß nur uniforme RISC gebildet werden. Im Gegensatz dazu können aus einer längeren dsRNA viele verschiedene siRNAs geschnitten werden, die in Einzelfällen off-target-Effekte verursachen könnten. Ebenfalls anhand von *D. melanogaster* Zell-Assays konnte allerdings gezeigt werden, dass hierbei 19+ nts ausreichen, um andere Transkripte signifikant herab zu regulieren. Ohne eine Kontrolle solcher sequenzbasierenden Fehlerquellen, kann der induzierten Phänotyp nicht allein auf das eigentliche Zielprotein zurückgeführt werden (vgl. Kulkarni, Booker u.a. 2006).

Für die Arbeiten in dieser Dissertation wurde ein Programm geschrieben, welches die gewünschten Zielsequenzen in alle möglichen 21bp-Fragmente beider Stränge zerlegt (Magdalena Stock). Die hieraus entstandenen *in silico* siRNAs wurden auf Sequenzhomologien in der Transkriptom-Datenbank untersucht (s. Mauskript 3). Die Bereiche, die in der zukünftigen dsRNA Übereinstimmungen von mehr als 20 Nucleotiden haben, ohne eine Lücke oder eine Diskrepanz aufzuweisen, wurden in der Folge aus der dsRNA-Sequenz herausgenommen. Eigene Untersuchungen mit 1500 nt langer dsRNA haben gezeigt, dass 21 bp mit einer einzelnen Diskrepanz in unseren Blattkäfern bereits ausreichen, um eine signifikante Reduktion des falschen Transkripts zu verursachen (Manuskript 3, Abb. S2). Dass neben der sequenzbasierenden Co-Regulation auch eine Gegenregulation des Körpers stattfinden kann, wird im nächsten Kapitel erläutert.

4.2.2 Metabolische Co-Regulation nach RNAi Induktion

Ein wichtiger Aspekt in der Validierung von Phänotypen mittels RNAi, ist die Kontrolle der Induktion der RNAi-Maschinerie selbst. Die alleinige Aktivierung des RNAi-Mechanismus' führt systemisch zu einer Veränderung des Stoffwechselprofils, weshalb dieses Ereignis mit einer speziellen Kontrolle normalisiert werden muss (vgl. Hansen, Burns u.a. 2005). Eine Behandlung mit dsRNA, welche zwar den Mechanismus in den Zellen aktiviert, die gebildeten RISC-Proteine jedoch keine passende mRNA erkennen können, würde diese Aufgabe erfüllen. Eine Injektion mit Injektionspuffer allein normalisiert zwar die durch die Injektion entstandene Verletzung, aber keinesfalls die RNAi-abhängige Reaktion. Mit Entdeckung der RNAi wurden oft (Lew-Tabor, Kurscheid u.a. 2011, Seinen, Burgerhof u.a. 2011, Zhai, Zhang u.a. 2013), solche Kontrollen angewendet. Diese reichen von zufällig zusammengesetzten RNA Sequenzen (z.B. Mitchell Iii, Ross u.a. 2007), bis hin zur Verwendung von dsRNA, die der bekannten Sequenz des GFP-gens entnommen wurde (z.B. Ghanim, Kontsedalov u.a. 2007). Die letztere Variante fand in dieser Arbeit Anwendung, nicht nur weil diese Sequenz weder in *C. populi* noch in *P. cochleariae* vorkommt,

A

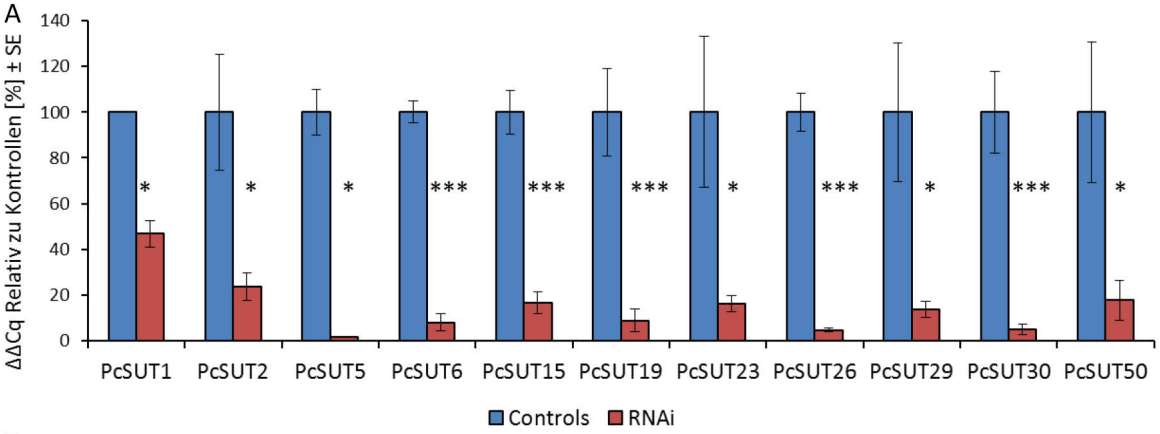

B

	PcSUT1	PcSUT2	PcSUT15	PcSUT19	PcSUT23	PcSUT26	PcSUT29	PcSUT30	PcSUT50
Kontrollen	100	100	100	100	100	100	100	100	100
PcSUT1 (-)	46,76	172,19	182,48	170,18	60,04	115,52	5,22	133,46	85,82
PcSUT2 (-)	62,54	23,65	138,21	95,23	262,47	86,05	715,92	105,58	276,11
PcSUT15 (-)	86,44	97,64	16,63	45,41	237,96	57,60	571,92	87,09	484,98
PcSUT19 (-)	47,15	77,53	97,55	8,87	128,54	66,88	860,84	98,11	317,54
PcSUT23 (-)	27,15	106,58	134,27	23,48	16,10	68,00	327,34	109,41	187,06
PcSUT26 (-)	43,94	133,86	165,46	72,23	219,43	4,65	425,68	190,87	240,23
PcSUT29 (-)	80,40	88,94	103,07	48,01	385,08	73,98	13,76	81,80	543,08
PcSUT30 (-)	61,21	57,37	83,90	61,68	312,66	48,23	720,39	4,96	410,84
PcSUT50 (-)	116,56	71,22	124,87	53,70	263,92	77,37	817,22	75,03	17,76

Abbildung 12: Differentielle Exprimierung von Zucker-Transportproteinen nach RNAi-Induktion.
RNAi wurde auf einzelne Zuckertransporter angewendet (markiert mit „(-)“) und ihre Expression nach der Gewinnung von cDNA aus ganzen Larven analysiert. A: RNAi-Effekt auf das Ziel- Transkript des gesilencten Zucker-Transporters, Controls: gfp-Kontrolle, RNAi: 200ng dsRNA Injektion, Sequenz vom in der X- Achse notierten Transporters. B: Expressionsanalyse aller getesteten Transporter, Farbcode in Relation zur gemessenen Transkriptmenge in *gfp*-Kontrollen: gelb: 100% grün <100%, rot> 100%. Stärke der Signifikanz: p≤0.05: *, p≤0.01:**, p≤0.001:***. R. Gretscher, tlw. unveröffentlichte Daten.

sondern auch weil durch das Fehlen eines Genoms nicht eindeutig gesagt werden kann, ob eine Zufalls-Sequenz nicht doch eine Entsprechung in den Blattkäfern hat.

Ein Phänomen, welches bei der Arbeit an Manuskript 2 ergründet wurde, ist das Herabregulieren von Transkripten, in Abhängigkeit vom metabolischen Pfad, der durch die RNAi Behandlung beeinträchtigt wird. Hierbei werden offenbar andere Transkripte endogen herauf- oder herabreguliert um auf den Verlust des RNAi-Zieltranskripts zu reagieren. Vergleichbares geschieht auch in herkömmlichen knock-out Systemen und auch in anderen RNAi Versuchen (z.B. Kippner, Finn u.a. 2011, Fraga, Ribeiro u.a. 2013). Dieses Phänomen wird in der Systembiologie auch mit Absicht genutzt, um in metabolischen Netzwerken einzelne Pfade durch die Herabregulierung von anderen zu betonen (Bartl, Kötzing u.a. 2013). Wenn es ein anderes Gen gibt, dass die Funktion des manipulierten Gens übernehmen kann, oder welches in den metabolischen Pfad eingreift, der durch das Fehlen des Zielgens gestört wird, kann es zur Gegenregulation durch den Organismus mittels zellulären Signalen kommen, die zu einer Veränderung in der normalen Expression von Genen führt. Im Falle der *Cpop*SAO (Manuskript 3) kann metabolisches Co-Silencing ausgeschlossen werden, da es derlei zelluläre Signale aus dem extrazellulären Raum des Reservoirs nicht zu geben scheint, gleichwohl konnte nach der RNAi gegen die *Pc*SODs in Manuskript 4 keine Gegenregulation festgestellt werden (Manuskript 4, Fig. 5*A*).

Durch anfängliche qPCR Versuche während der Arbeit an Manuskript 2 wurde beobachtet, dass auch die Zucker-Transporter sich in solchen differentiellen Netzwerken zu organisiert scheinen (Abb. 12). Daraufhin wurden RNAseq-Daten von mRNA aus Wehrdrüsengewebe generiert um anhand einer Transkriptom-weiten Analyse Hinweise auf die betroffenen Gene zu finden. Die in Manuskript 2 gezeigte differentielle Expression zahlreicher als Transportproteine annotierter mRNAs aus den Proben in denen RNAi auf *PcSUT*s angewendet wurde, stellte für uns eine Erklärung dar, weshalb das Ausschalten eines prominenten Transporters aus den Wehrdrüsen, nicht zu einem Erliegen der ATP abhängigen Wehrbiochemie führte. Andere Transporter, die ebenso einen Transport dieses Glucosids bewerkstelligen konnten, wurden heraufreguliert und übernahmen die Funktion des herabregulierten Proteins. Eine RNAseq basierende Kontrolle einer dsRNA-Behandlung stellt daher die Vollendung der RNAi-Methode dar, da sowohl der Erfolg der RNAi am Transkript gemessen werden kann, als dass man auch in der Lage ist signifikante Gegenreaktionen des Organismus zu identifizieren (Manuskript 2, Fig. S10).

4.2.3 Auslöser von RNAi, siRNA *versus* dsRNA

Da RNAi im Prinzip auch durch die direkte Injektion von siRNA induziert werden kann, was die Vermeidung von off-target-Effekten begünstigen würde, wurde auch getestet, ob RNAi mittels 27 bp siRNAs induziert werden kann. Hierzu wurde aus der kodierenden Sequenz von *PcSOD3.1* unter

Beachtung der von Reynolds et al. (2004) publizierten Spezifikationen für effektive siRNAs eine Sequenz ausgewählt und synthetisiert (siMax, MWG eurofins operon). Es wurden Test-Injektionen mit 100 pmol siRNA je L3-Larve, vorgenommen, was einer Injektion mit 1,78 µg dsRNA entspricht. Dabei wurde die siRNA zum einen ausschließlich in Injektionspuffer gelöst, ein anderes Mal mit Lipofectamine (life technologies) nach Herstellerangaben versetzt und für eine dritte Testreihe wurde IsiFect (BianoScience) als Transfektionshilfe verwendet. In allen Fällen konnte nach drei Tagen keine Reduktion des Transkripts in Gewebe von *P. cochleariae* festgestellt werden, was exemplarisch in Abbildung 13 am Beispiel mit IsiFect gezeigt ist.

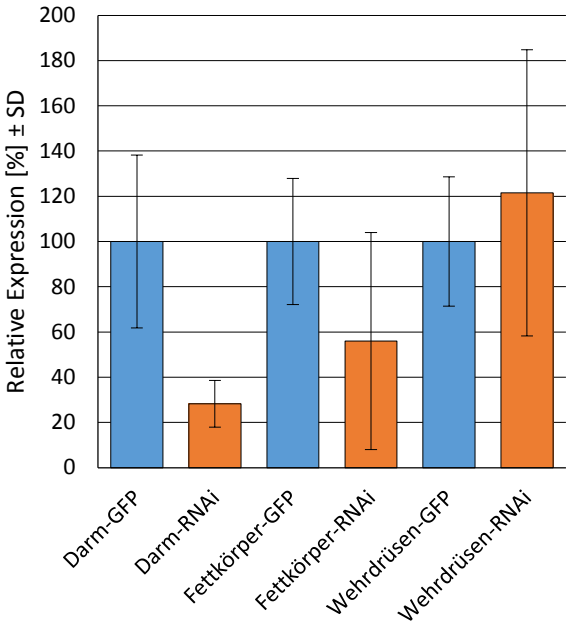

Abbildung 13: Transkript von *PcSOD3.1* nach Injektion mit siRNA. Drei Tage nach der Injektion mit IsiFect und 100pmol siRNA wurden die Larven präpariert, die Expression von *PcSOD3.1* via qPCR analysiert und zur Kontrolle normalisiert. Referenzgen war *PcRP-L6*. n=3. (eigene unveröffentlichte Daten)

Auch in *T. castaneum* war bisher eine künstliche Induktion von RNAi durch siRNAs nicht erfolgreich (Wang, Wu u.a. 2013), obwohl der Modellkäfer bekanntermaßen sehr sensitiv für dsRNA ist.

In der hier vorliegenden Arbeit variiert die Länge der dsRNA stets in Abhängigkeit der verfügbaren Sequenz nach der off-target Vorhersage. Die injizierte Menge richtete sich allerdings stets nach der Einwaage der dsRNA im Injektionspuffer, sodass bei gleichen Konzentrationen immer die gleiche Menge an dsRNA injiziert wurde, trotz der Unterschiede in der Länge der dsRNA (z.B. 1 µg einer 500 bp dsRNA ergibt 3,03 pmol, 1 µg einer 1500 bp dsRNA ergibt 1.01 pmol). Die Injektion von dsRNA mit einer Länge von 173 bp (*PcSOD3.3*) führte indes genauso zum Erfolg, wie die Injektion mit der 1500 bp dsRNA von *CpopSAO*. Gleichermaßen hatte die Menge an dsRNA keinen positiven Einfluss auf die Induktionsgeschwindigkeit oder das Ausmaß des RNAi-Phänotyps (Manuskript 3, Fig. 3*d*) (vgl. He, Cao u.a. 2010).

Obwohl anhand von *CpopSAO* gezeigt werden konnte, dass eine Injektion mit 100 ng dsRNA ausreicht um RNAi auszulösen wurde in dieser Arbeit standardmäßig eine Menge von 200 ng injiziert. Damit sollte zum einen abgesichert werden, dass die dsRNA nicht durch möglicherweise vorhandene RNAse III-Enzyme abgebaut wird, bevor sie das Zielgewebe erreich. Dass derartige Enzyme zumindest im Mitteldarm der Larven von *P. cochleariae* zu finden sind, wurde von Sher Afzal Khan (persönliche Mitteilung) experimentell belegt, ob das auch auf die Hämolymphe zutrifft,

wurde nicht untersucht. Zum anderen wurde beobachtet, dass Transkripte, die Proteine mit geringerer Abundanz codieren, bei kleineren Mengen von dsRNA nicht so effektiv herabreguliert werden, wie höher abundante Proteine mit der gleichen Menge an dsRNA (Arbeiten im Zusammenhang mit Manuskript 1, unveröffentlicht). Das würde vermuten lassen, dass der RNAi-Mechanismus an Effektivität zunimmt, wenn die RISC-Proteine im Zytosol häufiger Basenpaarung mit mRNA eingehen, sodass bspw. auf eine akute Infektion mit Viren heftiger reagiert wird als auf das kontinuierliche, aber seltenere Auftreten von dsRNAs die von Transposons kodiert werden. Beides ist allerdings höchst spekulativ und wird durch die Forschungen anderer Gruppen am RNAi-Mechanismus geklärt werden müssen.

4.2.4 Injektionsprozedur bei Larven, Puppen und Adulten

In Anlehnung an die Etablierung der Methode in Prof. Buchers Labor (z.B. Nico Posnien, Schinko u.a. 2009) wurde auch hier eine Position für die Injektion gesucht, die über alle Larvenstadien hinweg und bei mehreren Blattkäfer-Arten, zugänglich ist und eine ausschließliche Injektion in die Hämolymphe erlaubt, ohne den Darm zu verletzen. Da die Tiere nur durch Herabkühlen verlangsamt und nicht mit CO_2 oder ähnlichen gasförmigen Neurostatika betäuben werden sollten, musste die Injektionsstelle auch für sich bewegende Larven gut erreichbar sein. Die Position, die für alle Blattkäferlarven gut zu funktionieren scheint, ist dorsomedian hinter dem prothorakalen Tergit (Abb. 14). Eine Injektion in die intersegmentale Membran an der Stelle kann mit größeren Volumina (bis 10% des Gewichtes der Larven) erfolgen, ohne, dass eine relevante Menge an Hämolymph-Injektionsflüssigkeitsgemisch nach dem Ziehen der Kapillare austritt. Puppen können erfolgreich mit bis zu 20% ihres Körpergewichtes an der gleichen Stelle wie die Larven injiziert werden und bei Imagines ist eine Injektion in die metathorakalen Coxen erfolgreich. Eine injektionsbedingte Mortalität kann nur bei L1 und L2-Stadien beobachtet werden, wo sie ca. 10% bzw. 5% betragen kann.

Abbildung 14: Injektionsstelle am Beispiel von *P. cochleariae* und RNAi-induzierbare Gewebe. Lila umrandet: „silencebare" Gewebe (Manuskript 4), Pfeile: Richtung des Hä,olymph-Stoms, Beschriftung siehe Abb. 4.

Nach der Injektion findet eine rasche Verteilung der Injektionsflüssigkeit im Körper statt, sodass die dsRNA, gelöst in der Hämolymphe, alle Organe umspült und von den Zellen aufgenommen werden kann (Huvenne und Smagghe 2010). Ob oder ob nicht in einem Organismus RNAi induziert

werden kann, liegt an einer Reihe von Faktoren (z.B. Terenius, Papanicolaou u.a. 2011, Melnyk, Molnar u.a. 2011) und muss jeweils empirisch für die Zielart erprobt werden. Allgemein gilt in Insekten allerdings, dass in phylogenetisch evolvierteren Gruppen jenseits der Coleoptera RNAi schwieriger zu etablieren ist, als bei denen darunter. Zum Beispiel kann in *D. melanogaster* kein systemisches Silencen durch die Injektion von dsRNA induziert werden (z.B. S. C. Miller, Brown u.a. 2008), wohingegen in hemimetabolen Insekten RNAi regelmäßig erfolgreich ist (z.B. Katoch, Sethi u.a. 2013).

Im Sinne des „Beyond *Drosophila*" Paradigmas wurde auch in dieser Arbeit belegt, dass RNAi und Sequenzierungstechniken tatsächlich die Tür für die funktionale Charakterisierung von Proteinen in Nicht-Modellorganismen geöffnet hat (vgl. Mito, Nakamura u.a. 2011). Nichts desto weniger konnte in der vorliegenden Arbeit auch gezeigt werden, dass die Integration von adäquaten Kontrollen im Vorausgang und wünschenswerterweise auch im Nachgang der Experimente, essentiell für die Absicherung der Effekte von RNAi ist. Richtlinien für die RNAi sollen dabei helfen falsch-positive Phänotypen zu erkennen (z.B. Kulkarni, Booker u.a. 2006), aber die Kontrolle etwaiger Feedback-Schleifen, die zu einer differentiellen Exprimierung führen, sind selten (z.B. Ciudad, Belles u.a. 2007), was auch daran liegt, dass RNAi traditionell vor allem für die Erforschung von Entwicklungsgenen eingesetzt wird, welche eben keine alternative Entsprechung im Genom zu haben scheinen, die i, Falle eines Ausfalls differentiell exprimiert werden kann. Ein genetisches Arbeiten jenseits von *T. castaneum* und *D. melanogaster* ist durchaus möglich und wurde bereits hundertfach angewendet (Katoch, Sethi u.a. 2013), aber es bedarf gerade wegen der prinzipiellen Leichtigkeit der Generierung von RNAi-Phänotypen, einer adäquaten Absicherung der selbigen unter Einbeziehung der größtmöglichen Menge an genetischer Information.

4.3 Ausblick

4.3.1 Zukünftige Arbeiten zu in Manuskript 4 beschriebenen *Pc*SODs

Der Nachweis der *in vivo* Funktionalität der in Manuskript 4 untersuchten SODs erwies sich als viel komplexer als zuvor angenommen, weshalb das Manuskript noch nicht vollständig vorliegt.

Nichtsdestoweniger stellen die Ergebnisse bereits zum jetzigen Zeitpunkt einen Nachweis dar, dass SODs in Insekten womöglich viel komplexer funktionieren als durch bisherige Veröffentlichungen gezeigt werden konnte. Wenn extrazelluläre SODs tatsächlich die Mediatoren von Signalkaskaden über die Produktion von H_2O_2 sind, oder eben eine Rolle in der Vernichtung von mikrobiellen Pathogenen spielen, müssen weitere Experimente zur Absicherung durchgeführt werden, gerade im Hinblick auf die Übertagbarkeit auf die unspezifische Immunantwort in anderen Eukaryoten.

Folgende Experimente würden die mechanistische Aufklärung der Rolle der *Pc*SODs entscheidend voranbringen:

1. Infektion mit entomopathogenen Bakterien (z.B. *Bacillus sphaericus*, Gram(+), DSM-28 und *Xenorhabdus nematophila*, Gram(-), DSM-3370, beides S1 Organismen.

Diese Experimente wären notwendig, um zu zeigen, dass die beobachteten Ergebnisse der Infektion mit *E. coli* und *M. luteus* auch auf Pathogene von Käfern zutreffen. *E. coli* uns *M. luteus* werden häufig in *in vitro* Assays genutzt um antimikrobielle Eigenschaften von biogenen Stoffen oder chemischen Komponenten auszutesten. Ihnen fehlt allerdings die Fähigkeit auf das Insekten-Immunsystem und die durch das Insekt angebotenen Nährstoffquellen, angepasst zu reagieren, da sie normalerweise für Insekten eben nicht virulent sind. Zeigt sich auch hierbei eine Unterscheidung der Funktion von *Pc*SOD3.1 zwischen Gram positiven und Gram negativen Bakterien, könnte das weitere Hinweise auf den Mechanismus von *Pc*SOD3.1 in *P. cochleariae* geben.

2. RNAseq von folgenden 48 Proben (RNA aus ganzen Larven, 2 biologische Replikate, ein Replikat aus 10 Larven des gleichen Gewichts)

Tabelle 1: Übersicht über die Proben, von denen RNAseq Analysen zu einem Verständnis der SOD Funktionalität beitragen würden.

	Wildtyp	gfp	*PcSOD1*(-)	*PcSOD3.1*(-)	*PcSOD3.2*(-)	*PcSOD3.3*(-)
Unbehandelt/ dsRNA behandelt	X	X	X	X	X	X
E. coli/ *X. nematophila*, $1x10^6$ Zellen	X	X	X	X	X	X
M. luteus /*B. sphaericus*, $1x10^6$ Zellen	X	X	X	X	X	X
M. anisopliae, 1 $x10^3$ Conidien	X	X	X	X	X	X

Im zweiten Experiment könnte deutlich werden, ob die Vielfältigkeit immunologischer Transkripte, die durch zelluläre Signale im Fall der Infektion mit verschiedenen Pathogenen exprimiert werden können, eine Abhängigkeit von einer SOD haben. Wenn die SOD eine Rolle in der Signaltransduktion nach der Infektion spielen sollte, verändern sich ohne die SOD die Expressionschemata im Vergleich zum Wildtyp, was durch eine anschließende bioinformatische Auswertung der differentiellen Expression zu einer neuen Einsicht in die SOD-abhängigen Immunantwort führen kann.

4.3.2 Verhaltensänderung der Blattkäfer durch RNAi gegen Duftbindende Proteine

In der Gruppe von Prof. Dr. Monika Hilker an der Freien Universität zu Berlin wurde in Experimenten gezeigt, dass Puppen und junge adulte *P. cochleariae* auf den Duft einer bestimmten Wirtspflanze geprägt werden können. Dazu wurden die genannten Stadien mit in Dichlormethan (DCM) gelöstem Phenylisothiocyanat (PEITC) behandelt und die Präferenz der auf diese Weise geprägten Käfer mittels Y-Olfaktometer dokumentiert. Eine Kontrollgruppe wurde lediglich dem Lösungsmittel ausgesetzt. Die Analyse von sequenziertem Antennengewebe von Imagines nach der Prägung zeigte ein duftbindendes Protein (odorant binding protein, OBP) welches bei geprägten Tieren im Gegensatz zu den nicht-geprägten Tieren, heraufreguliert worden ist. Duftbindende Proteine werden in Sensillen der „riechenden" Organe von Insekten exprimiert, also Tarsen und Antennen, und stellen die Vermittler zwischen Stimulus und der Reizleitung her, indem sie die Duftstoffe binden und an einen Rezeptorkomplex an der Neuron-Oberfläche weiterleiten (Grosse-Wilde, Kuebler u.a. 2011).

In meinen eigenen Vorarbeiten sollte die RNAi-Methodik für dieses Zielgen entwickelt und induziert werden, wobei die Tiere dann in Berlin im Olfaktometer getestet werden sollten. Dank der Versuche in Manuskript 4 war bereits bekannt, dass RNAi, die in Larven, Puppen und Imagines induziert wird bis an das Ende des adulten Lebensstadiums aktiv bleiben würde.

Nach der off-target-Vorhersage für das OBP, wurde die 450 bp lange dsRNA in späte L3-larven injiziert. Erste Experimente haben gezeigt, dass eine Induktion der RNAi im larvalen Stadium nötig ist, einerseits, um die Prägephase nicht zu stören und andererseits aber auch, damit das Transkript signifikant reduziert wird (Abb. 15).

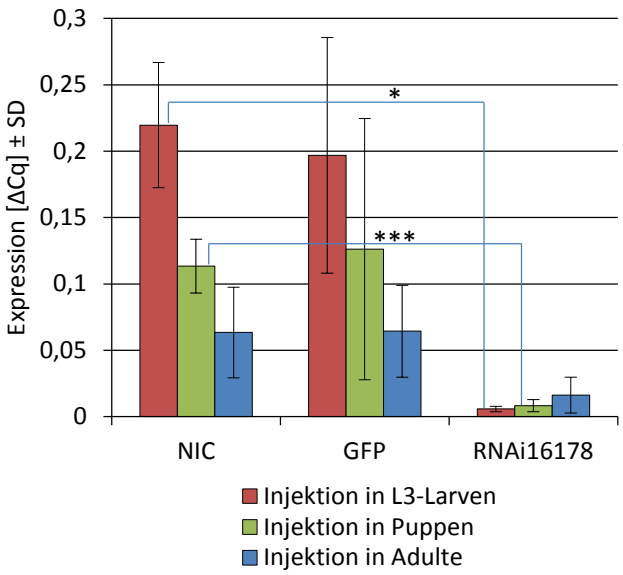

Abbildung 15: Expression von *Pcoc*OBP1 nach RNAi Induktion in verschiedenen Stadien. Jeweils 100 ng dsRNA von *gfp* oder *Pcoc*OBP1 wurden in Larven, Puppen oder adulte Weibchen gespritzt oder ohne Behandlung gelassen. RNA aus ganzen weiblichen Käfern wurde aus ca. a zweiwöchige weibliche Käfer entnommen und nach Umschrift in cDNA in der qPCR analysiert. Es zeigt sich, dass die RNAi unbedingt im larvalen oder Puppen-Stadium induziert werden muss um signifikante Ergebnisse zu liefern. Eine Induktion im bereits adulten Tier führt zu keiner Herabregulierung im Vergleich zu den Kontrollen. Stärke der Signifikanz: p≤0.05: *, p≤0.01:**, p≤0.001:***. R.Gretscher, unveröffentlichte Daten.

Tatsächlich ergab sich durch die Anwendung von RNAi auf *PcocOBP1*, dass sich die Käfer nicht mehr auf einen Duft prägen ließen. In Wahlversuchen konnte keine Präferenz für PEITC festgestellt werden. So wählten die Tiere der RNAi-Behandlung gleich oft

den DCM- Y-Ast, wie den mit PEITC. In der gleichen Weise verhielten sich auch die nicht-geprägten Tiere der Kontrollgruppe (Abb. 16).

Diese erfolgreichen Experimente ebnen den Weg für weitere Untersuchungen an anderen Arten, die Wirtspflanzenwechsel vollziehen oder vollzogen haben. Am Beispiel der auf ihre jeweilige Wirtspflanze spezialisierten Ökotypen von *C. lapponica* (s. Kap. 1.2.1), wäre es von größerer ökologischer Bedeutung, dass die Manifestation dieser biochemisch begründeten Präferenz sich in exprimierten Genen für den Geruchs- und Geschmacksinn der Tiere wiederfinden ließe. Es ist bereits bekannt, dass der Birken-bewohnende Ökotyp seine einstmals funktionale SAO nicht mehr im Sekret exprimiert (Kirsch, Vogel u.a. 2011a). Ein Sequenzvergleich dieses Enzyms mit den Entsprechungen aus anderen Chrysomelina, seien sie nun charakterisiert, oder nur als Sequenz vorhanden, hat weitere Einblicke in die Evolution der Salicyladehyd-Abwehr innerhalb der Chrysomelina gebracht (Kirsch, Vogel u.a. 2011b). Wenn man nun die Transkripte mittels RNAi identifiziert, die dafür verantwortlich sind, dass die beiden Ökotypen jeweils Birke und Weide finden, könnte man mittels eines Sequenzvergleichs und einer Expressionsstudie der selbigen auch Rückschlüsse ziehen, wie sich der mehrmalige Wirtspflanzenwechsels auf die Geruchsperzeption ausgewirkt hat. Das Aufklären der molekularen Ursache dieses zentralen Punktes bei der Entstehung von Ökotypen und später auch der sympatrischen Speziation: der Entscheidung für eine Wirtspflanze, gerät zunehmend in den Fokus (Smadja, Canback u.a. 2012, Unbehend, Hänniger u.a. 2013) und die bereits gut etablierte Ökologie von *C. lapponica* kann dazu beitragen das System besser zu verstehen.

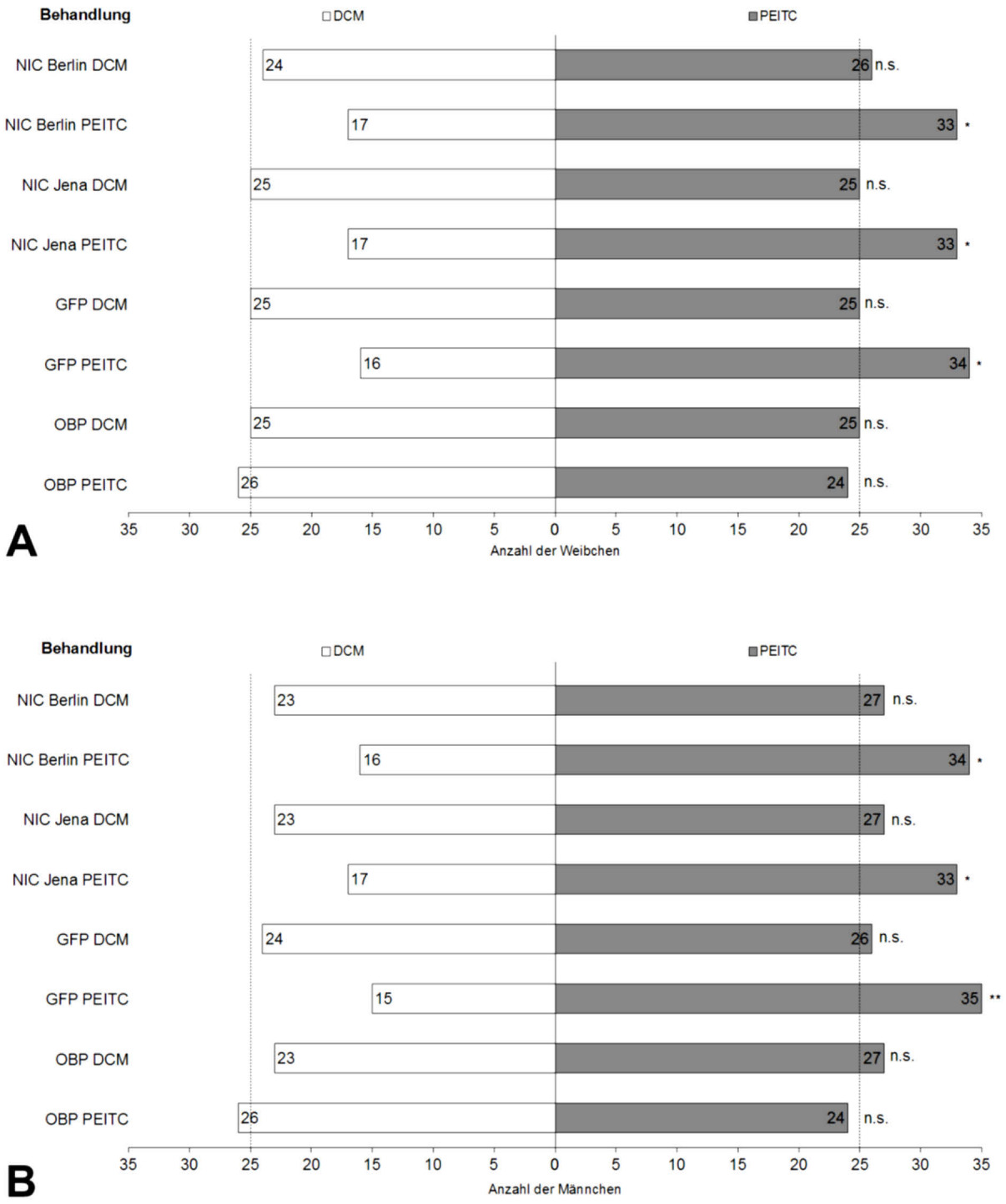

Abbildung 16: Verhalten A) weiblicher und B) männlicher Meerrettichblattkäfer (*Phaedon cochleariae*) (1-Tag alte adulte Käfer) im dynamischen Y-Olfaktometer. Der Test erfolgte mit Tieren, die als Larven keine Injektion von dsRNA erhielten (NIC) oder denen als Larven dsRNA des *green fluorescent protein* (GFP) Gens bzw. PcocOBP1 (OBP) injiziert wurde. Alle Tiere waren während des Puppen- und frühen Imaginalstadiums entweder PEITC (+) oder DCM (-) exponiert. Die Larven aller Gruppen stammten aus Jena (J), mit Ausnahme von NICB, die aus Berlin (B) stammten. Im Y-Olfaktometer bestand die Wahl zwischen DCM und 350 ng PEITC. Je Prägestimulus und Geschlecht wurden 50 Tiere getestet (n = 50), die anschließende statistische Auswertung erfolgte nach dem Vorzeichentest von MacKinnon. DCM: Dichlormethan; PEITC: Phenetylisothiocynat. n.s.: $P > 0,05$; * $P < 0,05$; ** $P < 0,01$. (entnommen aus (Battefeld 2013), Abbildung 3.1)

5. Zusammenfassung

Die chemische Abwehr von Blattkäferlarven stellt ein komplexes System von interzellulären Transportvorgängen und enzymatischen Konversionen dar, welche oftmals bereits im Sekundärmetabolismus der Pflanze beginnt und in der Abwehr eines Prädator, oder der Hemmung eines mikrobiellen Pathogenes endet. Sie wird hauptsächlich durch ein Wehrsekret realisiert, welches in neun paarigen Drüsenapparaten in den Larven produziert wird und im Falle eines Angriffes als Tropfen auf dorsalen Papillen erscheint. Vorhergehende Arbeiten lieferten für diesen Mechanismus bereits den Nachweis eines selektiven Transportsystems (Kuhn, Pettersson u.a. 2004, Kuhn, Pettersson u.a. 2007, Maritta Kunert, Soe u.a. 2008, Discher, Burse u.a. 2009) und wiesen die enzymatischen Schritte der Biosynthese der transportierten Vorstufen hin zum bioaktiven Allomon im Wehrsekret nach (Pasteels, Duffey u.a. 1990, Soetens, Pasteels u.a. 1993, Veith, Oldham u.a. 1997, Brueckmann, Termonia u.a. 2002, Tolzin-Banasch 2009). Initiiert durch die Erstellung von Transkriptom-Bibliotheken von *P. cochleariae* und in der Folge weiteren Mitgliedern des Unterstammes der Chrysomelina und der somit verfügbaren Menge an Sequenzdaten, konnten Themen wie die Aufklärung des Sekretoms der Wehrsekrete und die Identifizierung der molekularen Grundlagen des Transportnetzwerkes bearbeitet werden. Die bereits 1998 auf Insekten angewendete Methode der RNAi (Kennerdell und Carthew) galt als vielversprechend für die Identifizierung von beteiligten Proteinen im System der Wehrbiochemie in Blattkäferlarven. Die in dieser Dissertation zusammengefassten Arbeiten umfassen eine Anwendung der RNAi auf die Fettkörper-Biosynthese, das interzelluläre Transportnetzwerk, die Synthese des Wehrsekretes im extrazellulären Reservoir und auf systemisch wirkende Enzyme des Immunsystems.

*Pc*IDS1 ist ein Enzym aus dem Fettkörper von *P. cochleariae*, das in *in vitro* Experimenten eine synthetische Aktivität von Dimethylallyl-Diphosphat und Isoprenyl-Diphosphat zu Geranly-diphosphat (GDP) oder Farnesyl-diphosphat (FDP) zeigte, abhängig vom vorhandenen metallischen Co-Faktor. GDP dient als Vorstufe von 8-OH-Geraniol-8-O-*β*-D-Glukosids, was wiederum die Vorstufe zur Hauptkomponente im larvalen Wehrsekret von *P. cochleariae*, Chrysomelidial, darstellt. FDP ist die Vorstufe für verschiedene Produkte des Primärmetabolismus. Eine Anwendung von RNAi auf *Pc*IDS1 zeigte, dass dieses Enzym tatsächlich eine entscheidende Rolle in der Bereitstellung von 8-OH-Geraniol-8-O-*β*-D-Glukosid spielt, da die Sekretproduktion zehn Tage nach Injektion mit dsRNA zum Erliegen kam.

Die Identifizierung von *Pc*SUT1 und *Pc*SUT2 als relevante Zucker-Transporter in der Wehrsekretbiosynthese von *P. cochleariae* gelang durch die Anwendung einer RNAi basierenden hochdurchsatz-Analyse. 17 Transporter, die im Transkriptom durch strukturelle Merkmale als solche identifiziert werden konnten, wurden einzeln durch RNAi herabreguliert. Hierbei ergab sich auch, dass die Zucker-Transporter in metabolischen Netzwerken organisiert sind, die die

Versorgung der Zellen mit Energieträgern selbst dann gewährleisten, wenn vier Transporter gleichzeitig herabreguliert werden. Derartige Netzwerke können den Erfolg von RNAi stark mindern, indem der Phänotyp nicht mehr klar definiert werden kann, oder trotz des verminderten Transkripts nicht eintritt. Eine RNAseq-Analyse von cDNA aus Geweben nach der Induktion von RNAi, konnte einen Hinweis darauf geben, dass derartige Gegenregulation stattfindet.

Eine Herabregulierung von *Cpop*SAO, der Oxidase von Saligenin zu Salicylaldehyd konnte dessen Funktion *in vivo* nachweisen, wobei auch die off-target-Vorhersage etabliert wurde, die in unseren Nicht-Modellorganismen ein hochpräzises Arbeiten mit RNAi ermöglicht.

Durch das Ausschalten aller Cu/Zn-SODs, wurden die Funktionen der einzelnen Enzyme (*Pc*SOD1, *Pc*SOD3.1-3.3) im Kontext von zusätzlich durchgeführten Behandlungen charakterisiert. Alle vier SODs spielen eine Rolle in der Detoxifikation von künstlich eingebrachtem oxidativem Stress, wohingegen nach dem Stand der Dinge keine SOD einen Einfluss auf die Lebensspanne von *P. cochleariae* hat. *Pc*SOD3.1 als extrazelluläre SOD, die sowohl im Wehrsekret als auch in der Hämolymphe vorkommt, spielt hingegen eine Rolle in der Resistenz gegen einen entomopathogenen Pilz und ein Gram positives Bakterium. Die Funktion dieses Enzyms wird in der Realisierung einer adäquaten Immunantwort vermutet.

Unter Integration der für das jeweilige Zielgen adäquaten Kontrollen und entsprechender Analysestrategie, konnten mittels RNAi zahlreiche Proteine als Bestandteil einer bestimmten Biosynthese oder eines bestimmten Transport-Prozesses im Körper identifiziert werden. Diese Arbeit hat das Wissen um die molekularen Grundlagen der Produktion und enzymatischen Konversion chemischer Vorstufen zum Nutzen als Allomon im Wehrsekret, sowie dem interzellulären Transport erweitert und eine Methodik etabliert die auch bei weiteren Fragestellungen ihren Wert beweisen kann. Durch RNAi-Experimente in buchstäblich jedem Themenbereich der laufenden und geplanten Forschung nicht nur in dieser Arbeitsgruppe, wird die Relevanz der Leistung deutlich, die im Laufe dieser Doktorarbeit erbracht wurde. Durch die fortlaufende Sequenzierung nahe verwandter Arten, kann auch hier eine Anwendung von RNAi relativ kurzfristig erfolgen. In einem vergleichenden Ansatz mit der Kenntnis der molekularen Grundlagen der veränderten Wehrbiochemie anderer Arten, könnten dann neue Einsichten in die Entwicklung und die Artbildung der Blattkäfer erreicht werden.

6. Summary

The chemical defense of leaf beetle larvae represents a complex system of intercellular transport processes and enzymatic conversions, which often begins in the secondary metabolism of the plant and ends in the deterrence of a predator, or the inhibition of microbial pathogens. This is realized mainly through defensive secretions, which is produced in nine pairs of accessory defense glands in the larvae and presents itself as droplets on dorsal papillae in the event of an attack. For this mechanisms, previous work provided already evidence of a selective transport system (Kuhn, Pettersson u.a. 2004, Kuhn, Pettersson u.a. 2007, Maritta Kunert, Soe u.a. 2008, Discher, Burse u.a. 2009) and revealed the enzymatic steps in the biosynthesis of the transported precursors to bioactive allomones in the defensive secretions (Pasteels, Duffey u.a. 1990, Soetens, Pasteels u.a. 1993, Veith, Oldham u.a. 1997, Brueckmann, Termonia u.a. 2002, Tolzin-Banasch 2009). Initiated by the generation of transcriptomic libraries of *P. cochleariae* and subsequently other members of the subtribe Chrysomelina, a large amount of sequence data was available, with which issues such as the elucidation of the secretome of the defense secretions and the identification of the molecular basis of the transport network could be processed. Kennerdell and Carthew (1998) already applied RNAi to insects, which was considered being a promising tool also for the identification of proteins involved in the system of defensive biochemistry in leaf beetle larvae. The results summarized in this thesis show an application of RNAi on the fat body biosynthesis, the intracellular transport network, the synthesis of the defense secretion in the extracellular reservoir and on systemically acting enzymes of the immune system.

*Pc*IDS1 is an enzyme from the fat body of *P. cochleariae*, which showed in *in vitro* experiments, a synthetic activity of dimethylallyl-diphosphate and isoprenyl-diphosphate to geranly-diphosphate (GDP) or farnesyl-diphosphate (FDP), depending on the available metallic co-factor. GDP serves as a precursor of 8-OH-geraniol-8-O-*β*-D-glucoside, which in turn is the precursor to chrysomelidial, the main component in the larval defensive secretions of *P. cochleariae*. FDP is the precursor for various products of primary metabolism. An application of RNAi to *Pc*IDS1 showed that this enzyme does play a crucial role in the production of 8-OH-geraniol-8-O-*β*-D-glucoside, as the secretion production stops ten days after the injection of dsRNA.

The identification of *Pc*SUT1 and *Pc*SUT2 as important sugar transporters in the biosynthesis of the defense secretions of *P. cochleariae* was achieved by the application of an RNAi-based high-throughput analysis. 17 candidates were identified in the transcriptome according to structural features and were individually down-regulated by RNAi. In this context, it was also found that the sugar transporters are organized in metabolic networks, which ensure supply of the cells with energy even when four transporters are down-regulated simultaneously. Such networks can greatly reduce the success of RNAi since the phenotype could not be clearly defined, or in spite of the

reduced transcript does not occur. An RNAseq analysis of cDNA from tissues after induction of RNAi could provide an indication that such counter-regulation takes place.

A down-regulation of *Cpop*SAO, the oxidase of saligenin to salicylaldehyde demonstrates its function *in vivo*. Further the off-target prediction was established, which enables a highly-precise work with RNAi in non- model organisms.

By turning off all Cu/Zn-SOD, the function of individual enzymes (*Pc*SOD1 , *Pc*SOD3.1 -3.3) have been characterized in the context of additional treatments. All four SODs plays a role in the detoxification of artificially induction of oxidative stress, whereas according to the state of things, no SOD has an influence on the life span regulation of *P. cochleariae*. *Pc*SOD3.1 as extracellular SOD, which occurs both in the defensive secretions as well as in the hemolymph, plays a role in the resistance against an entomopathogenic fungus and Gram-positive bacterium. The activity of this enzyme is believed to contribute in the realization of a sufficient immune response.

By the integration of the adequate controls for each target gene and a corresponding analysis strategy, many proteins have been identified as part of a specific biosynthesis or transport process in the body by means of RNAi. This work has extended the knowledge of the molecular basis of intercellular transport and the production and enzymatic conversion of chemical precursors for the use as allomon in the defensive secretions. A methodology was established which can also be applied to other topics. By RNAi experiments in virtually every subject area of current and planned research, not only in this working group, the relevance of the work in this thesis is apparent. Due to the ongoing sequencing of closely related species, a comparable approach could be done relatively quickly. With the knowledge of the molecular base of the altered defense biochemistry of other species, new insights into the evolution and speciation of the leaf beetles could be obtained.

7. Literaturverzeichnis

Aldrich, J. R.,Blum, M. S.,Hefetz, A.,Fales, H. M.,Lloyd, H. A. und Roller, P. (1978): Proteins in a nonvenomous defensive secretion: biosynthetic significance. Science, 201**,** S. 452-4.

Alston, T. A.,Mela, L. und Bright, H. J. (1977): 3-Nitropropionate, Toxic Substance of Indigofera, Is a Suicide Inactivator of Succinate-Dehydrogenase - (Rat-Liver Mitochondria Carbanion-N-5 Flavin Adducts 2-Proton Abstraction Mechanism). Proceedings of the National Academy of Sciences of the United States of America, 74**,** S. 3767-3771.

Altincicek, B.,Knorr, E. und Vilcinskas, A. (2008): Beetle immunity: Identification of immune-inducible genes from the model insect Tribolium castaneum. Dev Comp Immunol, 32**,** S. 585-95.

Altschul, Stephen F.,Madden, Thomas L.,Schaeffer, Alejandro A.,Zhang, Jinghui,Zhang, Zheng,Miller, Webb und Lipman, David J. (1997): Gapped BLAST and PSI-BLAST: A new generation of protein database search programs. Nucleic Acids Research, 25**,** S. 3389-3402.

Ammann, B. (2000): Biotic responses to rapid climatic changes: Introduction to a multidisciplinary study of the Younger Dryas and minor oscillations on an altitudinal transect in the Swiss Alps. Palaeogeography Palaeoclimatology Palaeoecology, 159**,** S. 191-201.

Araujo, R. N.,Santos, A.,Pinto, F. S.,Gontijo, N. F.,Lehane, M. J. und Pereira, M. H. (2006): RNA interference of the salivary gland nitrophorin 2 in the triatomine bug Rhodnius prolixus (Hemiptera : Reduviidae) by dsRNA ingestion or injection. Insect Biochemistry and Molecular Biology, 36**,** S. 683-693.

Arbi, M.,Pouliliou, S.,Lampropoulou, M.,Marmaras, V. J. und Tsakas, S. (2011): Hydrogen peroxide is produced by E-coli challenged haemocytes and regulates phagocytosis, in the medfly Ceratitis capitata. The active role of superoxide dismutase. Developmental and Comparative Immunology, 35**,** S. 865-871.

Bacsi, A.,Woodberry, M.,Widger, W.,Papaconstantinou, J.,Mitra, S.,Peterson, J. W. und Boldogh, I. (2006): Localization of superoxide anion production to mitochondrial electron transport chain in 3-NPA-treated cells. Mitochondrion, 6**,** S. 235-244.

Bartl, Martin,Kötzing, Martin,Schuster, Stefan,Li, Pu und Kaleta, Christoph (2013): Dynamic optimization identifies optimal programmes for pathway regulation in prokaryotes. Nat Commun, 4.

Battefeld, Dominique. (2013): Rolle eines *odorant binding proteins* bei der Prägung des Meerrettichblattkäfers *Phaedon cochleariae* (Coleoptera: Chrysomelidae) auf Wirtspflanzenduftstoffe. Bachelorarbeit, Freie Universität.

Belles, X. (2010): Beyond Drosophila: RNAi In Vivo and Functional Genomics in Insects. Annual Review of Entomology, 55**,** S. 111-128.

Bellés, Xavier,Martín, David und Piulachs, Maria-Dolors (2005): THE MEVALONATE PATHWAY AND THE SYNTHESIS OF JUVENILE HORMONE IN INSECTS. Annual Review of Entomology, 50**,** S. 181-199.

Blum, M. S.,Brand, J. M.,Wallace, J. B. und Fales, H. M. (1972): Chemical characterisation of devensive secretions of a chrysomelid larva. Life Sciences Pt-2 Biochemistry General and Molecular Biology, 11**,** S. 525-531.

Bodemann, R. R.,Rahfeld, P.,Stock, M.,Kunert, M.,Wielsch, N.,Groth, M.,Frick, S.,Boland, W. und Burse, A. (2012): Precise RNAi-mediated silencing of metabolically active proteins in the defence secretions of juvenile leaf beetles. Proceedings of the Royal Society B-Biological Sciences, 279**,** S. 4126-4134.

Boelsterli, Urs, A. (2009): Mechanistic toxicology, the molecular basis of how chemicals disrupt biological target, 2 ed. Chippenham and Eastbourne.

Brueckmann, M.,Termonia, A.,Pasteels, J. M. und Hartmann, T. (2002): Characterization of an extracellular salicyl alcohol oxidase from larval defensive secretions of Chrysomela populi

and Phratora vitellinae (Chrysomelina). Insect Biochemistry and Molecular Biology, 32**,** S. 1517-1523.
Bucher, G.,Scholten, J. und Klingler, M. (2002): Parental RNAi in Tribolium (Coleoptera). Current Biology, 12**,** S. R85-R86.
Burand, John P. und Hunter, Wayne B. (2013): RNAi: Future in insect management. Journal of Invertebrate Pathology, 112**,** S. S68-S74.
Burse, A.,Frick, S.,Discher, S.,Tolzin-Banasch, K.,Kirsch, R.,Strauss, A.,Kunert, M. und Boland, W. (2009): Always being well prepared for defense: the production of deterrents by juvenile Chrysomelina beetles (Chrysomelidae). Phytochemistry, 70**,** S. 1899-909.
Burse, A.,Schmidt, A.,Frick, S.,Kuhn, J.,Gershenzon, J. und Boland, W. (2007): Iridoid biosynthesis in Chrysomelina larvae: Fat body produces early terpenoid precursors. Insect Biochemistry and Molecular Biology, 37**,** S. 255-265.
Burse, Antje,Frick, Sindy,Schmidt, Axel,Buechler, Rita,Kunert, Maritta,Gershenzon, Jonathan,Brandt, Wolfgang und Boland, Wilhelm (2008): Implication of HMGR in homeostasis of sequestered and de novo produced precursors of the iridoid biosynthesis in leaf beetle larvae. Insect Biochemistry and Molecular Biology, 38**,** S. 76-88.
Carton, Y.,Poirie, M. und Nappi, A. J. (2008): Insect immune resistance to parasitoids. Insect Science, 15**,** S. 67-87.
Cavener, D. R. (1992): Gmc oxidoreductases - a newly defined family of homologous proteins with diverse catalytic activities. Journal of Molecular Biology, 223**,** S. 811-814.
Cerenius, L.,Lee, B. L. und Soderhall, K. (2008): The proPO-system: pros and cons for its role in invertebrate immunity. Trends in Immunology, 29**,** S. 263-271.
Ciudad, Laura,Belles, Xavier und Piulachs, Maria-Dolors (2007): Structural and RNAi characterization of the German cockroach lipophorin receptor, and the evolutionary relationships of lipoprotein receptors. Bmc Molecular Biology, 8**,** S. 53.
Colinet, D.,Cazes, D.,Belghazi, M.,Gatti, J. L. und Poirie, M. (2011): Extracellular superoxide dismutase in insects: characterization, function, and interspecific variation in parasitoid wasp venom. J Biol Chem, 286**,** S. 40110-21.
Cottrell, J. E.,Krystufek, V.,Tabbener, H. E.,Milner, A. D.,Connolly, T.,Sing, L.,Fluch, S.,Burg, K.,Lefevre, F.,Achard, P.,Bordacs, S.,Gebhardt, K.,Vornam, B.,Smulders, M. J. M.,Broeck, A. H. V.,Van Slycken, J.,Storme, V.,Boerjan, W.,Castiglione, S.,Fossati, T.,Alba, N.,Agundez, D.,Maestro, C.,Notivol, E.,Bovenschen, J. und van Dam, B. C. (2005): Postglacial migration of Populus nigra L.: lessons learrit from chloroplast DNA. Forest Ecology and Management, 206**,** S. 71-90.
Daloze, D. und Pasteels, J. M. (1994): Isolation of 8-hydroxygeraniol-8-o-beta-d-glucoside, a probable intermediate in biosynthesis of iridoid monoterpenes, from defensive secretions of Plagiodera versicolora and Gastrophysa viridula (Coleoptera, Chrysomelidae). Journal of Chemical Ecology, 20**,** S. 2089-2097.
Dettner, K. (1987): Chemosystematics and evolution of beetle chemical defenses. Annual Review of Entomology, 32**,** S. 17-48.
Dettner, K. und Schwinger, G. (1987): Chemical Defense in the Larvae of the Leaf Beetle Gonioctena-Viminalis L (Coleoptera, Chrysomelidae). Experientia, 43**,** S. 458-460.
Diaz-Albiter, H.,Mitford, R.,Genta, F. A.,Sant'Anna, M. R. V. und Dillon, R. J. (2011): Reactive Oxygen Species Scavenging by Catalase Is Important for Female Lutzomyia longipalpis Fecundity and Mortality. Plos One, 6.
Discher, Sabrina,Burse, Antje,Tolzin-Banasch, Karla,Heinemann, Stefan H.,Pasteels, Jacques M. und Boland, Wilhelm (2009): A versatile transport network for sequestering and excreting plant glycosides in leaf beetles provides an evolutionary flexible defense strategy. ChemBioChem, 10**,** S. 2223-2229.
Dossey, A. T. (2010): Insects and their chemical weaponry: New potential for drug discovery. Natural Product Reports, 27**,** S. 1737-1757.

Eisner, T. (1971): Chemical ecology: on arthropods and how they live as chemists. Verhandlungen dt. zool. Ges., 65**,** S. 123-137.

Eisner, T. und Meinwald, J. (1966): Defensive secretions of arthropods. Science, 153**,** S. 1341-50.

Feld, Birte K.,Pasteels, Jacques M. und Boland, Wilhelm (2001): Phaedon cochleariae and Gastrophysa viridula (Coleoptera: Chrysomelidae) produce defensive iridoid monoterpenes de novo and are able to sequester glycosidically bound terpenoid precursors. CHEMOECOLOGY, 11**,** S. 191-198.

Fire, A.,Xu, S. Q.,Montgomery, M. K.,Kostas, S. A.,Driver, S. E. und Mello, C. C. (1998): Potent and specific genetic interference by double-stranded RNA in Caenorhabditis elegans. Nature, 391**,** S. 806-811.

Fraga, Amanda,Ribeiro, Lupis,Lobato, Mariana,Santos, Vitória,Silva, José Roberto,Gomes, Helga,da Cunha Moraes, Jorge Luiz,de Souza Menezes, Jackson,de Oliveira, Carlos Jorge Logullo,Campos, Eldo und da Fonseca, Rodrigo Nunes (2013): Glycogen and Glucose Metabolism Are Essential for Early Embryonic Development of the Red Flour Beetle Tribolium castaneum. Plos One, 8**,** S. e65125.

Frick, S.,Nagel, R.,Schmidt, A.,Bodemann, R. R.,Rahfeld, P.,Pauls, G.,Brandt, W.,Gershenzon, J.,Boland, W. und Burse, A. (2013): Metal ions control product specificity of isoprenyl diphosphate synthases in the insect terpenoid pathway. Proc Natl Acad Sci U S A, 110**,** S. 4194-9.

Ghanim, Murad,Kontsedalov, Svetlana und Czosnek, Henryk (2007): Tissue-specific gene silencing by RNA interference in the whitefly Bemisia tabaci (Gennadius). Insect Biochemistry and Molecular Biology, 37**,** S. 732-738.

Giulianini, P. G.,Bertolo, E.,Battistella, S. und Amirante, G. A. (2003): Ultrastructure of the hemocytes of Cetonischema aeruginosa larvae (Coleoptera, Scarabaeidae): involvement of both granulocytes and oenocytoids in in vivo phagocytosis. Tissue & Cell, 35**,** S. 243-251.

Gretscher, René R.,Stock, Magdalena,Strauss, Anja,Frick, Sindy,Boland, Wilhelm und Burse, Antje (tba): Extracellular Superoxide-dismutases take an active part in fitness, oxidative Stress and pathogen resistance in juvenile Phaedon cochleariae (Coleoptera: Chrysomelidae: Chrysomelina). In Preparation.

Gross, J.,Müller, C.,Vilcinskas, A. und Hilker, M. (1998): Antimicrobial activity of exocrine glandular secretions, hemolymph, and larval regurgitate of the mustard leaf beetle Phaedon cochleariae. Journal of Invertebrate Pathology, 72**,** S. 296-303.

Gross, J.,Podsiadlowski, L. und Hilker, M. (2002): Antimicrobial activity of exocrine glandular secretion of Chrysomela larvae. Journal of Chemical Ecology, 28**,** S. 317-331.

Gross, J.,Schumacher, K.,Schmidtberg, H. und Vilcinskas, A. (2008): Protected by fumigants: Beetle perfumes in antimicrobial defense. Journal of Chemical Ecology, 34**,** S. 179-188.

Grosse-Wilde, E.,Kuebler, L. S.,Bucks, S.,Vogel, H.,Wicher, D. und Hansson, B. S. (2011): Antennal transcriptome of Manduca sexta. Proceedings of the National Academy of Sciences of the United States of America, 108**,** S. 7449-7454.

Grünler, Jacob,Ericsson, Johan und Dallner, Gustav (1994): Branch-point reactions in the biosynthesis of cholesterol, dolichol, ubiquinone and prenylated proteins. Biochimica et Biophysica Acta (BBA) - Lipids and Lipid Metabolism, 1212**,** S. 259-277.

Gunaratna, R. T. und Jiang, H. B. (2013): A comprehensive analysis of the Manduca sexta immunotranscriptome. Developmental and Comparative Immunology, 39**,** S. 388-398.

Ha, E. M.,Oh, C. T.,Bae, Y. S. und Lee, W. J. (2005): A direct role for dual oxidase in Drosophila gut immunity. Science, 310**,** S. 847-850.

Häger, Wiebke. (2013): Charakterisierung von beta-Glucosidasen aus dem Wehrsekret der juvenilen Blattkäfer *Phaedon cochleariae* und *Chrysomela populi*. Bachelor Bachelorarbeit, Friedrich-Schiller-Universität.

Hajek, A. E. und Stleger, R. J. (1994): INTERACTIONS BETWEEN FUNGAL PATHOGENS AND INSECT HOSTS. Annual Review of Entomology, 39**,** S. 293-322.

Hansen, Klavs R.,Burns, Gavin,Mata, Juan,Volpe, Thomas A.,Martienssen, Robert A.,Bähler, Jürg und Thon, Geneviève (2005): Global Effects on Gene Expression in Fission Yeast by Silencing and RNA Interference Machineries. Molecular and Cellular Biology, 25**,** S. 590-601.

He, Z. B.,Cao, Y. Q. und Xia, Y. X. (2010): Optimization of parental RNAi conditions for hunchback gene in Locusta migratoria manilensis (Meyen). Insect Science, 17**,** S. 1-6.

Hoek, W. Z. (1997): Late-glacial and early Holocene climatic events and chronology of vegetation development in the Netherlands. Vegetation History and Archaeobotany, 6**,** S. 197-213.

Hoffmann, Jules A. (2003): The immune response of Drosophila. Nature, 426**,** S. 33-38.

Huvenne, H. und Smagghe, G. (2010): Mechanisms of dsRNA uptake in insects and potential of RNAi for pest control: A review. Journal of Insect Physiology, 56**,** S. 227-235.

Iyer, S.,Deutsch, K.,Yan, X. W. und Lin, B. Y. (2007): Batch RNAi selector: A standalone program to predict specific siRNA candidates in batches with enhanced sensitivity. Computer Methods and Programs in Biomedicine, 85**,** S. 203-209.

Jackson, Aimee L.,Bartz, Steven R.,Schelter, Janell,Kobayashi, Sumire V.,Burchard, Julja,Mao, Mao,Li, Bin,Cavet, Guy und Linsley, Peter S. (2003): Expression profiling reveals off-target gene regulation by RNAi. Nature Biotechnology, 21**,** S. 635-637.

Johansson, M. W.,Holmblad, T.,Thornqvist, P. O.,Cammarata, M.,Parrinello, N. und Soderhall, K. (1999): A cell-surface superoxide dismutase is a binding protein for peroxinectin, a cell-adhesive peroxidase in crayfish. Journal of Cell Science, 112**,** S. 917-925.

Jolivet, Pierre H. A. (1995): Host-plants of Chrysomelidae of the world an essay about the relationships between the leaf-beetles and their food-plants, Leiden, Backhuys.

Katoch, Rajan,Sethi, Amit,Thakur, Neelam und Murdock, Larry (2013): RNAi for insect control: current perspective and future challenges. Applied biochemistry and biotechnology, 171**,** S. 847.

Kawahara, T.,Quinn, M. T. und Lambeth, J. D. (2007): Molecular evolution of the reactive oxygen-generating NADPH oxidase (Nox/Duox) family of enzymes. Bmc Evolutionary Biology, 7.

Kennerdell, J. R. und Carthew, R. W. (1998): Use of dsRNA-mediated genetic interference to demonstrate that frizzled and frizzled 2 act in the wingless pathway. Cell, 95**,** S. 1017-26.

Kippner, Linda,Finn, Nnenna,Shukla, Shreya und Kemp, Melissa (2011): Systemic remodeling of the redox regulatory network due to RNAi perturbations of glutaredoxin 1, thioredoxin 1, and glucose-6-phosphate dehydrogenase. BMC Systems Biology, 5**,** S. 164.

Kirsch, Roy,Vogel, Heiko,Muck, Alexander,Reichwald, Kathrin,Pasteels, Jacques M. und Boland, Wilhelm (2011a): Host plant shifts affect a major defense enzyme in Chrysomela lapponica. Proceedings of the National Academy of Sciences of the United States of America, 108**,** S. 4897-4901.

Kirsch, Roy,Vogel, Heiko,Muck, Alexander,Vilcinskas, Andreas,Pasteels, Jacques M. und Boland, Wilhelm (2011b): To be or not to be convergent in salicin-based defence in chrysomeline leaf beetle larvae: evidence from Phratora vitellinae salicyl alcohol oxidase. Proceedings of the Royal Society Biological Sciences Series B, 278**,** S. 3225-3232.

Komarov, D.A.,Slepneva, I.A.,Dubovskii, I.M.,Grizanova, E.V.,Khramtsov, V.V. und Glupov, V.V. (2006): Generation of Superoxide Radical and Hydrogen Peroxide in Insect Hemolymph in the Course of Immune Response. In: V. K. Shumnyi (Hrsg.).

Kuhn-Nentwig, L.,Schaller, J. und Nentwig, W. (2004): Biochemistry, toxicology and ecology of the venom of the spider Cupiennius salei (Ctenidae). Toxicon, 43**,** S. 543-553.

Kuhn, J.,Pettersson, E. M.,Feld, B. K.,Burse, A.,Termonia, A.,Pasteels, J. M. und Boland, W. (2004): Selective transport systems mediate sequestration of plant glucosides in leaf beetles: A molecular basis for adaptation and evolution. Proceedings of the National Academy of Sciences of the United States of America, 101**,** S. 13808-13813.

Kuhn, J.,Pettersson, E. M.,Feld, B. K.,Nie, L. H.,Tolzin-Banasch, K.,M'Rabet, S. M.,Pasteels, J. und Boland, W. (2007): Sequestration of plant-derived phenolglucosides by larvae of the leaf

beetle Chrysomela lapponica: Thioglucosides as mechanistic probes. Journal of Chemical Ecology, 33**,** S. 5-24.

Kulkarni, M. M.,Booker, M.,Silver, S. J.,Friedman, A.,Hong, P.,Perrimon, N. und Mathey-Prevot, B. (2006): Evidence of off-target effects associated with long dsRNAs in Drosophila melanogaster cell-based assays. Nat Methods, 3**,** S. 833-8.

Kunert, M.,Rahfeld, P.,Shaker, K. H.,Schneider, B.,David, A.,Dettner, K.,Pasteels, J. M. und Boland, W. (2013): Beetles Do It Differently: Two Stereodivergent Cyclisation Modes in Iridoid-Producing Leaf-Beetle Larvae. ChemBioChem, 14**,** S. 353-360.

Kunert, Maritta,Soe, Astrid,Bartram, Stefan,Discher, Sabrina,Tolzin-Banasch, Karla,Nie, Lihua,David, Anja,Pasteels, Jacques und Boland, Wilhelm (2008): De novo biosynthesis versus sequestration: A network of transport systems supports in iridoid producing leaf beetle larvae both modes of defense. Insect Biochemistry and Molecular Biology, 38**,** S. 895-904.

Leschen, Richard, A. B. und Beutel, Rolf, G. (2014): Arthropoda: Insecta: Coleoptera, Volume 3: Morphology and Systematics (Phytophaga), Berlin, DeGruyter.

Lew-Tabor, A. E.,Kurscheid, S.,Barrero, R.,Gondro, C.,Moolhuijzen, P. M.,Valle, M. Rodriguez,Morgan, J. A. T.,Covacin, C. und Bellgard, M. I. (2011): Gene expression evidence for off-target effects caused by RNA interference-mediated gene silencing of Ubiquitin-63E in the cattle tick Rhipicephalus microplus. International Journal for Parasitology, 41**,** S. 1001-1014.

Li, J. W.,Lehmann, S.,Weissbecker, B.,Naharros, I. O.,Schutz, S.,Joop, G. und Wimmer, E. A. (2013): Odoriferous Defensive Stink Gland Transcriptome to Identify Novel Genes Necessary for Quinone Synthesis in the Red Flour Beetle, Tribolium castaneum. PLoS Genetics, 9**,** S. 18.

Lorenz, M.,Boland, W. und Dettner, K. (1993): Biosynthesis of iridodials in the defense glands of beetle larvae (Chrysomelinae). Angewandte Chemie-International Edition in English, 32**,** S. 912-914.

Maraghi, Hakima El. (1993): Etude ultrastructurale comparée des glandes défensive chez les larves de Gastrophysa viridula, Chrysomela tremulae et Phratora vitellinae (Chrysomelidae). docteur en sciences Thèse pou l'obtention di grade de docteur en sciences, Université Libre.

Mardulyn, P.,Othmezouri, N.,Mikhailov, Y. E. und Pasteels, J. M. (2011): Conflicting mitochondrial and nuclear phylogeographic signals and evolution of host-plant shifts in the boreo-montane leaf beetle Chrysomela lapponica. Molecular Phylogenetics and Evolution, 61**,** S. 686-696.

McCord, J. M. und Fridovich, I. (1969): Superoxide dismutase. An enzymic function for erythrocuprein (hemocuprein). J Biol Chem, 244**,** S. 6049-55.

Meister, G. und Tuschl, T. (2004): Mechanisms of gene silencing by double-stranded RNA. Nature, 431**,** S. 343-349.

Melnyk, C. W.,Molnar, A. und Baulcombe, D. C. (2011): Intercellular and systemic movement of RNA silencing signals. EMBO Journal, 30**,** S. 3553-3563.

Michalski, C.,Mohagheghi, H.,Nimtz, M.,Pasteels, J. und Ober, D. (2008): Salicyl alcohol oxidase of the chemical defense secretion of two chrysomelid leaf beetles - Molecular and functional characterization of two new members of the glucose-methanol-choline oxidoreductase gene family. Journal of Biological Chemistry, 283**,** S. 19219-19228.

Miller, A. F. (2004): Superoxide dismutases: active sites that save, but a protein that kills. Current Opinion in Chemical Biology, 8**,** S. 162-168.

Miller, S. C.,Brown, S. J. und Tomoyasu, Y. (2008): Larval RNAi in Drosophila? Development Genes and Evolution, 218**,** S. 505-510.

Mitchell Iii, Robert D.,Ross, Elizabeth,Osgood, Christopher,Sonenshine, Daniel E.,Donohue, Kevin V.,Khalil, Sayed M.,Thompson, Deborah M. und Michael Roe, R. (2007): Molecular characterization, tissue-specific expression and RNAi knockdown of the first vitellogenin receptor from a tick. Insect Biochemistry and Molecular Biology, 37**,** S. 375-388.

Mito, T.,Nakamura, T.,Bando, T.,Ohuchi, H. und Noji, S. (2011): The advent of RNA interference in Entomology. Entomological Science, 14**,** S. 1-8.
Moreau, S. J. M. (2013): "It stings a bit but it cleans well": Venoms of Hymenoptera and their antimicrobial potential. Journal of Insect Physiology, 59**,** S. 186-204.
Moretto, A. und Colosio, C. (2013): The role of pesticide exposure in the genesis of Parkinson's disease: Epidemiological studies and experimental data. Toxicology, 307**,** S. 24-34.
Naito, Y.,Yamada, T.,Matsumiya, T.,Ui-Tei, K.,Saigo, K. und Morishita, S. (2005): dsCheck: highly sensitive off-target search software for double-stranded RNA-mediated RNA interference. Nucleic Acids Research, 33**,** S. W589-W591.
Nappi, A. J. und Christensen, B. M. (2005): Melanogenesis and associated cytotoxic reactions: Applications to insect innate immunity. Insect Biochemistry and Molecular Biology, 35**,** S. 443-459.
Nappi, A. J.,Vass, E.,Frey, F. und Carton, Y. (1995): Superoxide anion generation in Drosophila during melanotic encapsulation of parasites. European Journal of Cell Biology, 68**,** S. 450-456.
Nicolaus, L. K.,Cassel, J. F.,Carlson, R. B. und Gustavson, C. R. (1983): Taste-Aversion Conditioning of Crows to Control Predation on Eggs. Science, 220**,** S. 212-214.
Ohnishi, Atsushi,Hashimoto, Kana,Imai, Kiyohiro und Matsumoto, Shogo (2009): Functional characterization of the Bombyx mori fatty acid transport protein (BmFATP) within the silkmoth pheromone gland. Journal of Biological Chemistry, 284**,** S. 5128-5136.
Oldham, N. J.,Veith, M.,Boland, W. und Dettner, K. (1996): Iridoid monoterpene biosynthesis in insects - evidence for a de novo pathway occurring in the defensive glands of Phaedon armoraciae (Chrysomelidae) leaf beetle larvae. Naturwissenschaften, 83**,** S. 470-473.
Pasteels, J. M.,Braekman, J. C.,Daloze, D. und Ottinger, R. (1982): Chemical defence in chrysomelid larvae and adults. Tetrahedron, 38**,** S. 1891-1897.
Pasteels, J. M.,Duffey, S. und Rowell-Rahier, M. (1990): Toxins in chrysomelid beetles possible evolutionary sequence from de novo synthesis to derivation from food-plant chemicals. Journal of Chemical Ecology, 16**,** S. 211-222.
Pasteels, J. M.,Gregoire, J. C. und Rowell-Rahier, M. (1983): The chemical ecology of defense in arthropods. Annual Review of Entomology, 28**,** S. 263-289.
Pasteels, J. M. und Rowell-Rahier, M. (1989): Defensive glands and secretions as taxonomical tools in the Chrysomelidae. Entomography, 6**,** S. 423-432.
Pasteels, J. M.,Rowell-Rahier, M.,Braekman, J. C. und Daloze, D. (1984): Chemical Defenses in Leaf Beetles and Their Larvae - the Ecological, Evolutionary and Taxonomic Significance. Biochemical Systematics and Ecology, 12**,** S. 395-406.
Pasteels, J. M.,Rowell-Rahier, M.,Braekman, J. C.,Daloze, D. und Duffey, S. (1989): Evolution of Exocrine Chemical Defense in Leaf Beetles (Coleoptera, Chrysomelidae). Experientia, 45**,** S. 295-300.
Pasteels, J. M.,Rowell-Rahier, M.,Braekman, J. C. und Dupont, A. (1983): Salicin from host plant as precursor of salicyl aldehyde in defensive secretion of chrysomeline larvae. Physiological Entomology, 8**,** S. 307-314.
Phillips, J. P.,Campbell, S. D.,Michaud, D.,Charbonneau, M. und Hilliker, A. J. (1989): Null mutation of copper/zinc superoxide dismutase in Drosophila confers hypersensitivity to paraquat and reduced longevity. Proc Natl Acad Sci U S A, 86**,** S. 2761-5.
Posnien, N.,Koniszewski, N. D. B.,Hein, H. J. und Bucher, G. (2011): Candidate Gene Screen in the Red Flour Beetle Tribolium Reveals Six3 as Ancient Regulator of Anterior Median Head and Central Complex Development. PLoS Genetics, 7.
Posnien, Nico,Schinko, Johannes,Grossmann, Daniela,Shippy, Teresa D.,Konopova, Barbora und Bucher, Gregor (2009): RNAi in the Red Flour Beetle (Tribolium). Cold Spring Harbor Protocols, 2009**,** S. pdb.prot5256.
Punta, M.,Coggill, P. C.,Eberhardt, R. Y.,Mistry, J.,Tate, J.,Boursnell, C.,Pang, N.,Forslund, K.,Ceric, G.,Clements, J.,Heger, A.,Holm, L.,Sonnhammer, E. L. L.,Eddy, S. R.,Bateman, A. und Finn,

R. D. (2012): The Pfam protein families database. Nucleic Acids Research, 40**,** S. D290-D301.

Quennedey, Andre (1998): Insect epidermal gland cells: Ultrastructure and morphogenesis.

Rahfeld, Peter,Kirsch, Roy,Kugel, Susann,Wielsch, Natalie,Stock, Magdalena,Groth, Marco,Boland, Wilhelm und Burse, Antje (2014): Independently recruited oxidases from the glucose-methanol-choline oxidoreductase family enabled chemical defences in leaf beetle larvae (subtribe Chrysomelina) to evolve. Proceedings of the Royal Society B: Biological Sciences, 281.

Randoux, T.,Braekman, J. C.,Daloze, D. und Pasteels, J. M. (1991): Denovo Biosynthesis of Delta-3-Isoxazolin-5-One and 3-Nitropropanoic Acid-Derivatives in Chrysomela-Tremulae. Naturwissenschaften, 78**,** S. 313-314.

Resh, Vincent H. (2009): Encyclopedia of insects, Amsterdam u.a., Elsevier.

Reynolds, A.,Leake, D.,Boese, Q.,Scaringe, S.,Marshall, W. S. und Khvorova, A. (2004): Rational siRNA design for RNA interference. Nature Biotechnology, 22**,** S. 326-330.

Rhee, S. G. (2006): H2O2, a necessary evil for cell signaling. Science, 312**,** S. 1882-1883.

Ruddle, F. H. (1984): Reverse Genetics and Beyond. American Journal of Human Genetics, 36**,** S. 944-953.

Schulz, S.,Gross, J. und Hilker, M. (1997): Origin of the defensive secretion of the leaf beetle Chrysomela lapponica. Tetrahedron, 53**,** S. 9203-9212.

Seinen, Erwin,Burgerhof, Johannes G. M.,Jansen, Ritsert C. und Sibon, Ody C. M. (2011): RNAi-induced off-target effects in Drosophila melanogaster: frequencies and solutions. Briefings in Functional Genomics, 10**,** S. 206-214.

Siomi, H. und Siomi, M. C. (2009): On the road to reading the RNA-interference code. Nature, 457**,** S. 396-404.

Siva-Jothy, M. T.,Moret, Y. und Rolff, J. (2005): Insect immunity: An evolutionary ecology perspective, In: S. J. Simpson (Hrsg.): Advances in Insect Physiology, Vol 32. San Diego: Elsevier Academic Press Inc.

Smadja, C. M.,Canback, B.,Vitalis, R.,Gautier, M.,Ferrari, J.,Zhou, J. J. und Butlin, R. K. (2012): Large-Scale Candidate Gene Scan Reveals the Role of Chemoreceptor Genes in Host Plant Specialization and Speciation in the Pea Aphid. Evolution, 66**,** S. 2723-2738.

Snyder, J. H. und Qi, X. Q. (2013): Biosynthesis Metal Matters. Nature Chemical Biology, 9**,** S. 295-296.

Soetens, P.,Pasteels, J. M. und Daloze, D. (1993): A simple method for invivo testing of glandular enzymatic activity on potential precursors of larval defensive compounds in phratora-species (coleoptera, chrysomelinae). Experientia, 49**,** S. 1024-1026.

Stock, Magdalena,Gretscher, R. René,Groth, Marco,Eiserloh, Simone,Boland, Wilhelm und Burse, Antje (2013): Putative sugar transporters of the mustard leaf beetle Phaedon cochleariae: their phylogeny and role for nutrient supply in larval defensive glands. Plos One.

Strauss, Anja S,Peters, Sven,Boland, Wilhelm und Burse, Antje (2013): ABC transporter functions as a pacemaker for sequestration of plant glucosides in leaf beetles. eLife, 2.

Tanaka, H. und Suzuki, K. (2005): Expression profiling of a diapause-specific peptide (DSP) of the leaf beetle Gastrophysa atrocyanea and silencing of DSP by double-strand RNA. Journal of Insect Physiology, 51**,** S. 701-707.

Terenius, O.,Papanicolaou, A.,Garbutt, J. S.,Eleftherianos, I.,Huvenne, H.,Kanginakudru, S.,Albrechtsen, M.,An, C. J.,Aymeric, J. L.,Barthel, A.,Bebas, P.,Bitra, K.,Bravo, A.,Chevalieri, F.,Collinge, D. P.,Crava, C. M.,de Maagd, R. A.,Duvic, B.,Erlandson, M.,Faye, I.,Felfoldi, G.,Fujiwara, H.,Futahashi, R.,Gandhe, A. S.,Gatehouse, H. S.,Gatehouse, L. N.,Giebultowicz, J. M.,Gomez, I.,Grimmelikhuijzen, C. J. P.,Groot, A. T.,Hauser, F.,Heckel, D. G.,Hegedus, D. D.,Hrycaj, S.,Huang, L. H.,Hull, J. J.,Iatrou, K.,Iga, M.,Kanost, M. R.,Kotwica, J.,Li, C. Y.,Li, J. H.,Liu, J. S.,Lundmark, M.,Matsumoto, S.,Meyering-Vos, M.,Millichap, P. J.,Monteiro, A.,Mrinal, N.,Niimi, T.,Nowara, D.,Ohnishi, A.,Oostra, V.,Ozaki, K.,Papakonstantinou, M.,Popadic, A.,Rajam, M. V.,Saenko, S.,Simpson, R.

M.,Soberon, M.,Strand, M. R.,Tomita, S.,Toprak, U.,Wang, P.,Wee, C. W.,Whyard, S.,Zhang, W. Q.,Nagaraju, J.,Ffrench-Constant, R. H.,Herrero, S.,Gordon, K.,Swelters, L. und Smagghe, G. (2011): RNA interference in Lepidoptera: An overview of successful and unsuccessful studies and implications for experimental design. Journal of Insect Physiology, 57**,** S. 231-245.

Termonia, A.,Hsiao, T. H.,Pasteels, J. M. und Milinkovitch, M. C. (2001): Feeding specialization and host-derived chemical defense in Chrysomeline leaf beetles did not lead to an evolutionary dead end. Proceedings of the National Academy of Sciences of the United States of America, 98**,** S. 3909-3914.

Theuerkauf, M. und Joosten, H. (2012): Younger Dryas cold stage vegetation patterns of central Europe - climate, soil and relief controls. Boreas, 41**,** S. 391-407.

Tolzin-Banasch, Karla. (2009): Wehrchemie in Blattkäfern Aufklärung eines neuen Acylierungskomplexes in Insekten am Beispiel von *Chrysomela lapponica*. Dissertation, Freidrich-Schiller-Universität.

Tolzin-Banasch, Karla,Dagvadorj, E.,Sammer, U.,Kunert, M.,Kirsch, R.,Ploss, K.,Pasteels, J. M. und Boland, W. (2011): Glucose and Glucose Esters in the Larval Secretion of Chrysomela Lapponica; Selectivity of the Glucoside Import System from Host Plant Leaves. Journal of Chemical Ecology, 37**,** S. 195-204.

Tomoyasu, Y.,Miller, S. C.,Tomita, S.,Schoppmeier, M.,Grossmann, D. und Bucher, G. (2008): Exploring systemic RNA interference in insects: a genome-wide survey for RNAi genes in Tribolium. Genome Biology, 9.

Unbehend, Melanie,Hänniger, Sabine,Meagher, RobertL,Heckel, DavidG und Groot, AstridT (2013): Pheromonal Divergence Between Two Strains of Spodoptera frugiperda. Journal of Chemical Ecology, 39**,** S. 364-376.

Veith, Martin,Lorenz, Michael,Boland, Wilhelm,Simon, Helmut und Dettner, Konrad (1994): Biosynthesis of iridoid monoterpenes in insects: Defensive secretions from larvae of leaf beetles (Coleoptera: Chrysomelidae). Tetrahedron, 50**,** S. 6859-6874.

Veith, Martin,Oldham, NeilJ,Dettner, Konrad,Pasteels, JacquesM und Boland, Wilhelm (1997): Biosynthesis of Defensive Allomones in Leaf Beetle Larvae: Stereochemistry of Salicylalcohol Oxidation in Phratora vitellinae and Comparison of Enzyme Substrate and Stereospecificity with Alcohol Oxidases from Several Iridoid Producing Leaf Beetles. Journal of Chemical Ecology, 23**,** S. 429-443.

Vilcinskas, A. (2013): Evolutionary plasticity of insect immunity. Journal of Insect Physiology, 59**,** S. 123-129.

Wain, R. L. (1944): The secretion of salicylaldehyde by the larvae of the brassy willow beetle (Phylbdecta vitellinae L.). Ann. Rep. agric. hort. Res. Sta. Long Ashton, Bristol, 1943**,** S. pp. 108-110.

Wang, Jinda,Wu, Min,Wang, Baoju und Han, Zhaojun (2013): Comparison of the RNA interference effects triggered by dsRNA and siRNA in *Tribolium castaneum*. Pest Management Science, 69**,** S. 781-786.

Whitman, D. W.,Blum, M. S. und Alsop, D. W. (1990): Allomones: chemicals for defense.

Wiesner, J. und Vilcinskas, A. (2010): Antimicrobial peptides The ancient arm of the human immune system. Virulence, 1**,** S. 440-464.

Zhai, Yifan,Zhang, Jianqing,Sun, Zhongxiang,Dong, Xiaolin,He, Yuan,Kang, Kui,Liu, Zhichao und Zhang, Wenqing (2013): Proteomic and Transcriptomic Analyses of Fecundity in the Brown PlanthopperNilaparvata lugens(Stål). Journal of Proteome Research, 12**,** S. 5199-5212.

Zhang, S. L.,Yeromin, A. V.,Zhang, X. H. F.,Yu, Y.,Safrina, O.,Penna, A.,Roos, J.,Stauderman, K. A. und Cahalan, M. D. (2006): Genome-wide RNAi screen of Ca2+ influx identifies genes that regulate Ca2+ release-activated Ca2+ channel activity. Proceedings of the National Academy of Sciences of the United States of America, 103**,** S. 9357-9362.

Zvereva, E. L.,Kozlov, M. V. und Hilker, M. (2010): Evolutionary variations on a theme: host plant specialization in five geographical populations of the leaf beetle Chrysomela lapponica. Population Ecology, 52**,** S. 389-396.

8. Abkürzungsverzeichnis

dsRNA	Doppelsträngige Ribonucleinsäure
RNA	Ribonucleinsäure (engl. Ribonuclein-acid)
GFP	green-fluorescent protein
NIC	Non-Injection-Control
m.	married (Namensänderung nach der Hochzeit)
GDP	Geranyl-Diphosphat
FDP	Farnesyl-Diphosphat
Cpop SAO	Salicyl-Alkohol-Oxidase von *C. populi*
Pc To-like	To-like-Protein von *P. cochleariae*
Pc SOD1	Cytosolische Superoxid dismutase von *P. cochleariae*
PcSOD3.1 - 3.3	drei extrazelluläre SOD Isozyme von *P. cochleariae*
PcIDS1	Isoprenyl-Diphosphat-Synthase1 aus *P. cochleariae*

9. Danksagung

Nach fast vier Jahren, sind die Beteiligten an dieser Dissertation so zahlreich geworden, dass es unmöglich ist sie in diesem Abschnitt, der ihnen ja gewidmet ist, namentlich zu nennen

Zuallererst danke ich meiner Frau Anja für ihre Liebe und Motivation während der ganzen Zeit. Trotzdem, dass sie ihre eigene Abschlussarbeit schreiben und die Prüfungen für das erste Staatsexamen ablegen musste beschwerte sie sich nie über die phasenweise notwendigen ausgedehnten Arbeitszeiten, während derer sie zuerst mit unserer Tochter und dann mit unseren Töchtern allein war. Sie trieb mich an, nach Fehlschlägen weiterzumachen und freute sich mit mir, für all die kleinen und großen Erfolge, die dieser Beruf zum Glück auch mit sich bringt. Unseren Töchtern Alana und Talea sei an dieser Stelle auch gedankt, dank ihnen fiel die Zerstreuung an den Wochenenden leicht und durch ihr Staunen und unser Staunen über sie, wird die Welt bunt.

Ganz herzlich möchte ich mich bei Dr. Carsten Milkowski bedanken, der mir zuerst mit seiner Professionalität während meiner Staatsexamensarbeit in 4 Monaten die Grundlagen der praktischen Molekularbiologie vermittelte und mir dann durch eine kleine Bemerkung den Gedanken in den Kopf setzte, es tatsächlich in der Wissenschaft zu versuchen.

Meinen HiWis sei gedankt für die vielen kleinen und oft großen Dienste, die es mir erlaubten, manchmal mit Siebenmeilenstiefeln voranzukommen. Namentlich: Toni Krause, Christin Meißner, Tim Baumeister, Franziska Eberl, Anthea Wirges und Maximilian Fraulob. Letzter ermöglichte es mir nebenher in einem komplett anderen Teilgebiet zu forschen.

Natürlich möchte ich mich auch bei den ehemaligen und gegenwärtigen Mitarbeitern des MPI und im Besonderen der Abteilung für Bioorganische Chemie bedanken. Ihr habt mir stets geholfen, wenn ich eurer Hilfe bedurfte und mir mit Geduld Methoden und Zusammenhänge erklärt, die mir neu waren. Ich hoffe ich konnte etwas zurückgeben. Dr. Maritta Kunert, Kerstin Ploß, Angelika Berg und Anja David seien für ihre technische Unterstützung in der Abteilung hier namentlich erwähnt.

Ganz besonders möchte ich mich auch bei Prof. Rolf G. Beutel von der Uni Jena bedanken. Nicht nur dafür, dass er sich bereit erklärt hat meine Doktorarbeit zu betreuen, sondern auch und insbesondere dafür, dass er sich bereit erklärte mich bei einem Projekt mit unklarem Ausgang durch Investition von Arbeitskraft und Zeit zu unterstützen, woraus in Kürze auch eine kleine Arbeit entstehen soll. Ferner durfte ich zweimal eines seiner Zoologischen Grundpraktika leiten, was mich zum einen enc
beibrachte.

Zum Abschluss sei Prof. Wilhelm Boland gedankt für das Vertrauen in mich und meine Arbeit und die Unterstützung sowie Förderung in jedem Moment meiner Zeit am MPI. Durch die verständlicherweise chemische Sichtweise auf unsere Themen wurde man stets animiert die Dinge

noch einmal aus einem anderen Blickwinkel zu überdenken. Vielen Dank auch für die kritische Durchsicht der hier vorliegenden Arbeit.

Frau Dr. Antje Burse gelten meine vorletzten Worte. Ihr Humor und ihre Art mit Rückschlägen aber auch mit Erfolg umzugehen, waren stets eine Hilfe und neuer Ansporn. Sie ließ mir den Raum mich tatsächlich durch eigenes Vorgehen auf die zukünftige selbstbestimmte Karriere in der Forschung einzustellen und half mir durch klare Worte auf den Weg zurück, der das jeweils aktuelle Projekt zum Abschluss brachte. Nicht zuletzt hat sie mir im Schreibprozess dieser Arbeit durch Hinweise und Anmerkungen geholfen, diese Arbeit zu dem zu machen, was sie jetzt ist.

Allen vergessenen und allen unerwähnten, aber nie vergessenen Kollegen sei hier der allerletzte Gruß vergeben, man kann heutzutage nicht mehr ohne Menschen wie euch Erfolg haben und eine funktionierende kommunikative und kooperative Grundlage sind die Basis jeglichen Fortschritts in unserer schnellen Welt.

10. Erklärung

Jena, 10.08.2014

Ich erkläre hiermit, dass mir die aktuelle Promotionsordnung der Biologisch-Pharmazeutischen Fakultät der Friedich-Schiller-Universität Jena bekannt ist.

Ich habe die vorliegende Dissertation selbstständig verfasst und alle Hilfsmittel, persönlichen Mitteilungen und Quellen in der Arbeit genannt.

Sämtliche Personen, die mir bei der Auswahl, der Auswertung und der Herstellung des Manuskriptes geholfen haben, sind in der Danksagung erwähnt.

Ich habe weder die Hilfe eines Promotionsberaters in Anspruch genommen, noch haben Dritte unmittelbar oder mittelbar geldwerte Leistungen von mir für Arbeiten erhalten, die im Zusammenhang mit dem Inhalt der vorliegenden Arbeit stehen.

Ich habe die Dissertation noch nicht als Prüfungsarbeit für eine staatliche oder andere wissenschaftliche Prüfung eingereicht. Ferner habe ich auch nicht versucht, die gleiche, eine wesentlich ähnliche oder eine andere Abhandlung bei einer anderen Hochschule als Dissertation einzureichen.

_____

René Roberto Gretscher

11. Lebenslauf

Persönliche Angaben:

Name:	René Roberto Gretscher, geb. Bodemann
Geburtsdatum, Geburtsort:	30.11.1983, Berlin
Anschrift:	Anna-Siemsen-Str. 4, 07745 Jena
Kinder:	Alana Catalina (2008), Talea Carlotta (2012)

Schulische Ausbildung

13.06.2003	Abitur am Sartre-Gymnasium Berlin-Hellersdorf

Beruflicher Werdegang

Feb 2014 – dato	Lehramtsanwärter für das Lehramt an Regelschulen für die Fächer Biologie und Geschichte am Studienseminar Ostthüringen
Mai 2010 – 27.05.2014	Dissertation am Max-Planck-Institut für chemische Ökologie in Jena, Abteilung Bioorganische Chemie, AG Dr. Antje Burse: Chemische Abwehr bei Blattkäferlarven.

Akademische Ausbildung

Nov. 2012	Abschluss an der IMPRS – Exploration of Ecological Interactions with Molecular and Chemical Techniques.
Okt. 2004 – Apr. 2010	Studium des Lehramts für Regelschulen in den Fächern Biologie und Geschichte, Abschlussarbeit zum Thema „Untersuchungen zum pflanzenähnlichen Cryptochrom in Chlamydomonas reinhardtii“, Erstes Staatsexamen, Note 1,6.

International Max-Planck-Research School – ausgewählte Kurse

Nov. 2012	MS-based Proteomics, speaker: Dr. A. Svatos, Dr. N. Wielsch, Dr. N. Hupfer
Jun. 2012	Adobe Illustrator, speaker: Nico Überschaar, HKI
Feb. 2011	Innovative Morphology and Phylogeny, speaker: Prof. Rolf Beutel
Nov. 2010	Statistics for Beginners, speaker: Christian Hummert
Sep. 2010	Communication, speaker: Kerstin Kathy Meyer-Ross
Sep. 2010	Project Management, speaker: Kerstin Kathy Meyer-Ross
Aug. 2010	Scientific Writing, speaker: Kerstin Kathy Meyer-Ross
Aug. 2010	Time and self-management, speaker: Kerstin Kathy Meyer-Ross

Apr. 2011- Nov. 2011	Fachbetreuer einer Seminarfacharbeit an der Grete-Unrein-Schule Jena zum Thema „Bestimmung der optimalen Lebensbedingungen des Meerettichblattkäfers und seiner Bedeutung für die Landwirtschaft als potentieller Schädling“ von Caroline Keil, Saskia Schmidt, Lisa Wolfram, Maik Hoffmann.
Jun.2011- Nov. 2011	Betreuung der 1. Staatsexamensarbeit zum Thema „Experimentelle Ökologie für den Biologieunterricht im 21. Jahrhundert – Der Meerrettichblattkäfer *Phaedon cochleariae* als Modellorganismus“ von Anja Gretscher.

12. Wissenschaftliche Veröffentlichungen und Präsentationen

Publikationen

Bodemann (m. Gretscher), R.R., Rahfeld, P., Stock, M., Kunert, M., Wielsch, N., Groth, M.,Frick, S., Boland, W. and Burse, A., "Precise RNAi-mediated silencing of metabolically active proteins in the defence secretions of juvenile leaf beetles", Proceedings of the royal society B-Biological sciences, volume: 279, Issue: 1745, pages: 4126-4134, DOI: 10.1098/rspb.2012.1342, published: OCT 22 2012.

Frick, S., Nagel, R., Schmidt, A., **Bodemann (m.Gretscher), R.R.**, Rahfeld, P., Pauls, G., Brandt, W., Gershenzon, J., Boland, W. and Burse, A., "Metal ions control product specificity of isoprenyl diphosphate synthases in the insect terpenoid pathway.", Proceedings of the National academy of sciences of the United States of America, volume: 110, issue: 11, pages: 4194-4199, DOI: 10.1073/pnas.1221489110, published: MAR 12 2013.

Stock, M., **Gretscher, R.R.**, Groth, M., Eiserloh, S., Boland, W. and Burse, A., "Putative Sugar Transporters of the Mustard Leaf Beetle Phaedon cochleariae: Their Phylogeny and Role for Nutrient Supply in Larval Defensive Glands", PLOSone, DOI: 10.1371/journal.pone.0084461, published: DEC 31 2013.

Strauss, A., Dang, D., Stock, M., **Gretscher, R.R.,** Groth, M., Boland, W. and Burse, A., "Tissue-Specific Transcript Profiling for ABC Transporters in the Sequestering Larvae of the Phytophagous Leaf Beetle Chrysomela populi", PLOSone, DOI: 10.1371/journal.pone.0098637, published: JUN 02 2014.

Präsentationen

Wissenschaftliche Fachvorträge

Gretscher, R.R., "Extracellular Cu/Zn-SODs playing an important role in anti-microbial immune response of leaf beetles. RNAi, infections and xenobiotics.", 47. Doktorandenworkshop: Naturstoffe: Chemie, Biologie, Ökologie, Universität Bayreuth, Deutschland, October 2013.

Bodemann (m.Gretscher), R.R., "To kill two birds with one stone. Systemic silencing of an extracellular superoxide dismutase in *Phaedon cochleariae* (coleoptera).", iBeetle symposium "New horizons in molecular Zoology", Göttingen, Deutschland, März 2013.

Bodemann (m.Gretscher), R.R., "'And what's that for?' Functional allocation of unknown proteins in defensive secretions of juvenile chrysomelid species using RNA interference." 11. IMPRS Symposium, MPI für chemische Ökologie, Dornburg, Deutschland, Februar 2012.

Bodemann (m.Gretscher), R.R., "Disarming leaf beetle larvae. RNAi mediated silencing of keystonecompounds of the defense system." ICE-Symposium, MPI für chemische Ökologie, Jena, Deutschland, September 2011.

Bodemann (m.Gretscher), R.R., "RNAi – a promising tool for exploration of the defense related secretome in leaf beetle larvae." 27th ISCE Meeting, international society of chemical ecology, Simon-Fraser University, Burnaby, Canada, July 2011.

Bodemann (m.Gretscher), R.R., "RNAi effects on the chemical defense of leaf beetle larvae.", 41. Doktorandenworkshop: Naturstoffe: Chemie, Biologie, Ökologie, Universität Bonn, Deutschland, Mai 2011.

Poster Präsentationen

Gretscher R.R., "The non-model approach. Transcriptome guided identification of secretory proteins from leaf beetle defense secretions via LC-MS^{E}". 7th Central and Eastern European Proteomics Conference (CEEPC), Max Planck Institute for Chemical Ecology, Jena, Deutschland, October 2013

Bodemann (m.Gretscher), R.R., "Transcriptome based protein-identification and functional elucidation via RNA interference", SAB Meeting 2012, MPI für chemische Ökologie, Jena, Deutschland, Oktober 2012.

Bodemann (m.Gretscher), R.R., "Functional evaluation of enzymes in defense secretions of leaf beetle larvae by RNAi.", 24. Irseer Naturstofftage, Dechema e.V., Irsee, Deutschland, Februar 2012.

Bodemann (m.Gretscher), R.R., "Silencing of a superoxide dismutase in Phaedon cochleariae (Coleoptera: Chrysomelidae) by using RNAi." 5th international qPCR Symposium & industrial Exhibition & Application Workshops, Technische Universität München, Freising, Deutschland, April 2011.

Bodemann (m.Gretscher), R.R., "Silencing of a superoxide dismutase in Phaedon cochleariae (Coleoptera: Chrysomelidae) by using RNAi." 10. IMPRS Symposium, MPI für chemische Ökologie, Dornburg, Deutschland, Februar 2011.

Auszeichnungen

2013 Poster presentation prize, 7th Central and Eastern European Proteomics Conference (CEEPC), Max Planck Institute for Chemical Ecology, Jena, Deutschland, October 2013